Preliminary Report
of
The Hakuhō Maru Cruise KH 82-4

July 23 - August 21, 1982

Geophysical and Geological Investigation of Seafloor
Around Ogasawara (Bonin) Islands, Amami Plateau and
Southwestern Part of the Sea of Japan

(WESTPAC, IPOD)

Ocean Research Institute
University of Tokyo
1983

Preliminary Report
of
The Hakuhō Maru Cruise KH 82-4

July 23 - August 21, 1982

Geophysical and Geological Investigation of Seafloor
Around Ogasawara (Bonin) Islands, Amami Plateau and
Southwestern Part of the Sea of Japan

(WESTPAC, IPOD)

by
The Scienfific Members of the Expedition
Edited by
Kazuo Kobayashi

PREFACE

The principal scientific objectives of the cruise KH82-4 of the Research Vessel Hakuho Maru were geological and geophysical investigation of deep-sea floor around Japan. The cruise was divided into two legs; the early one aimed to clarify geotectonic and geodynamic settings of two colliding plate boundaries of the northern Philippine Sea. Oceanic plateaus and seamounts in the Pacific plate are colliding with the Philippine-sea plate east off the Bonin (Ogasawara) Islands. We investigated a fore-arc high southeast of Hahajima Island and collected hard rock samples. Results of visual and some microscopic examination of rocks collected by this operation are included in this report and would provide clue information on fore-arc structure with complementary data obtained by the former cruise KH80-3 in the same area.

In the northwestern margin of the Philippine-sea plate an oceanic plateau called Amami Plateau is colliding with the Asian plate. Our survey in this region included geophysical methods such as multichannel seismic profiling, seismic refraction and seismicity observation by ocean bottom seismometers deployed on the plateau, etc.

In leg 2 of this cruise the paleoenvironmental studies of the southern part of the Sea of Japan were attempted by collecting many sediment cores by piston corer. Distribution of surface layers of sediment was surveyed by a 3.5 kHz echo sounder and a single-channel seismic profiler.

This cruise was collaborated by the WESTPAC program of UNESCO-IOC. Participation of three scientists from three Asian countries in this cruise was made possible by thoughtful arrangement of the coordinators of the UNESCO-IOC-WESTPAC and Ministry of Education, Science and Culture (MONBUSHO), Japan. I am heartily grateful to those concerned.

Selection of survey areas and sites as well as compilation of bathymetric charts in these regions were greatly helped by unpublished data made available from Geological Survey of Japan and Japan Oceanographic Data Center, Hydrographic Department, Maritime Safety Agency of Japan (Marine Geophysical Data 81-043 and 82-065). I wish to express my sincere thanks to them for their help.
This cruise was also for the IPOD future site selection in the northwestern Pacific margins.

March 1983

Kazuo KOBAYASHI
Chief Scientist of the Cruise

CONTENTS

1. SCIENTISTS ABOARD THE R.V. HAKUHO MARU FOR THE CRUISE KH 82-4

KOBAYASHI, Kazuo (Chief Scientist)	Ocean Research Institute, University of Tokyo
AMAMIYA, Hideki	Department of Earth Sciences, Chiba University
ASANUMA, Toshio	Department of Earth Sciences, Chiba University
BRAVO, Angel**	Bureau of Mines and Geosciences (Philippines)
FUJII, Naoyuki*	Department of Earth Sciences, Kobe University
FUJISAWA, Hideyuki**	Earthquake Research Institute, University of Tokyo
FURUTA, Toshio	Ocean Research Institute, University of Tokyo
FUTAKUCHI, Katsuto	Department of Geology, Kanazawa University
ISEZAKI, Nobuhiro	Department of Earth Sciences, Kobe University
ISHII, Teruaki*	Ocean Research Institute, University of Tokyo
HASHIMOTO, Jun*	Japan Marine Science and Technology Center
KITAZATO, Hiroshi**	Department of Earth Sciences, Shizuoka University
KOBAYASHI, Hiroaki**	Department of Geology and Paleontology, Tohoku University
KONG, Young Sae*	Ocean Research Institute, University of Tokyo
KONISHI, Kenji*	Department of Geology, Kanazawa University
LIU, Zhong Chen	National Bureau of Oceanography (China)
MATSUBARA, Yoshikazu	Department of Earth Sciences, Kobe University
MATSUMOTO, Takeshi	Ocean Research Institute, University of Tokyo
MIYATA, Yuichiro**	Department of Geology, Kyushu University
MORIWAKI, Hiroshi**	Department of Geology, Tokyo Metropolitan University
NAKA, Jiro*	Department of Geology, Kyushu University
NISHIZAWA, Azusa*	Department of Geophysics, Tohoku Universtiy
OBA, Tadamichi**	Educational College, Kanazawa University
OGAWA, Yujiro**	Department of Geology, Kyushu University
OHARA, Hideki	Department of Geology, Kanazawa University
OHYAMA, Naomi	Department of Earth Sciences, Chiba University
OMURA, Akio**	Department of Geology, Kanazawa University
SHIMIZU, Hiroshi*	Department of Geophysics, Tohoku University
SUYEHIRO, Kiyoshi*	Department of Geophysics, Tohoku University
TANAKA, Takeo	Ocean Research Institute, University of Tokyo
TANIMURA, Yoshihiro**	National Science Museum
MASUZAWA, Toshiyuki**	Institute for Hydrosphere Sciences, Nagoya University

TOKUYAMA, Hidekazu*	Ocean Research Institute, University of Tokyo
YAMANO, Makoto	Earthquake Research Institute, University of Tokyo
YOO, Tong Hoon	Korean Ocean Research and Development Institute (Republic of Korea)
WATANABE, Masaharu	Ocean Research Institute, University of Tokyo

* From Tokyo to Fukuoka only

** From Fukuoka to Tokyo only

2. INDEX MAP OF KH 82-4

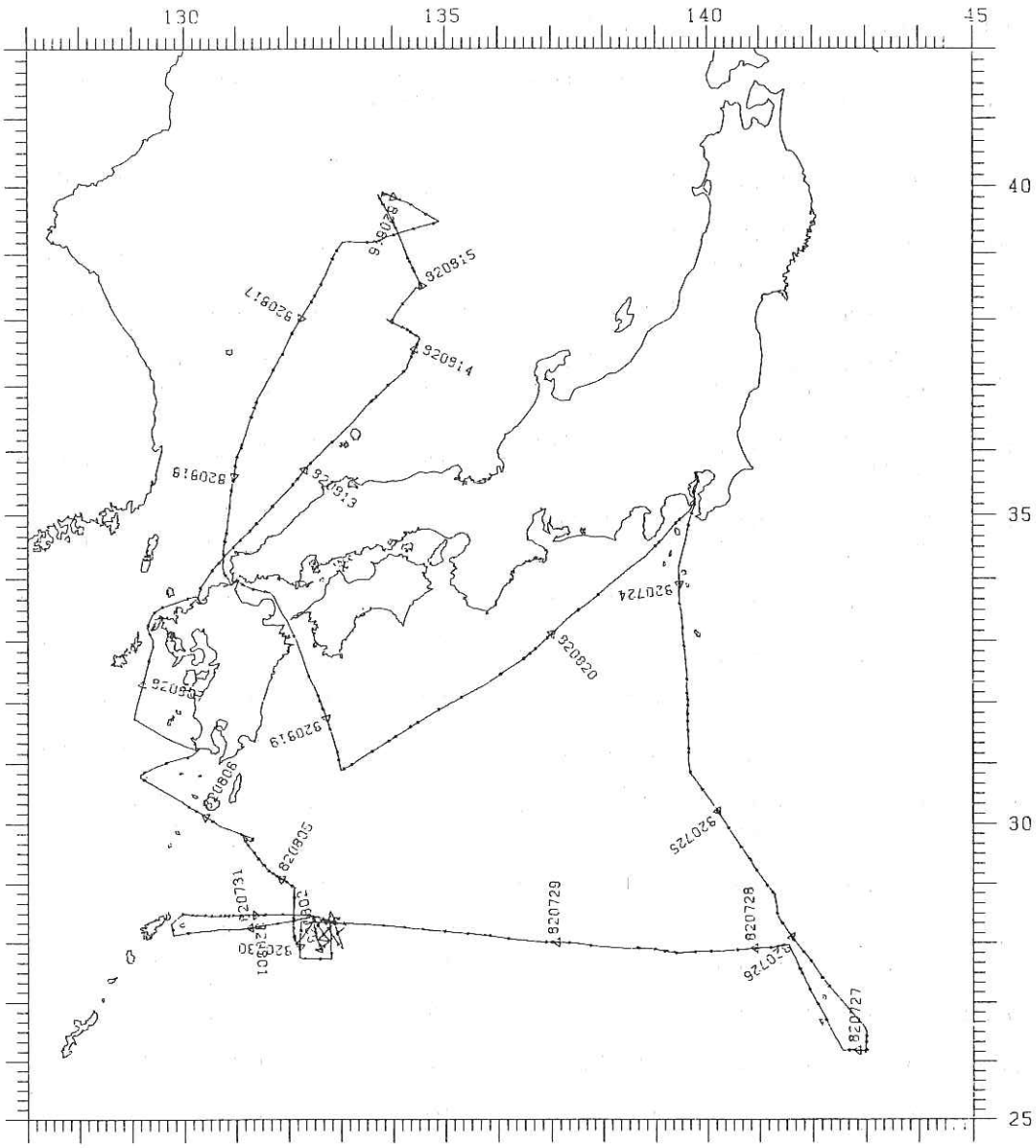

Fig.2-1. Cruise tracks of KH 82-4. Numerical figures indicate positions at 00:00 (Local time) of year-month-day.

3. LIST OF RESEARCH STATIONS IN THE CRUISE KH 82-4

Leg 1 (Tokyo to Fukuoka (Hakata pier))

Site No.	Position Lat. (N)	Long.(E)	Investigation	Water Depth(m)	Date	& Time	Remarks
1	28°51.1'	141°14.1'	Piston Coring	4020	July 25	11:42	Hit on Bottom
1(B)	28°50.6	141°15.0	Camera (pop-up)	4010	25	10:18	Start
	28°51.1	141°15.0		4020	25	13:14	on Deck
2	28°29.6	141°20.8	Piston Coring	4100	25	16:44	Hit on Bottom
2(B)	28°28.5	141°21.0	Heat Flow	4100	25	19:24	Hit no.1
	28°27.9	141°20.7		4100	25	20:14	Hit no.2
3	26°08.8	142°59.2	Dredge Haul	2740	26	14:27	on Bottom
	26°11.1	143°01.3		1970	26	17:45	final on Bottom
4	26°10.8	143°02.9	Dredge Haul	1620	26	19:11	on Bottom
	26°12.2	143°03.8		1150	26	22:30	final on Bottom
5	27°58.2	142°31.9	Piston Coring	4160	27	15:26	Hit on Bottom
6	27°56.5	142°19.2	Piston Coring	4100	27	18:45	Hit on Bottom
6(B)	27°55.6	142°18.5	Heat Flow	4100	27	21:03	Hit on Bottom
7	27°49.4	139°28.9	Piston Coring	3230	28	09:30	Hit on Bottom
7(B)	27°49.6	139°29.1	Camera (pop-up)	3330	28	08:29	Start
	27°49.7	139°29.0		3330	28	11:00	on Deck
8	28°23.1	132°45.9	Piston Coring	2630	30	10:15	Hit on Bottom
8(B)	28°23.7	132°46.3	Camera (pop-up)	2630	30	09:12	Start
	28°23.2	132°46.1		2650	30	11:32	on Deck
OBS-1	28°20.9	132°52.5	OBS (1)	2610	30	14:14	Set
OBS-2	28°03.2	132°33.2	OBS (2)	2930	30	16:20	Set
OBS-3	28°27.3	132°27.6	OBS (3)	3045	30	18:59	Set

Site No.	Position Lat.(N)	Long.(E)	Investigation	Water Depth(m)	Date & Time		Remarks
					Aug		
SB-1	28°24.5'	132°39.0'	Sonobuoy	2955	02	07:10	Set
	28°23.4	132°38.6		2810	02	20:33	on Deck
SB-2	28°21.8	132°49.2	Sonobuoy	2630	02	10:57	Set
	28°21.1	132°48.5		2650	02	17:53	on Deck
9	27°55.1	133°00.7	Dredge Haul	1580	03	00:36	on Bottom
	27°55.5	133°00.9		1400	03	01:49	final on Bottom
OBS-1	28°20.8	132°52.3	OBS-1	2640	03	07:06	on Deck
OBS-2	28°02.7	132°33.2	OBS-2	2940	03	11:02	on Deck
OBS-3	28°27.0	132°27.3	OBS-3	3040	03	15:07	on Deck
10	28°26.3	132°27.7	Heat Flow	3040	03	16:28	Hit no.1
	28°26.0	132°27.7		3040	03	16:59	Hit no.2
	28°25.8	132°27.7		3050	03	17:27	Hit no.3
10(B)	28°25.5	132°28.1	Camera	3050	03	18:42	Start
	28°24.3	132°28.5		3050	03	21:10	on Deck
11	27°59.4	132°09.7	Dredge Haul	2770	04	00:43	on Bottom
	28°00.1	132°07.7		2600	04	03:24	final on Bottom
12	28°08.3	132°07.3	Dredge Haul	2040	04	05:49	on Bottom
	28°07.6	132°07.1		1920	04	07:03	final on Bottom
13	29°45.1	131°17.9	Heat Flow	3400	05	16:57	Hit no.1
	29°45.0	131°18.2				17:29	Hit no.2
	29°45.4	131°18.3				18:31	Hit no.3
14	31°44.4	129°02.1	Piston Coring (12m)	740	06	21:15	Hit on Bottom

Port of Call at Hakata pier, Fukuoka

August 07 to August 12

Leg 2 Sea of Japan (Fukuoka to Tokyo)

Site No.	Position Lat.(N)	Long.(E)	Investigation	Water Depth	Date & Time		Remarks
					Aug.		
15	36°44.3'	133°33.6'	Piston Coring	1090	13	10:08	Hit on Bottom
16	37°00.2	133°54.2	Piston Coring	1745	13	13:13	Hit on Bottom
17	37°15.5	134°16.2	Piston Coring	2450	13	16:40	Hit on Bottom
17(B)	37°15.4	134°15.6	Heat Flow	2445	13	18:46	Hit no.1
	37°15.5	134°15.4		2430	13	19:13	Hit no.2
18	37°57.9	133°58.7	Piston Coring	640	14	10:47	Hit on Bottom
19	38°29.1	134°34.6	Piston Coring	3010	14	16:32	Hit on Bottom
19(B)	38°28.5	134°35.2	Heat Flow	3020	14	18:33	Hit no.1
	38°28.4	134°35.4		3010	14	19;32	Hit no.2
19(C)	38°28.1	134°35.9	Camera	3010	14	20:56	Start
	38°27.2	134°36.4	(wired)	3010	14	23:32	on Deck
20	39°49.3	133°45.9	Dredge Haul	674	15	16:21	on Bottom
	39°50.5	133°46.2		580	15	18:36	final on Bottom
21	39°53.2	132°49.8	Dredge Haul	440	15	22:15	on Bottom
	39°53.6	132°49.5		470	15	22:25	final on Bottom
22	39°13.4	133°46.1	Piston Coring	2110	16	12:12	Hit on Bottom
23	36°48.4	131°24.9	Piston Coring	2070	17	09:43	Hit on Bottom
24	36°25.6	131°15.3	Piston Coring	2020	17	13:20	Hit on Bottom
25	36°02.7	131°05.6	Piston Coring	1570	17	16.35	Hit on Bottom
25(A)	36°02.4	131°04.7	Heat Flow	1550	17	18:07	Hit no.1
	36°01.8	131°04.6		1550	17	19:04	Hit no.2
25(B)	36°01.6	131°04.5	Camera (wired)	1520	17	20:04	Start
	36°01.4	131°03.7		1525	17	21:37	on Deck

4. GRAVIMETRY AND BATHYMETRY

T. MATSUMOTO

Gravimetry :

Gravity measurement at sea was carried out during the whole cruise by use of the equipment described below.

Gravity meter system : T.S.S.G.

Gravity meter : Model Z-68-7-14 (string type)

Vertical gyro : Model 82-A (a pair of single freedom gyros)

Data processing system : Model 76-1 (0.05 sec. sampling rate)

Fig. 4-1 shows some examples of profiles of gravity anomalies and topography along the track where the gravity values are obtained in desirable accuracy. Ship position was fixed by use of both Loran C and NNSS. NNSS system was out of order from Aug.06 1130 to Aug.07 0220 due to the wrong update fixing. In this period position fixing was conducted on the basis of Loran C and dead reckoning.

The type of the vertical gyro was renewed from the previous KH-82-3 Cruise, and the observation also had the role of the second trial of the new gravity meter system.

Bathymetry :

Bathymetry was carried out by use of PDR during the whole cruise. Bathymetric data of every 5 minutes were digitized from the topographic profiles on the record chart, and the correction of sound velocity for these data was made by Matthews'table. Profiles accompanied by magnetic data of the whole cruise are shown in Fig. 6-2. From Jul.31 1800 to Aug.02 0000 and from Aug.15 2300 and Aug. 16 0700 S/N ratio of echo sounder was not large enough due to the bad sea condition, and bathymetric data possibly include errors of several tens of meters.

Bathymetric charts with a scale of 1/250,000 and contours of 200 m were compiled for Ogasawara fore-arc region and Amami Plateau, which are attached with this report in a separate foldout envelope.

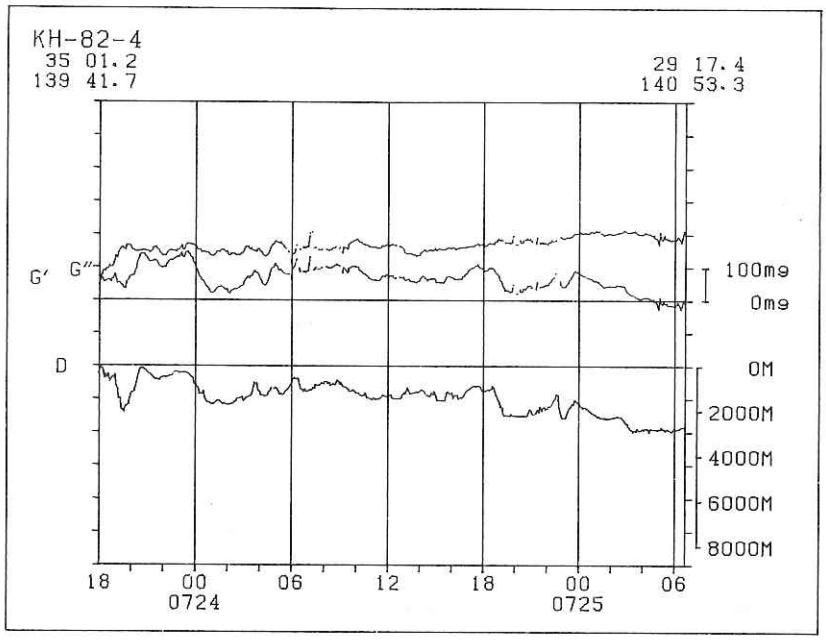

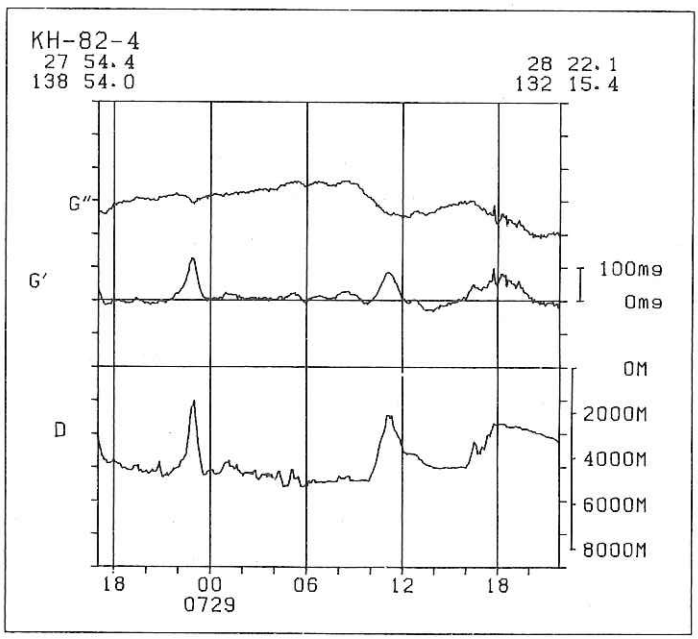

Fig. 4-1. Two examples of gravity and topographical profiles obtained in this cruise. D indicates water depth, G' free air anomaly and G" Bouguer anomaly.

5. SURFACE CURRENTS BASED ON NNSS

T. MATSUMOTO

Apparent surface currents can be obtained by NNSS system, on the basis of the difference between the position fixed by the Doppler counts and that calculated by dead reckoning by use of the output data of gyrocompass and electro-magnetic log. Fig. 5-1 shows the surface current data of the region of Kuroshio obtained by the method mentioned above. Fig. 5-2 shows currents observed actually in the same period. These figures show that current speed and direction based on NNSS have fairly good agreement with those directly observed, showing that position fixing by NNSS is available for the method of monitoring of ocean currents.

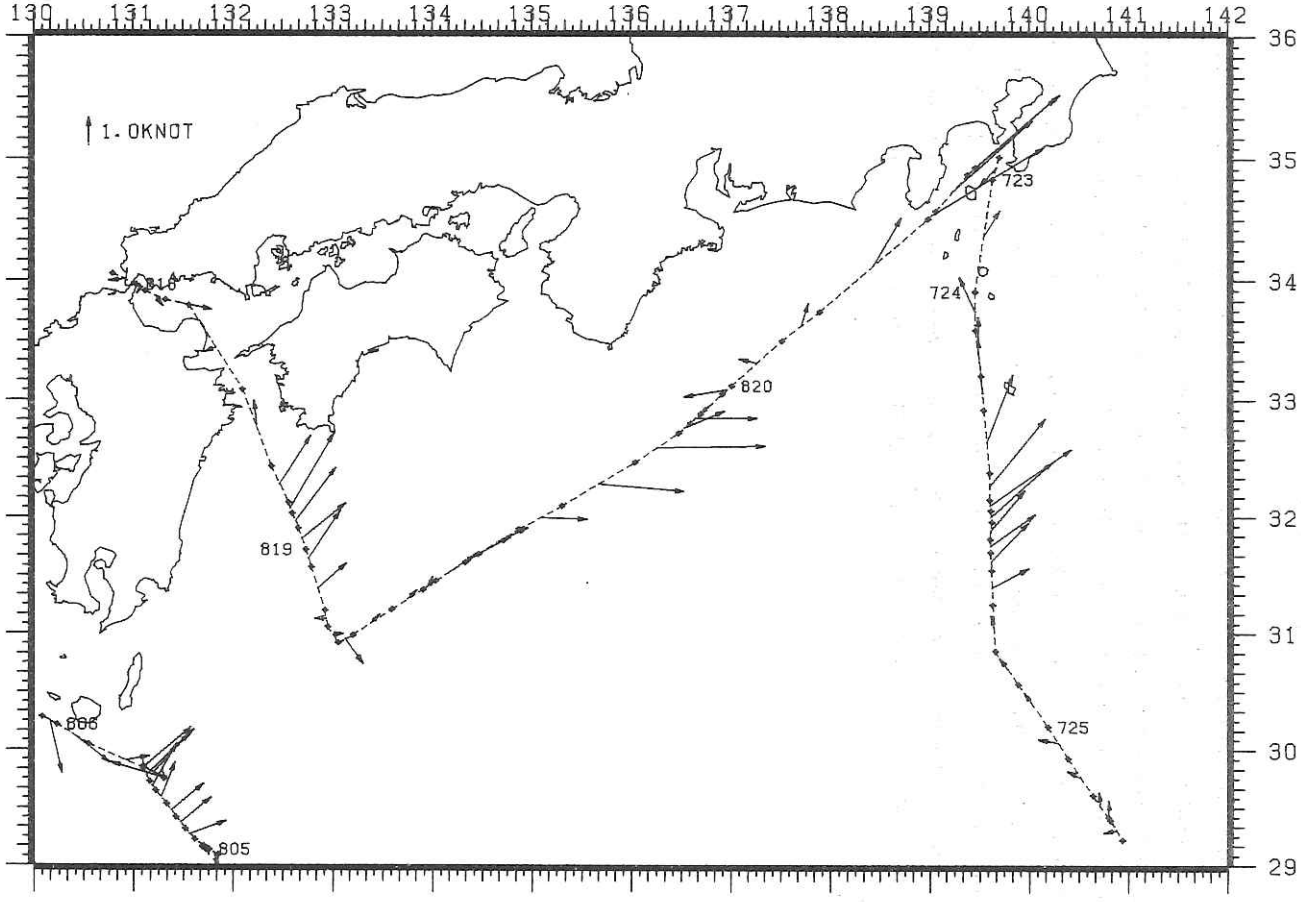

Fig. 5-1. Velocity and direction of surface currents based on NNSS position fixing in this cruise.

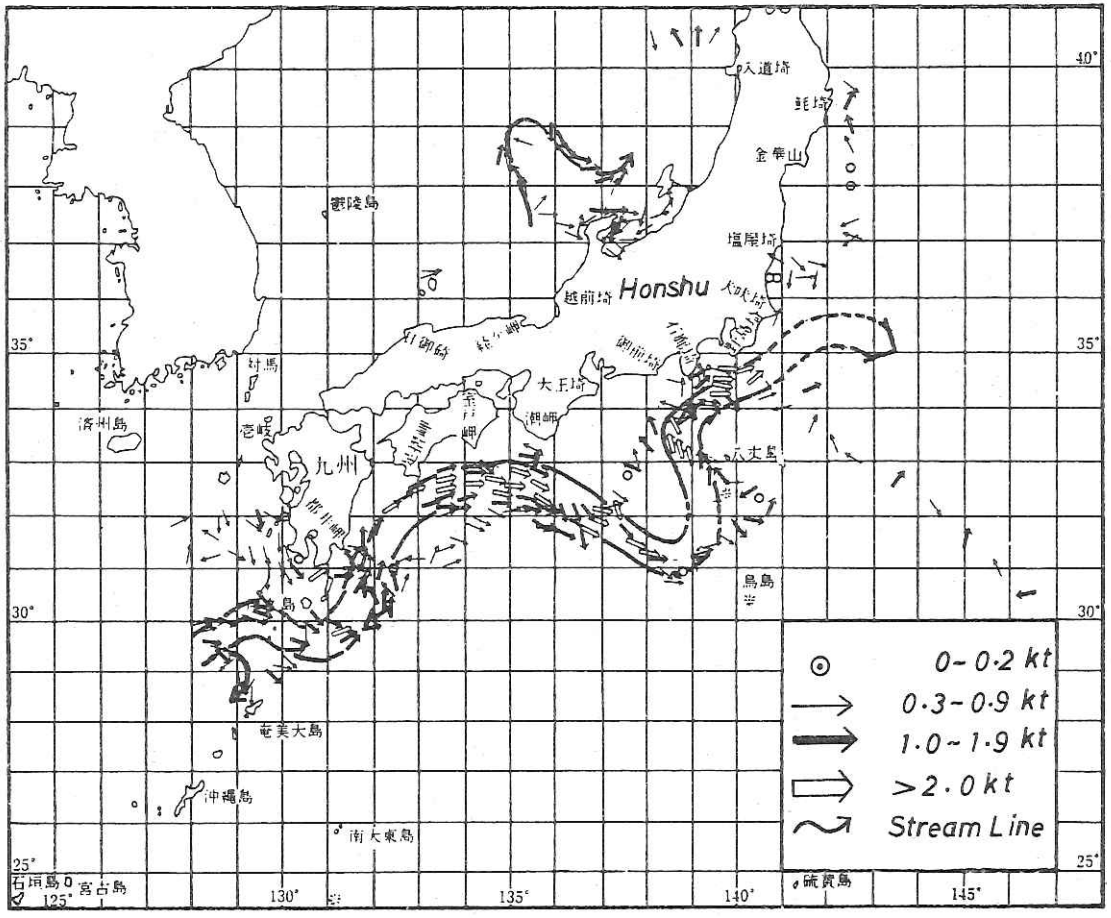

Fig. 5-2. Observed surface currents from Aug.06 to Aug.19---from Kaiyo-Sokuho (Prompt Report of the Sea Conditions) issued by the Hydrographic Department of Maritime Safety Agency, Japan.

6. MEASUREMENT OF THE THREE COMPONENTS OF GEOMAGNETIC FIELD

Y. MATSUBAYA and N. ISEZAKI

1. Method of measurement

Geomagnetic total field was measured by a proton precession magnetometer, and three components of the geomagnetic field were measured by the shipboard three components magnetometer (STCM), which we developed. The STCM is a fluxgate type magnetometer. The three sensors (which are assembled rectangular to each other) are hung with an almost frictionless fulcrum, and set on the antirolling tank by the tripod. We also measured the ship's heading direction and rolling, pitching angles by the gyrocompass and the vertical gyroscope, respectively. Data sampling was controlled by the microcomputer and observed values were stored in the minifloppy disk every one minute.

2. Data processing

The values measured by the STCM are not the real three components of the geomagnetic field,because they include the magnetic field induced by the ship's body. So we have to reduce the induced field in order to obtain the real three components of geomagnetic field. Then we assumed that measured three components of the magnetic field were the vector sum of following three magnetic fields, (1) real geomagnetic field, (2) magnetic field caused by the permanent magnetic moments of the ship's body, (3) magnetic field due to the magnetic moments of the ship'd body which were induced by the real geomagnetic field. As the STCM sensors were fixed on the ship, magnetic field of (2) is always the same value. Distribution of the magnetic moments of (3) is thought to be complicated, however the magnetic moments as a whole are in proportion to the real geomagnetic field. So the induced field is thought to be linear to the real geomagnetic field. If we rotate the ship at one point (where the three components of the geomagnetic field are known), and measure the magnetic field, ship's heading direction and rolling, pitching angles, we can obtain the relation between the real geomagnetic field and observed magnetic field.

In this cruise, in order to obtain this relation, rotating observations were carried out at 4 points. Fig.6-1shows the locations of the magnetic profiles and Fig. 6-2 shows the profiles of the magnetic anomalies and water depths.

Because the correction for the list of the ship due to rolling and pitching is not sufficient, on almost all the profiles there are the low amplitude (less than 50 nT) and the short wave length anomlies which will be shown as the difference between cT and pT. However, the measurements were thought to be done with the accuracy less than 25 nT as a whole for the measurement of the ralative change of the three components.

3. Profiles of magnetic anomalies and water depths

In Fig.6-2,, X, Y and Z are the profiles of north, east and vertical components of the geomagnetic field respectively and cT is the profile of the total intensity calculated by X, Y and Z ($cT=\sqrt{X^2+Y^2+Z^2}$) and pT is the total intensity measured by the proton precession magnetometer. If cT and pT are the same, it can be said that three components of the geomagnetic field are obtained correctly. Each magnetic profile is made of the running mean of 7 data. The IGRF-80 fields were subtracted from all data of the profiles.

Profile A-A'

This profile runs along the axis of the Shichito-Iwoto ridge. Because of the bad condition of the proton precession magnetometer, almost a half of the pT is lost and the data around the point "a" on the profile are much disturbed by the short wave length anomalies which were not due to the real geomagnetic field. Large anomaly (about 1000 nT) of the point "a" is thought to be caused by Hachijojima island. Probably Hachijojima island is highly magnetized, that is the geologically young volcano.

Profile A'-A"

This profile runs from Shichito-Iwoto ridge to Ogasawara basin. Though water depth changed largely, magnetic anomalies do not change so much.

Profile B-B'

This profile crosses the Ogasawara ridge and X, Y, X, cT and pT are influenced by this uplift. The difference between cT and pT becomes gradually large. It may be caused by gradual change of the list of the ship. In the method of analysis used in this report, this phenomenon is not sufficiently corrected. Z component anomalies show the clear change corresponding to the ridge but X and Y component anomalies do not, which could mean the structure of the ridge of the area B-B' does not extend north to south.

Profile C-C'

This profile also crosses the Ogasawara ridge. The large anomaly of the point "b" is not the real anomaly. At this point, ship rotated by 360° in a few minutes, and rolling and pitching angles largely changed, so that the anomaly of the point "b" is due to the insufficient correction for the rapid change of heading, rolling and pitching angles. Both profiles B-B' and C-C' show that the anomalies are not so large as expected from the specific height of the Ogasawara ridge, which could mean that the ridge is not made of oceanic nor young basic rocks.

Profile D-D'

This profile crosses the Shichito-Iwoto ridge. There seems to be no clear correlation between bottom topography and the magnetic anomaly. The west side of the profile shows the clear linear structure of the magnetic source extending north to south, because there are almost no anomalies in X component but there are rather large anomalies in Y and Z components.

Profile E-E'

This profile runs from east to west in the southern part of the Shikoku basin. The uplift of the point "c", "d" and "e" are the Kinan sea mountains, Kyushu-Palau ridge and Amami rise respectively. Magnetic anomalies caused by these uplift are not so large. Between the point"e"and "d", anomaly amplitude of Y and Z are clearly larger than X. This phenomenon is thought to be caused by the linear magnetic source whose trend is north to south.

Profile F-F'

This profile runs from east of Amamioshima island to Amami rise. Anomaly of the point "f" is due to the rapid change of ship's heading direction. Both profiles E-E' and F-F' show that the anomalies are very calm on the Amami rise.

Profile G-G'

There are almost no anomalies in total intensity, however anomaly of X and Z are very large on the slope of the continental side of the Ryukyu trench.

Profile H-H'

Anomaly of the point "g" is due to Tokara island, and the anomaly of the point "h" is caused by the rapid change of the ship's heading direction.

Profile I-I'

Though the topography is very smooth, there are large magnetic anomalies. This is thought to be caused by the rough topography of the basement. Anomaly of the point "i" is thought to be caused by the basement topography which elongates north to south, because there are no anomaly at this point in X component.

Profile J-J' and J'-J"

In profile J-J', anomalies seen in the left part of X and Y component are due to the small change of the ship's heading direction, so there might be almost no magnetic anomalies in J-J'. The anomaly of the point "j" in profile J'-J" is caused by the rapid change of the ship's heading direction.

Profile K-K'

This profile crosses the Yamato ridge. There are almost no magnetic anomalies in this area.

Profile L-L'

Because of the rough condition of the sea, heading, rolling and pitching angles changed largely, so there are large noises in X and Y components.

Profile L"-L"

There are large anomalies in Y component compared with other X and Z components.

Profile M-M'

Anomaly of the point "k" is due to the Takeshima island. In the left side of the profile, there are anomalies in X and Y components caused by the rapid change of rolling and pitching angles due to the rough condition of the sea.

Profile N-N'

There are large magnetic anomalies in the south part of this profile. These anomalies are caused by the rough topography of the basement as seen in the profile I-I'.

Profile O-O', O'-O" and O"-O"'

There are no significant magnetic anomalies in the profile O-O'. Profiles O'-O" and O"-O"' run from south-west to north-east in the northern part of Shikoku basin. The gradual decrease of X component seen in the profile O'-O" and in the first part of the profile O"-O"' is thought to be due to the gradual change of rolling angle. As described before, there are north-south trending magnetic lineations, and anomaly amplitude of Y and Z is larger than that of X.

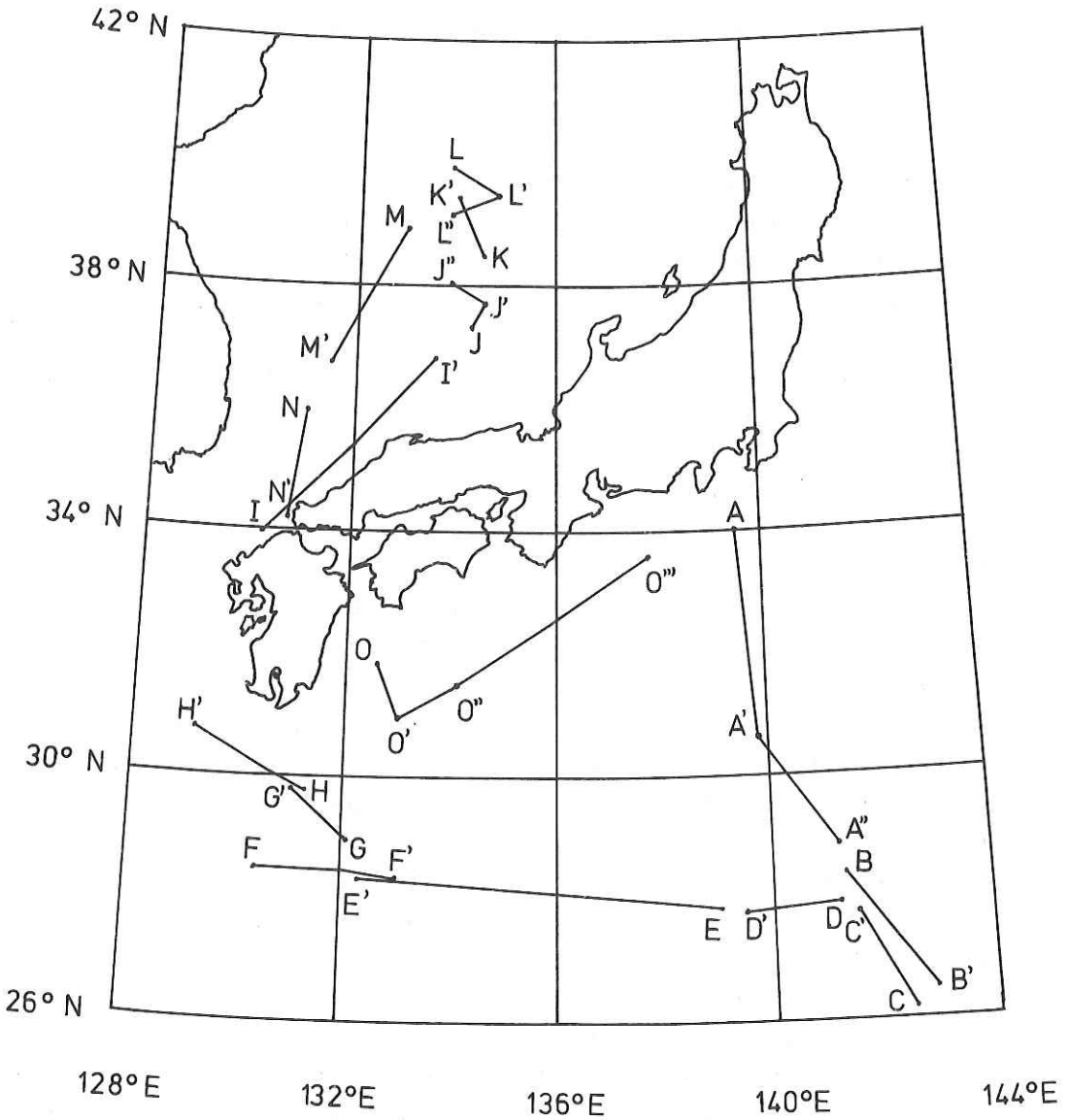

Fig. 6-1. Location of magnetic and bathymetric profiles.

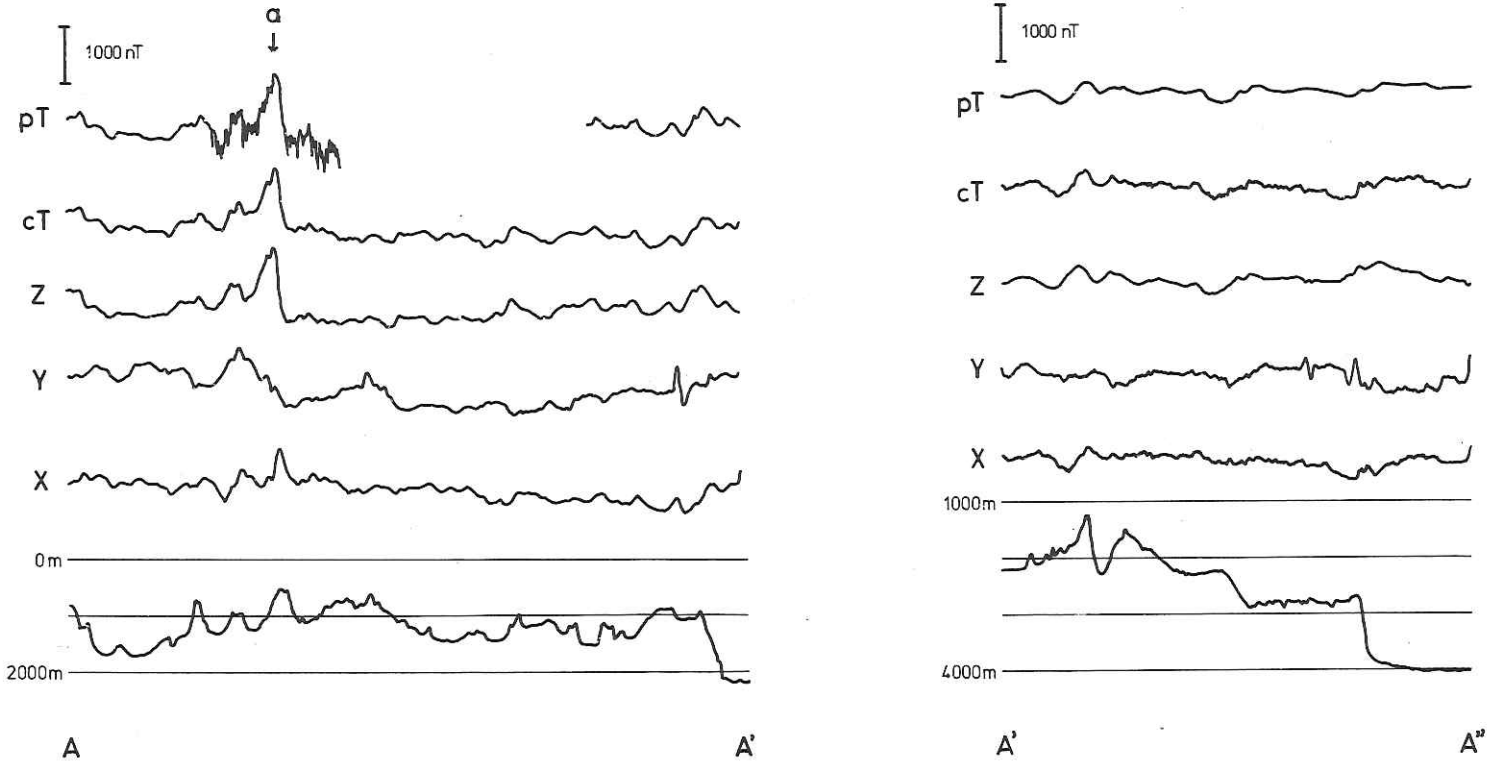

Fig. 6-2. Profiles of magnetic anomalies and water depths.

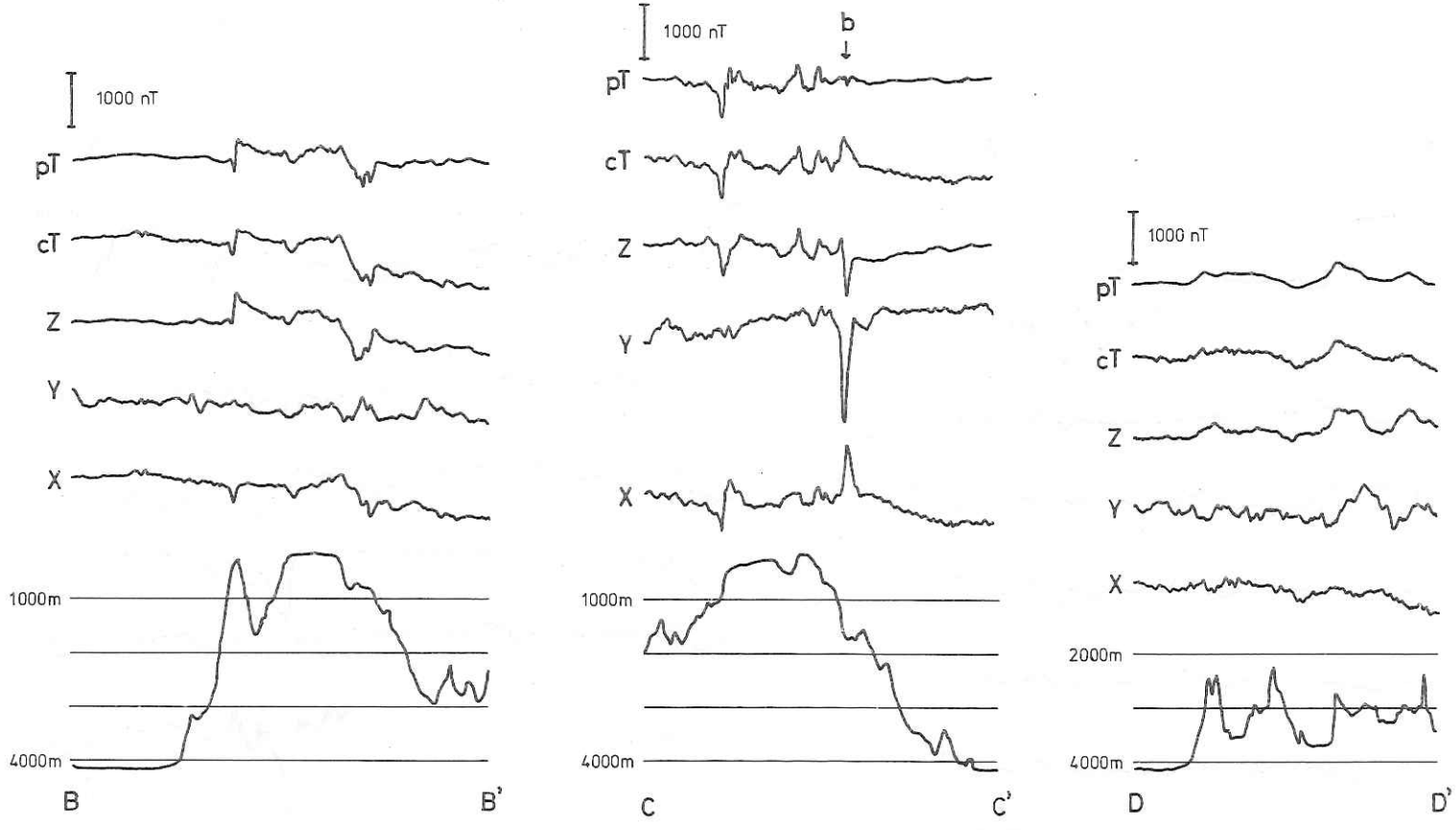

Fig. 6-2. Profiles of magnetic anomalies and water depths.

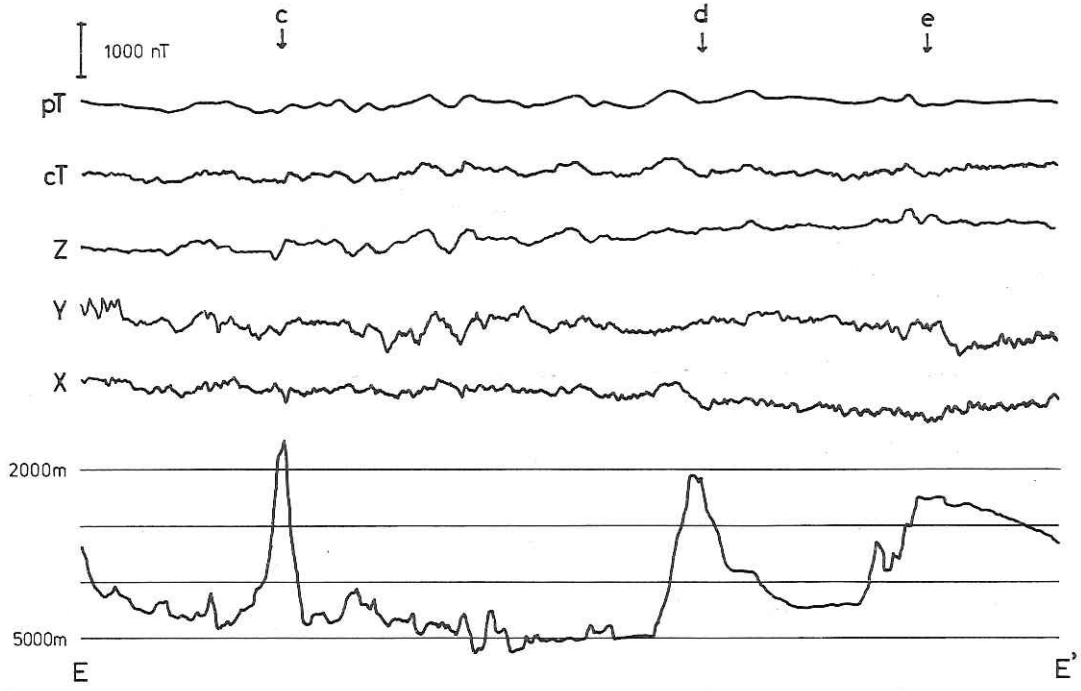

Fig. 6-2. Profiles of magnetic anomalies and water depths.

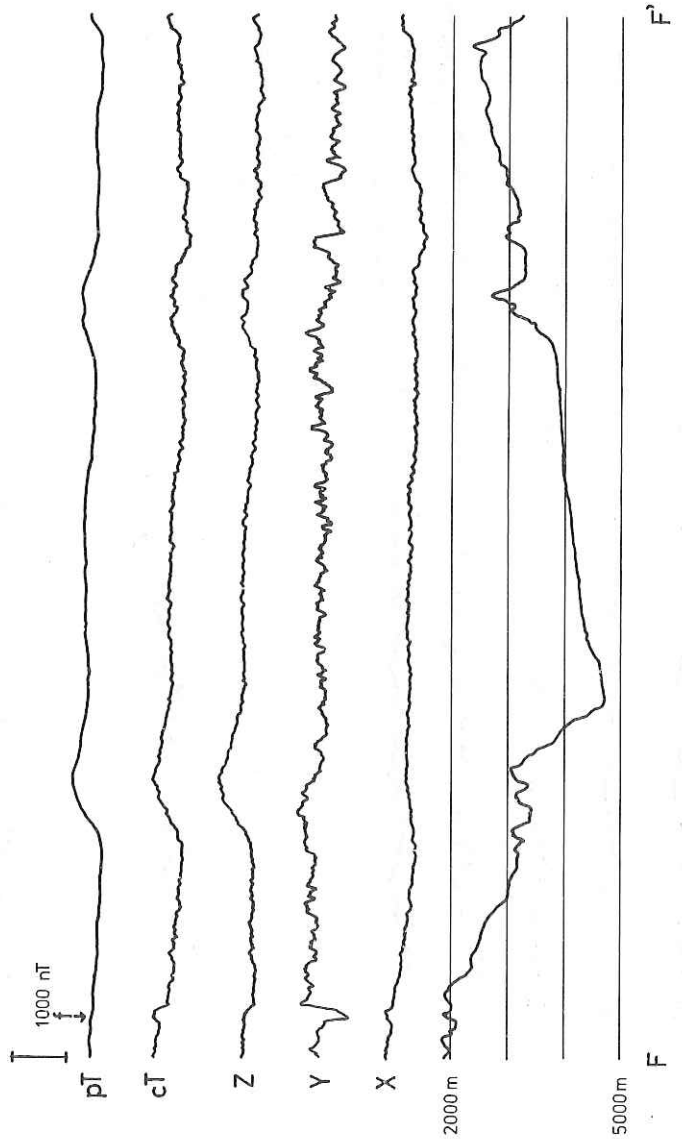

Fig. 6-2. Profiles of magnetic anomalies and water depths.

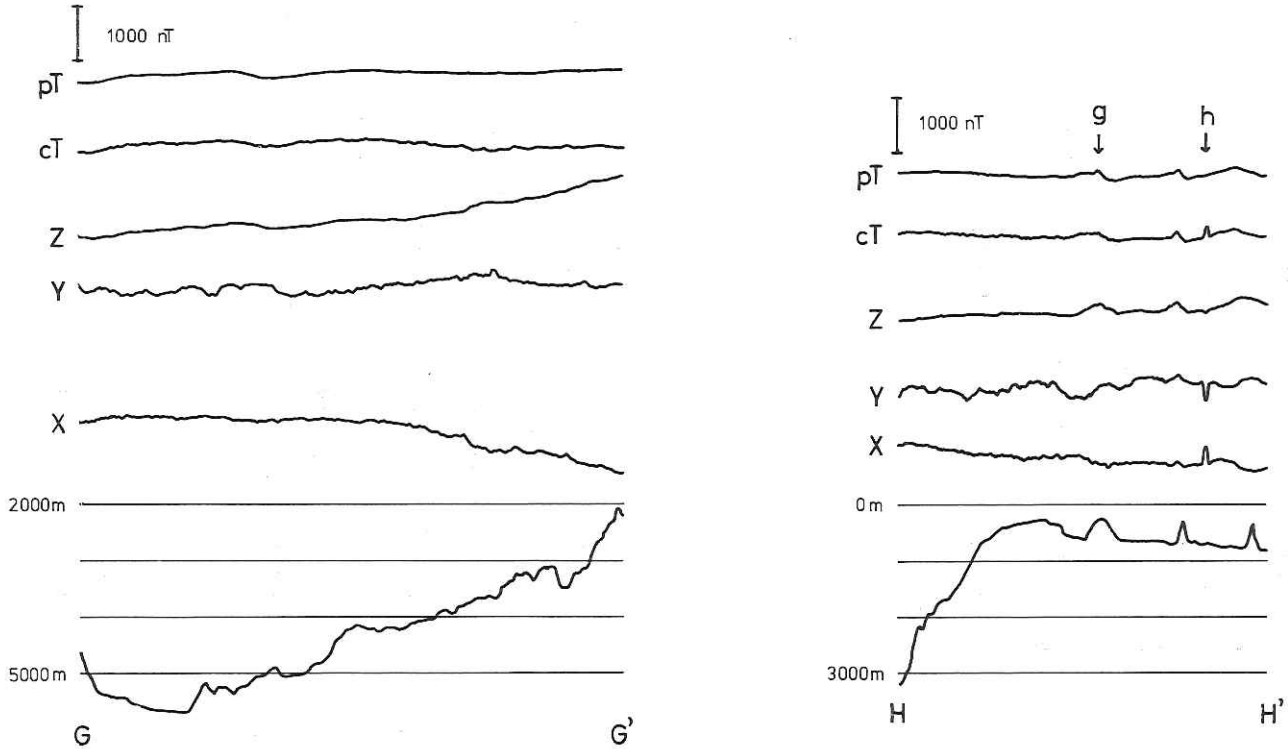

Fig. 6-2. Profiles of magnetic anomalies and water depths.

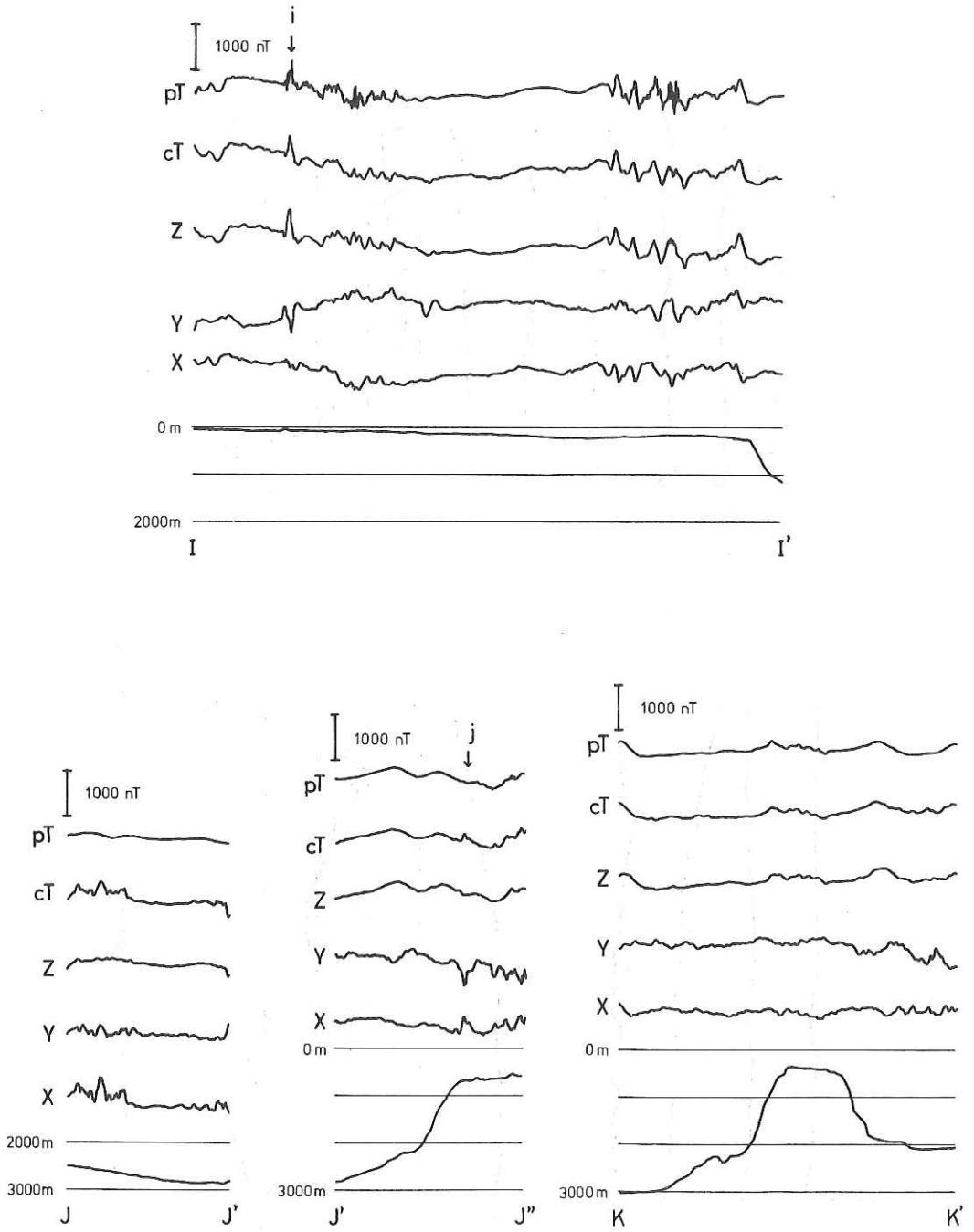

Fig. 6-2. Profiles of magnetic anomalies and water depths.

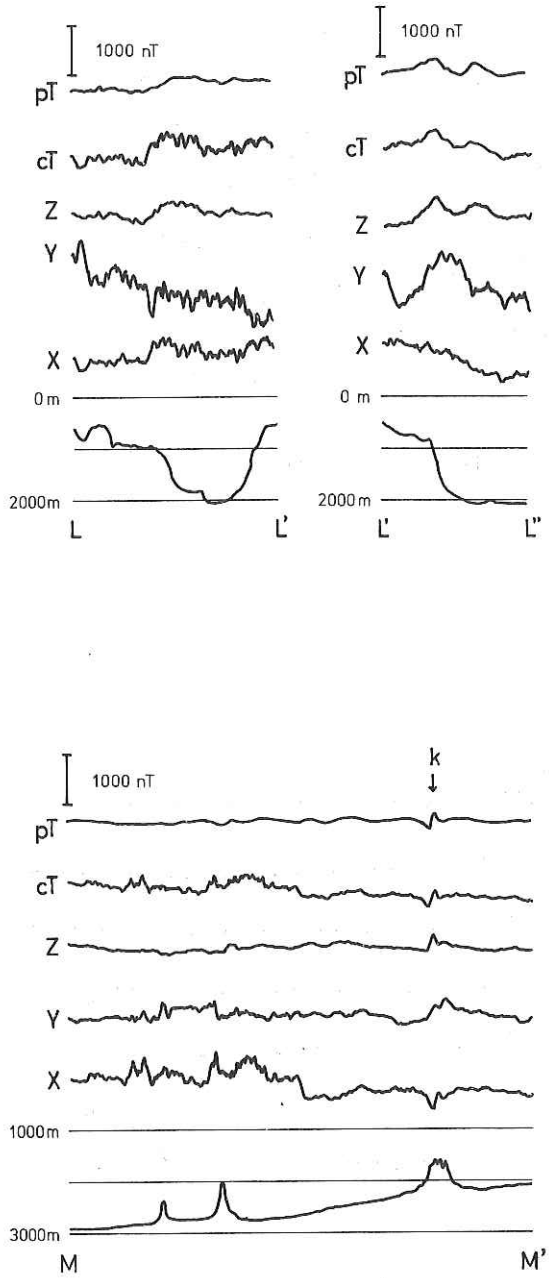

Fig. 6-2. Profiles of magnetic anomalies and water depths.

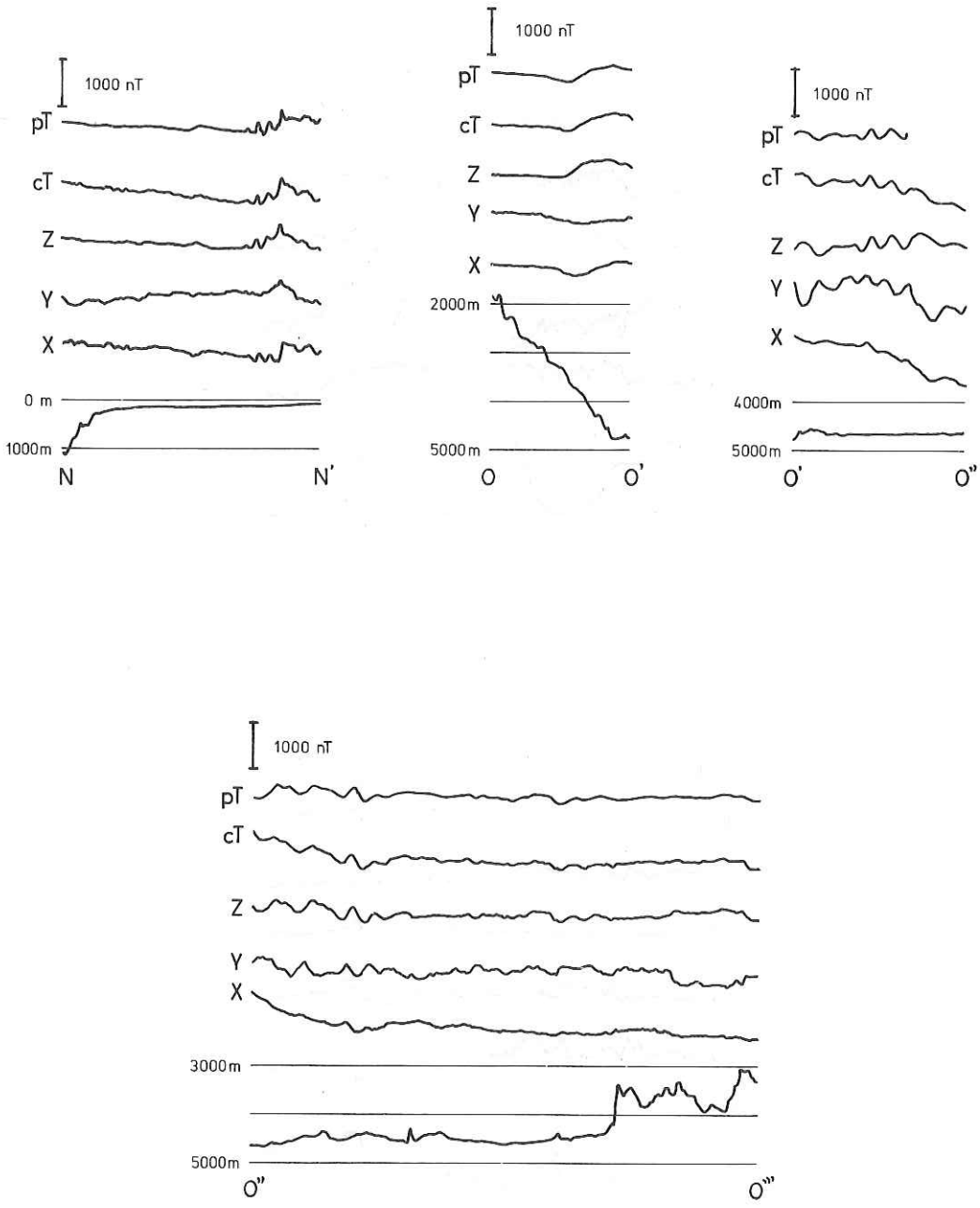

Fig. 6-2. Profiles of magnetic anomalies and water depths.

7. PISTON CORING

7-1. OPERATION LOGS

Date July 25, 1982 Ship Hakuho Maru KH 82-4 Station 1
Latitude 28°51.1'N Longitude 141°14.1'E
Location Ogasawara Trough (north)
Sea calm Weather cloudy
Bottom Topography flat Profiler sediment

Length of Core Pipe 4 m Wall Thickness mm Material stainless steel
ID of Pipe 80 mm Core Head Wt. 400 Kg Trigger Wt. 30 Kg
Length Main Line 12.58m Length Trigger Line14.2m Length Free Fall m
Response at Hit good Response at Pull-out good
Time Lowered 10 h 39 m; Uncorrected Water Depth 4020 m
Time Hit 11 h 42 m; Uncorrected Water Depth 4020 m
Wire Angle at Hit 0 °; Wire-out at Hit 4043 m

Cored Length ≒315 cm Trigger Cored Length 0 cm
Method of Storage vertical storage No. of Pipe filled 1

Date July 25, 1982 Ship Hakuho Maru KH 82-4 Station 2
Latitude 28°29.7'N Longitude 141°20.0'E
Location Ogasawara Trough
Sea calm Weather cloudy to fine
Bottom Topography flat-gentle slope Profiler sediment cover

Length of Core Pipe 4 m Wall Thickness mm Material stainless steel
ID of Pipe 80 mm Core Head Wt. 400 kg Trigger Wt. 30 kg
Length Main Line 12.58m Length Trigger Line14.2m Length Free Fall m
Response at Hit good Response at Pull-out unclear
Time Lowered 15 h 34 m; Uncorrected Water Depth 4110 m
Time Hit 16 h 44 m; Uncorrected Water Depth 4100 m
Wire Angle at Hit 0 °; Wire-out at Hit 4118 m

Cored Length 220 cm Trigger Cored Length cm
Method of Storage No. of Pipe Filled 1

Date July 27, 1982 Ship Hakuho Maru KH 82-4 Station 5
Latitude 27°58.2'N Longitude 142°31.9'E
Location Ogasawara Trough
Sea calm, low swell Weather clear 6m/s, 78°E
Bottom Topography flat Profiler sediment cover

Length of Core Pipe 4 m Wall Thickness mm Material stainless steel
ID of Pipe 80 mm Core Head Wt. 400 Kg Trigger Wt. 30 Kg
Length Main Line m Length Trigger Line m Length Free Fall m
Response at Hit good Response at Pull-out unclear
Time Lowered 14 h 12 m; Uncorrected Water Depth 4160 m
Time Hit 14 h 25 m; Uncorrected Water Depth 4160 m
Wire Angle at Hit 0 °; Wire-out at Hit 4166 m

Cored Length 115 cm Trigger Cored Length 50 cm
Method of Storage No. of Pipe filled 1
Length of Cores in Pipe 1. cm, 2. cm, 3. cm, 4. cm,
5. cm, 6. cm.
No. of Cubic Samples for Paleomagnetism (No. No.)

Date July 27, 1982 Ship Hakuho Maru KH 82-4 Station 6
Latitude 27°56.5'N Longitude 142°19.2'E
Location Ogasawara Trough west
Sea calm, low swell Weather breeze 6m/s, N75°E
Bottom Topography west of 75m cliff Profiler rugged, thin soft sediment
Length of Core Pipe 4 m Wall Thickness mm Material stainless steel
ID of Pipe 80 mm Core Head Wt. 400 kg Trigger Wt. 30 kg
Length Main Line m Length Trigger Line m Length Free Fall m
Response at Hit Response at Pull-out
Time Lowered 17 h 38 m; Uncorrected Water Depth 4105 m
Time Hit 18 h 45 m; Uncorrected Water Depth 4100 m
Wire Angle at Hit 0 °; Wire-out at Hit 4129 m

Cored Length 365 cm Trigger Cored Length cm
Method of Storage No. of Pipe Filled 1
Length of Core in Pipe 1. cm, 2. cm, 3. cm, 4. cm
5. cm, 6. cm.
No. of Cubic Samples for Paleomagnetism (No. No.)

Date July 28, 1982 Ship Hakuho Maru KH 82-4 Station 7
Latitude 27°49.4'N Longitude 139°28.9'E
Location west of Iwojima ridge
Sea calm Weather partly cloudy
Bottom Topography rugged Profiler

Length of Core Pipe 4 m Wall Thickness mm Material stainless steel
ID of Pipe 80 mm Core Head Wt. 400 Kg Trigger Wt. 30 Kg
Length Main Line m Length Trigger Line m Length Free Fall m
Response at Hit good Response at Pull-out good
Time Lowered 08 h 37 m; Uncorrected Water Depth 3230 m
Time Hit 09 h 30 m; Uncorrected Water Depth 3220 m
Wire Angle at Hit 0 °; Wire-out at Hit 3247 m

Cored Length 310 cm Trigger Cored Length cm
Method of Storage No. of Pipe filled 1
Length of Cores in Pipe 1. cm, 2. cm, 3. cm, 4. cm,
5. cm, 6. cm.
No. of Cubic Samples for Paleomagnetism (No. No.)

Date July 30, 1982 Ship Hakuho Maru KH 82-4 Station 8
Latitude 28°23.1'N Longitude 132°45.9'E
Location Amami plateau NE
Sea large swell-Typhoon 10 nearby Weather cloudy-partly clear, 8m/s N43°E
Bottom Topography NE of Amami crest, N of small high Profiler sediment cover recognized
Length of Core Pipe 12 m Wall Thickness 7.5 mm Material Al
ID of Pipe 65 mm Core Head Wt. 550 kg Trigger Wt. 30 kg
Length Main Line 20 m Length Trigger Line 22 m Length Free Fall 8 m
Response at Hit clear Response at Pull-out strong
Time Lowered 09 h 22 m; Uncorrected Water Depth 2630 m
Time Hit 10 h 15 m; Uncorrected Water Depth 2630 m
Wire Angle at Hit 0 °; Wire-out at Hit 2635 m

Cored Length 754.5 cm Trigger Cored Length cm
Method of Storage 2m container No. of Pipe Filled 6
Length of Core in Pipe 1. 153 cm, 2. 150.5 cm, 3. 180 cm, 4. 483.5 cm
5. 175 cm, 6. 96 cm.
No. of Cubic Samples for Paleomagnetism 329 (No. 12001 - No. 12329)

Date Aug. 06, 1982 Ship Hakuho Maru KH 82-4 Station 14
Latitude 31°44.4'N Longitude 129°02.1'E
Location east of Koshikijima Islands
Sea calm Weather clear, partly cloudy
Bottom Topography flat, gentle slope Profiler No. reflector ? in PDR
Length of Core Pipe 12 m Wall Thickness 7.5 mm Material Al
ID of Pipe 65 mm Core Head Wt. 550 Kg Trigger Wt. 30 Kg
Length Main Line 20 m Length Trigger Line 22 m Length Free Fall 8 m
Response at Hit clear Response at Pull-out very clear
Time Lowered 20 h 56 m; Uncorrected Water Depth 740 m
Time Hit 21 h 15 m; Uncorrected Water Depth 740 m
Wire Angle at Hit 0 °; Wire-out at Hit 723 m

Cored Length 1075.5 cm Trigger Cored Length cm
Method of Storage 2m container No. of Pipe filled 7
Length of Cores in Pipe 1. 33 cm, 2. 189 cm, 3. 194 cm, 4. 188 cm,
5. 199 cm, 6. 190 cm. 7. 88.5 cm.
No. of Cubic Samples for Paleomagnetism 477 (No. 12401 -No. 12877)

Date Aug. 13, 1982 Ship Hakuho Maru KH 82-4 Station 15
Latitude 36°44.3'N Longitude 133°33.6'E
Location slope of Yamato basin off Oki Islands
Sea calm Weather clear, partly cloudy
Bottom Topography slope, slump deposit nearly but not here? Profiler no clear reflector in 3.5 KHz record
Length of Core Pipe 12 m Wall Thickness 7.5 mm Material Al
ID of Pipe 65 mm Core Head Wt. 550kg Trigger Wt. 30 kg
Length Main Line 20 m Length Trigger Line 22 m Length Free Fall 8 m
Response at Hit clear Response at Pull-out clear
Time Lowered 09 h 43 m; Uncorrected Water Depth 1070 m
Time Hit 10 h 07 m; Uncorrected Water Depth 1095 m
Wire Angle at Hit 0 °; Wire-out at Hit 1051 m

Cored Length 1054 cm Trigger Cored Length cm
Method of Storage 2m container No. of Pipe Filled 6
Length of Core in Pipe 1. 191 cm, 2. 189 cm, 3. 193 cm, 4. 197 cm
5. 199 cm, 6. 85 cm.
No. of Cubic Samples for Paleomagnetism 472 (No. 12901 -No. 13372)

Date Aug. 13, 1982 Ship Hakuho Maru KH 82-4 Station 16
Latitude 37°00.2'N Longitude 133°54.2'E
Location down-slope off Oki Islands, Yamato basin
Sea calm, very low swell Weather cloudy 2m/s breeze N150°E
Bottom Topography slope-down Profiler thick sed layer in 3.5 KHz
Length of Core Pipe 12 m Wall Thickness 7.5mm Material Al
ID of Pipe 65 mm Core Head Wt. 550 Kg Trigger Wt. 30 Kg
Length Main Line 20 m Length Trigger Line 22 m Length Free Fall 8 m
Response at Hit clear Response at Pull-out clear
Time Lowered 12 h 38 m; Uncorrected Water Depth 1730 m
Time Hit 13 h 12 m; Uncorrected Water Depth 1740 m
Wire Angle at Hit 0 °; Wire-out at Hit 1695 m

Cored Length 983 cm Trigger Cored Length cm
Method of Storage 2m container No. of Pipe filled 6
Length of Cores in Pipe 1. 104 cm, 2. 195 cm, 3. 191 cm, 4. 196 cm, 5. 175 cm, 6. 122 cm.
No. of Cubic Samples for Paleomagnetism 439 (No. 13401 -No. 13839)

Date Aug. 13, 1982 Ship Hakuho Maru KH 82-4 Station 17
Latitude 37°15.5'N Longitude 134°16.2'E
Location SW edge of Yamato basin down slope off Oki Islands
Sea calm, low swell Weather cloudy 2m/s breeze
Bottom Topography slope Profiler clear layered sediment in 3.5 KHz
Length of Core Pipe 12 m Wall Thickness 7.5mm Material Al
ID of Pipe 65 mm Core Head Wt. 550 kg Trigger Wt. 30 kg
Length Main Line 20 m Length Trigger Line 22 m Length Free Fall 8 m
Response at Hit clear Response at Pull-out no, no tension!
Time Lowered 15 h 58 m; Uncorrected Water Depth 2460 m
Time Hit 16 h 39 m; Uncorrected Water Depth 2455 m
Wire Angle at Hit 0 °; Wire-out at Hit 2397 m

Cored Length 870 cm Trigger Cored Length cm
Method of Storage 2m container No. of Pipe Filled 5
Length of Core in Pipe 1. 191 cm, 2. 198 cm, 3. 198 cm, 4. 195 cm, 5. 88 cm, 6. cm.
No. of Cubic Samples for Paleomagnetism 386 (No. 13901 -No. 14286)

Date Aug. 14, 1982 Ship Hakuho Maru KH 82-4 Station 18
Latitude 37°57.9'N Longitude 133°58.7'E
Location crest of Oki Tai
Sea calm, very low swell Weather cloudy 4m/s breeze
Bottom Topography rugged Profiler pond of sediment

Length of Core Pipe 12 m Wall Thickness 7.5 mm Material Al
ID of Pipe 65 mm Core Head Wt. 550 Kg Trigger Wt. 30 Kg
Length Main Line 20 m Length Trigger Line 22 m Length Free Fall 8 m
Response at Hit Response at Pull-out
Time Lowered 10 h 29 m; Uncorrected Water Depth 630 m
Time Hit 10 h 47 m; Uncorrected Water Depth 640 m
Wire Angle at Hit °; Wire-out at Hit 610 m

Cored Length 0 cm Trigger Cored Length cm
Method of Storage corer lost by broken wire No. of Pipe filled
Length of Cores in Pipe 1. cm, 2. cm, 3. cm, 4. cm,
5. cm, 6. cm.
No. of Cubic Samples for Paleomagnetism (No. No.)

Date Aug. 14, 1982 Ship Hakuho Maru KH 82-4 Station 19
Latitude 38°29.1'N Longitude 134°34.6'E
Location NW of Yamato basin close to NE of Kita-Oki Tai
Sea calm, no swell Weather cloudy 2m/s, N245°E breeze
Bottom Topography flank of Kita-Oki Tai Profiler thick(>100m) sediment cover in 3.5KHz
Length of Core Pipe 12 m Wall Thickness 7.5 mm Material Al
ID of Pipe 65 mm Core Head Wt. 550 kg Trigger Wt. 30 kg
Length Main Line 20 m Length Trigger Line 22 m Length Free Fall 8 m
Response at Hit clear Response at Pull-out second shot after 10m up
Time Lowered 15 h 40 m; Uncorrected Water Depth 3010 m
Time Hit 16 h 32 m; Uncorrected Water Depth 3010 m
Wire Angle at Hit 0 °; Wire-out at Hit 2968 m

Cored Length 867 cm Trigger Cored Length cm
Method of Storage 2m container No. of Pipe Filled 5
Length of Core in Pipe 1. 202 cm, 2. 197 cm, 3. 194 cm, 4. 191 cm
5. 83 cm, 6. cm.
No. of Cubic Samples for Paleomagnetism (No. No.)

Date Aug.16, 1982 Ship Hakuho Maru KH 82-4 Station 22
Latitude 39°13.4'N Longitude 133°46.1'E
Location Kita-Yamato Trough W portion
Sea rough, low swell Weather cloudy 20m/s, N20°E
Bottom Topography flat Profiler thick, irregular

Length of Core Pipe 12 m Wall Thickness 7.5mm Material Al
ID of Pipe 65 mm Core Head Wt. 550Kg Trigger Wt. 30 Kg
Length Main Line 20 m Length Trigger Line 22m Length Free Fall 8 m
Response at Hit Response at Pull-out
Time Lowered 11 h 23 m; Uncorrected Water Depth 2110 m
Time Hit 12 h 12 m; Uncorrected Water Depth m
Wire Angle at Hit 20 °; Wire-out at Hit 2212 m

Cored Length 0 cm Trigger Cored Length cm
Method of Storage No. of Pipe filled
Length of Cores in Pipe 1. cm, 2. cm, 3. cm, 4. cm,
5. cm, 6. cm.
No. of Cubic Samples for Paleomagnetism (No. No.)

Date Aug. 17, 1982 Ship Hakuho Maru KH 82-4 Station 23
Latitude 36°48.4'N Longitude 131°24.9'E
Location Tsushima basin, south of Takeshima
Sea calm, low swell waves Weather clear partly cloudy 9m/s, N20°E
Bottom Topography flat Profiler sediment

Length of Core Pipe 12 m Wall Thickness 7.5 mm Material Al
ID of Pipe 65 mm Core Head Wt. 550 kg Trigger Wt. 30 kg
Length Main Line 20 m Length Trigger Line 22 m Length Free Fall 8 m
Response at Hit clear Response at Pull-out clear
Time Lowered 09 h 07 m; Uncorrected Water Depth 2080 m
Time Hit 09 h 43 m; Uncorrected Water Depth 2080 m
Wire Angle at Hit 0 °; Wire-out at Hit 2029 m

Cored Length 848 cm Trigger Cored Length cm
Method of Storage 2m container No. of Pipe Filled 5
Length of Core in Pipe 1. 165 cm, 2. 198 cm, 3. 197 cm, 4. 195 cm
5. 93 cm, 6. cm.
No. of Cubic Samples for Paleomagnetism 379 (No.14301 -No.14679)

Date Aug. 17, 1982 Ship Hakuho Maru KH 82-4 Station 24
Latitude 36°48.4'N Longitude 131°24.9'E
Location Tsushima basin, S portion
Sea calm Weather clear
Bottom Topography flat Profiler sediment

Length of Core Pipe 12 m Wall Thickness 7.5 mm Material Al
ID of Pipe 65 mm Core Head Wt. 550 Kg Trigger Wt. 30 Kg
Length Main Line 20 m Length Trigger Line 22 m Length Free Fall 8 m
Response at Hit clear Response at Pull-out very clear
Time Lowered 12 h 41 m; Uncorrected Water Depth 2010 m
Time Hit 13 h 20 m; Uncorrected Water Depth 2010 m
Wire Angle at Hit 0 °; Wire-out at Hit 1969 m

Cored Length 820 cm Trigger Cored Length cm
Method of Storage 2m container No. of Pipe filled 5
Length of Cores in Pipe 1. 152 cm, 2. 194 cm, 3. 192 cm, 4. 193 cm,
5. 119 cm, 6. cm.
No. of Cubic Samples for Paleomagnetism No (No. No.)

Date Aug. 17, 1982 Ship Hakuho Maru KH 82-4 Station 25
Latitude 36°25.6'N Longitude 131°15.3'E
Location S margin of Tsushima basin
Sea calm Weather clear 5m/s N wind
Bottom Topography slope Profiler 20m sediment

Length of Core Pipe 12 m Wall Thickness 7.5 mm Material Al
ID of Pipe 65 mm Core Head Wt. 550 kg Trigger Wt. 30 kg
Length Main Line 20 m Length Trigger Line 22 m Length Free Fall 8 m
Response at Hit clear Response at Pull-out clear
Time Lowered 16 h 05 m; Uncorrected Water Depth 1580 m
Time Hit 16 h 35 m; Uncorrected Water Depth 1570 m
Wire Angle at Hit 0°; Wire-out at Hit 1517 m

Cored Length 877 cm Trigger Cored Length cm
Method of Storage 2m container No. of Pipe Filled 6
Length of Core in Pipe 1. 15 cm, 2. 193 cm, 3. 195 cm, 4. 194 cm
5. 190.5 cm, 6. 89.5 cm.
No. of Cubic Samples for Paleomagnetism No (No. No.)

7-2. MEGASCOPIC CORE DESCRIPTION

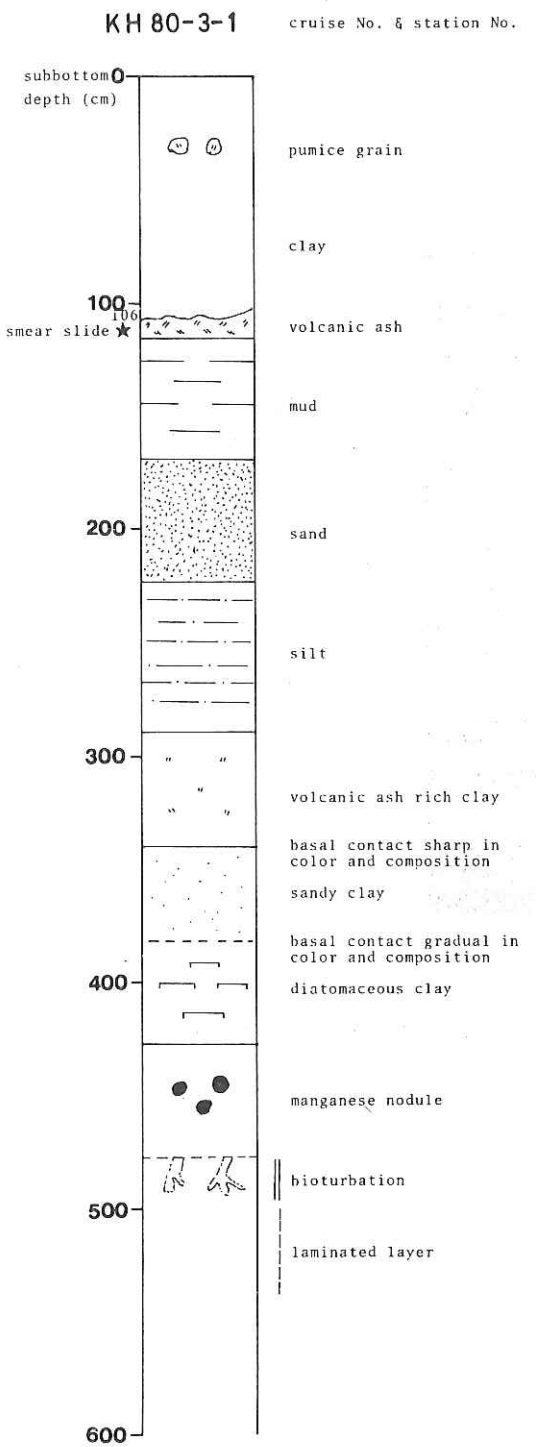

Fig. 7-2-1 Legend of core description.

KH82-4-1

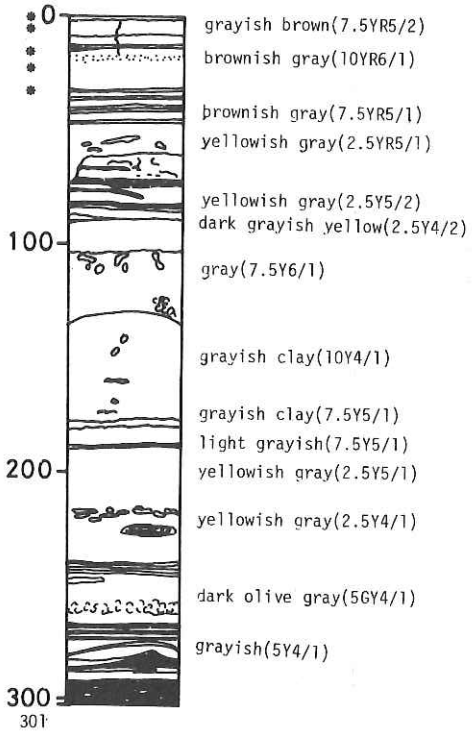

Fig. 7-2-2 Megascopic core description of cores.

KH82-4-2

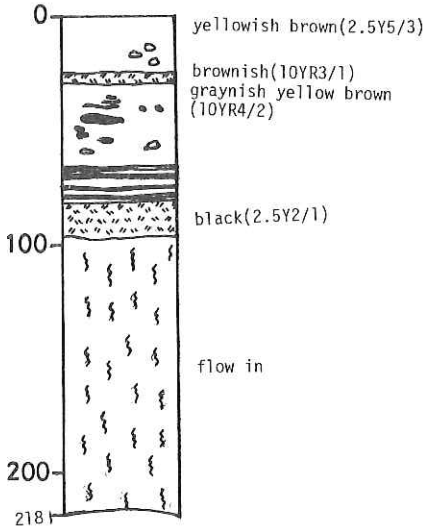
0
100
200
218
yellowish brown(2.5Y5/3)
brownish(10YR3/1)
graynish yellow brown
(10YR4/2)
black(2.5Y2/1)
flow in

KH82-4-5

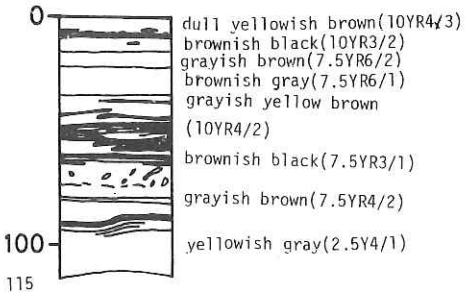
0
100
115
dull yellowish brown(10YR4/3)
brownish black(10YR3/2)
grayish brown(7.5YR6/2)
brownish gray(7.5YR6/1)
grayish yellow brown
(10YR4/2)
brownish black(7.5YR3/1)
grayish brown(7.5YR4/2)
yellowish gray(2.5Y4/1)

KH82-4-6

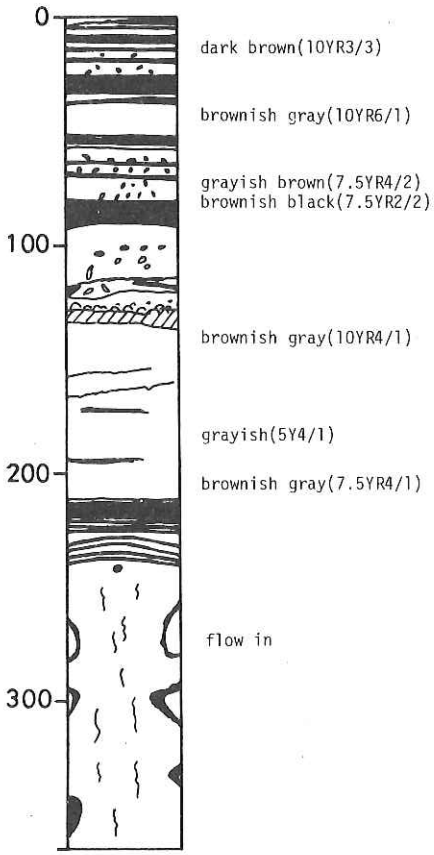
0
100
200
300
dark brown(10YR3/3)
brownish gray(10YR6/1)
grayish brown(7.5YR4/2)
brownish black(7.5YR2/2)
brownish gray(10YR4/1)
grayish(5Y4/1)
brownish gray(7.5YR4/1)
flow in

KH82-4-7

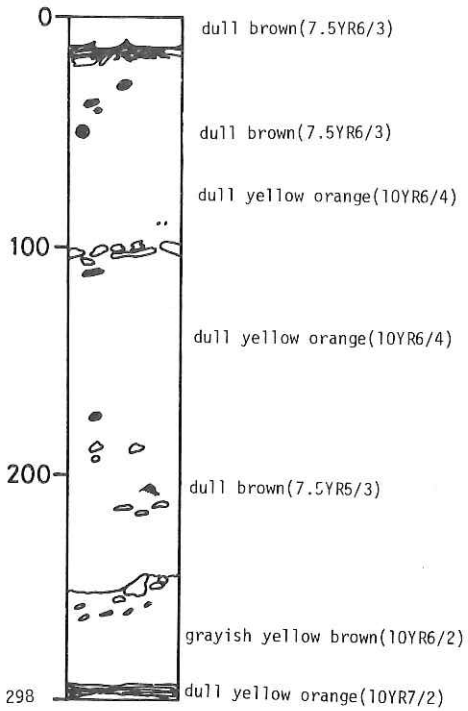
0
100
200
298
dull brown(7.5YR6/3)
dull brown(7.5YR6/3)
dull yellow orange(10YR6/4)
dull yellow orange(10YR6/4)
dull brown(7.5YR5/3)
grayish yellow brown(10YR6/2)
dull yellow orange(10YR7/2)

KH82-4-8

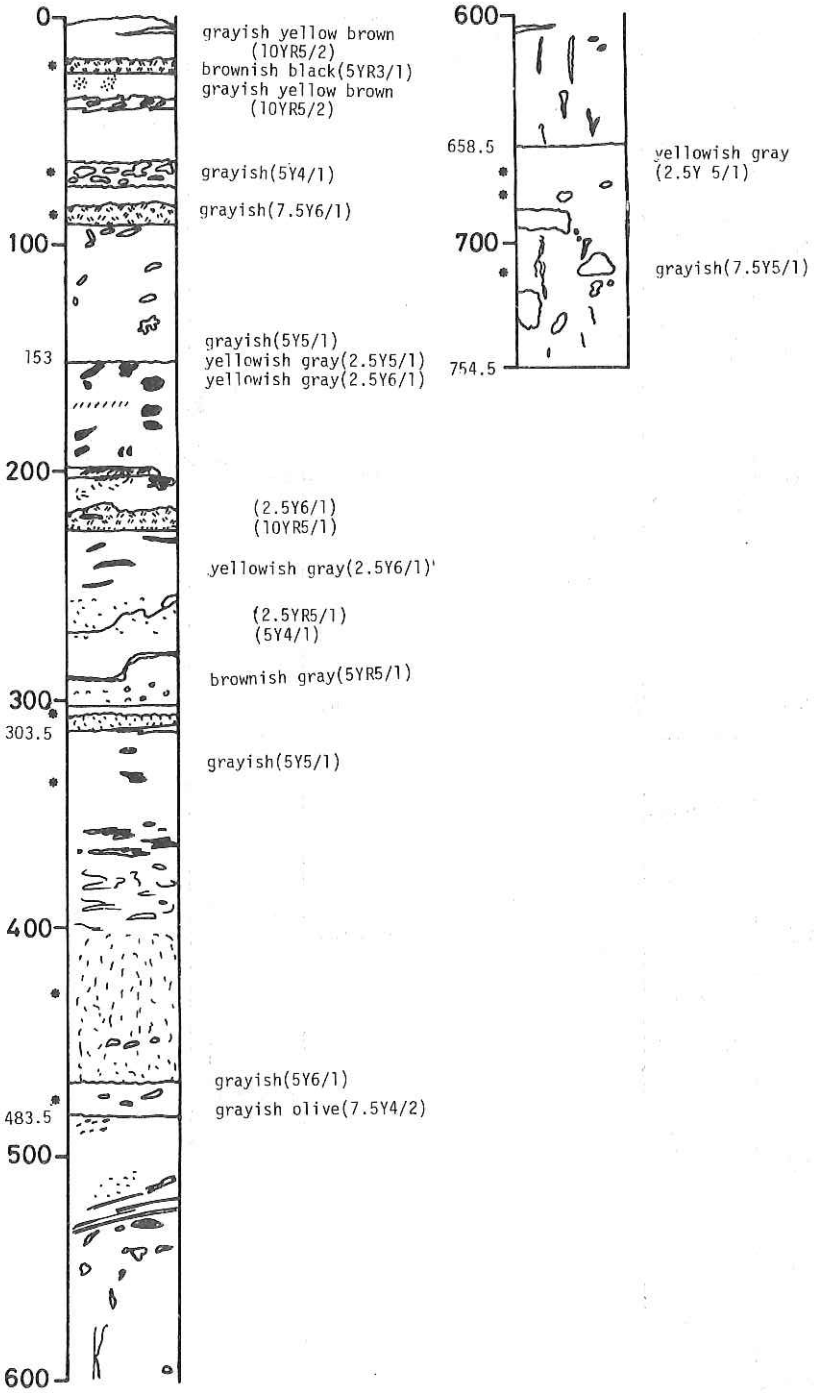
0
100
153
200
300
303.5
400
483.5
500
600
600
658.5
700
754.5
grayish yellow brown (10YR5/2)
brownish black(5YR3/1)
grayish yellow brown (10YR5/2)
grayish(5Y4/1)
grayish(7.5Y6/1)
grayish(5Y5/1)
yellowish gray(2.5Y5/1)
yellowish gray(2.5Y6/1)
(2.5Y6/1)
(10YR5/1)
yellowish gray(2.5Y6/1)
(2.5YR5/1)
(5Y4/1)
brownish gray(5YR5/1)
grayish(5Y5/1)
grayish(5Y6/1)
grayish olive(7.5Y4/2)
yellowish gray (2.5Y 5/1)
grayish(7.5Y5/1)

KH82-4-14

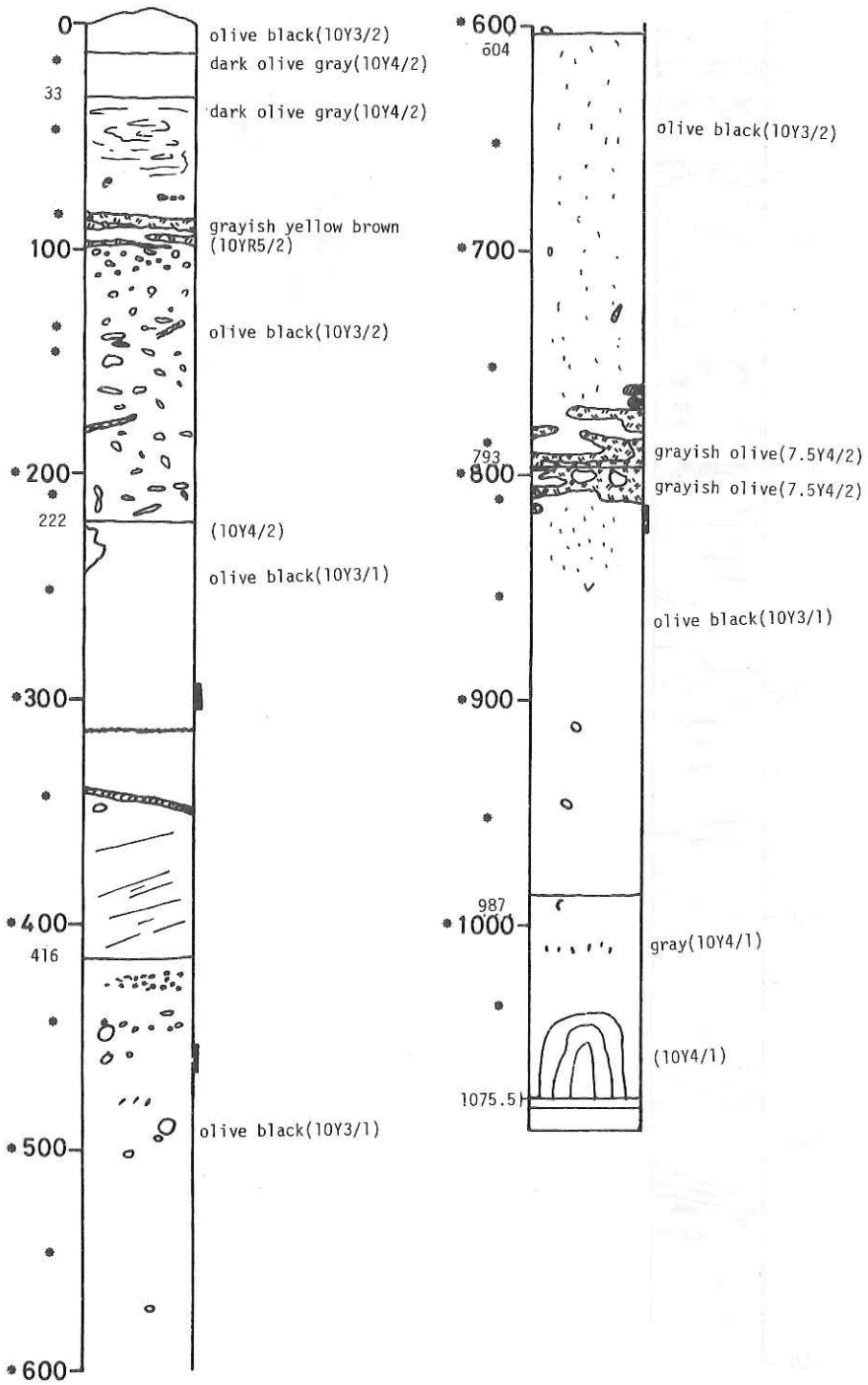
0
olive black(10Y3/2)
dark olive gray(10Y4/2)
33
dark olive gray(10Y4/2)
grayish yellow brown
(10YR5/2)
100
olive black(10Y3/2)
200
222
(10Y4/2)
olive black(10Y3/1)
300
400
416
olive black(10Y3/1)
500
600
600
604
olive black(10Y3/2)
700
793
grayish olive(7.5Y4/2)
800
grayish olive(7.5Y4/2)
olive black(10Y3/1)
900
987
1000
gray(10Y4/1)
(10Y4/1)
1075.5

KH82-4-15

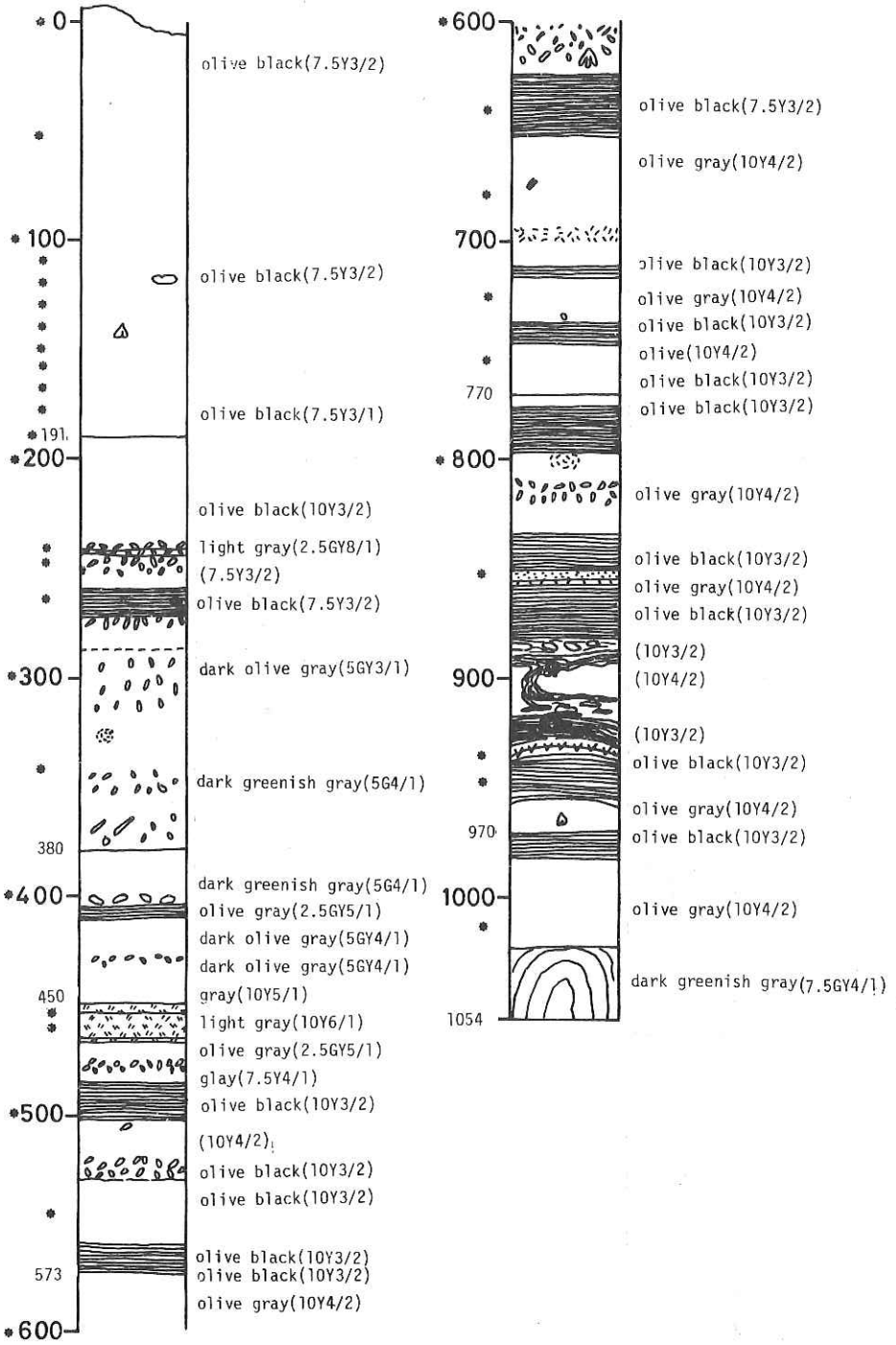
0
olive black(7.5Y3/2)
100
olive black(7.5Y3/2)
olive black(7.5Y3/1)
191
200
olive black(10Y3/2)
light gray(2.5GY8/1)
(7.5Y3/2)
olive black(7.5Y3/2)
300
dark olive gray(5GY3/1)
dark greenish gray(5G4/1)
380
400
dark greenish gray(5G4/1)
olive gray(2.5GY5/1)
dark olive gray(5GY4/1)
dark olive gray(5GY4/1)
450
gray(10Y5/1)
light gray(10Y6/1)
olive gray(2.5GY5/1)
glay(7.5Y4/1)
olive black(10Y3/2)
500
(10Y4/2)
olive black(10Y3/2)
olive black(10Y3/2)
olive black(10Y3/2)
573
olive black(10Y3/2)
olive gray(10Y4/2)
600
600
olive black(7.5Y3/2)
olive gray(10Y4/2)
700
olive black(10Y3/2)
olive gray(10Y4/2)
olive black(10Y3/2)
olive(10Y4/2)
olive black(10Y3/2)
770
olive black(10Y3/2)
800
olive gray(10Y4/2)
olive black(10Y3/2)
olive gray(10Y4/2)
olive black(10Y3/2)
(10Y3/2)
(10Y4/2)
900
(10Y3/2)
olive black(10Y3/2)
olive gray(10Y4/2)
970
olive black(10Y3/2)
1000
olive gray(10Y4/2)
dark greenish gray(7.5GY4/1)
1054

KH82-4-16

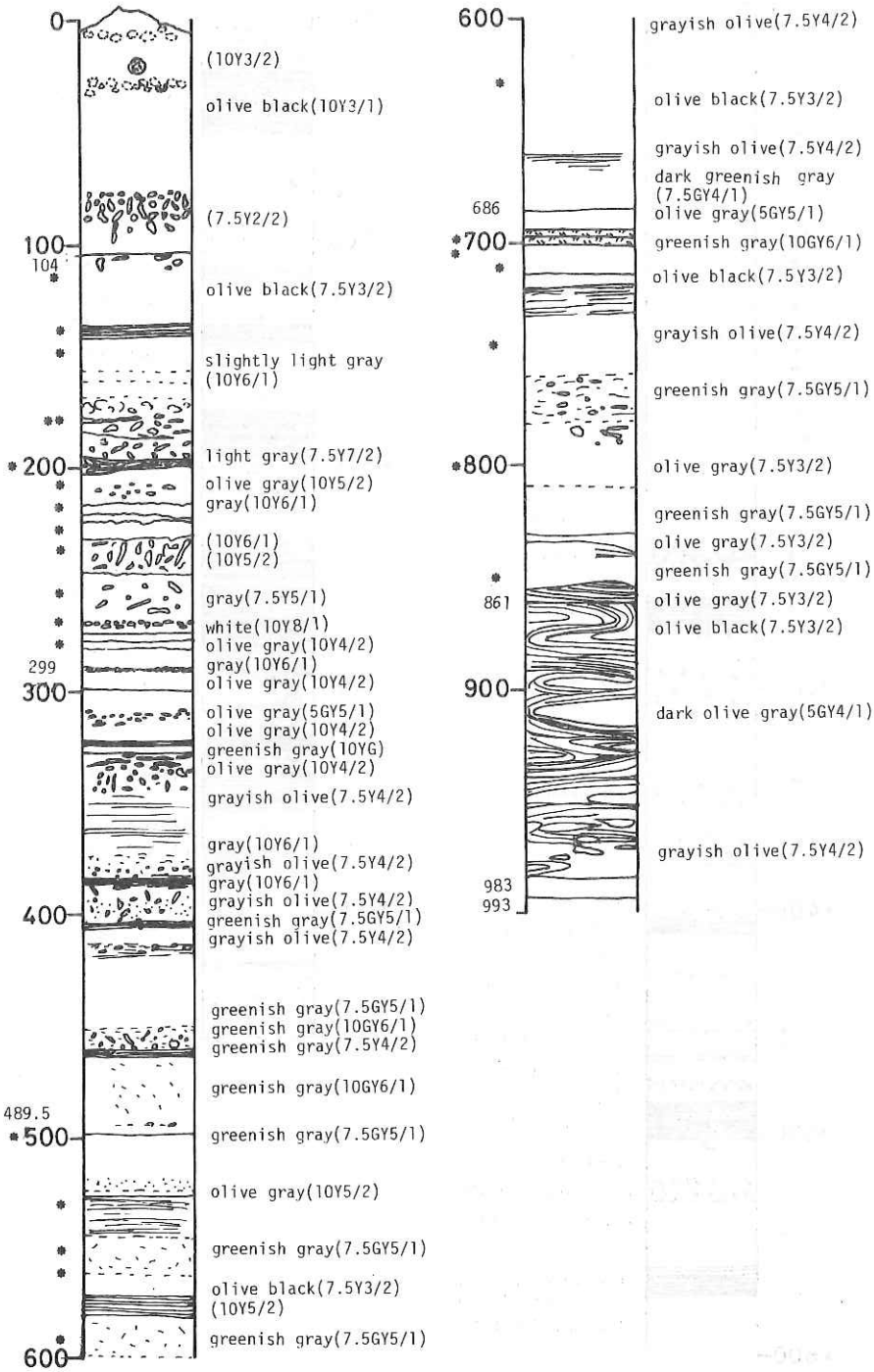
0
(10Y3/2)
olive black(10Y3/1)
(7.5Y2/2)
100
104
olive black(7.5Y3/2)
slightly light gray
(10Y6/1)
light gray(7.5Y7/2)
200
olive gray(10Y5/2)
gray(10Y6/1)
(10Y6/1)
(10Y5/2)
gray(7.5Y5/1)
white(10Y8/1)
olive gray(10Y4/2)
gray(10Y6/1)
299
olive gray(10Y4/2)
300
olive gray(5GY5/1)
olive gray(10Y4/2)
greenish gray(10YG)
olive gray(10Y4/2)
grayish olive(7.5Y4/2)
gray(10Y6/1)
grayish olive(7.5Y4/2)
gray(10Y6/1)
grayish olive(7.5Y4/2)
400
greenish gray(7.5GY5/1)
grayish olive(7.5Y4/2)
greenish gray(7.5GY5/1)
greenish gray(10GY6/1)
greenish gray(7.5Y4/2)
greenish gray(10GY6/1)
489.5
500
greenish gray(7.5GY5/1)
olive gray(10Y5/2)
greenish gray(7.5GY5/1)
olive black(7.5Y3/2)
(10Y5/2)
greenish gray(7.5GY5/1)
600
grayish olive(7.5Y4/2)
olive black(7.5Y3/2)
grayish olive(7.5Y4/2)
dark greenish gray
(7.5GY4/1)
686
olive gray(5GY5/1)
700
greenish gray(10GY6/1)
olive black(7.5Y3/2)
grayish olive(7.5Y4/2)
greenish gray(7.5GY5/1)
800
olive gray(7.5Y3/2)
greenish gray(7.5GY5/1)
olive gray(7.5Y3/2)
greenish gray(7.5GY5/1)
861
olive gray(7.5Y3/2)
olive black(7.5Y3/2)
900
dark olive gray(5GY4/1)
grayish olive(7.5Y4/2)
983
993

KH82-4-17

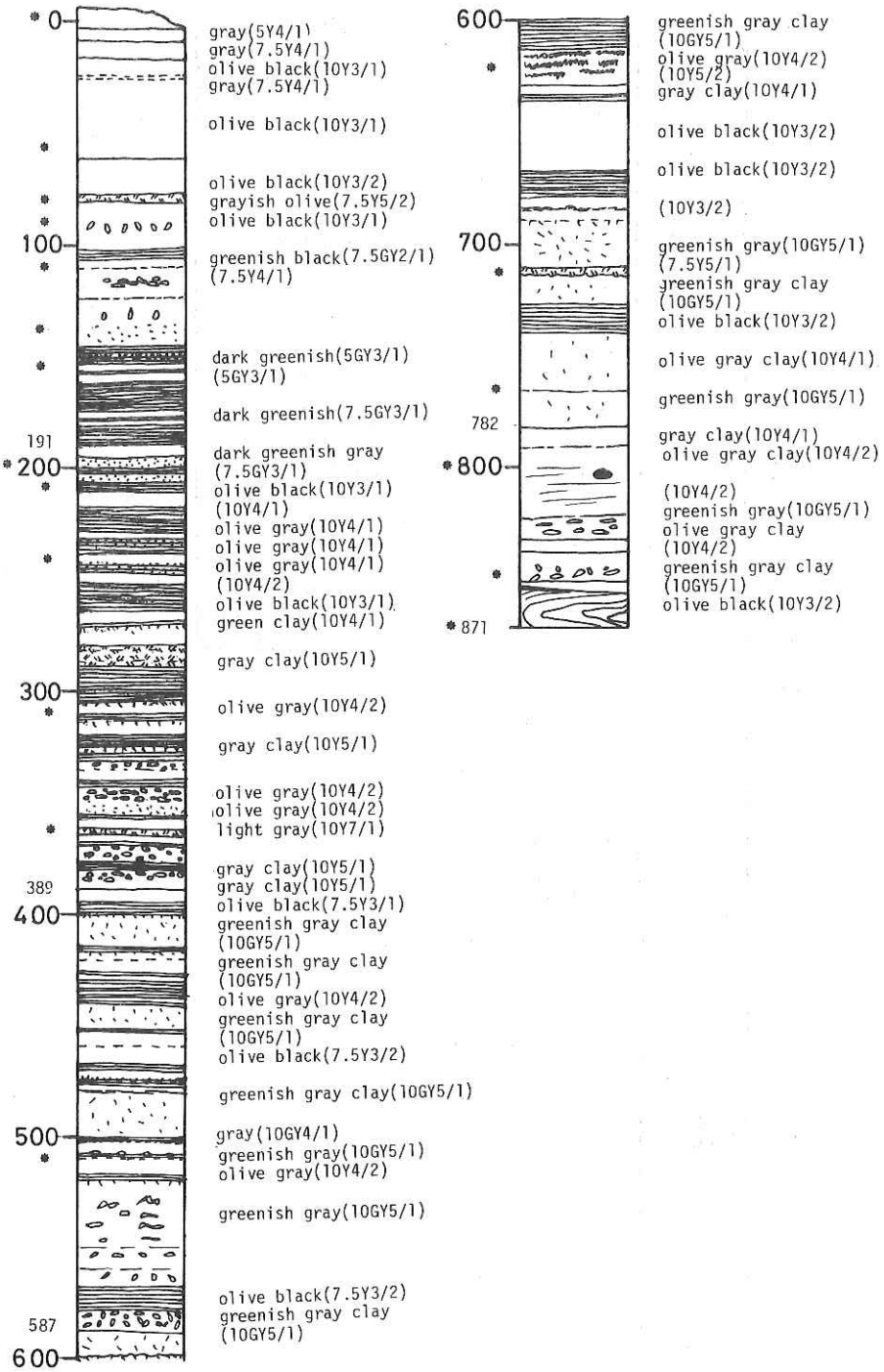
0
100
191
200
300
389
400
500
587
600
gray(5Y4/1)
gray(7.5Y4/1)
olive black(10Y3/1)
gray(7.5Y4/1)
olive black(10Y3/1)
olive black(10Y3/2)
grayish olive(7.5Y5/2)
olive black(10Y3/1)
greenish black(7.5GY2/1)
(7.5Y4/1)
dark greenish(5GY3/1)
(5GY3/1)
dark greenish(7.5GY3/1)
dark greenish gray
(7.5GY3/1)
olive black(10Y3/1)
(10Y4/1)
olive gray(10Y4/1)
olive gray(10Y4/1)
olive gray(10Y4/1)
(10Y4/2)
olive black(10Y3/1)
green clay(10Y4/1)
gray clay(10Y5/1)
olive gray(10Y4/2)
gray clay(10Y5/1)
olive gray(10Y4/2)
olive gray(10Y4/2)
light gray(10Y7/1)
gray clay(10Y5/1)
gray clay(10Y5/1)
olive black(7.5Y3/1)
greenish gray clay
(10GY5/1)
greenish gray clay
(10GY5/1)
olive gray(10Y4/2)
greenish gray clay
(10GY5/1)
olive black(7.5Y3/2)
greenish gray clay(10GY5/1)
gray(10GY4/1)
greenish gray(10GY5/1)
olive gray(10Y4/2)
greenish gray(10GY5/1)
olive black(7.5Y3/2)
greenish gray clay
(10GY5/1)
600
700
782
800
871
greenish gray clay
(10GY5/1)
olive gray(10Y4/2)
(10Y5/2)
gray clay(10Y4/1)
olive black(10Y3/2)
olive black(10Y3/2)
(10Y3/2)
greenish gray(10GY5/1)
(7.5Y5/1)
greenish gray clay
(10GY5/1)
olive black(10Y3/2)
olive gray clay(10Y4/1)
greenish gray(10GY5/1)
gray clay(10Y4/1)
olive gray clay(10Y4/2)
(10Y4/2)
greenish gray(10GY5/1)
olive gray clay
(10Y4/2)
greenish gray clay
(10GY5/1)
olive black(10Y3/2)

KH82-4-19

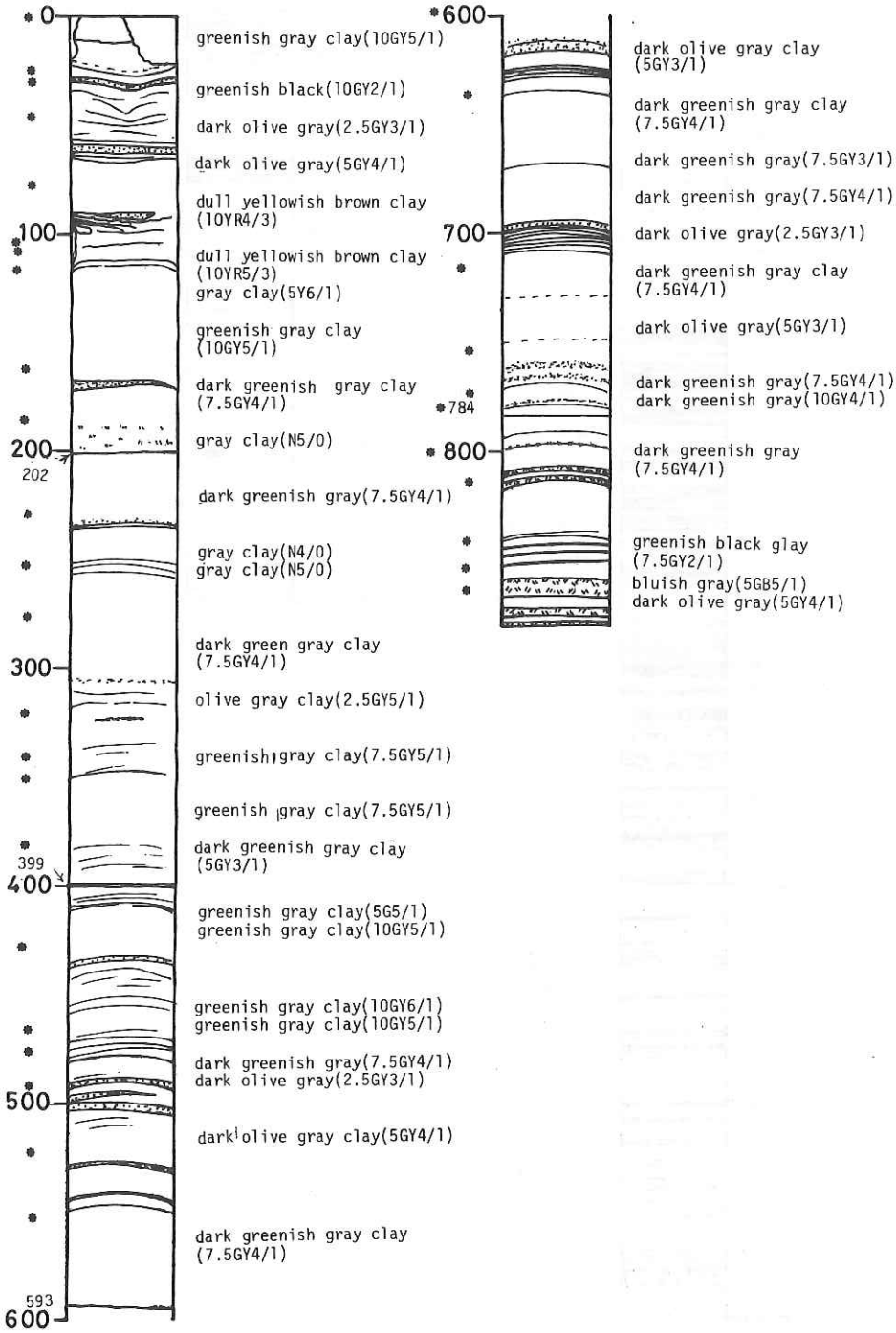
0
100
200
202
300
399
400
500
593
600
greenish gray clay(10GY5/1)
greenish black(10GY2/1)
dark olive gray(2.5GY3/1)
dark olive gray(5GY4/1)
dull yellowish brown clay (10YR4/3)
dull yellowish brown clay (10YR5/3)
gray clay(5Y6/1)
greenish gray clay (10GY5/1)
dark greenish gray clay (7.5GY4/1)
gray clay(N5/0)
dark greenish gray(7.5GY4/1)
gray clay(N4/0)
gray clay(N5/0)
dark green gray clay (7.5GY4/1)
olive gray clay(2.5GY5/1)
greenish gray clay(7.5GY5/1)
greenish gray clay(7.5GY5/1)
dark greenish gray clay (5GY3/1)
greenish gray clay(5G5/1)
greenish gray clay(10GY5/1)
greenish gray clay(10GY6/1)
greenish gray clay(10GY5/1)
dark greenish gray(7.5GY4/1)
dark olive gray(2.5GY3/1)
dark olive gray clay(5GY4/1)
dark greenish gray clay (7.5GY4/1)
600
700
784
800
dark olive gray clay (5GY3/1)
dark greenish gray clay (7.5GY4/1)
dark greenish gray(7.5GY3/1)
dark greenish gray(7.5GY4/1)
dark olive gray(2.5GY3/1)
dark greenish gray clay (7.5GY4/1)
dark olive gray(5GY3/1)
dark greenish gray(7.5GY4/1)
dark greenish gray(10GY4/1)
dark greenish gray (7.5GY4/1)
greenish black clay (7.5GY2/1)
bluish gray(5GB5/1)
dark olive gray(5GY4/1)

KH82-4-23

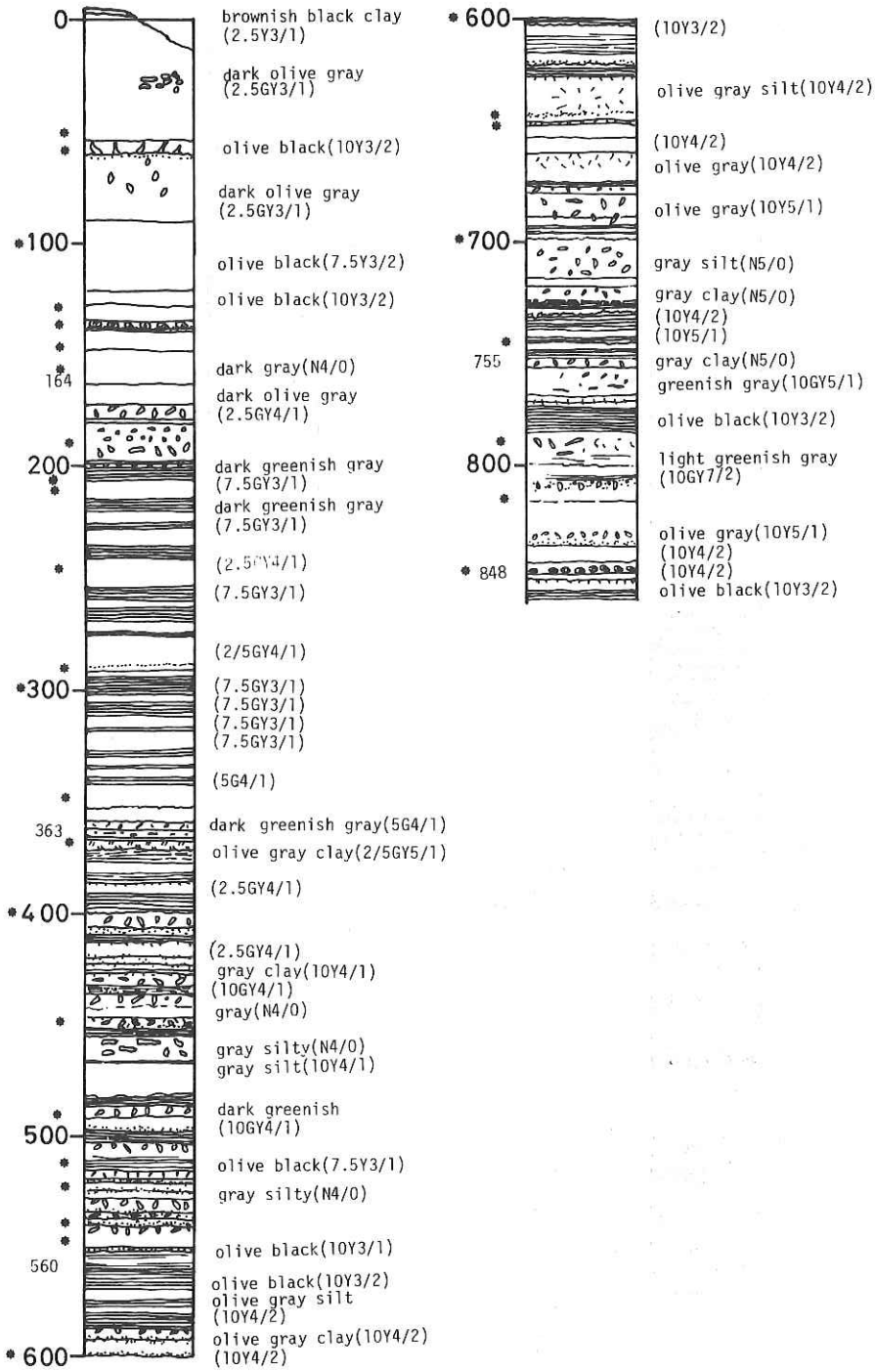
0
100
164
200
300
363
400
500
560
600
brownish black clay (2.5Y3/1)
dark olive gray (2.5GY3/1)
olive black(10Y3/2)
dark olive gray (2.5GY3/1)
olive black(7.5Y3/2)
olive black(10Y3/2)
dark gray(N4/0)
dark olive gray (2.5GY4/1)
dark greenish gray (7.5GY3/1)
dark greenish gray (7.5GY3/1)
(2.5GY4/1)
(7.5GY3/1)
(2/5GY4/1)
(7.5GY3/1)
(7.5GY3/1)
(7.5GY3/1)
(7.5GY3/1)
(5G4/1)
dark greenish gray(5G4/1)
olive gray clay(2/5GY5/1)
(2.5GY4/1)
(2.5GY4/1)
gray clay(10Y4/1)
(10GY4/1)
gray(N4/0)
gray silty(N4/0)
gray silt(10Y4/1)
dark greenish (10GY4/1)
olive black(7.5Y3/1)
gray silty(N4/0)
olive black(10Y3/1)
olive black(10Y3/2)
olive gray silt (10Y4/2)
olive gray clay(10Y4/2)
(10Y4/2)
600
700
755
800
848
(10Y3/2)
olive gray silt(10Y4/2)
(10Y4/2)
olive gray(10Y4/2)
olive gray(10Y5/1)
gray silt(N5/0)
gray clay(N5/0)
(10Y4/2)
(10Y5/1)
gray clay(N5/0)
greenish gray(10GY5/1)
olive black(10Y3/2)
light greenish gray (10GY7/2)
olive gray(10Y5/1)
(10Y4/2)
(10Y4/2)
olive black(10Y3/2)

KH82-4-24

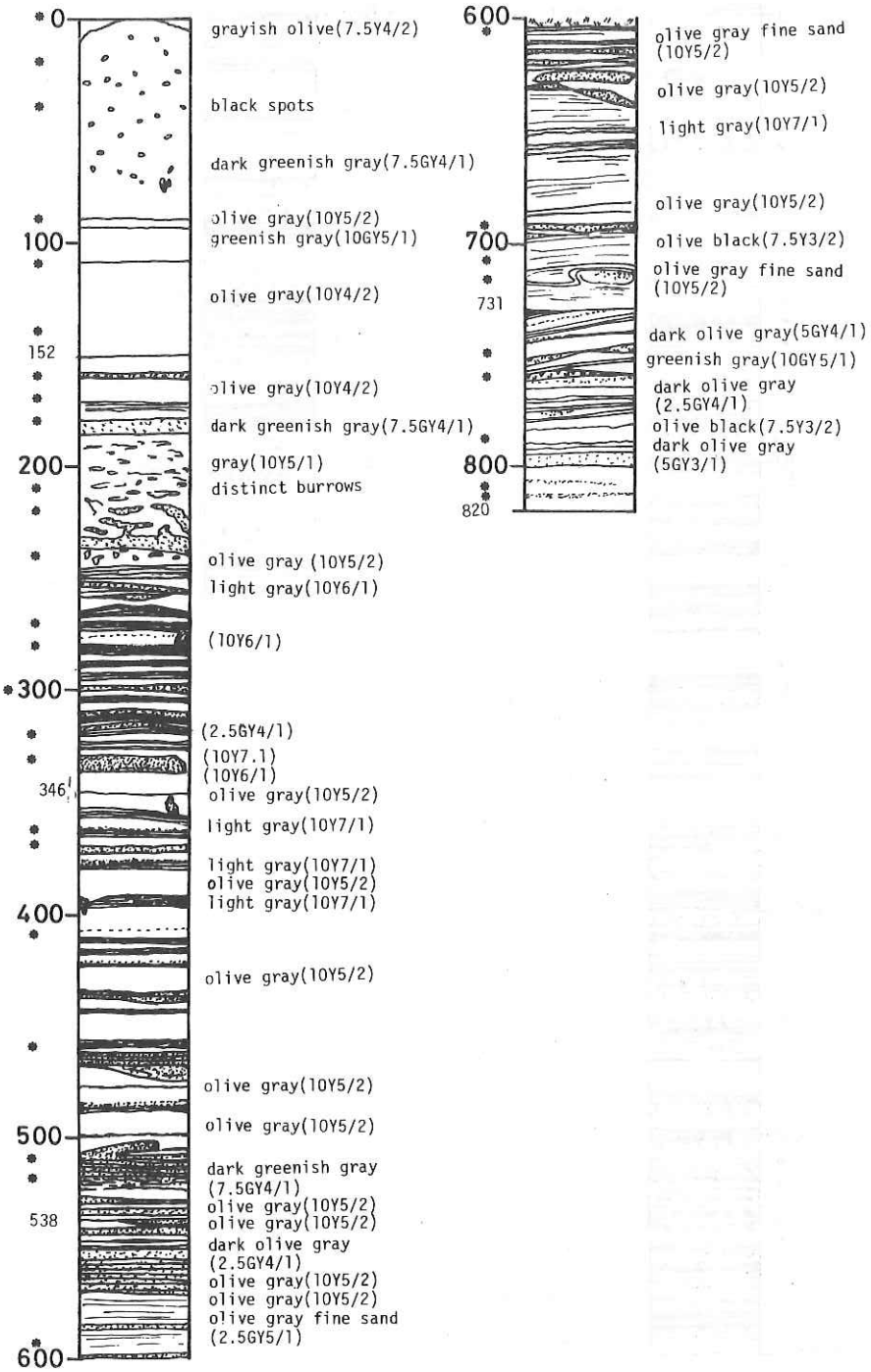
0
grayish olive(7.5Y4/2)
black spots
dark greenish gray(7.5GY4/1)
olive gray(10Y5/2)
greenish gray(10GY5/1)
100
olive gray(10Y4/2)
152
olive gray(10Y4/2)
dark greenish gray(7.5GY4/1)
200
gray(10Y5/1)
distinct burrows
olive gray (10Y5/2)
light gray(10Y6/1)
(10Y6/1)
300
(2.5GY4/1)
(10Y7.1)
(10Y6/1)
346
olive gray(10Y5/2)
light gray(10Y7/1)
light gray(10Y7/1)
olive gray(10Y5/2)
light gray(10Y7/1)
400
olive gray(10Y5/2)
olive gray(10Y5/2)
olive gray(10Y5/2)
500
dark greenish gray
(7.5GY4/1)
olive gray(10Y5/2)
538
olive gray(10Y5/2)
dark olive gray
(2.5GY4/1)
olive gray(10Y5/2)
olive gray(10Y5/2)
olive gray fine sand
(2.5GY5/1)
600
600
olive gray fine sand
(10Y5/2)
olive gray(10Y5/2)
light gray(10Y7/1)
olive gray(10Y5/2)
700
olive black(7.5Y3/2)
olive gray fine sand
(10Y5/2)
731
dark olive gray(5GY4/1)
greenish gray(10GY5/1)
dark olive gray
(2.5GY4/1)
olive black(7.5Y3/2)
dark olive gray
(5GY3/1)
800
820

KH82-4-25

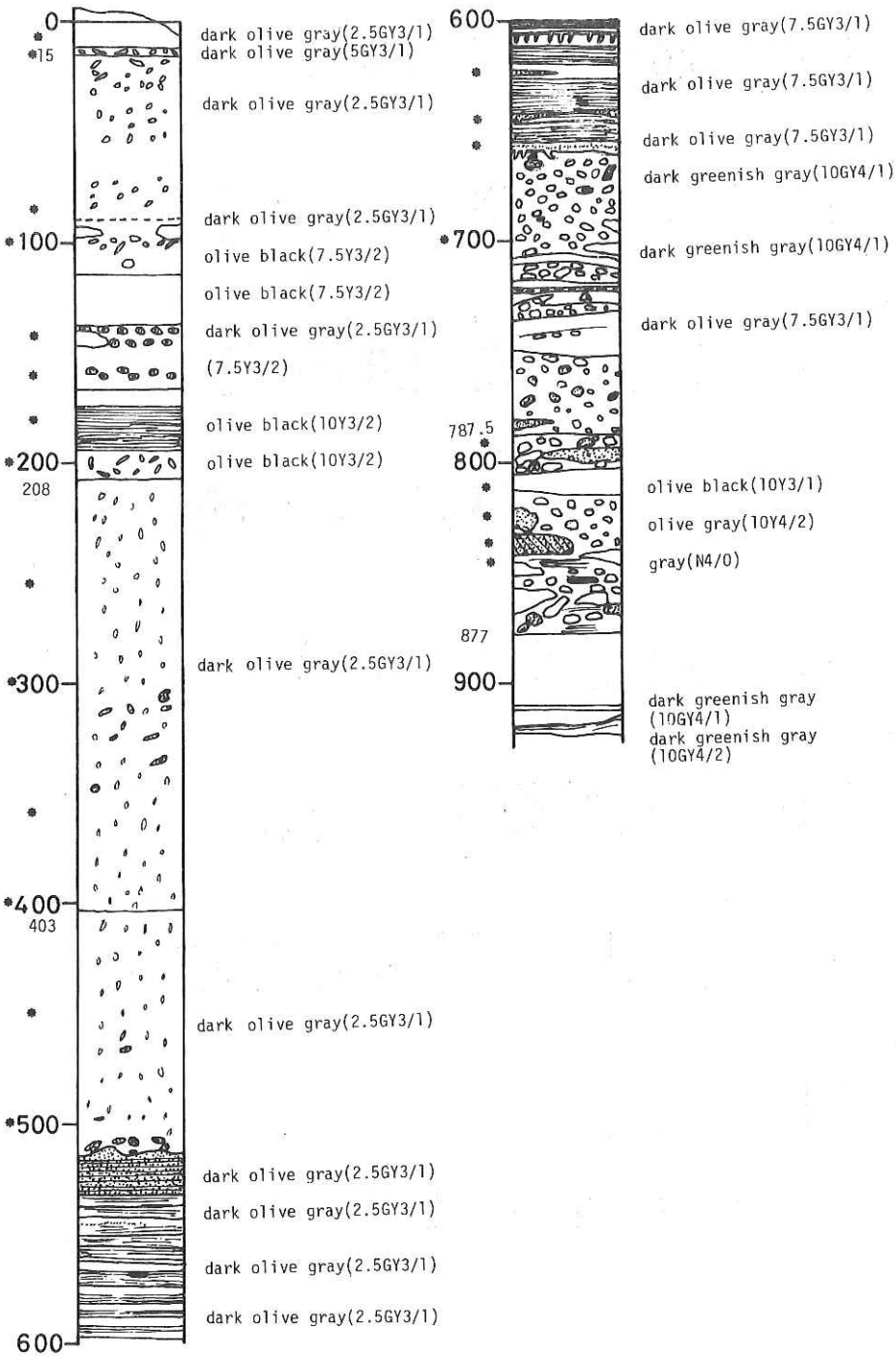
0
15
100
200
208
300
400
403
500
600
dark olive gray(2.5GY3/1)
dark olive gray(5GY3/1)
dark olive gray(2.5GY3/1)
dark olive gray(2.5GY3/1)
olive black(7.5Y3/2)
olive black(7.5Y3/2)
dark olive gray(2.5GY3/1)
(7.5Y3/2)
olive black(10Y3/2)
olive black(10Y3/2)
dark olive gray(2.5GY3/1)
dark olive gray(2.5GY3/1)
dark olive gray(2.5GY3/1)
dark olive gray(2.5GY3/1)
dark olive gray(2.5GY3/1)
600
700
787.5
800
877
900
dark olive gray(7.5GY3/1)
dark olive gray(7.5GY3/1)
dark olive gray(7.5GY3/1)
dark greenish gray(10GY4/1)
dark greenish gray(10GY4/1)
dark olive gray(7.5GY3/1)
olive black(10Y3/1)
olive gray(10Y4/2)
gray(N4/0)
dark greenish gray (10GY4/1)
dark greenish gray (10GY4/2)

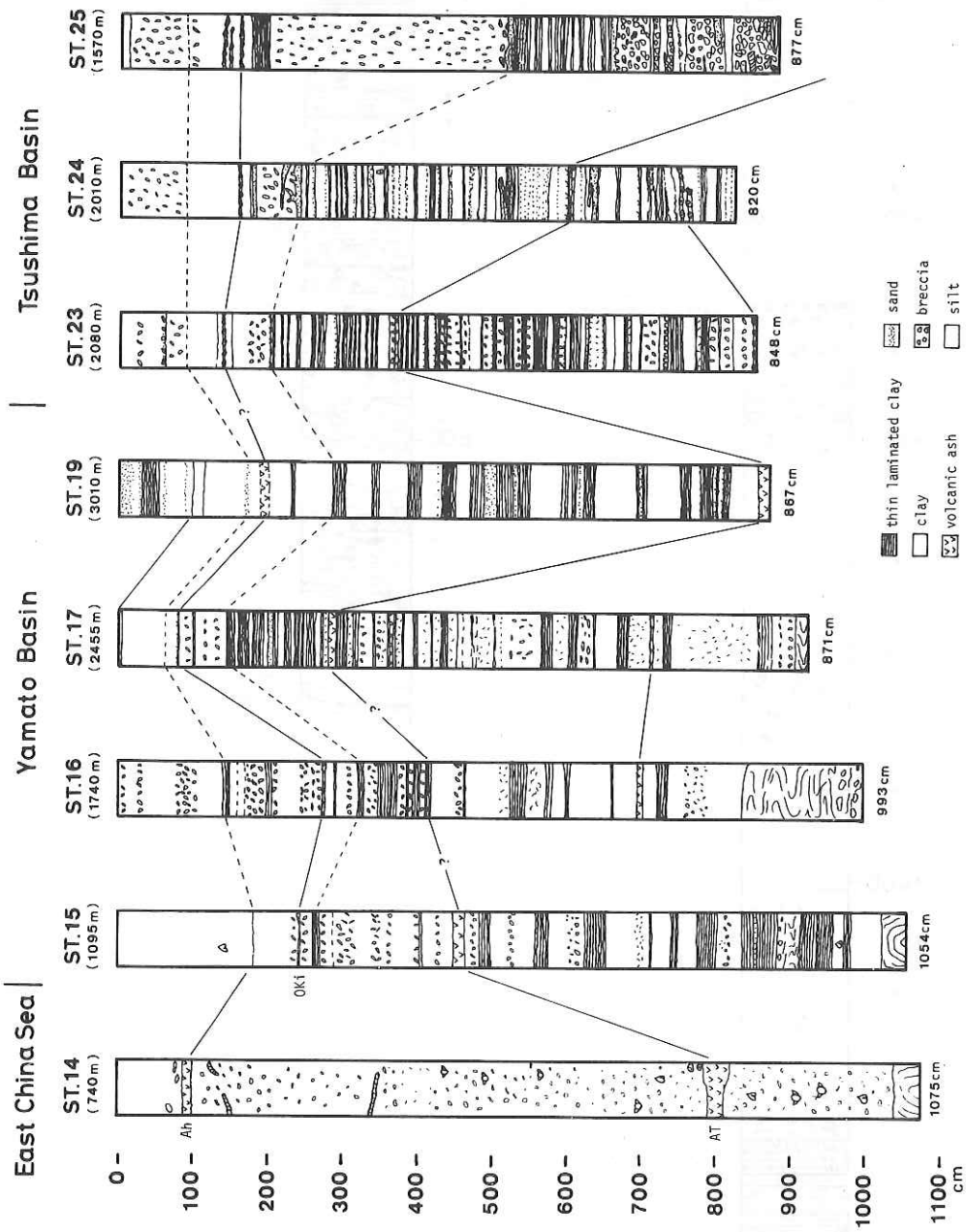

Fig. 7-2-3 Summary of long piston cores collected during KH 82-4.

7-3. PHYSICAL PROPERTY (SHEAR STRENGTH) OF PISTON CORE SAMPLES

Y. MIYATA AND T. TANAKA

MATERIALS AND PROCEDURES

Shear strength of twelve piston core samples was measured with an aid of a vane-type torque driver (Max. 1.0 kg and 5.0 kg, see Fig.7-3-1.). The general relationship between shear stress (torque) and strain (rotation angle of vane) of most samples is shown in Fig.7-3-2. Shear stress firstly increases with a very slight increase of strain toward the point f_1. In the next stage, stress increases as strain increases and reaches the maximam value M. Then strain increases with decreasing stress. At the point f_2, the sediments moving with the vane are separated from the surroundings, and no more stress are needed for further deformation.

If samples were destroyed during measuring, they could not be used for further examinations. In such a case, torque values were estimated as f_1 but not M. Vane shear strength S_V is given by.

$$S_V = T_m / (D^2H/2 + D^3/6),$$

where S_V : vane shear strength [g/cm^2],

T_m : torque [g],

D : vane diameter (=2.0cm),

H : vane height (=1.0cm),

RESULTS AND DISCUSSIONS

The results of the measurements are shown in Fig.7-3-3. Core samples P1 to P5 were cut and examined in the laboratory about one month after coring due to the inner tube sampling method. Core P14 was examined 6 days after sampling, while others were measured on ship. As shown in Fig. 7-3-3, P15 to P25 show a significant correlation between the subbottom depth and the vane shear strength. P14 is, however, less correlatable and P1 to P5 show no significant correlations. The results imply that the measurement of the shear stress of sediments should be made as soon as cores were obtained. An aluminium tube is, therefore, more useful for prompt measurements than a stainless tube with an inner tube.

The increasing rate of shear strength with subbottom depth varies from station to station. The relationships between shear strength and the following features were examined;

(1) Subbottom depth and lithofacies

Although shear strength increases with increasing subbottom depth, the horizon of sand and sand-size ash layers (indicated by A of P14 and S of P24 in Fig.7-3-3)has a large value as compared with the silt or clay layers above and below.

The sediments of P19 has a high water content and show a lower shear strength, while P16 shows a higher strength and a steeper slope (Fig.7-3-3). Such a difference reflects the difference of the sedimentation rate; P16 has a rate about 9cm/1000yr and P19 about 35cm/1000yr. Thus, shear strength may be a function of sedimentation and compaction history rather than a function of lithofacies.

In order to confirm this hypothesis let us consider the loading to the sediments of a known age. Shear strength may be formed by consistent effective pressure. Being the sedimentation rate R[g/cm^2.1000yr] assumed to be constant, the effective pressure P at the horizon of age T is given by

$P=R(r_s-r_f)T/r_s$,

where r_s : density of solid particle [g/cm^3],

r_f : density of pore fluid [g/cm^3].

The total effective pressure P_s subjected to the increasing weight of overlying sediments accumulated in a period of TX1000yr is

$P_s=(r_s-r_f)RT^2/2r_s$ ----------(1).

While, the thickness of the sediments is reduced by compaction. The void ratio e is given by

$e = e_o-C_c\log P$,

where e_o: initial value of the void ratio [-],

C_c : coefficient of compression.

The thickness of the sediments D[cm] is, therefore, given as

$D = (R/r_s)\{(1+e_o) - C_c\int_0^T \log Rtdt\}$

$= (R/r_s)\{(1+e_0) - C_cT(\log RT - 1)\}$ ----------(2)

If the age and the subbottom depth of a certain ash layer were known, R is calculated by equation (2). The values of P_s were calculated for P15 to P25, with R by D, T, r_s, D_c, where T=9.3x1000yr and =22x1000yr (ash layer Oki and AT respectively), r_s=2.7 and C_c=0.86. In Fig. 7-3-4, the

measured strengths S at the horizons of silt or clay just above the Oki (A) and AT (B) ash layers were plotted against the calculated values of Rt . Both Figs.(A) and (B) show that S is proportional to Rt and the shear strength had been formed by consistent effective pressure. However, only P19 shows a less strength than the expected value in both cases. The following two alternative interpretations may be possible;

(i) Dehydration was interrupted by too large rate of sedimentation and the effective pressure could not increase.

(ii) The piston corer put through the sediments obliquely and the apparent subbottom depth was overestimated.

(2) wire tension

No apparent relationship was found between shear strength and wire tension.

(3) 3.5kHz seismic profiles

Fig. 7-3-5 shows 3.5kHz seismic profiles of coring site P15 to P25. The profile of P19 shows many clear reflections even in deeper part, suggesting that these sediments absorb and reflect less seismic waves than those in other sites. Such a characteristic feature is expected from our observation showing that the sediments of P19 contain much water.

(4) Mode of deformation of soft sediments

In addition to slump fold and breccia observed in the sediments (*e.g.* P16 and P25), deformation structures of soft sediments by "piston effect" were found at the levels of 340cm and 510cm in P24 as a clast of a sand layer in a clay matrix. The mud layer above and below these sand layers however, did not neccessarily show a lower shear strength. Problems remain unsolved for such cases.

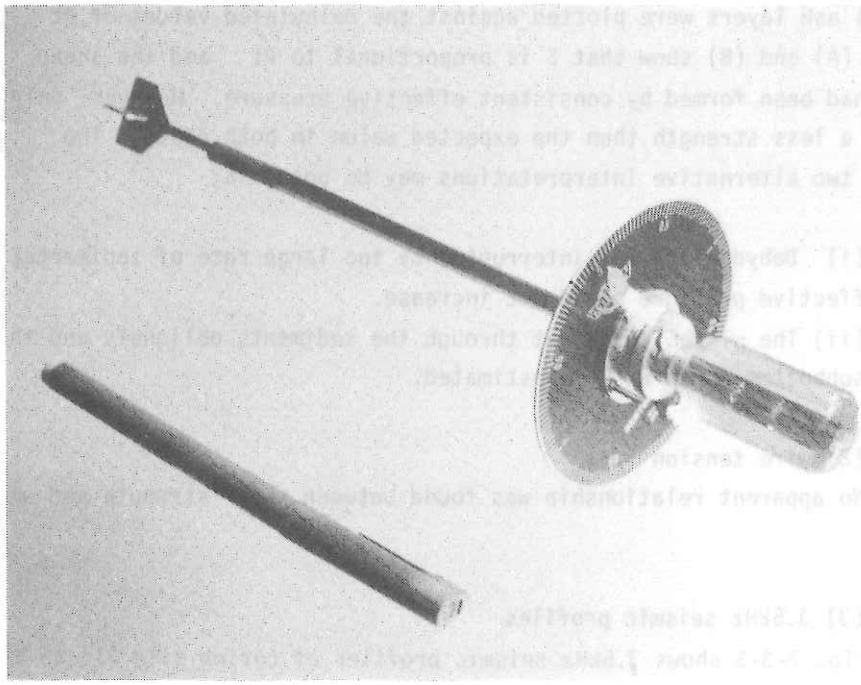

Fig.7-3-1.Simplified illustration of a vane-type torque driver.

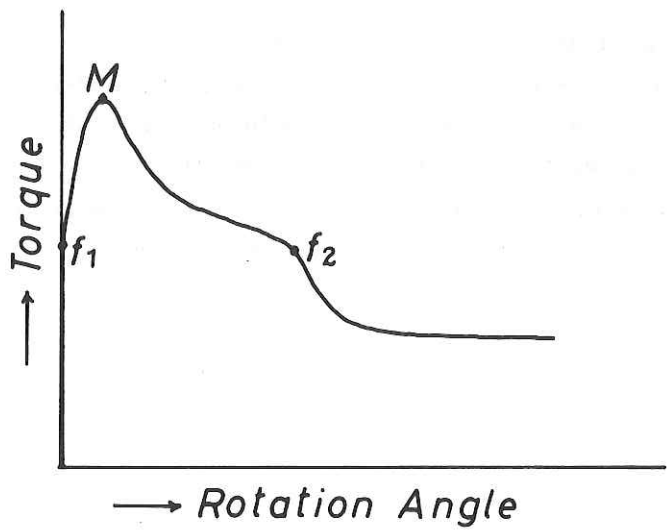

Fig.7-3-2. A typical stress-strain curve of soft sediments, replaced by a torque and a rotation angle of vane.

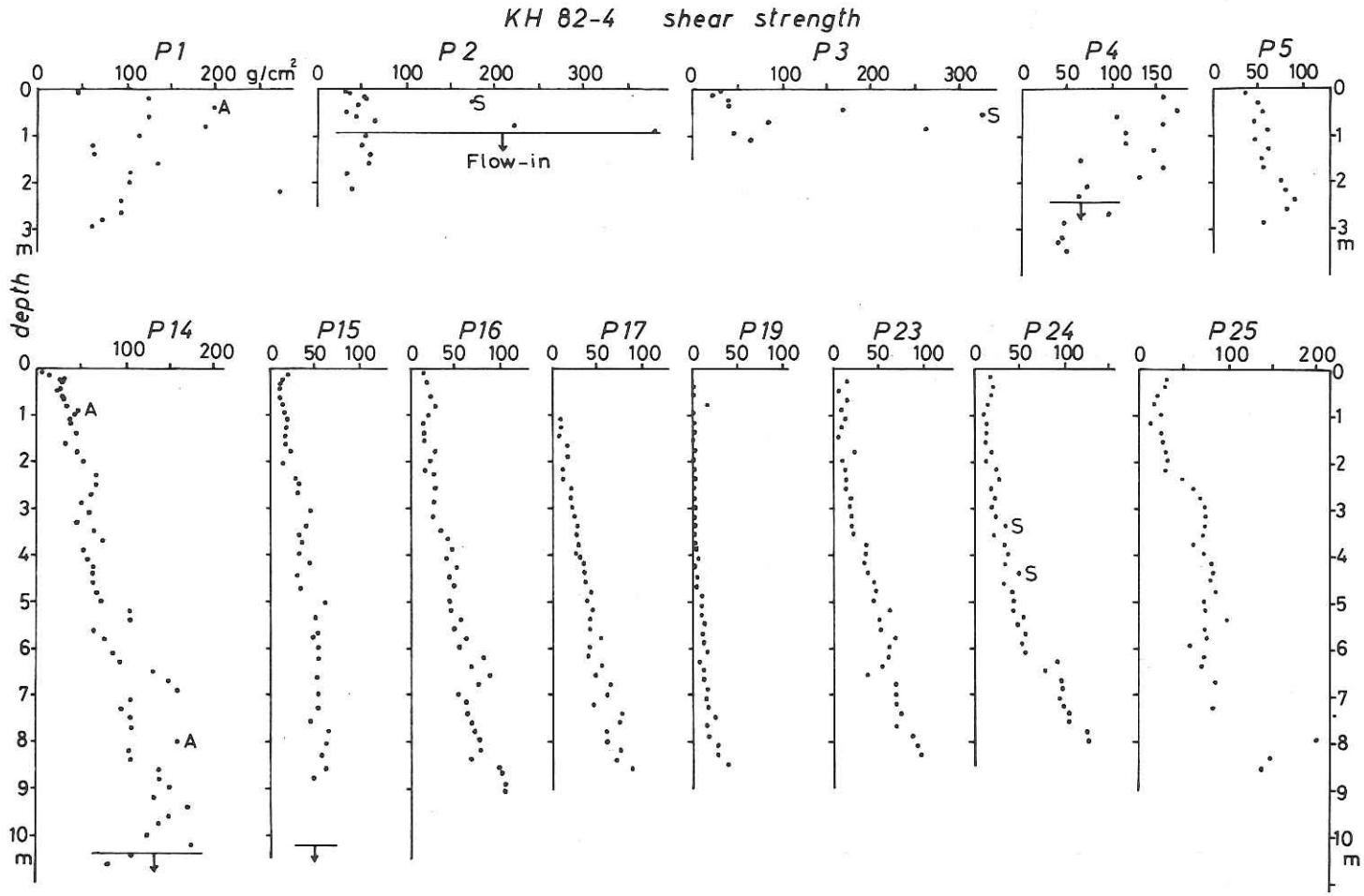

Fig.7-3-3. The vane shear strength of KH82-4 piston core samples.

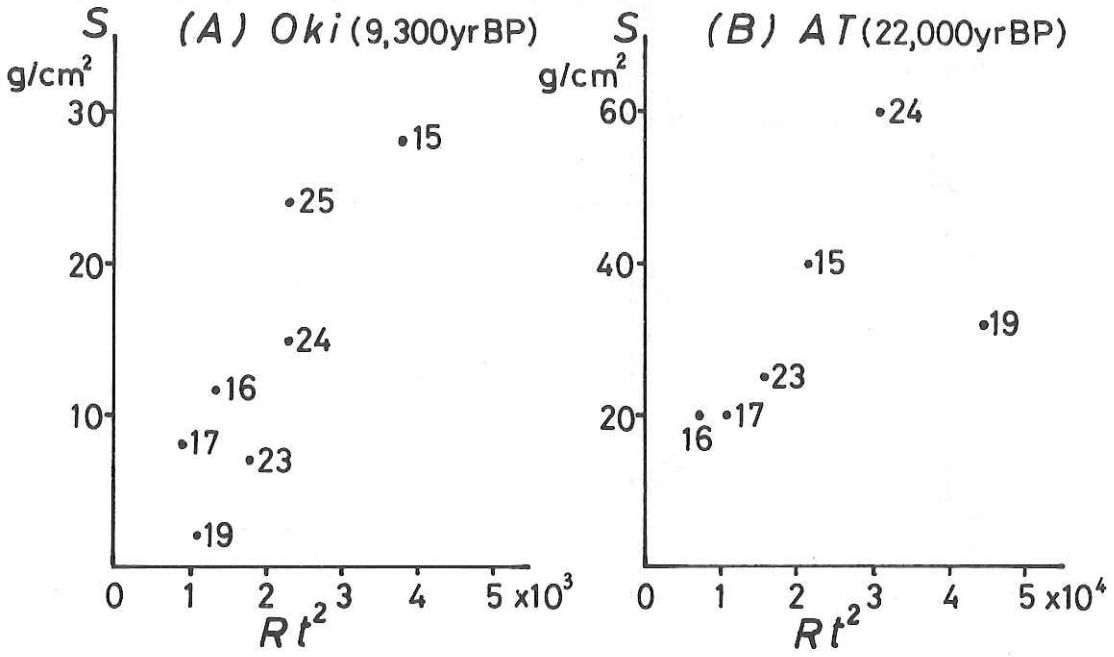

Fig.7-3-4. The diagrams showing the relationship between the time-integrated effective pressure Rt calculated with the sedimentation rate and the measured shear strength S of the sediments above the ash layer Oki (A) and AT (B) of core samples P15- P25.

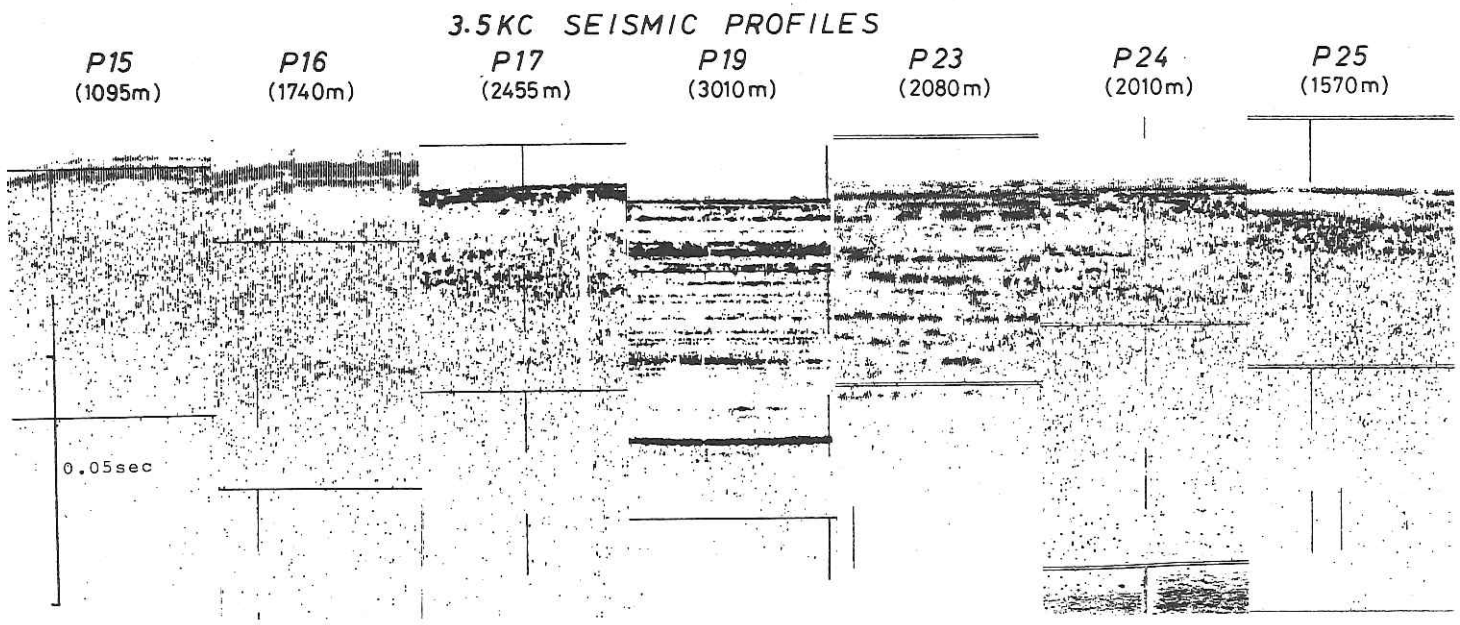

Fig.7-3-5. The 3.5kHz seismic profiles of coring site #15 - #25.

7-4. 3.5 kHz SUBBOTTOM PROFILING SURVEY IN THE CRUISE KH-82-4

T. TANAKA and Y. OGAWA

In tha last decade, many workers investigated 3.5 kHz subbottom profiles and demonstrated that certain echo types reflect the sedimentary processes which have been active in that region. They classified and mapped the areal distributions of various types of bottom echoes (Damuth, 1975; Damuth and Hayes, 1975; Tanahashi et al., 1981). It is important and indispensable to combine these informations with piston cores, bottom-photographs and other methods in an attempt to understand the sedimentary processes which have formed the sedimentary column in that area.

3.5 kHz subbottom profiling survey was carried out along the survey tracks in the present cruise in order to clarify the surface sedimentary structure and distribution of sediment and to decide the coring location. The subbottm profiling system is composed of 3.5 kHz transducers, PTR 105B, CESP II and UGR, which were manufatured by Raytheon Co.. Ship speed in the survey area was about 10 knots. Unfortunately, we can not get the profiles in the Amami Plateau and Ryukyu Trench regions because of the mechanical failure. Figs. 7-4-3 and -5 show the ship tracks and 3.5 kHz profile lines in the regions of Ogasawara, Sea of Japan and Nankai Trough, respectively.

Generally bottom echoes recorded with 3.5 kHz sound pulses consist of two principal classes: distinct and indistinct echoes. Three types of distinct echoes are recognized on the basis of the presence or absence of subbottom reflectors. Indistinct echoes are subdivided into two sub-classes: prolonged and hyperbolic (Damuth and Hayes, 1977). We attempted to classify the profiles based on these criteria. It should be noted that gradational variations are present within each echo type.

OGASAWARA REGION

Tanahashi et al. (1981) classified the subbottom profiles into five types in this region, Type a, b, c, d and e. Generally the subbottom profiles in the KH-82-4 cruise correspond to their results, although the echo type b was not found in our records.

Type a is recognizable in the Torishima Depression and the Ogasawara Trough. The nature of this echo pattern is semi-prolonged bottom echoes with intermittent zones of semi-prolonged, discontinuous, parallel subbottom reflectors.

However, there are minor variations in the penetration depth, continuity and strength of subbottom reflectors, site by site. Jacobi and Mrozowski (1979) discussed migrating sediment waves in the northern part of the Ogasawara Trough. Our profiles in that area show gentle undulated bottom topography with continuous parallel subbottom reflectors. But ship speed was too fast to observe the detailed structures. We carried out a piston coring (P-2) in this area. The sediment core shows no remarkable difference from cores P-1 and P-3.

Type c is characterized by the regular overlapping hyperbolae with varying vertex elevations above the sea floor. This echo type shows the sediment facies which are induced by sediment slide.

Type d shows regular, overlapping hyperbolae with relatively uniform vertex elevations above the sea floor on a gentle slope.

Type e is characterized by large irregular overlapping or single hyperbolae with widely varying vertex elevations above the sea floor. These echoes are due to the very rough topography of the Ogasawara Ridge.

THE SEA OF JAPAN REGION AND THE NANKAI TROUGH REGION

Two echo patterns are distinguished on the continental shelf and the ridges of the Japan Sea.

Type I-A. Continuous, sharp, bottom echoes with no subbottom reflectors

Type I-B. Continuous, sharp, bottom echoes with discontinuous folded subbottom reflectors which are truncated obliquely by sea floor.

In general, echo type I-A is recorded largely on the continental shelf which is a broad platform of consolidated sediments with an intermittent, thin covering of sand and gravel. Coarse sediments are very good reflectors of sound energy and consequently little or no sound penetrates to buried sediment interfaces. Therefore subbottom reflectors are seldom recorded on echograms from shelf regions (Damuth and Hayes, 1977). It seems the area of Type I-B is covered by fine sediments.

Three echo patterns are distinguished in the Yamato Basin, Tsushima Basin and Nankai Trough.

Type I-C. Continuous, sharp, bottom echoes with continuous, sharp, parallel subbottom reflectors.

Type II-A. Semi-prolonged bottom echoes with intermittent zones of semi-prolonged, discontinuous, parallel subbottom reflectors.

Type II-B. Very prolonged bottom echoes with no subbottom reflectors. Echo type I-C occurs in the Kita-Yamato Trough and the northeastern part of the Yamato Basin, and also represent the thin cover on the Ridge of the Sea of Japan. The type II-A is the most widespread echoes observed in the research area. The type II-B occurs in the basin between Ulreung Island and the Yamato Ridge, and in the part of trough axis off Shionomisaki.

The echo patterns at the coring sites are described in another report of this volume (Tanaka et al.). In general, sediments from regions of distinct echoes with continuous parallel subbottoms (I-C) contain minor amounts (less than 5 %) of bedded silt/sand. In contrast, regions of very prolonged echoes with no subbottom reflectors (II-B) generally contain high amounts (20 to 100 %) of bedded silt/sand. Sediments from the regions of semi-prolonged echoes with intermittent zones of subbottoms (II-A) indicate that the abundance of bedded silt/sand in these regions is relatively low to moderate, and therefore intermediate between those of I-C and II-B regions (Damuth and Hayes, 1977). These results are correspondable with the results from the piston cores in the Sea of Japan. It suggests that coarse sediments are distributed in the eastern part of the Nankai Trough rather than the western part.

The echo patterns from steep slopes are characterized by blocky surfaces, truncation of reflectors and unrecognizable sequences of reflectors. It suggests that slides, slumps and debris flow deposits are extensively deposited on the surrounding slopes.

REFERENCES

Damuth, J. E., 1975. Echo character of the western Equatorial Atlantic floor and its relationship to the dispersal and distribution of terrigenous sediments. Mar. Geol., 18, 17-45.

Damuth, J. E. and Hayes, D. E., 1977. Echo character of the east Brazilian continental margin and its relationship to sedimentary processes. Mar. Geol., 24, 73-95.

Jacobi, R. D. and Mrozowski, C. L., 1979. Sediments slides and sediment waves in the Bonin Trough, western Pacific. Mar. Geol., 29, M1-M9.

Tanahashi,M., Tamaki, K. and Okuda, Y., 1981. 3.5 kHz subbottom profiling survey in cruise GH-79-2, 3 and 4. Geol. Surv. Japan Cruise Report, no.14, 36-44.

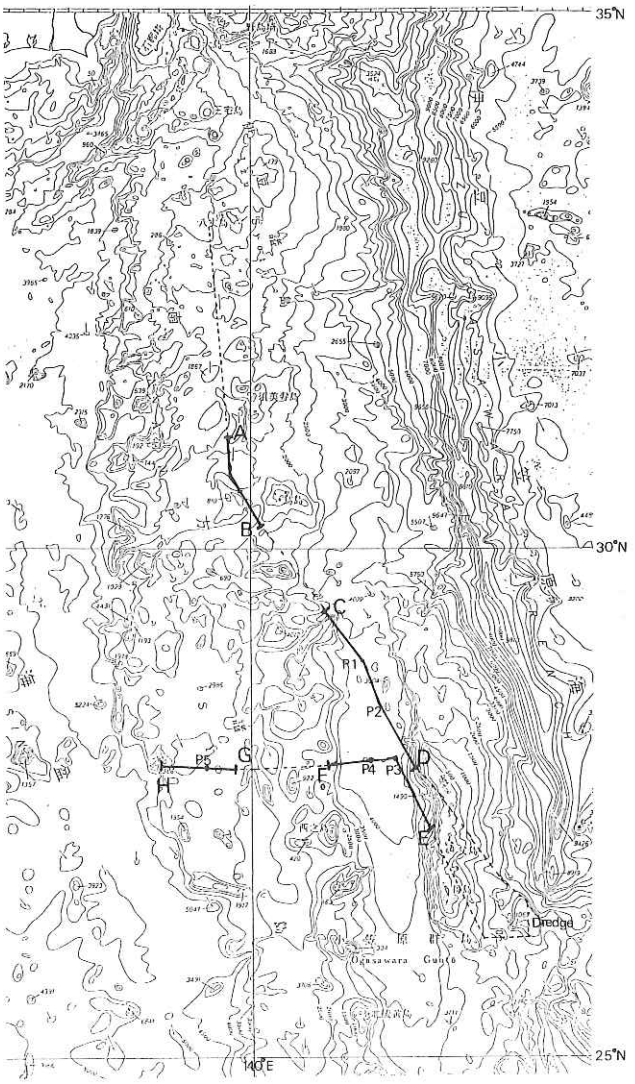

Fig. 7-4-1. Chart showing 3.5 kHz track lines and core location in the Ogasawara region. Thickened track lines with letter code correspond to selected profiles illustrated, in Fig. 7-4-2.

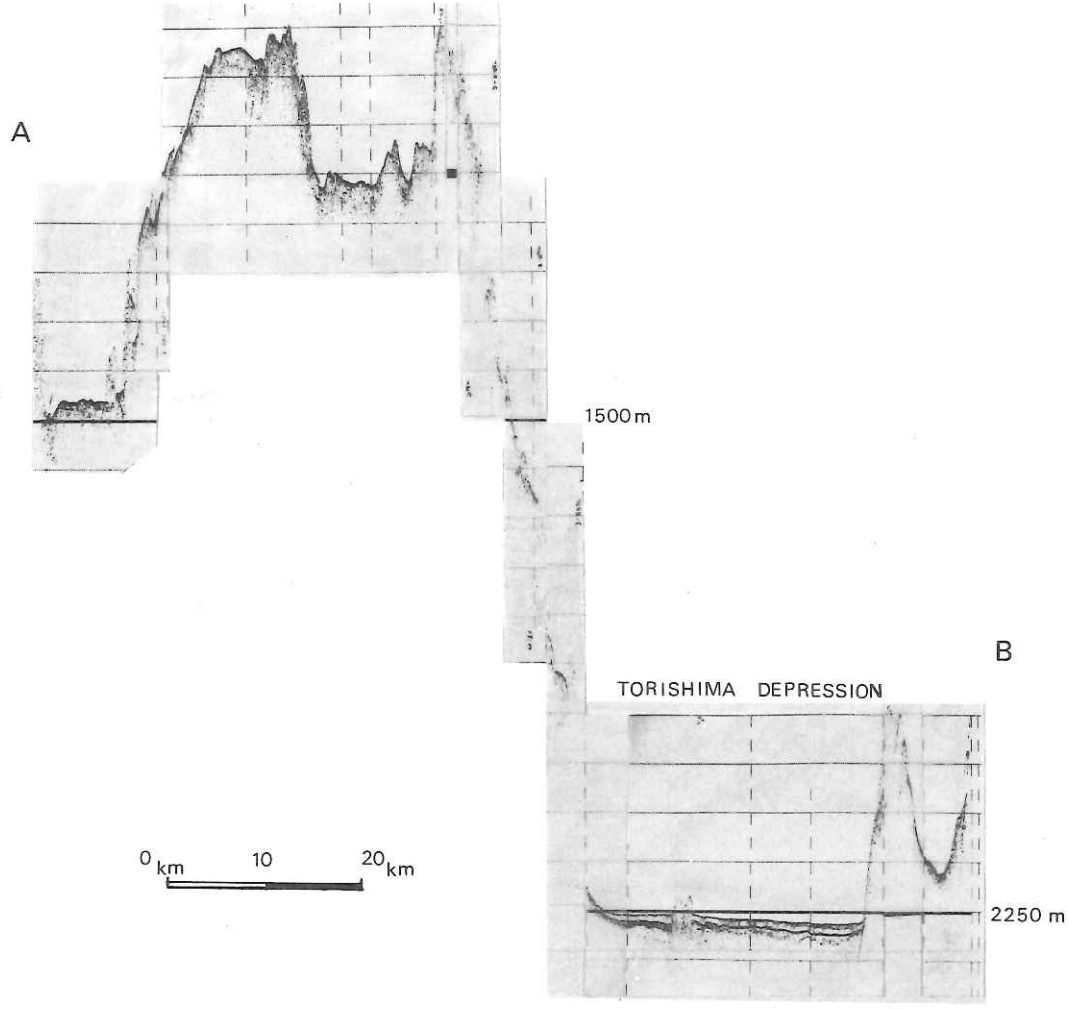

Fig. 7-4-2. Selected 3.5 kHz profiles in the Ogasawara area (depth in m).

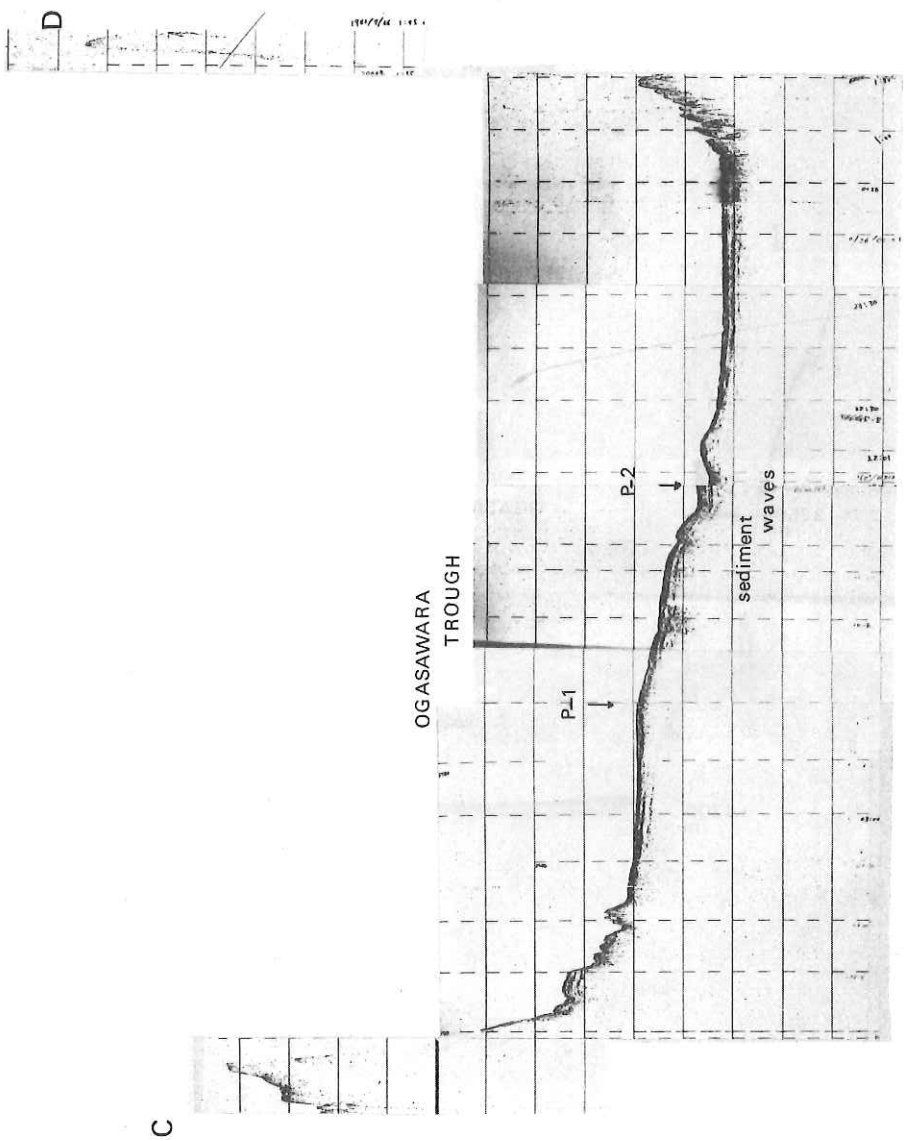
D
C
OGASAWARA
TROUGH
P-1
P-2
sediment
waves

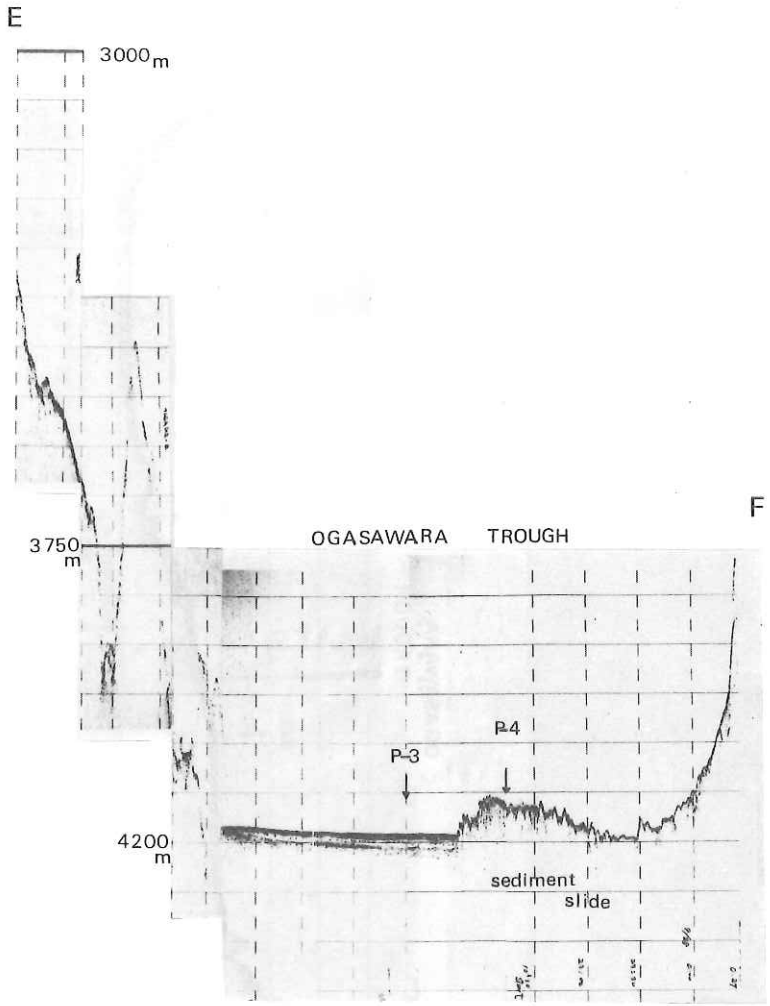
E
3000 m
3750 m
OGASAWARA TROUGH
F
P-4
P-3
4200 m
sediment slide

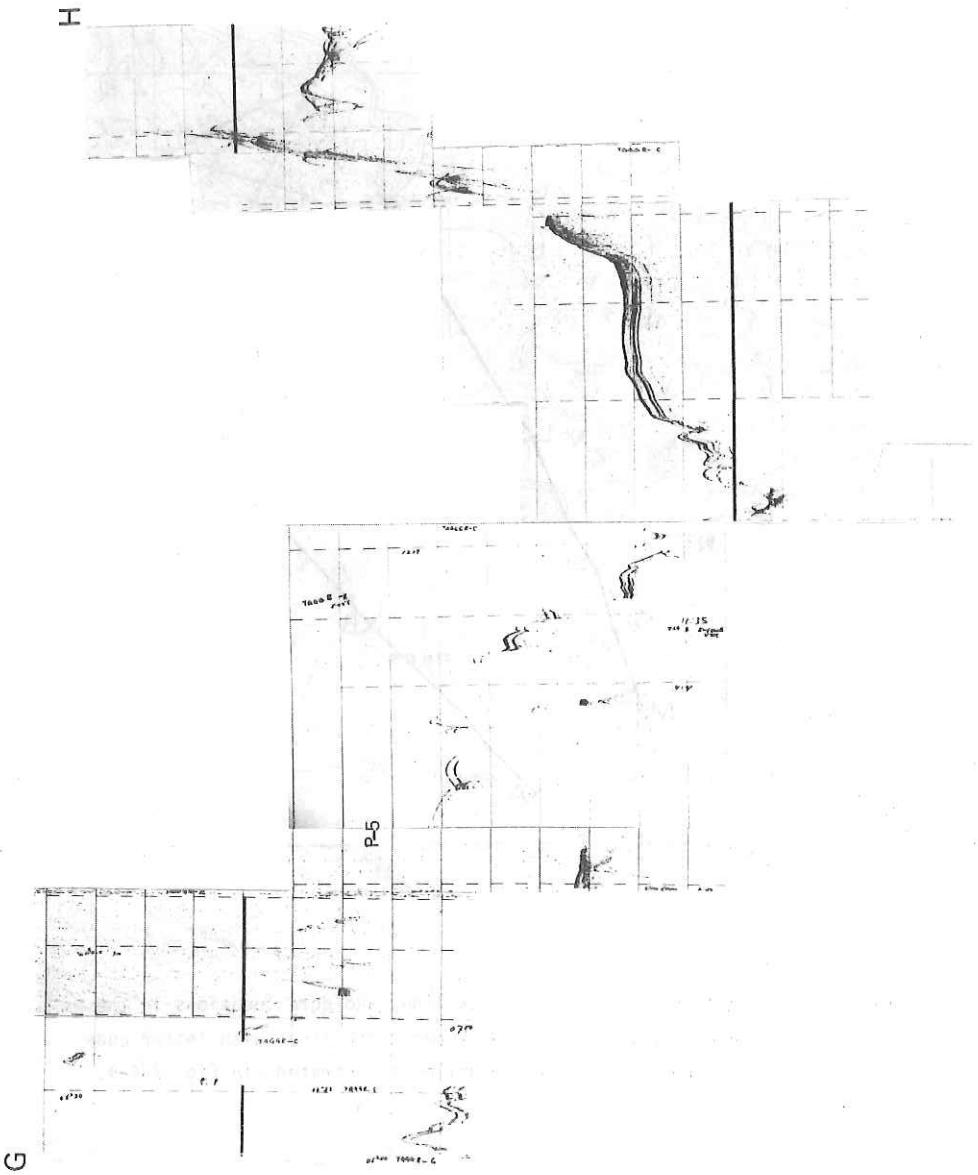
H
P-5
G

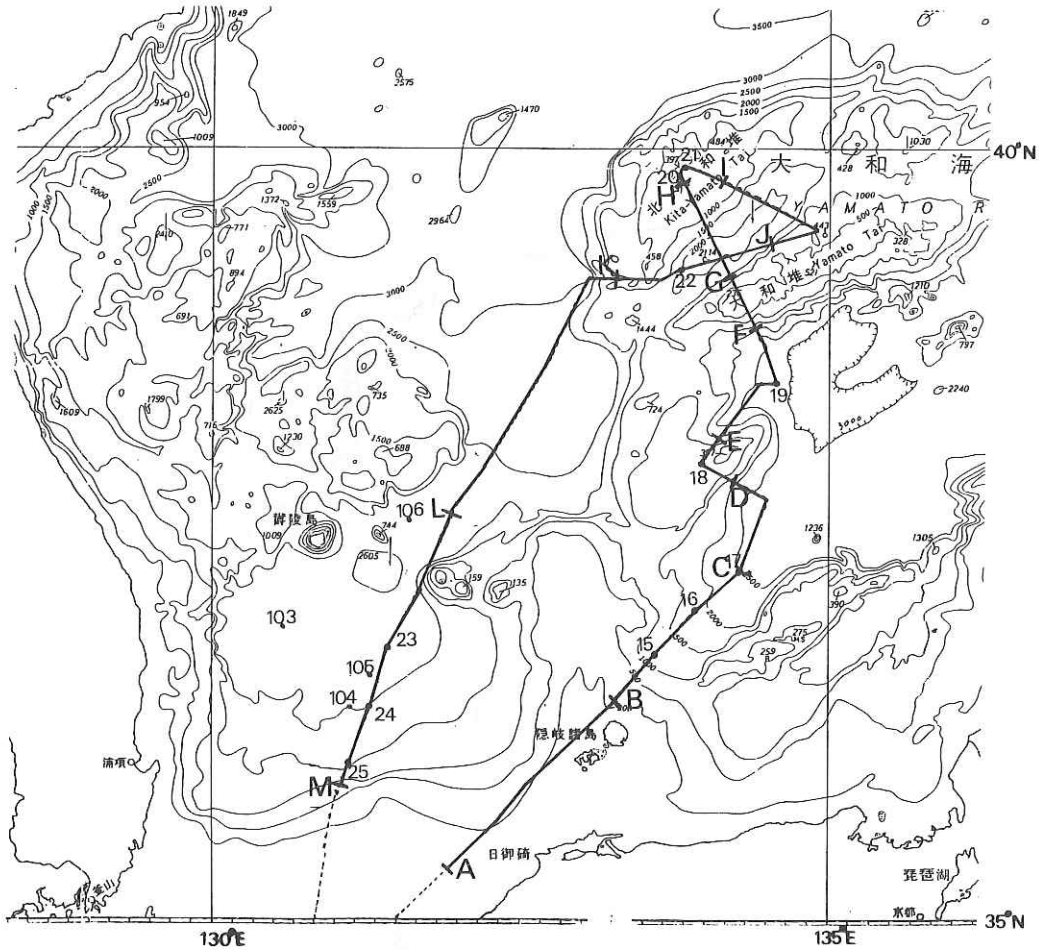

Fig. 7-4-3. Chart showing 3.5 kHz track lines and core locations in the Sea of Japan region. Thickened track lines with letter code correspond to selected profiles illustrated, in Fig. 7-4-4.

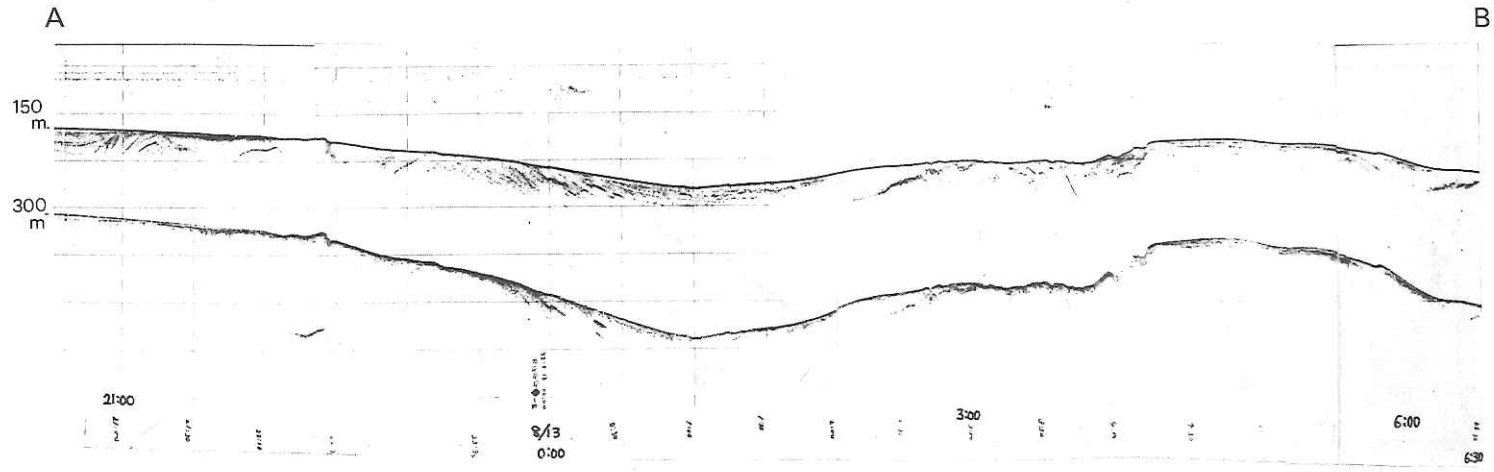

Fig. 7-4-4. Selected 3.5 kHz profiles in the Sea of Japan region (depth in m).

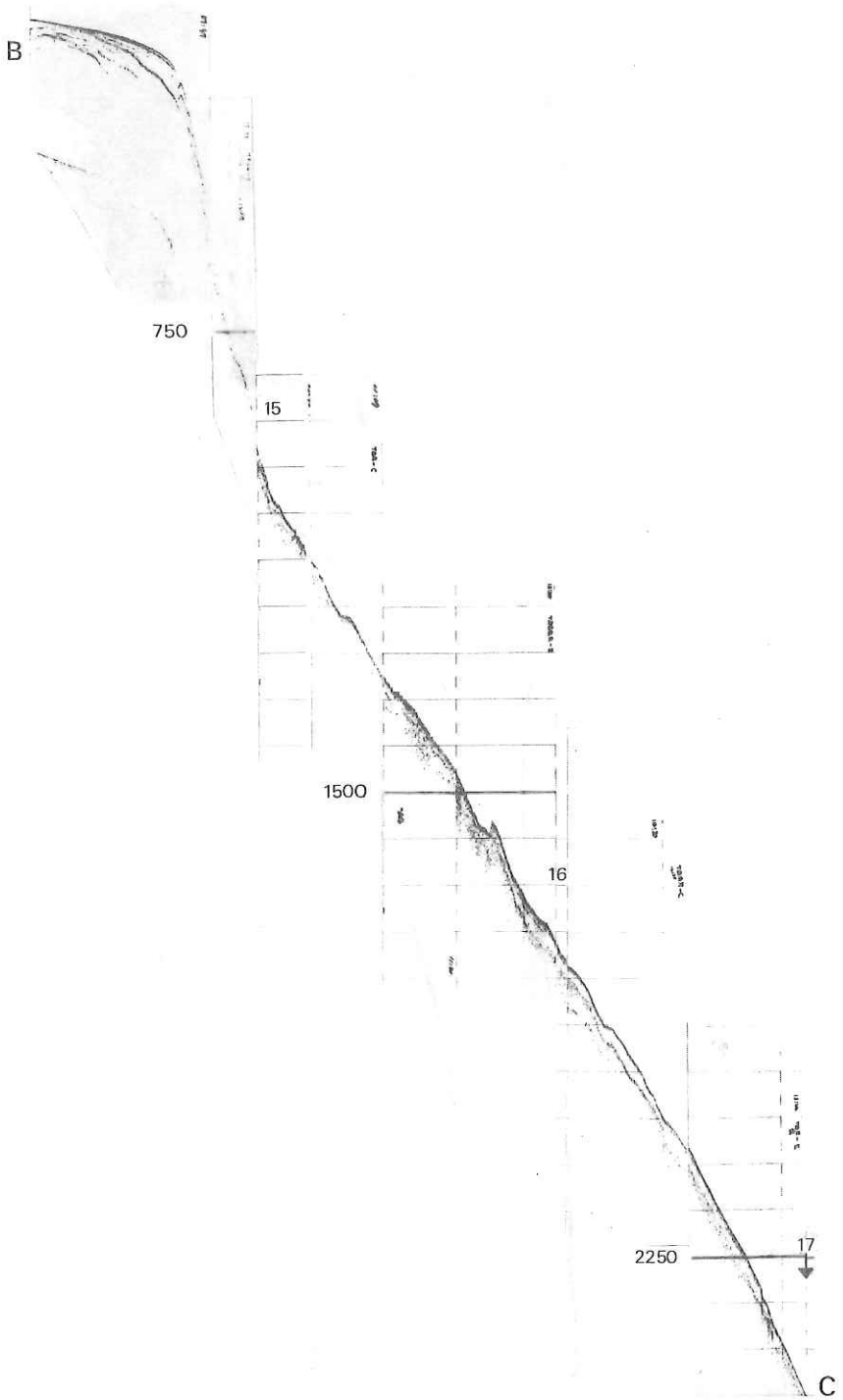
B
750
15
1500
16
2250
17
C

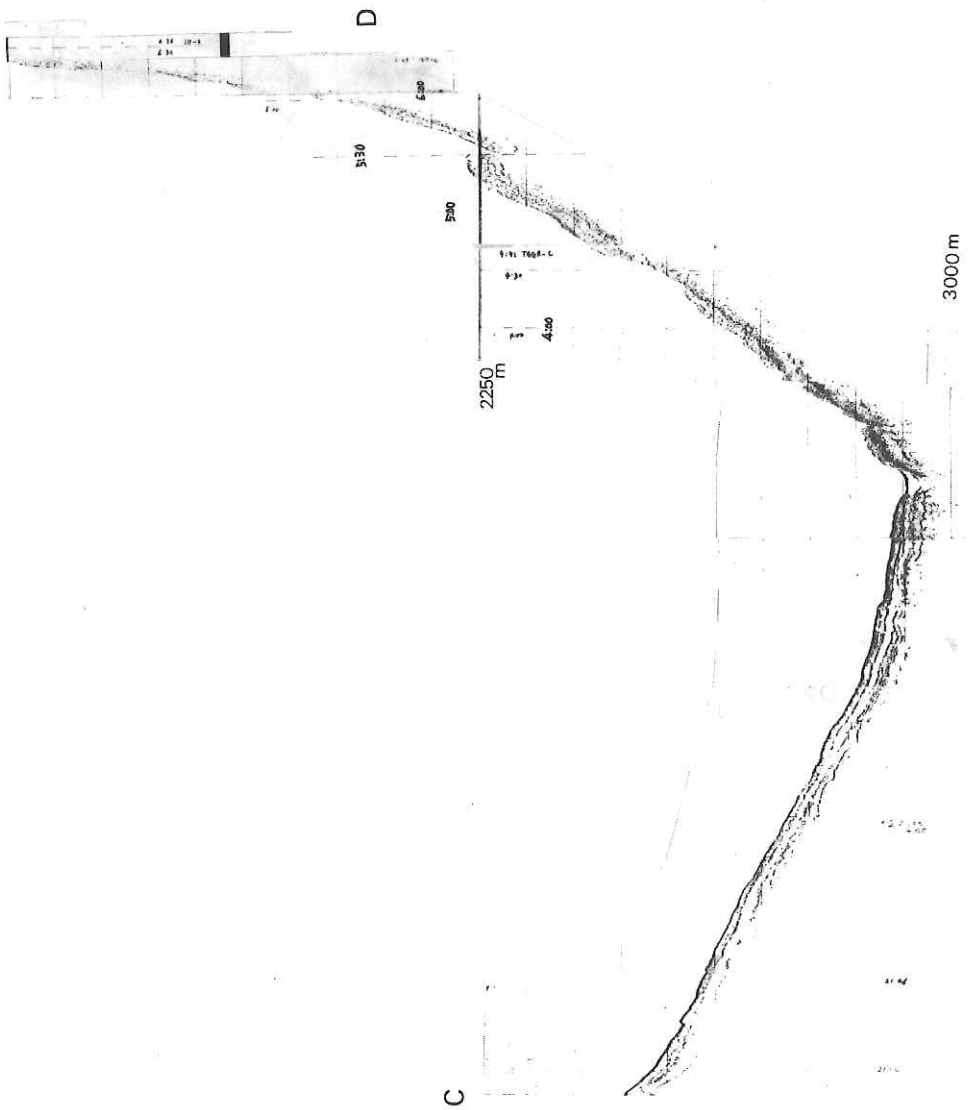
D
C
2250 m
3000 m

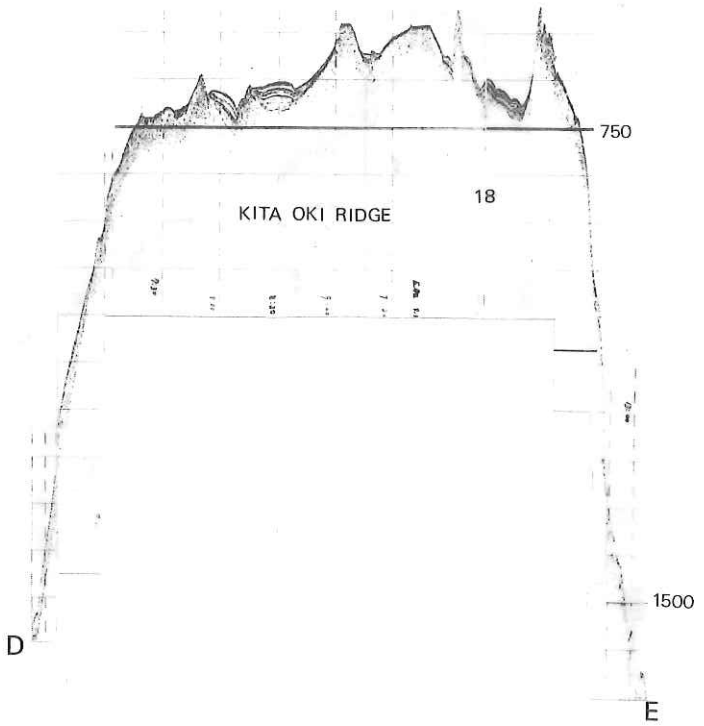
750
KITA OKI RIDGE
18
1500
D
E

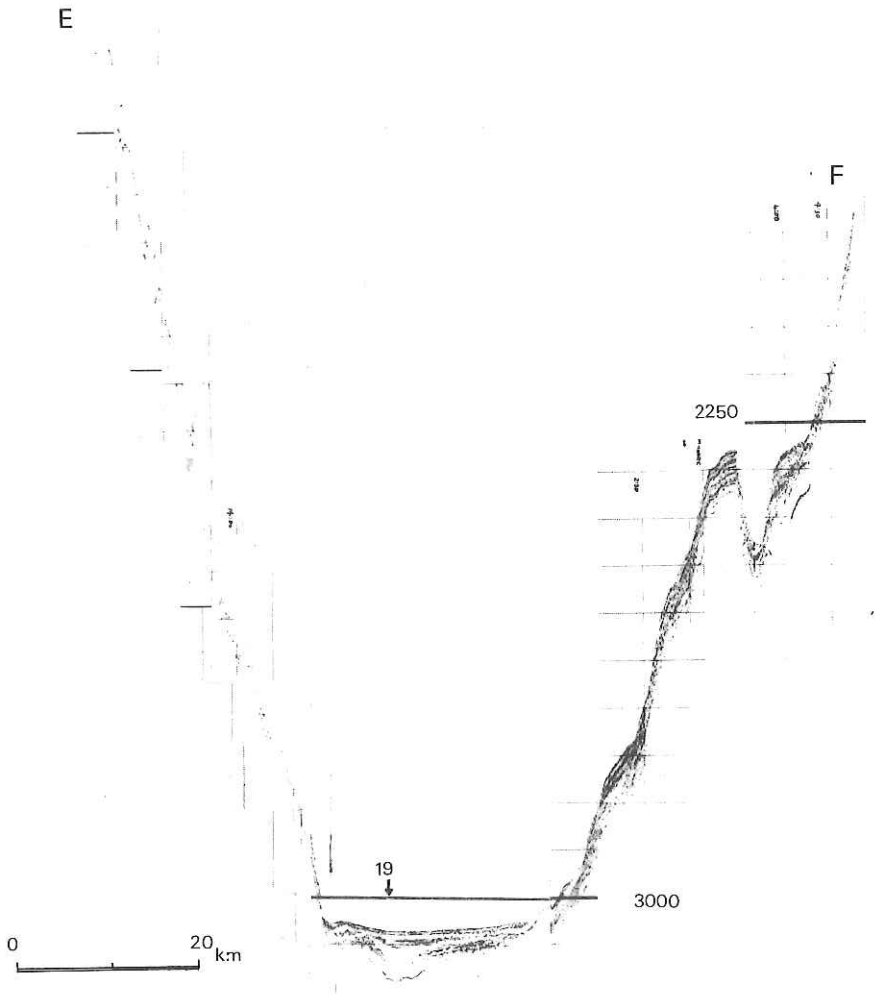
E
F
2250
19
3000
0
20
km

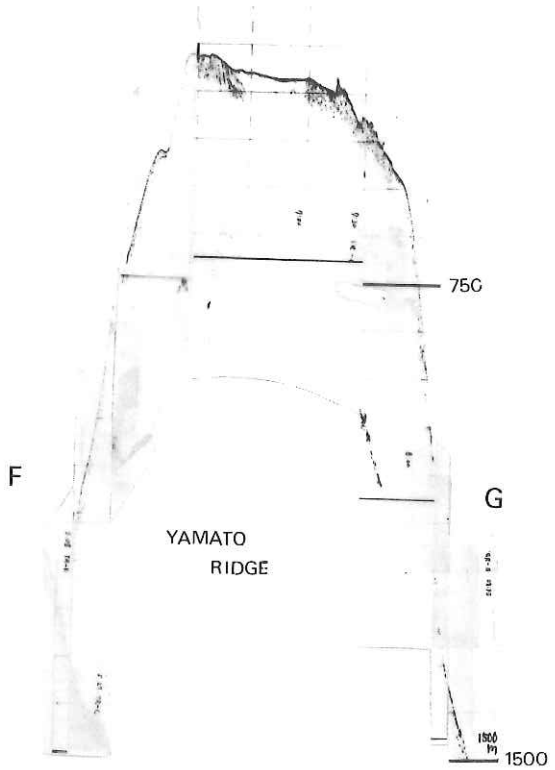
750
F
G
YAMATO
RIDGE
1500

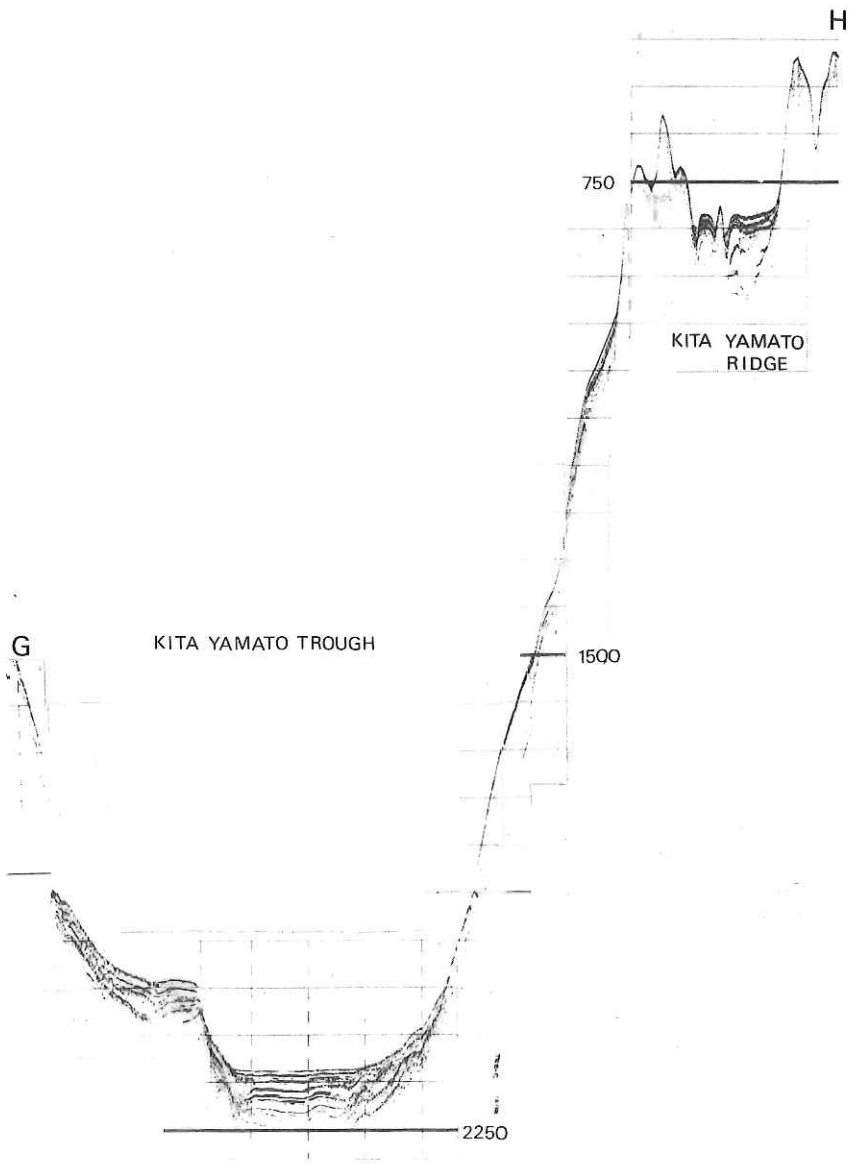
H
750
KITA YAMATO
RIDGE
G
KITA YAMATO TROUGH
1500
2250

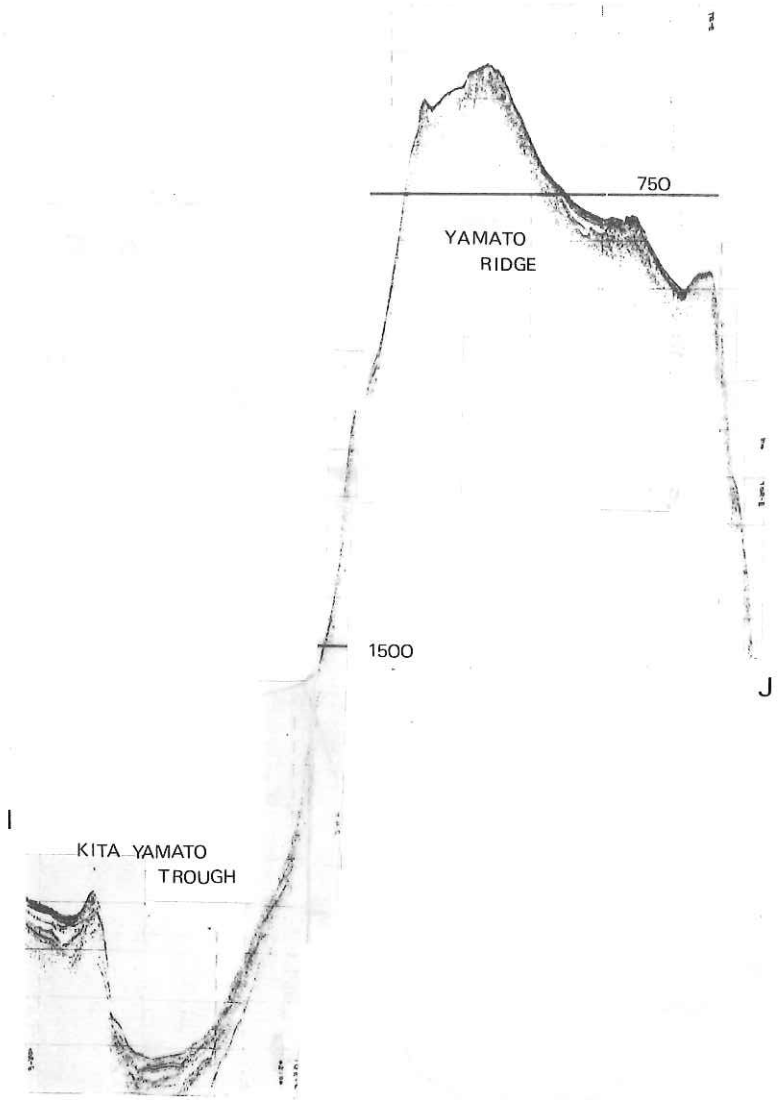
750
YAMATO
RIDGE
1500
J
I
KITA YAMATO
TROUGH

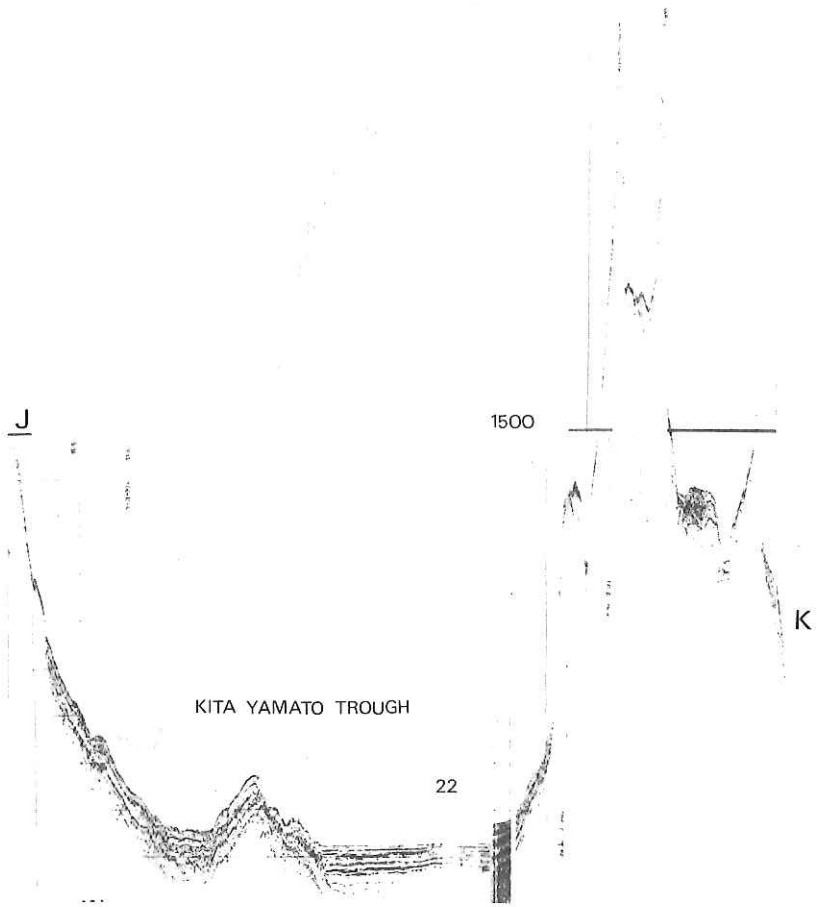
J
1500
K
KITA YAMATO TROUGH
22

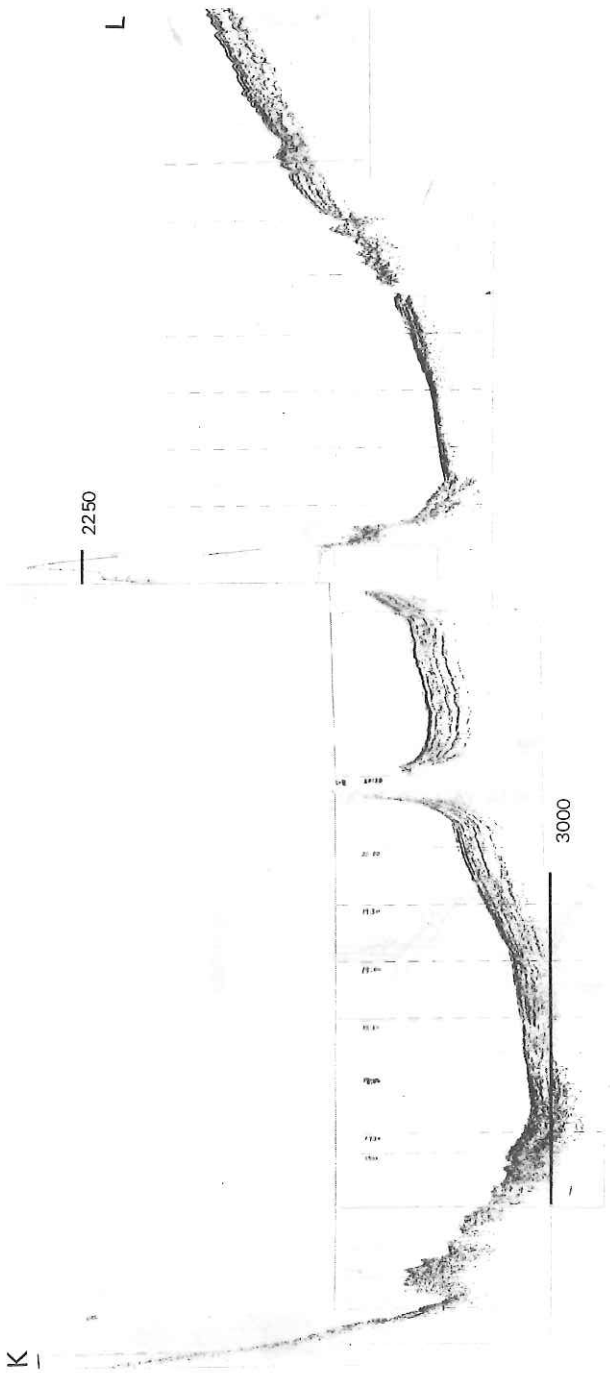
K
L
2250
3000

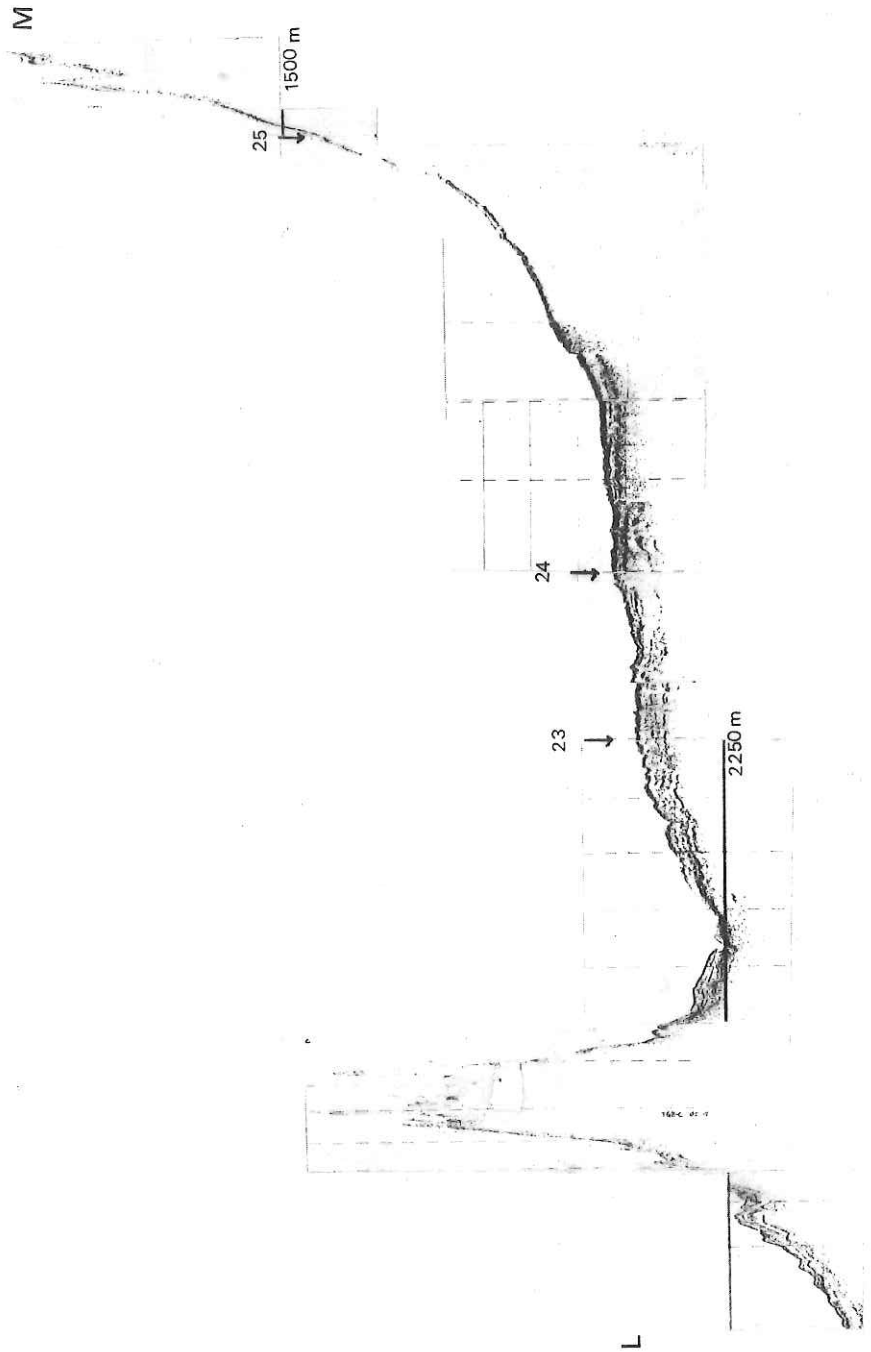
M
1500 m
25
24
23
2250 m
L

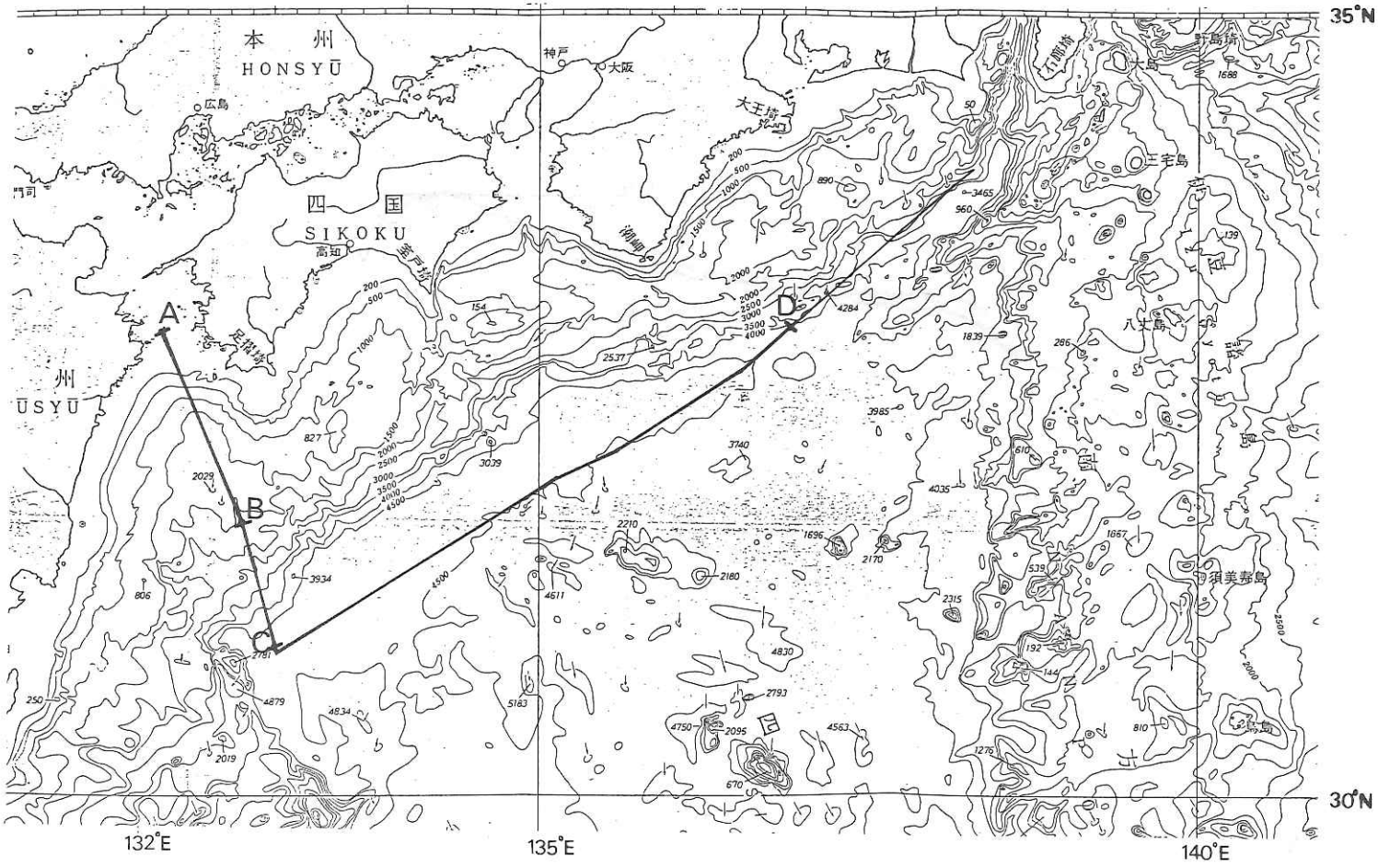

Fig. 7-4-5. Chart shwoing 3.5 kHz track lines in the Nankai Trough region. Thickened track lines with letter code correspond to selected profiles illustrated, in Fig. 7-4-6.

Fig. 7-4-6. Selected 3.5 kHz profiles in the Nankai Trough region.

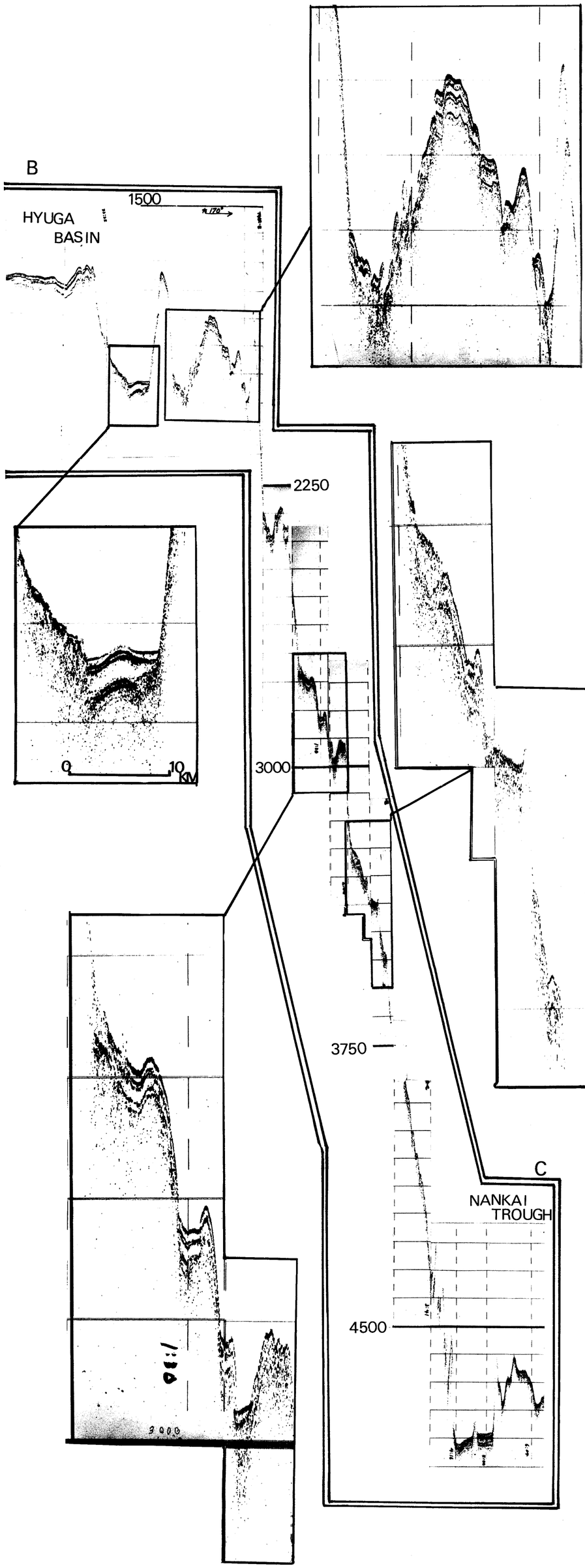
B
1500
HYUGA
BASIN
2250
3000
3750
C
NANKAI
TROUGH
4500
0
10
KM

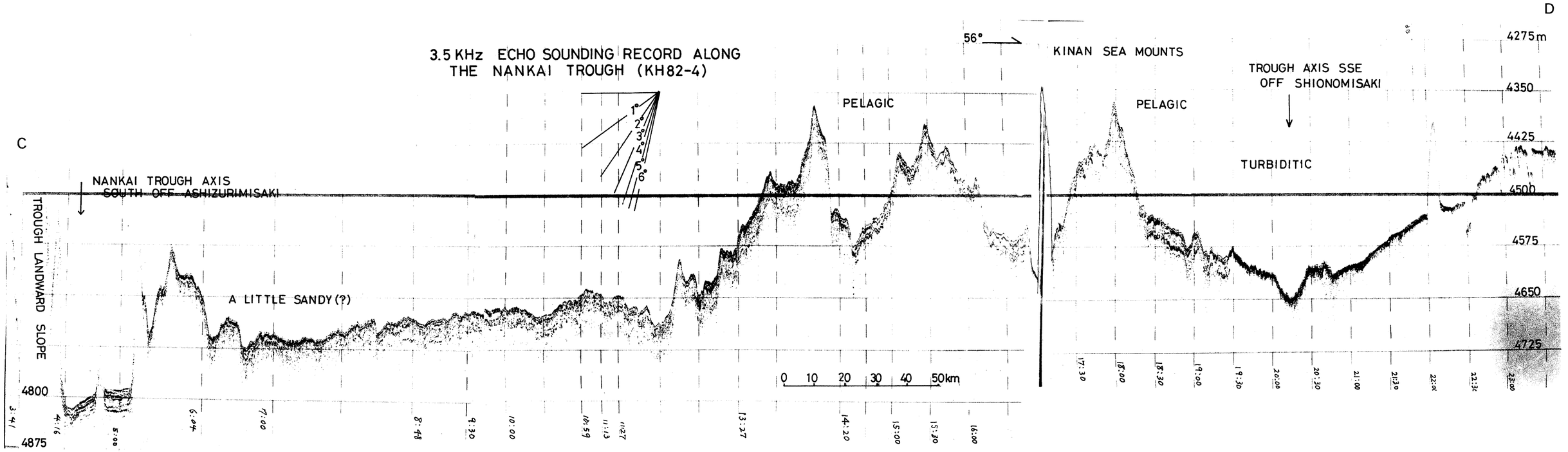
3.5 KHz ECHO SOUNDING RECORD ALONG
THE NANKAI TROUGH (KH82-4)
C
D
NANKAI TROUGH AXIS
SOUTH OFF ASHIZURIMISAKI
TROUGH LANDWARD SLOPE
A LITTLE SANDY(?)
PELAGIC
56°
KINAN SEA MOUNTS
PELAGIC
TROUGH AXIS SSE
OFF SHIONOMISAKI
TURBIDITIC
1°
2°
3°
4°
5°
6°
0 10 20 30 40 50km
4800
4875
4275m
4350
4425
4500
4575
4650
4725
3:41
4:16
5:00
6:04
7:00
8:48
9:30
10:00
10:59
11:13
11:27
13:27
14:20
15:00
15:30
16:00
17:30
18:00
18:30
19:00
19:30
20:00
20:30
21:00
21:30
22:00
22:30
23:00

7-5. PRELIMINARY STUDY ON THE SEDIMENT CORES FROM THE IZU-OGASAWARA REGION

T. TANAKA and N. OHYAMA

The greater part of the Izu-Ogasawara Arc is submerged and the topography of this area is diversified and complicated. There are various types of sedimentary basins in the Izu-Ogasawara Arc which include the broad and deep basins (Ogasawara Trough and Nishinoshima Trough), narrow and deep basins (Torishima Depression, etc.) and many small basins. The knowledge of the sediments and sedimentary processes in these intra-arc basins is very useful to understand the development of the island arc. During the cruise of KH-82-4, five 4m-piston cores were recovered in the middle part of the Izu-Ogasawara Arc in order to study the compositions of the sediments and to get representative sedimentary sequences in this area.

CORINGS AND METHODS OF ANALYSES

The 4m-piston corer is composed of a stainless pipe and an inner tube of vinyl chloride. We prospected that it was too hard for aluminium pipe piston corer to penetrate the volcanogenic substrata. Then we used the short and solid corer in the Izu-Ogasawara region. The piston core locations in the Ogasawara Trough are presented in Fig. 7-5-1, in association with the recently derived microphysiographic province map (Jacobi and Mrozowski, 1979). The photographs of the cores taken from the Ogasawara area are shown in Fig. 7-5-3 and the onboard visual core descriptions are presented in 7-2.

The cores were sliced using the plastic boxes (8 x 200 x 7 mm) and a fine steel wire. The plastic boxes were pushed into the sediment surface and undercut with the wire. The sample was then sealed with another box and wrapping sheet. For soft-X-radiograph these boxes were placed at a time on Fuji HS Softex Film. Source to sample distance on a X-ray unit was 60 cm. Voltage ranged between 45 and 50 kV, exposure time between 30 and 50 seconds. Amperage was kept constant at about 3 mA. Based on the X-radiographs, petrographical and sedimentological observations are carried out (Fujioka and Tanaka, in prep.).

CORE DESCRIPTIONS

Visual characteristics of all the cores in the Ogasawara Trough are the wide development of the volcanic ash turbidite layers which are mainly composed of brownish green volcanic glass, plagioclase, pyroxene and opaque minerals. Radiolaria rich foraminiferal nanno-oozes are intercalated with those volcanic ash turbidite layers. The mud parts are strongly mottled by bioturbation. Compared with the hemipelagic mud, the volcanic ash turbidite layers show marked differences in water content, shear strength and grain size. Fine lamination, normal grading and a sharp lower boundary are typical for all such tubidite layers. Occasionally middle parts of those turbidite layers show the convolute laminations and other distorted structures.

In some parts of these cores, sediments are already consolidated to a certain degree and show remarkable difference of vane shear strength from surrounding soft sediments. The grains of volcanic ash in the semiconsolidated part are slightly altered and transformed into clay minerals.

P-1

This core was taken from northwestern flat plain in the Ogasawara Trough (lat. 28°51.1'N, long. 141°14.1'E; water depth 4020 m). This site is slightly shallower than the main basin. The core length is 301 cm. The 3.5kHz echogram pattern in this area is semi-prolonged bottom reflector with continuous subbottom reflectors (Fig. 7-5-2). But the penetration depth is rather shallow (about 20 m). Sediment core is characterized by fine sand sized volcanic ash turbidite layers alternating with yellowish gray (2.5 Y 5/1) radiolaria rich foraminiferal nanno-oozes. The uppermost part of this core (0 to 15 cm) consists of grayish brown to brownish gray oxidized mud. Further down the colour becomes slightly greenish gray. The components of turbidite layers in this core are rich in translucent (acidic) volcanic glass, pale greenish brown volcanic glass, volcanic glass with microphenocryst, volcanic fragments and plagioclase grains. These layers show also compositional grading.

Core P-1 contains six volcanic ash turbidite layers (T-1: 15 to 44 cm, T-2: 66 to 92 cm, T-3: 120 to 130 cm, T-4: 226 to 249 cm: T-5: 255 to 273 cm, T-6: 282 to 300 cm). T-1 layer is rich in acidic volcanic glass shards, but

andesitic volcanic glass shards and microphenocryst containing glass are distinctly poor. The amount of volcanic fragments, benthic foraminifera fragments, feldspar grains increase in the lower part of this layer. T-2 layer is characterized by the high contents of brownish green glass shards and opaque grains. Ash particles are partly altered. The edge of these glass shards are worn out by probable moving processes.

According to the cross laminae of T-1 and T-2 layers, the turbidity current which formed the T-1 layer had flowed down from right to left and that of T-2 had flowed down in inverse sense (Fig. 7-5-4). Probably this is the reason of the difference of the compositions of sediments between the two turbidite layers. We will attempt to determine the azimuth of this core by magnetic analysis.

There are thin (1 cm) consolidated greenish layers at 105 cm and 188 cm. These layers contain greenish yellow clay lumps. At the intervals of 101 to 104 cm, 157 to 160 cm and 255 to 262 cm, sediments are semi-consolidated.

The layers of hemipelagic nanno-oozes are mottled by burrowing organisms. The types of bioturbation in this core are mainly *Planolites*(ϕ=1 to 2 cm) and *Chondrites* burrows. The burrows of *Zoophycus* are found at the upper part of T-1 layer.

P-2

The core P-2 was taken from the migrating sediment wave zone (lat. 28°29.3'N, long, 141°21.1'E: water depth 4100 m). The core length is 218 cm but the lower part below 96 cm from the top is flow-in. This core contains three volcanogenic turbidite layers and hemipelagic clay (T-1: 11 to 30 cm, T-2: 36 to 44 cm. T-3: 67 to 96 cm). All volcanogenic turbidite layers are mainly composed of greenish brown volcanic glass and feldspar grains. Two layers (T-1 and T-3) show fine parallel laminations in the middle part. As shown in the soft-X-radiographs these cross laminae represent oversteepened or recumbent-folded structure(Fig.7-5-4). This structure is similar to the water escape structure (Lowe, 1975). The hemipelagic nanno-oozes are moderately mottled by bioturbation (*Planolites*). From top to 96 cm this core does not show the sign of consolidation.

P-3

The core P-3 was recovered from the main flat plain in the central Ogasawara Trough (lat. 27°58.2'N, long. 142°31.9'E: water depth 4160 m). The 3.5 kHz subbottom profile shows semi-prolonged bottom echoes with discontinuous subbottom echoes, and the penetration depth was rather shallow (about 30 m) (Fig. 7-5-2). The core length is 115 cm. The characteristics of this core P-3 are the development of the well laminated mud layers and black ash layers with normal grading. Well laminated mud layers are found at the interval of 10 to 36 cm and 81 to 115 cm. They are relatively thick sections of distinct, thin (1 mm to a few mm), parallel laminae observable in X-radiographs. Some layers show gradings, and this is reflected by fining-up texture and vertical compositional changes. Bioturbation is absent in this mud type. Black ash layers are found at the intervals of 8 to 10 cm, 43 to 44 cm and 89 to 91 cm. These layers show normal grading and sharp lower boundary. There is no distinct compositional difference among the cores of P-1, P-2 and P-3.

P-4

The core P-4 was taken from the "sediment slide zone" in the western part of the Ogasawara Trough (lat. 27°56.7'N, long. 142°19.2'E: water depth 4100 m). The core length is 365 cm, but the part from 242 cm to bottom is flow-in. Although it was attempted to penetrate the surface sediment cover and reach to the "sediment slide" facies, P-4 core was too short to get the disturbed sediments. Piston core V 21-84 (Jacobi and Mrozowski, 1979) taken from this area showed the disturbed sediment facies below 290 cm. The sedimentary environments in this site can be divided into at least two stages after the large sediment slide.

Stage 1 (0 to 93 cm) Repeated Volcanogenic Turbidite Facies

This unit shows the high activity of turbidity currents. Eleven turbidite layers show the normal grading and parallel laminations, and the lower boudaries of these layers are sharp. Main components of these layers are volcanic glass, plagioclase, pyroxene and a few olivine grains. The grain size of this unit is the coarsest in all the cores obtained from the

Ogasawara Trough.

Stage 2 (93 to 242 cm)

This stage suggests the relatively calm sedimentary environment. The number and grain size of the volcanic turbidite layers decrease. Bioturbation in this stage is weaker than upper stage.

The age and cause of the change of sedimentary environment are unknown. It may be influenced by the change of volcanic activity in this area or the change of the flow pattern due to the slight change of the rugged topography.

P-5

The core P-5 was taken from the flank of a submarine high in the Nishinoshima Trough (lat. 27°29.4'N, Long. 139°28.9'E: water depth 3,230 m). The core length is 298 cm. The 3.5 kHz subbottom profile is not clear but shows hyperbolic echoes. The sediments are characterized by dull yellow orange (10YR6/4) homogeneous foraminiferal nanno-oozes and a few pumice grains, volcanic fragments and pebble sized calcareous siltstone with Mn-coating. Bioturbation is strong throughout the core. Coarse fraction of this sediment are composed of acidic volcanic glass and volcanic fragments. Coloured glass shards are rare.

REFERENCES

Fujioka, K. and Tanaka, T.: The preliminary study on the sediment cores from the Japan Trench region. Prel. Rep. of the Hakuho Maru Cruise KH-81-3 (in prep.).

Jacobi, R. D. and Mrozowski, C. L. (1979): Sediments and sediment waves in the Bonin Trough, western Pacific. Mar. Geol., 29, M1-M9.

Lowe, D. R. (1975): Water escape structures in coarse-grained sediments. Sedimentology, 22, 157-204.

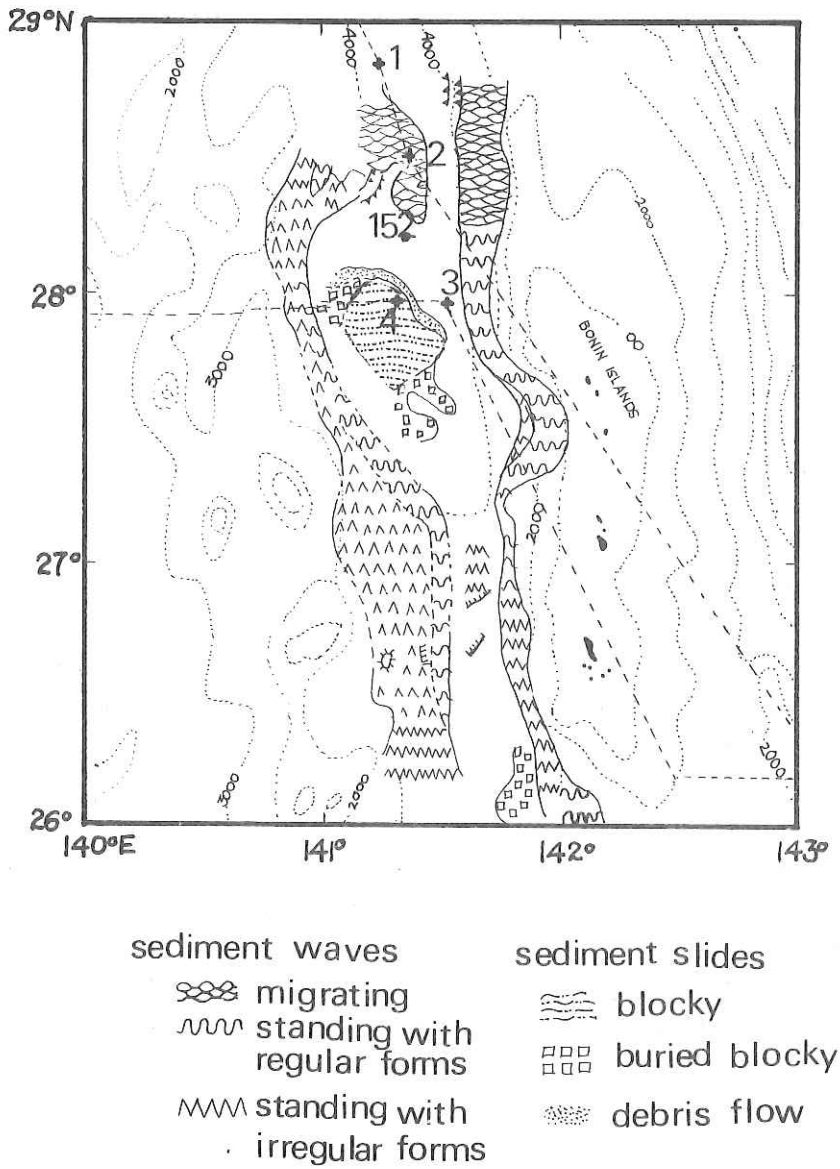

Fig. 7-5-1. Microphysiographic province map of the Ogasawara Trough (Jacobi and Mrozowski, 1979). 1, 2, 3 and 4 are the coring locations of P-1, P-2, P-3 and P-4, respectively. 152 indicates the location of core P-152, GH 79-3.

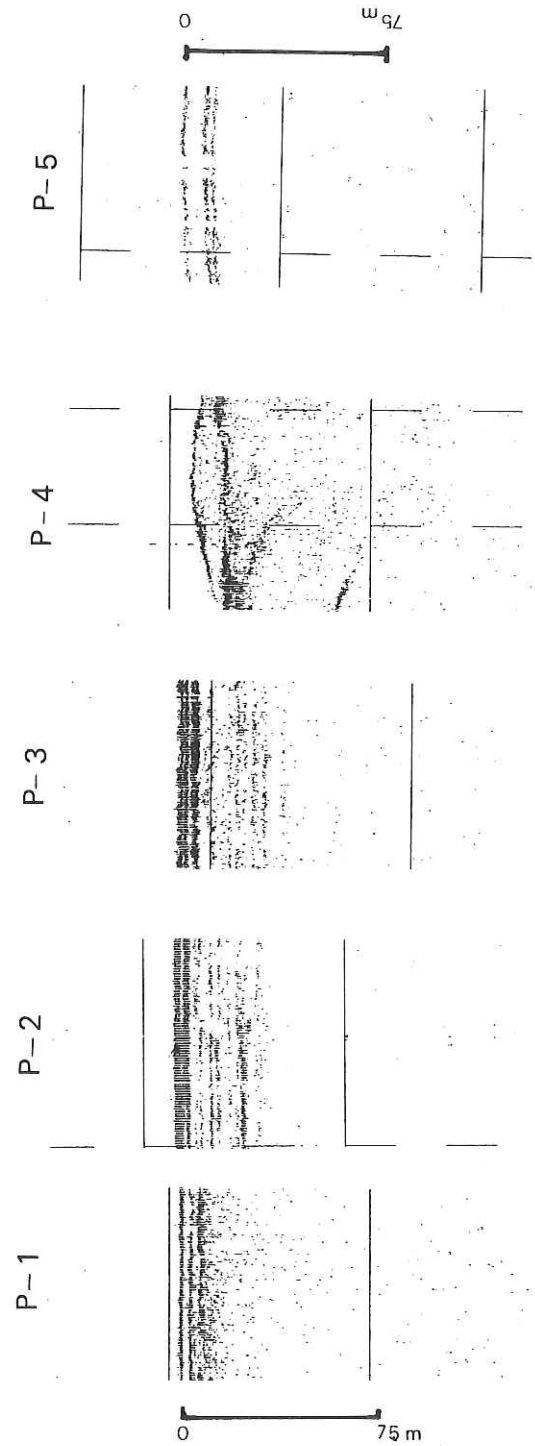

Fig. 7-5-2. 3.5 kHz echograms of coring sites P-1 to P-5.

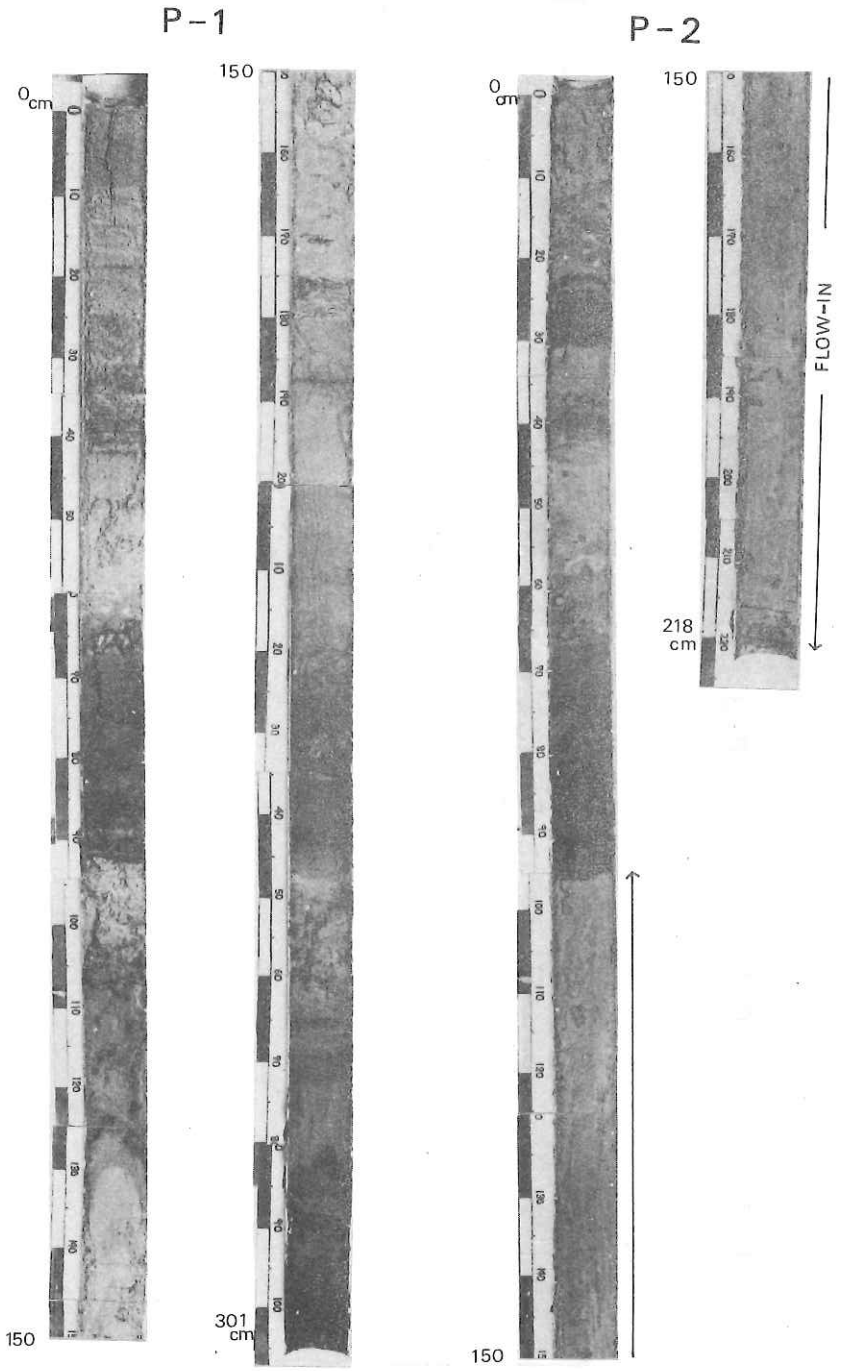

Fig. 7-5-3. Photographs of split piston cores P-1 to P-5. Length in cm.

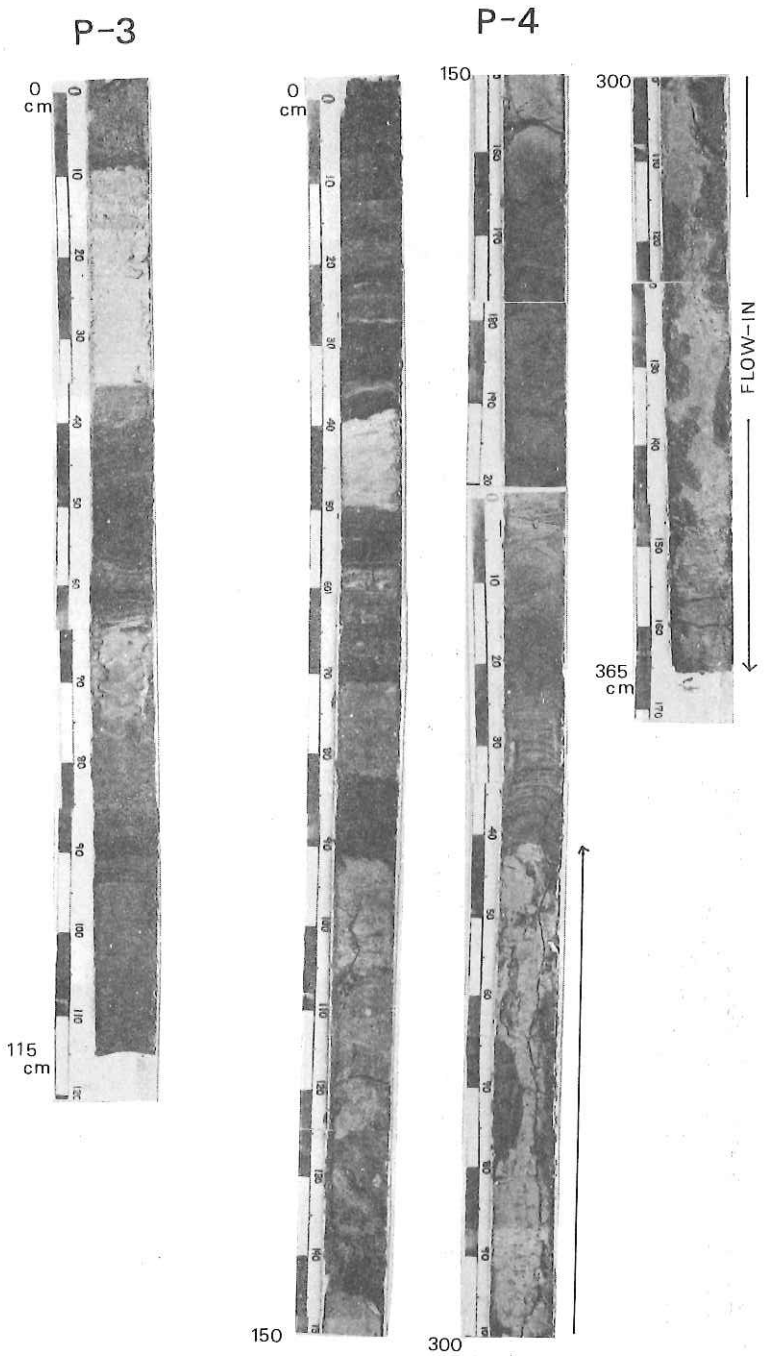
P-3
0
cm
115
cm
P-4
0
cm
150
150
300
300
365
cm
FLOW-IN

P-5

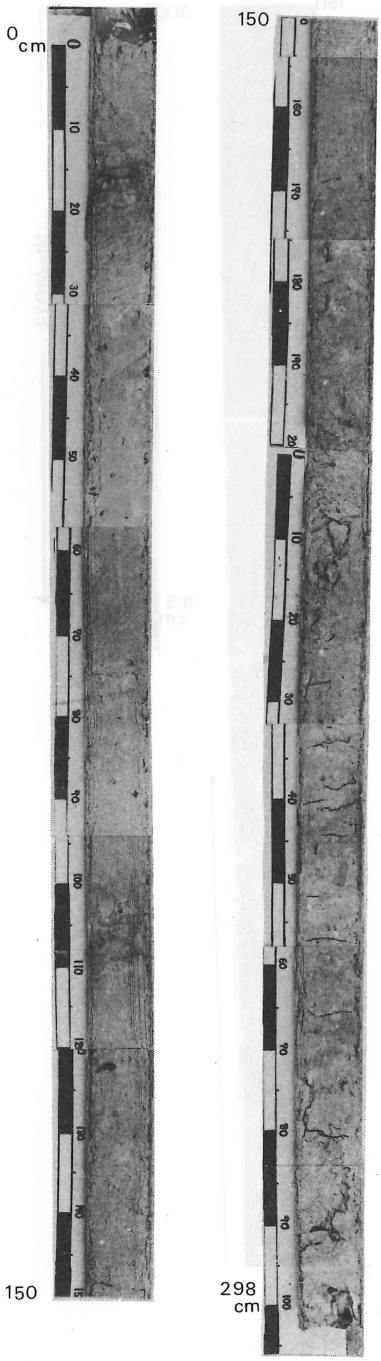

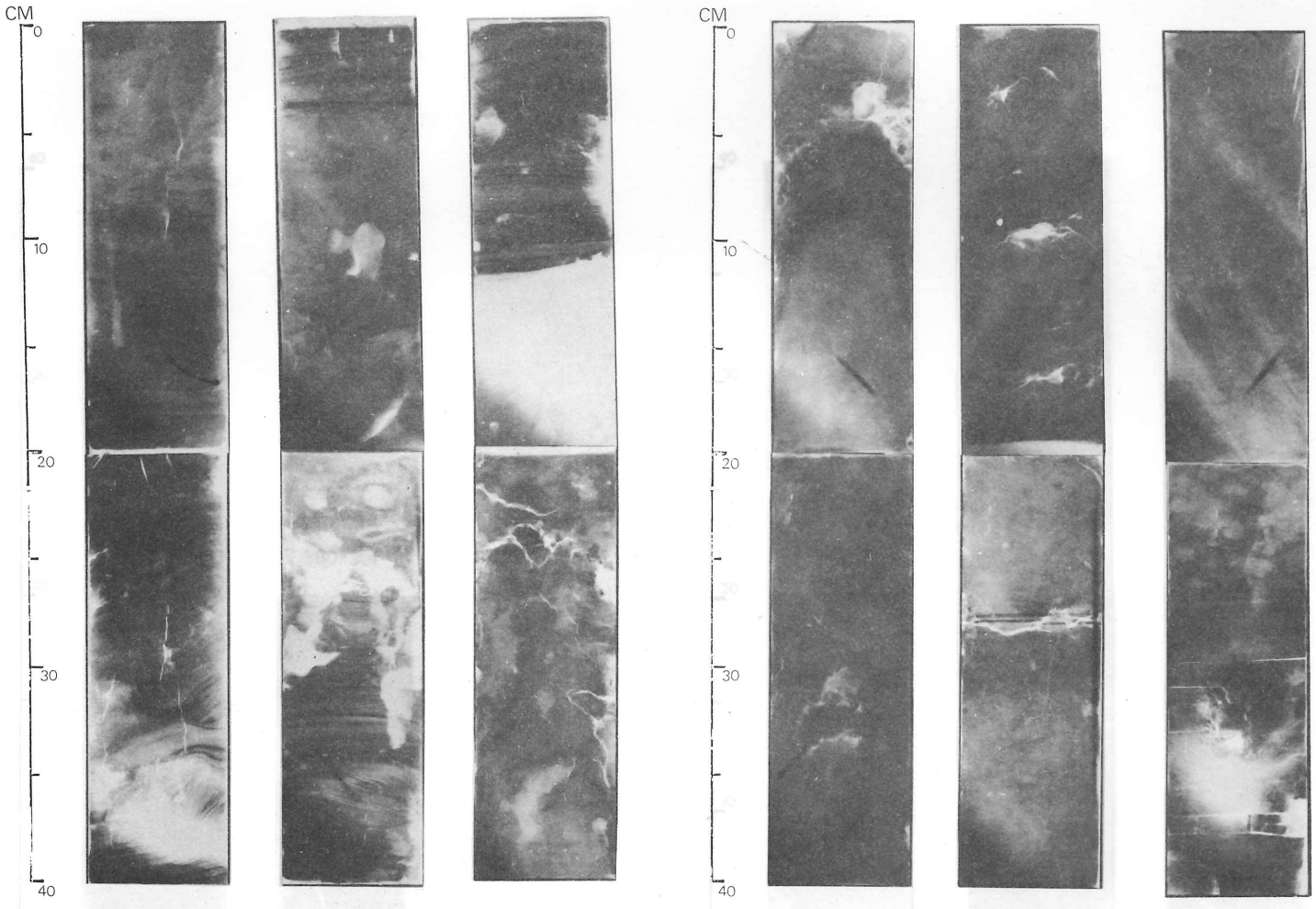

Fig. 7-5-4. X-radiographs of cores, P-1 to P-5. Numbers under the X-radiographs depict depth (in cm) from top of core.

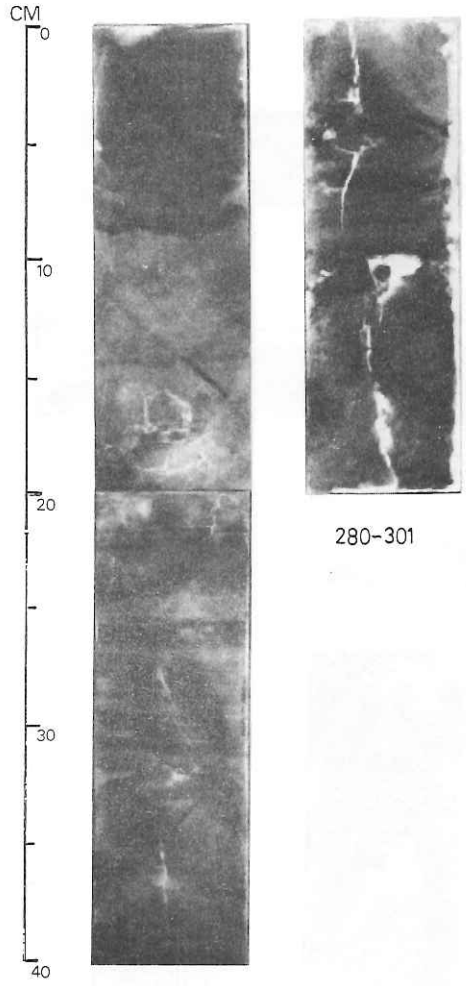
CM
0
10
20
30
40
280-301
240-280
P-1

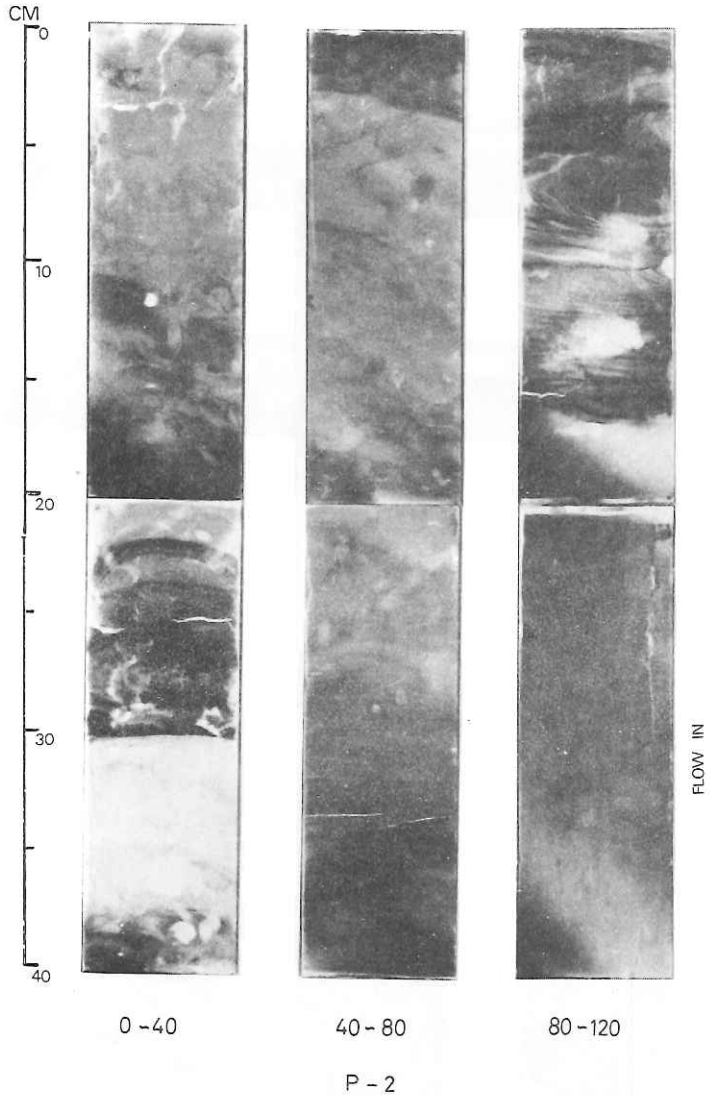
CM
0
10
20
30
40
FLOW IN
0-40
40-80
80-120
P-2

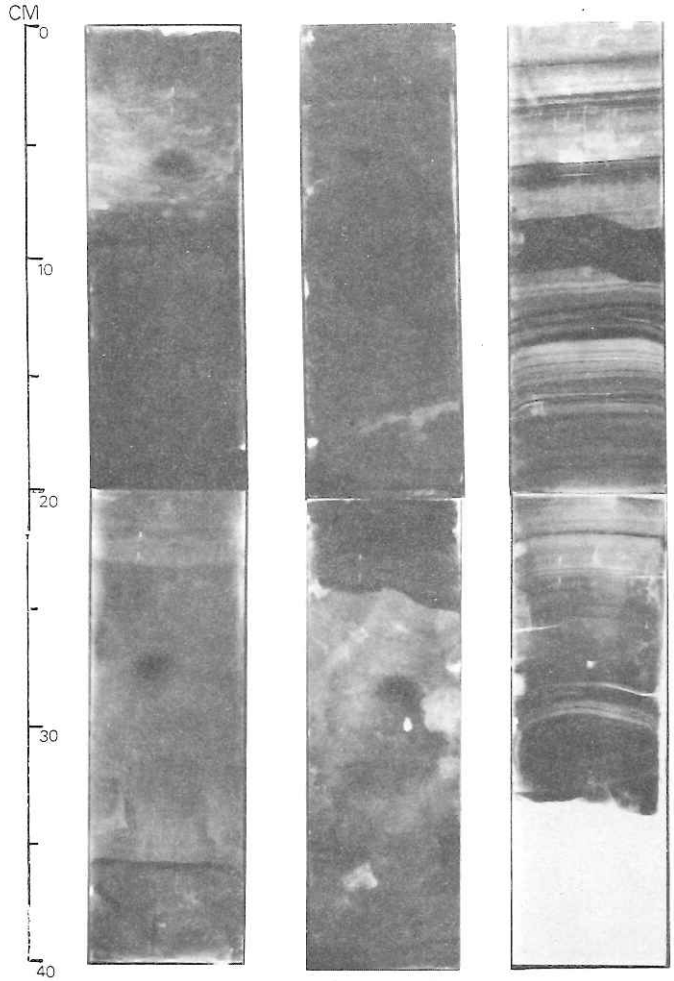

1 - 41 41 - 81 81 - 115

P - 3

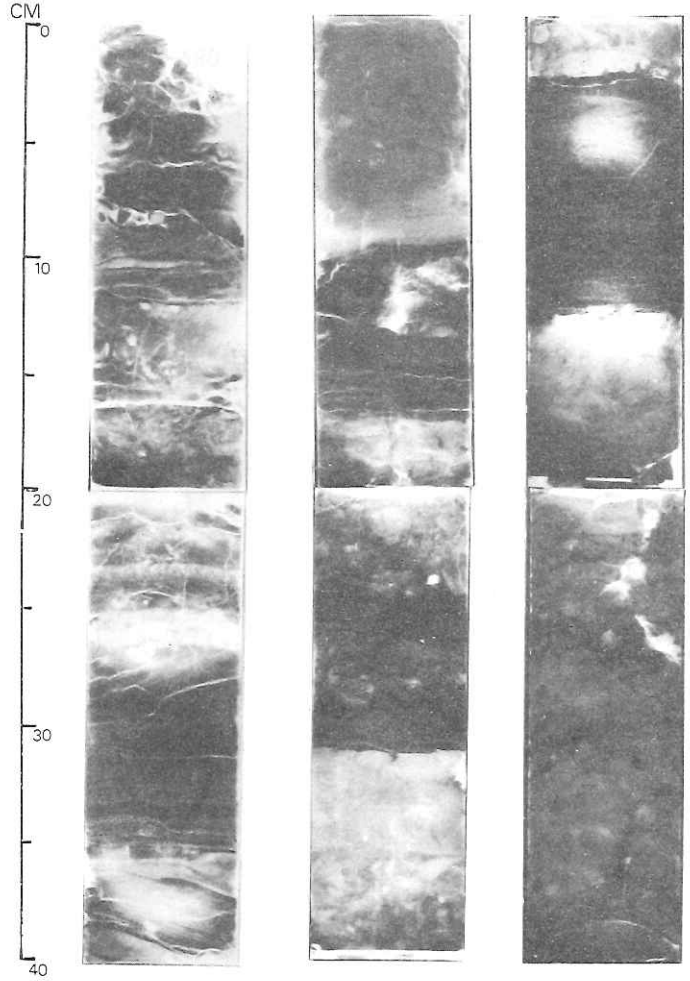

0 - 40 40 - 80 80 - 120

P - 4

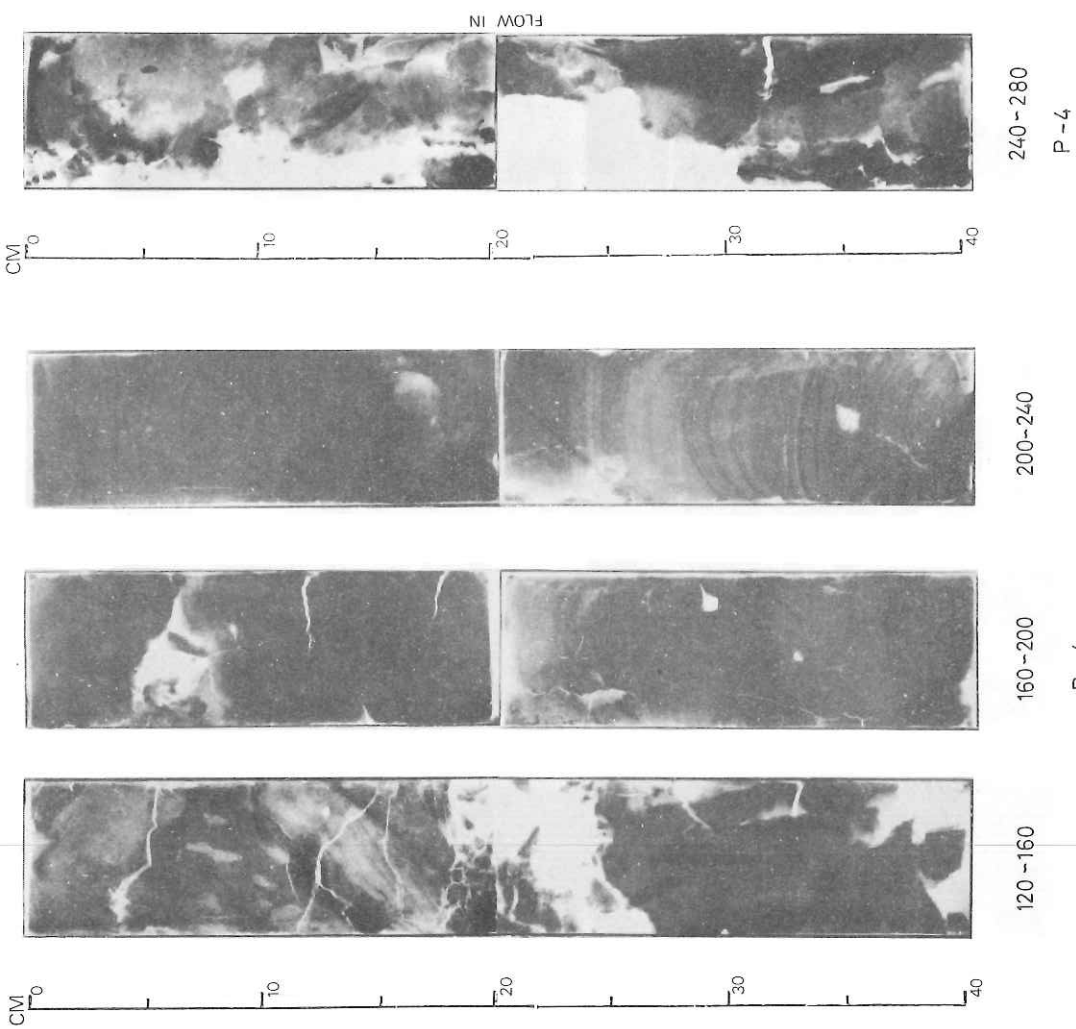
FLOW IN
CM
0
10
20
30
40
240-280
P-4
200-240
160-200
120-160
P-4

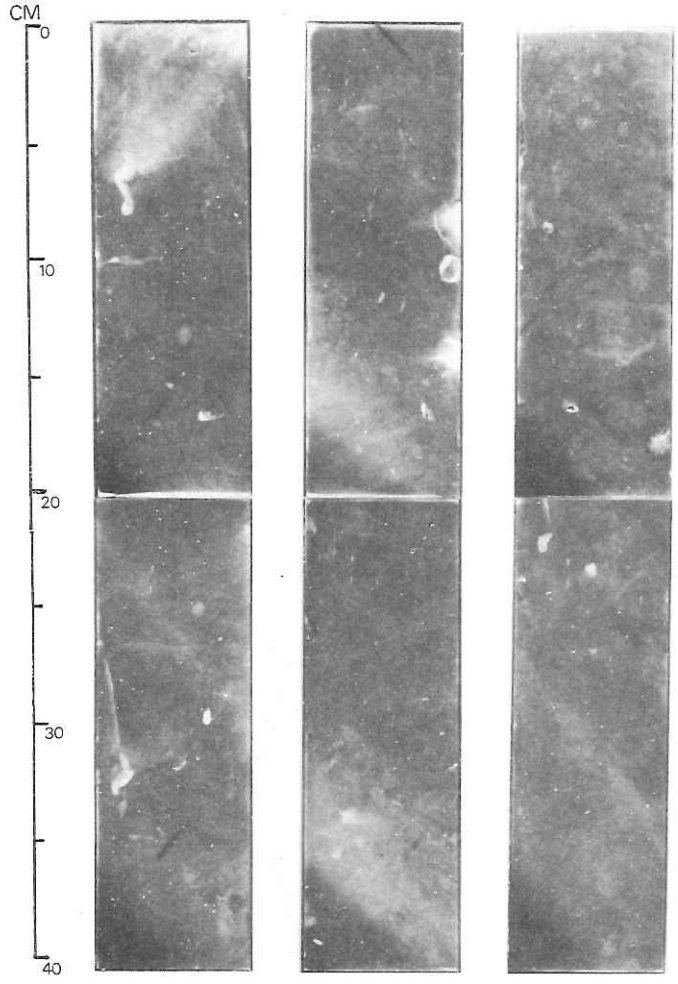

0 - 40 40-80 80 - 120

P - 5

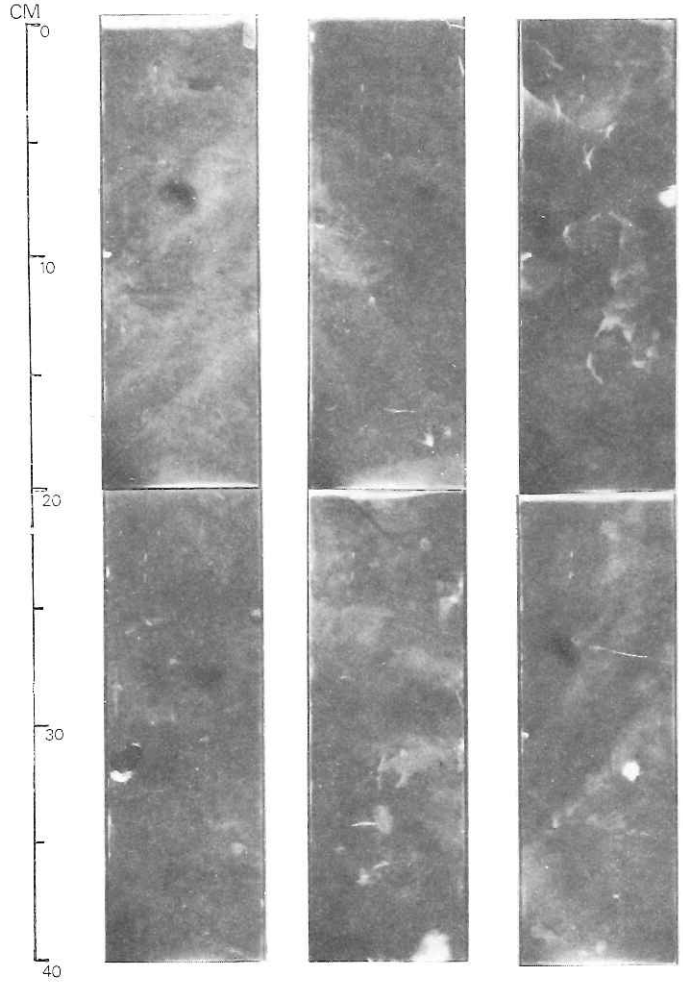

120-160 160-200 200-240

P - 5

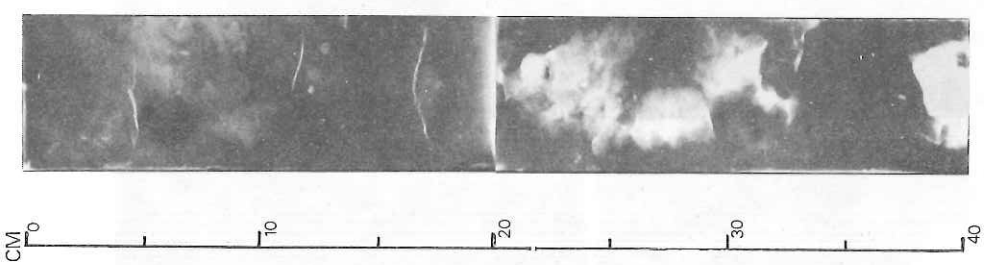
CM
0
10
20
30
40
240- bottom
P - 5

7-6. PRELIMINARY STUDY OF THE SEDIMENT CORES FROM THE SEA OF JAPAN REGION

T. TANAKA, Y. MIYATA. N. OHYAMA and Y. OGAWA

In the last decade, many workers have reported about the surface sediment of the Sea of Japan, and the history of oceanographic environment from late Pleistocene to Recent age has been made clear particularly by micro-paleontological studies (Ichikura and Ujiie, 1976; Arai et al., 1981; Tanimura, 1981). However, there have been few detailed investigations of sedimentary environment and their processes. One of the important purposes of the KH-82-4 cruise is to construct the maps showing the types of sediment and to infer the sedimentary processes based on the piston cores, bottom photographs and seismic profiles.

Nine piston corings were tried in the Sea of Japan region during the KH-82-4 cruise. Three cores (KH-82-4-15, -16 and -17) were obtained from the continental slope of Oki Island to the Yamato Basin and one core (KH82-4-19) was obtained in the northwestern deep part of the Yamato Basin deeper than 3,000 m. Three corings (KH82-4-23, -24 and -25) were carried out in the Tsushima Basin and on the middle part of slope. The other two trials failed.

The core locations are indicated in Fig. 7-6-1. The core logs record the lithology, texture, sedimentary and biogenic structures, colour and other characteristics observed visually onboard.

These cores were cut into slice of 8 mm thick and soft-X-radiographed in the shore laboratory with a standard method and observed, and some detailed descriptions have been added to the core logs. Smear slides of most characteristic sediment types are being analysed under a polarizing microscope. The columnar sections of these cores are shown in 7-2.

TOPOGRAPHY

According to the bathymetric charts and the 3.5 kHz subbottom profiles, these cores are subdivided into the following four groups;

1. Slope from the Oki Island to the Yamato Basin (KH 82-4-15, -16 and -17).
   This slope is 50-100 km wide and has a moderate seaward slope of 1.3%. It is covered by homogeneous hemipelagic mud and thinly

laminated mud rich in foraminifera. Bioturbation is moderate to high. The lower part of these cores show the folding structure which may be induced by slumping.

2. The foot of the steep slope from the Kita-Oki Ridge in the northwestern end of the Yamato Basin (KH 82-4-19)

   This core intercalates some foraminifera-rich layers and is characterized by the high water content. The sedimentation rate is very high and the vane shear strength is very small.

3. The rugged floor of the Tsushima Basin (KH 82-4-23 and 24)

   The most characteristic feature of the sediments in this area is the existence of well-developed turbiditic thin sand and mud layers. But it seems that the extent of each turbiditic layer is rather narrow and its lithology varies due to the bottom topography.

4. The middle slope of the Tsushima shelf to the Tsushima Basin (KH 82-4-25)

   The sediments at this location are characterized by dark olive gray mud strongly mottled by bioturbation and well laminated silt layers. The lower part of the core is composed of the disturbed sediment owing to debris flow.

DESCRIPTIONS OF CORES

Preliminary petrographical and sedimentological examinations of these cores revealed several sediment types. The colour of these sediment is variable and complicated basically by the contents of terrigenous material and pyritic micronodules. In this report we describe the core KH 82-4-23 particularly in detail as a representative of the sedimentary sequences in this area. The main reason of the choice is that the other cores taken from the Sea of Japan have appearence similar to the core -23 and slight differences in lithology of the others seem to be controlled by their individual sedimentary environments. We include photographs as many as possible in this report. The soft-X-radiographs should facilitate the distinction between various types of sediments and assist sample selection from the core meterial in future.

STATION 23

The core KH 82-4-23 was recovered at a station of a slightly rugged floor

east of the Tsushima Basin with depth of 2,080 m. The 3.5 kHz subbottom profile represents semi-prolonged bottom echoes with semi-prolonged, discontinuous subbottom reflectors, and the penetration depth is about 80 m.

0-147 cm: The uppermost part of this core is brownish black (2.5 Y 3/1) clay which has a lot of diatom and sponge spicule fragments, and quite a few calcareous biogenic components are contained. The main lithology between the top of the core and the horizon of Oki ash (135 cm) is dark olive gray (2.5 GY 3/1) to olive black (10 Y 3/2) homogeneous mud. This mud has no definite structures other than intercalating only a thin laminated sand layer (at 60 cm) which is slightly bioturbed. Tiny pyritized worm burrows (ϕ=0.5 mm) were observed around the Oki ash layer.

147-148 cm: Foraminiferal thinly laminated layer.

148-200 cm: Tiny pyritized worm burrows are scattered. The mud has many terriginious components and pyritic micronodules and few siliceous biogenic components.

201-202 cm: This non-transparent layer for soft-X-ray is composed of fine silt sized calcite and ankerite grains.

202-340 cm: This interval is the alternation of the foraminifera rich dark greenish gray (7.5 Y 3/1) thinly laminated mud and the dark olive gray (2.5 GY 4/1) turbiditic mud which is composed entirely of very poorly sorted slity clay. Based on a microscopic observation, it was made clear that such foraminiferal laminite is the alternation of the pyritic micronodules rich clay layer which contains foraminiferal fragments and the very thin (1-2 mm) layer of well sorted terrigenous silts. Thin sand layers are sometimes underlain by the turbiditic mud layer. These sands consist of quartz, feldspar, hornblende, pyroxene, glauconite, benthic foraminiferal fragments, unspecified carbonate fragments and sometimes olivine. Such heavy mineral assemblage suggests that most sand fraction of the terrigenous sediments at this coring site has been supplied from San-in district and not from Korea Peninsula (Chough et al., 1981). The turbiditic mud layers are very poorly sorted silty clay rich in diatom and sponge spicule, and show a vague normal grading. The uppermost part of such mud layers are very rich in diatom and sponge spicule fragments.

The following sedimentary sequences are recognized by soft-X-ray radiographs.

Foraminiferal thinly laminated layer

↑

Turbiditic mud layer

↑

Thin sand layer

However, the average sizes of quartz grain in each layer differ as follows.

Thin sand layer > Thinly laminated layer > Turbiditic mud layer

367-373 cm: At ash layer showing normal grading slightly.

400-450 cm, 520-550 cm and 590-660 cm: The turbiditic sand layers become thicker and coarser and form the parallel laminations. But foraminiferal thinly laminated layers are absent. In place of the laminated layers there are homogeneous dark greenish gray (7.5 Y 3/1) mud layers which have the tiny pyritized worm burrows. The sand layers are strongly disturbed by large (ϕ=5 to 10 mm) burrows. The sedimentary sequence of this interval is as follows;

Bioturbed homogeneous mud

↑

Turbiditic mud layer

↑

Laminated turbiditic sand layer

375-400 cm, 560-585 cm and 730-750 cm: These intervals are characterized by the alternation of the foraminiferal thinly laminated layer and the turbiditic mud layer which underlies the very thin turbiditic sand layer. Such sedimentary sequence is similar to that of the sediments at an interval from 202 to 340 cm.

450-480 cm, 500-520 cm, 660-725 cm and 750-830 cm: These sediments are thickly deposited homogeneous grayish clay layers with tiny pyritized worm burrows.

The sediment column of core KH 82-4-23 is constructed by the repeated sequences of that mentioned above.

The results of the above observations, showing the remarkable change in sedimentary regime with time, may reflect the modification in the supply processes of terrigenous component into the basin and the change of the effect of bioturbation.

The followings are the brief core descriptions of the other cores.

STATION 15

The core KH 82-4-15 was taken from the upper slope in the southwestern part of the Yamato Basin (lat. 36°44.3'N, long. 133°33.6'E) at a station with depth of 1,080 m. The sediment of this core is mainly composed of olive black (7.5 Y 3/2) to dark greenish gray (5 G 4/1) homogeneous silty clay. The foraminiferal thinly laminated layers are observed in places below the Oki ash layer. There are few turbiditic sand and mud layers. Activity of the bioturbation is moderate. The large burrow structure (ϕ=3 to 5 mm) is main bioturbation type at this location and the activity of the tiny pyritized worm burrows is not so intense.

According to Furuta (Furuta et al., this volume) two volcanic ash layers can be correlated to the specific key ash layers, they are Oki ash (242-244 cm) and at ash (450-464.5 cm).

Although the appearence of the foraminiferal thinly laminated layers seem to be coincident with that in the core 82-4-23 in the Tsushima Basin, the tendency of the increase in the turbidity current activities below the At ash layer is not observed.

STATION 16

The core KH 82-4-16 was recovered from a station at the middle part of this slope (lat. 37°06.2'N, long, 133°54.2'E) with depth of 1,740 m. Oki, At and Aso-4 ash layers are found at the interval of 104-106cm, 202-203 cm and 700 -702 cm, respectively. The upper part of this core is olive black homogeneous clay which is strongly disturbed by 3 to 5 mm diameter worm burrows. Throughout the core, the lithology is quite similar to the core of St. 15 without the type and activity of bioturbation. The lower part of this core is deformed by slump fold.

STATION 17

The core KH 82-4-17 from the lower part of this slope (lat. 37°15.4'N, long. 134°16.2'E; water depth 2455 m) contains five identified ash layers (Ah: 60-65 cm; Oki: 76-78 cm; at: 280-290 cm; Ym: 364-366 cm; Aso-4: 711-714 cm).

But below the At ash layer the lithofacies is similar to that of KH 82-4-16. The influence of turbidity current is not detectable at this site. The peculiar character of this core is the unusual development of tiny pyritized worm burrows.

STATION 19

The core KH 82-4-19 was taken from the foot of the steep slope in the northwestern end of the Yamato Basin (lat. 38°29.1'N, long. 134°34.6'E; water depth 3010 m). The 3.5 kHz reflection profiles show the continuous sharp bottom echoes with some continuous, parallel subbottom reflectors and a relatively large penetration depth. This core intercalates some foraminifera rich layers, and has a extremely high water content. Dark greenish gray (7.5 GY 3/1) clay is alternating with dark olive gray (2.5 GY 3/1) foraminifera rich thinly laminated mud throughout the core. The type of bioturbation is tiny pyritized worm burrows but its activity is weak.

STATION 24

The core KH 82-4-24 was recovered from the rugged floor at the foot of the Tsushima Shelf (lat. 36°25.6'N, long. 131°15.3'E; water depth 2020 m). The 3.5 kHz echogram at this site represents that the surface reflector is considerably prolonged and the subbottom reflectors are discontinuous and the maximum penetration depth is shallower than that at 82-4-23. From the top of the core to the foraminiferal thinly laminated layer (171 cm) the sediment type is quite similar to that of 82-4-23. Below this layer, however, the sediment is characterized by the well developed thick alternation of turbiditic sand and mud layers. The sedimentation rate in this part is as twice as that of KH 82-4-23. The slight difference of subbottom echogram pattern of KH 82-4-23 from that of KH 82-4-24 reflects the difference in concentration of coarse and bedded sediments. The lower part of the core shows slump structures.

STATION 25

The core KH 82-4-25 was taken from middle slope of the continental shelf (lat. 36°02.9'N, long. 131°05.9'E). The subbottom profile of 3.5 kHz represents the hummocky reflection patterns when the ship kept its position for piston coring.

From the top of the core to 520 cm excluding 100-200 cm this core displays bioturbation facies. Parallel laminated coarse silt to fine sand layers are intercalated from 517 cm to 660 cm. From 660 cm to the bottom the sediment shows the debris flow facies which is composed of varied coloured soft to semi-consolidated angular pebble sized clasts of mud with the matrix of dark olive gray mud.

REFERENCES

Arai, F., Oba, T., Kitazato, H., Horibe, Y. and Machida, H., 1981. Late Quaternary tephrochronology and paleo-oceanography of the sediments of the Japan Sea. Quaternary Res., 20, 209-230.

Chough, S. K., Tamaki, K., Bahk, K. S., Inoue, E. and Yuasa, M., 1981. Heavy minerals from the Oki Spur, Japan Sea. Bull. Geol. Surv. Japan, 32, 487-501.

Ichikura, M. and Ujiie, H., 1976. Lithology and planktonic foraminifera of the Sea of Japan piston cores. Bull. Nat. Sci. Mus., Ser. C. (Geol), 2, 151-178.

Tanimura, Y., 1981. Late Quaternary diatoms and paleo-oceanography of the Sea of Japan. Quaternary Res. 20, 231-242.

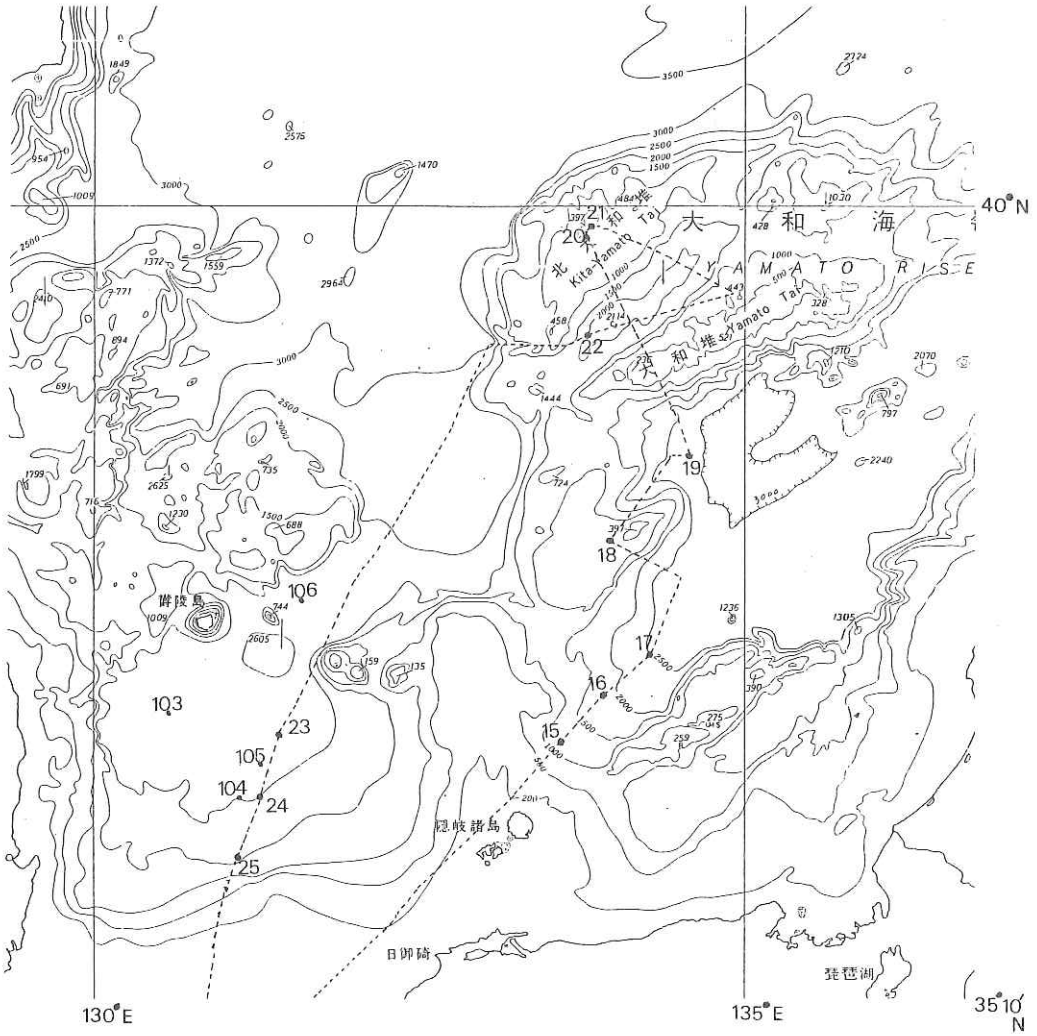

Fig. 7-6-1. Chart of the southwestern region of the Sea of Japan showing the ship tracks and sampling locations. 103 to 106 are the coring sites of GH-77-2.

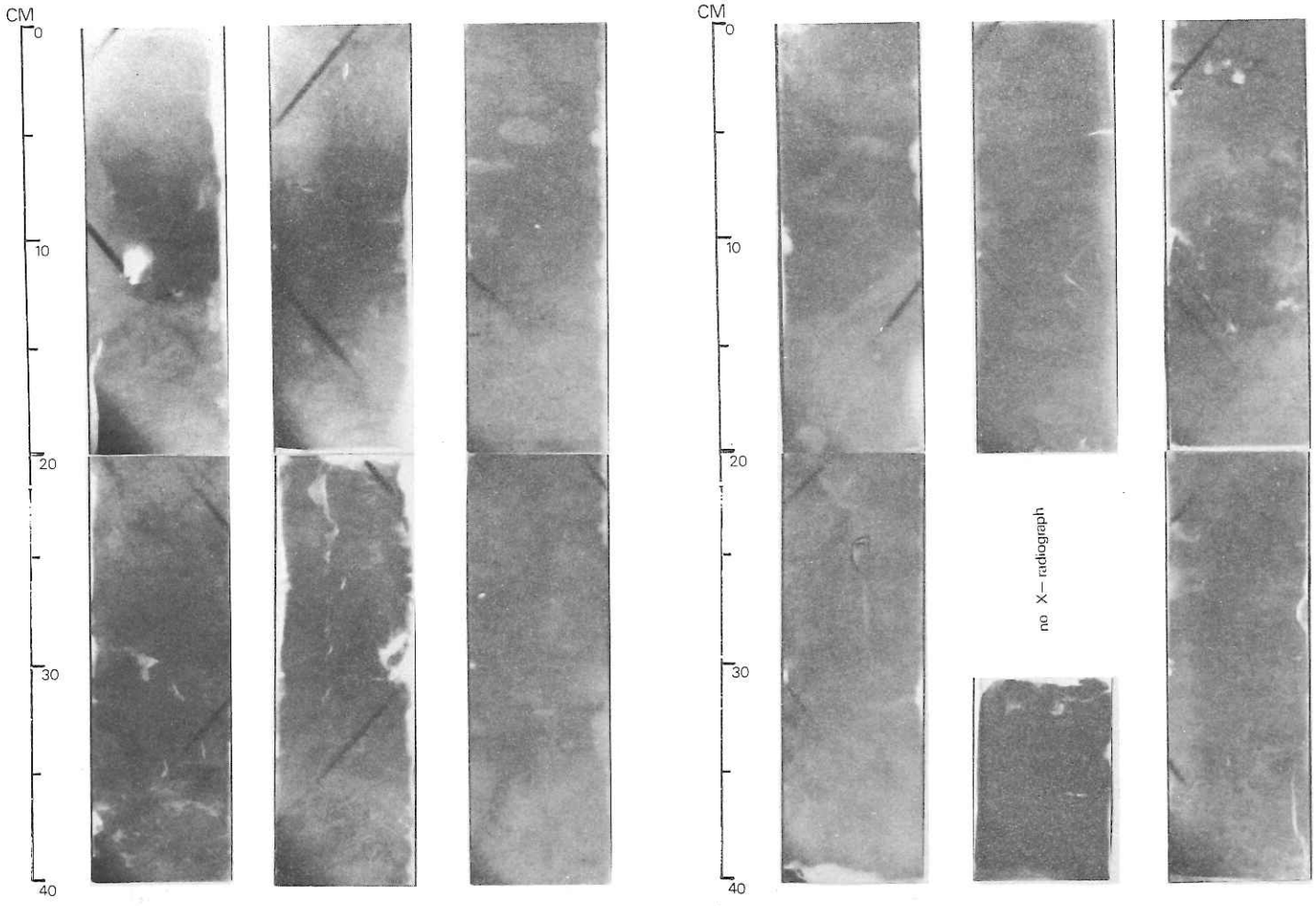

Fig. 7-6-2. X-radiographs of cores KH 82-4-15 to -17 and -23 to -25. Numbers under the X-radiographs depict depth (in cm) from top of core.

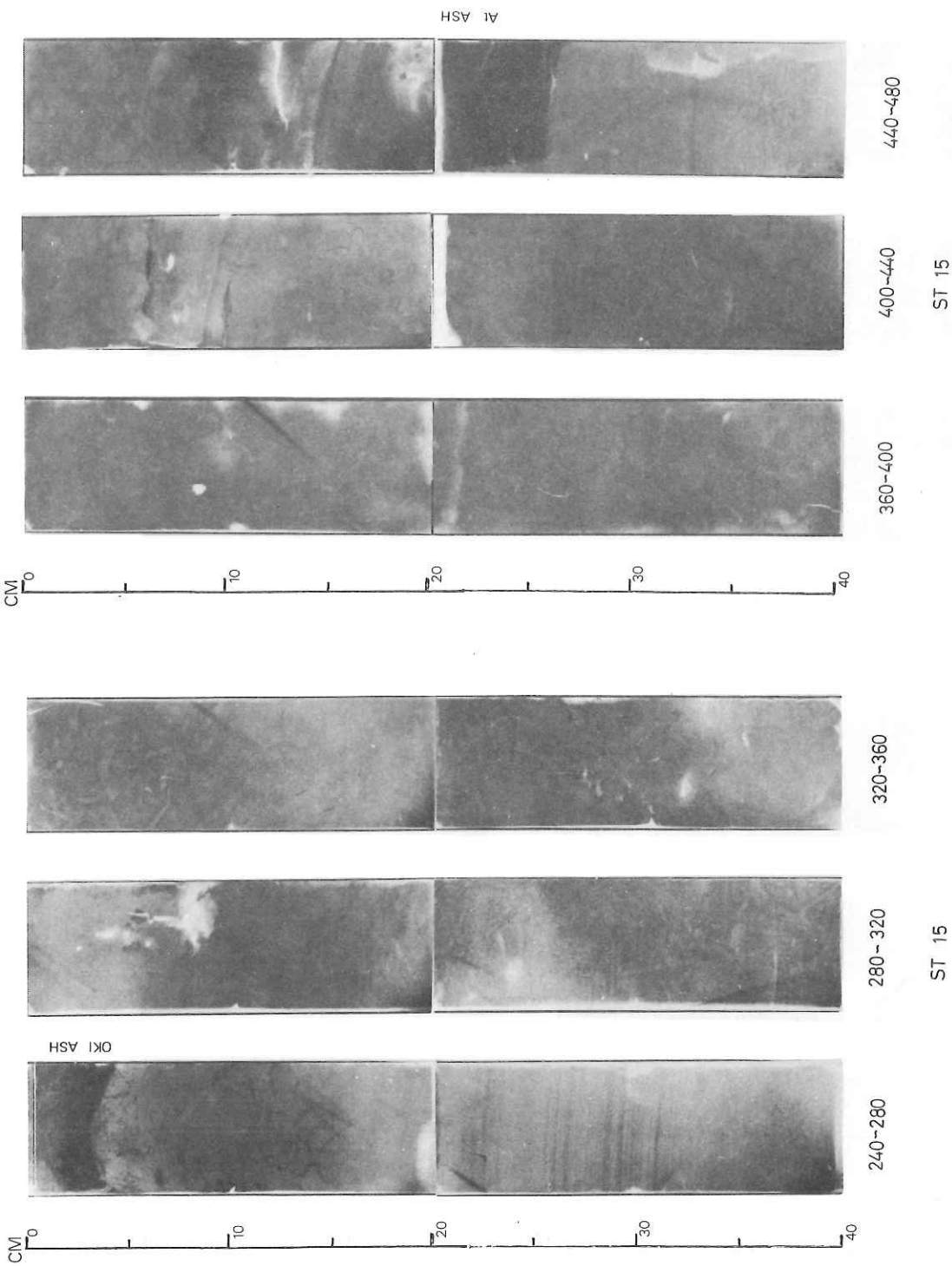
OKI ASH
AT ASH
CM
0
10
20
30
40
240-280
280-320
320-360
360-400
400-440
440-480
ST 15
ST 15

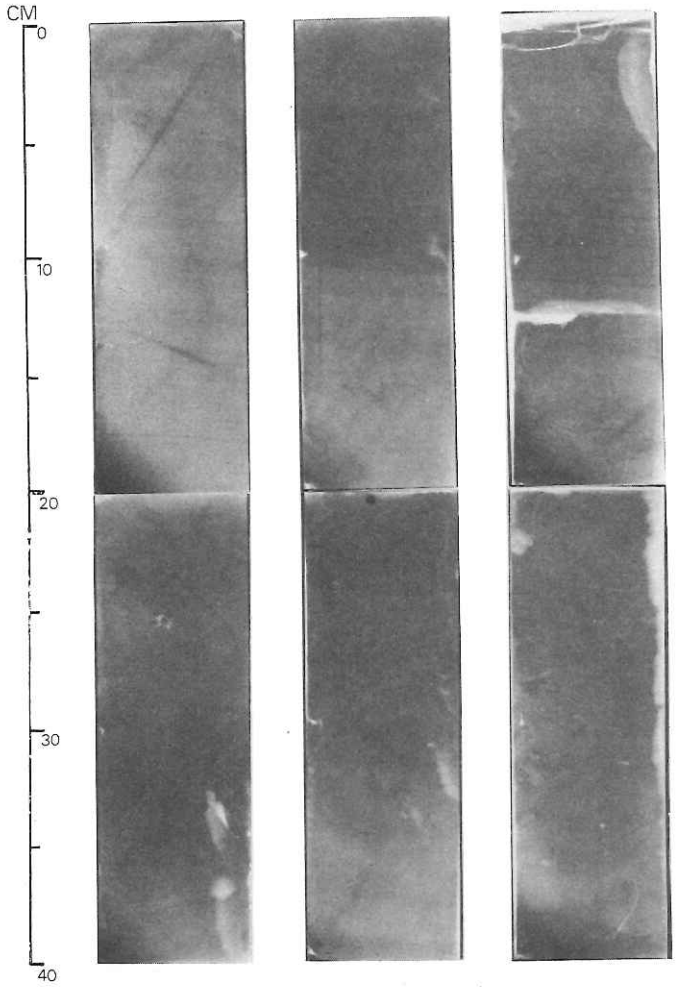
CM
0
10
20
30
40
480-520
520-560
560-600
ST 15

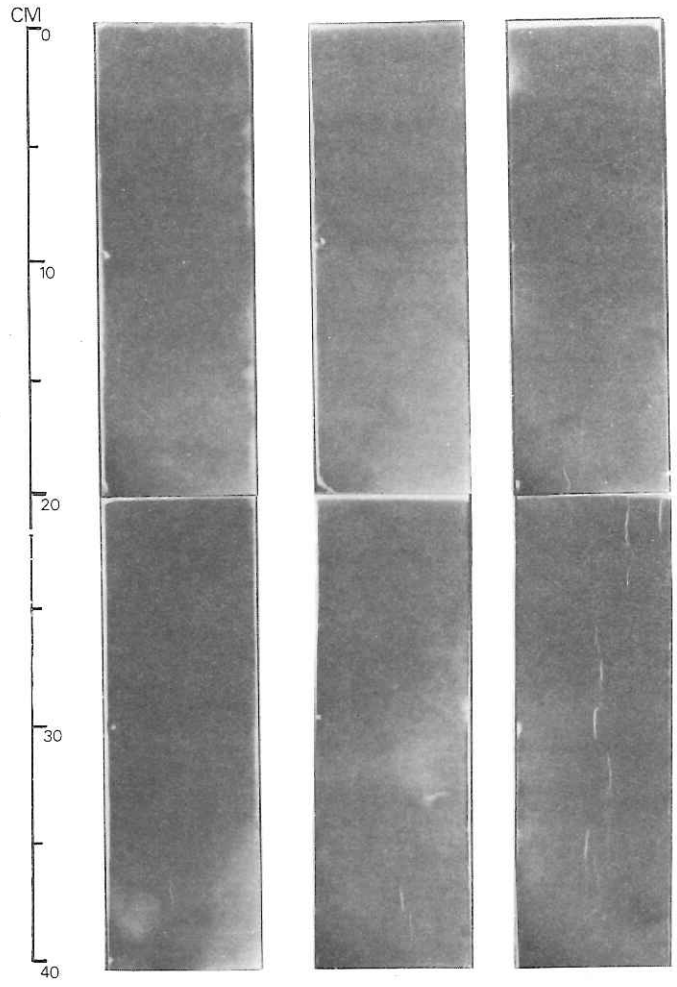
CM
0
10
20
30
40
600-640
640-680
680-720
ST 15

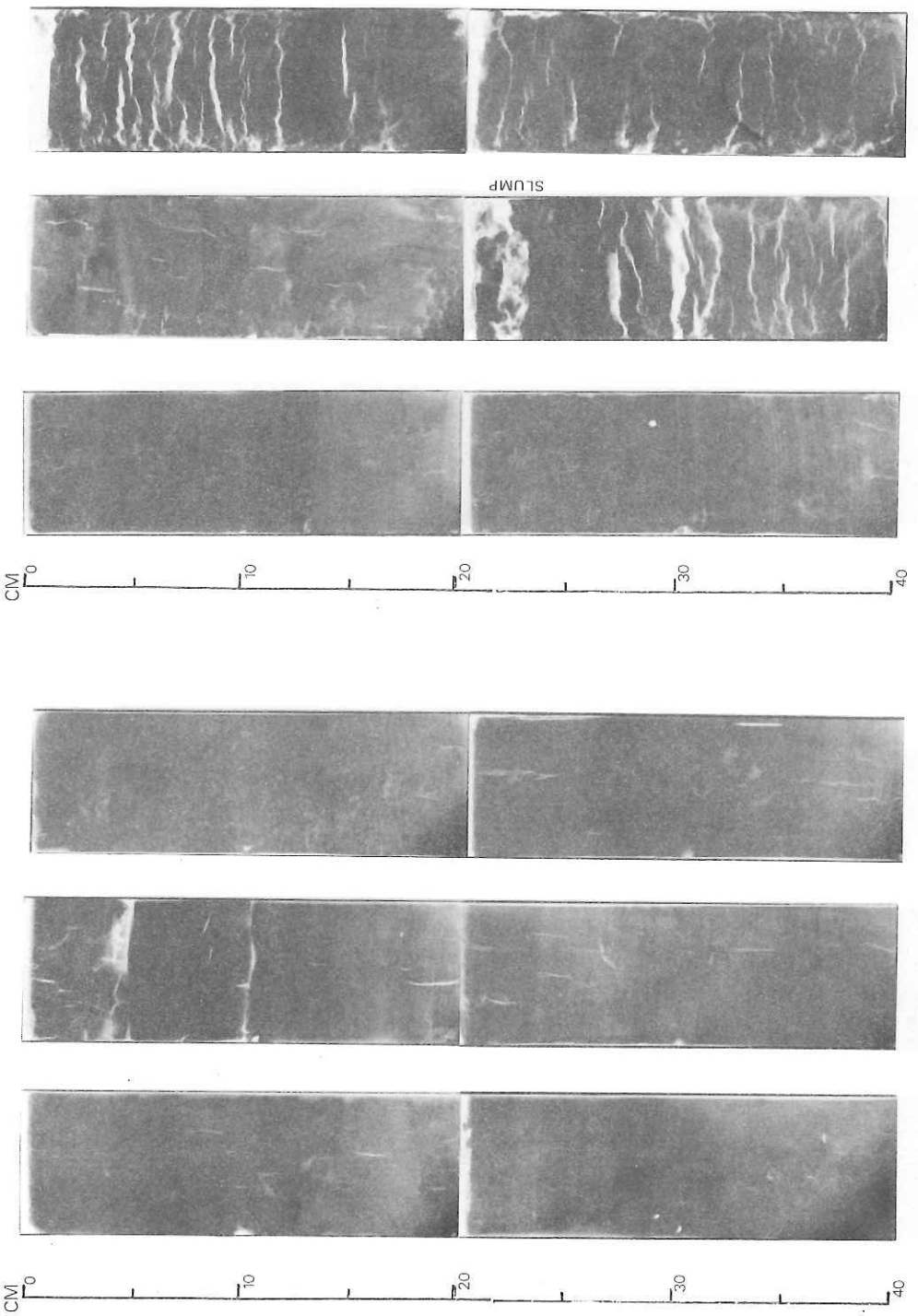
CM
0
10
20
30
40
720-760
760-800
800-840
ST 15
CM
0
10
20
30
40
840-880
880-920
SLUMP
920-960
ST 15

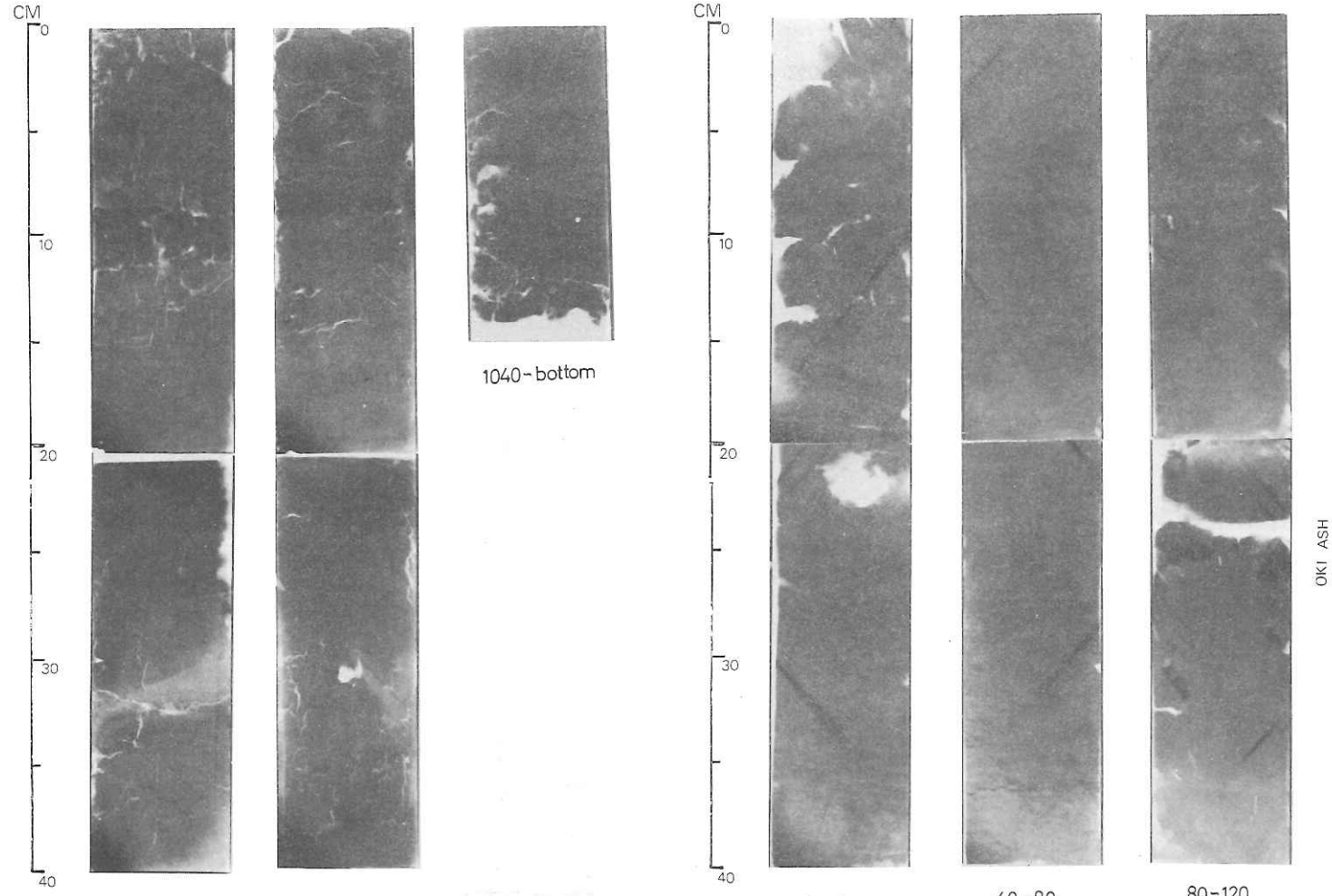
CM
0
10
20
30
40
960-1000
1000-1040
1040-bottom
ST 15
CM
0
10
20
30
40
0 - 40
40-80
80-120
ST 16
OKI ASH

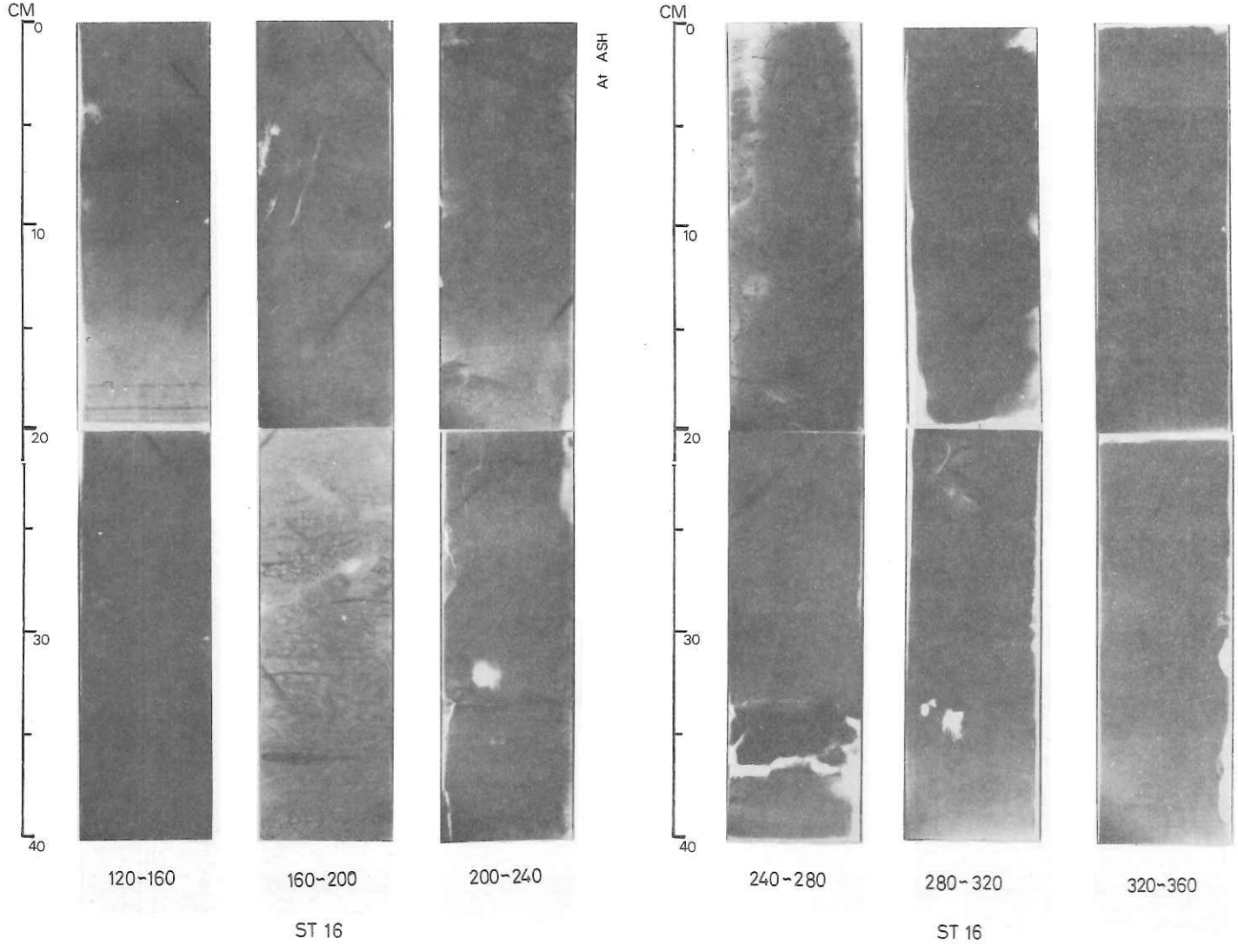
CM
0
10
20
30
40
At ASH
120-160
160-200
200-240
ST 16
CM
0
10
20
30
40
240-280
280-320
320-360
ST 16

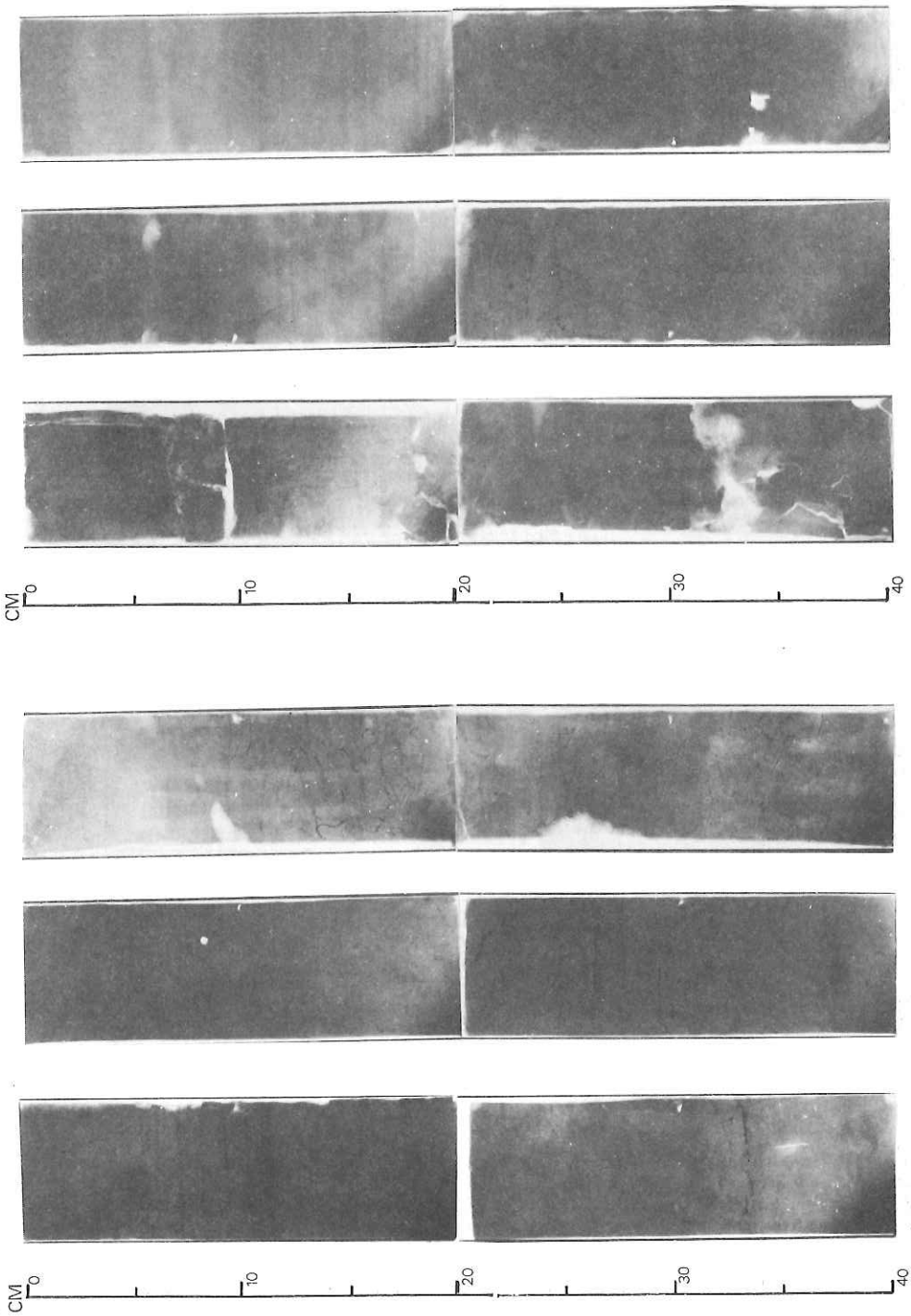
CM
0
10
20
30
40
360~400
400~440
440~480
ST 16
CM
0
10
20
30
40
480~520
520~560
560~600
ST 16

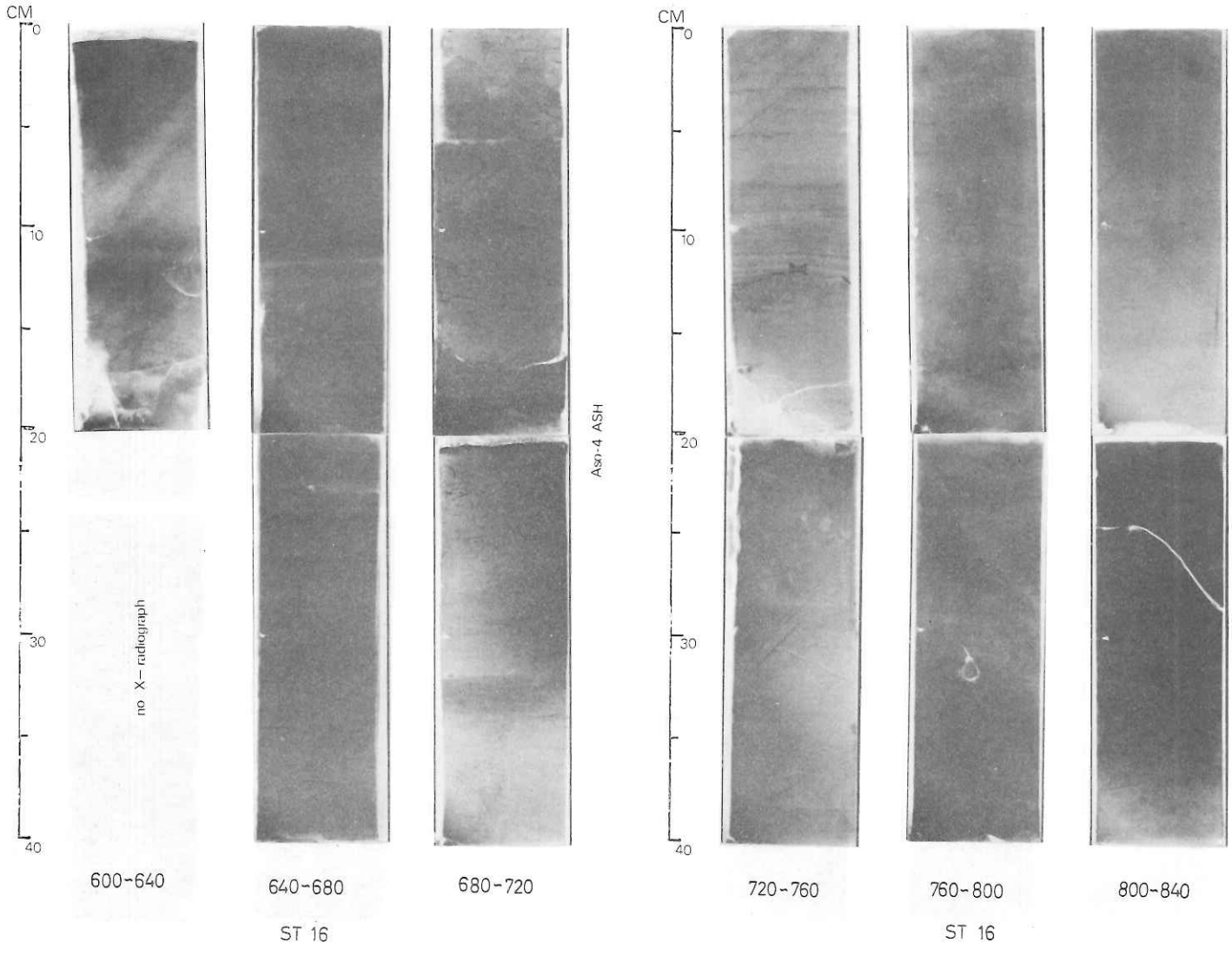
CM
0
10
20
30
40
no X-radiograph
Asn-4 ASH
600-640
640-680
680-720
ST 16
CM
0
10
20
30
40
720-760
760-800
800-840
ST 16

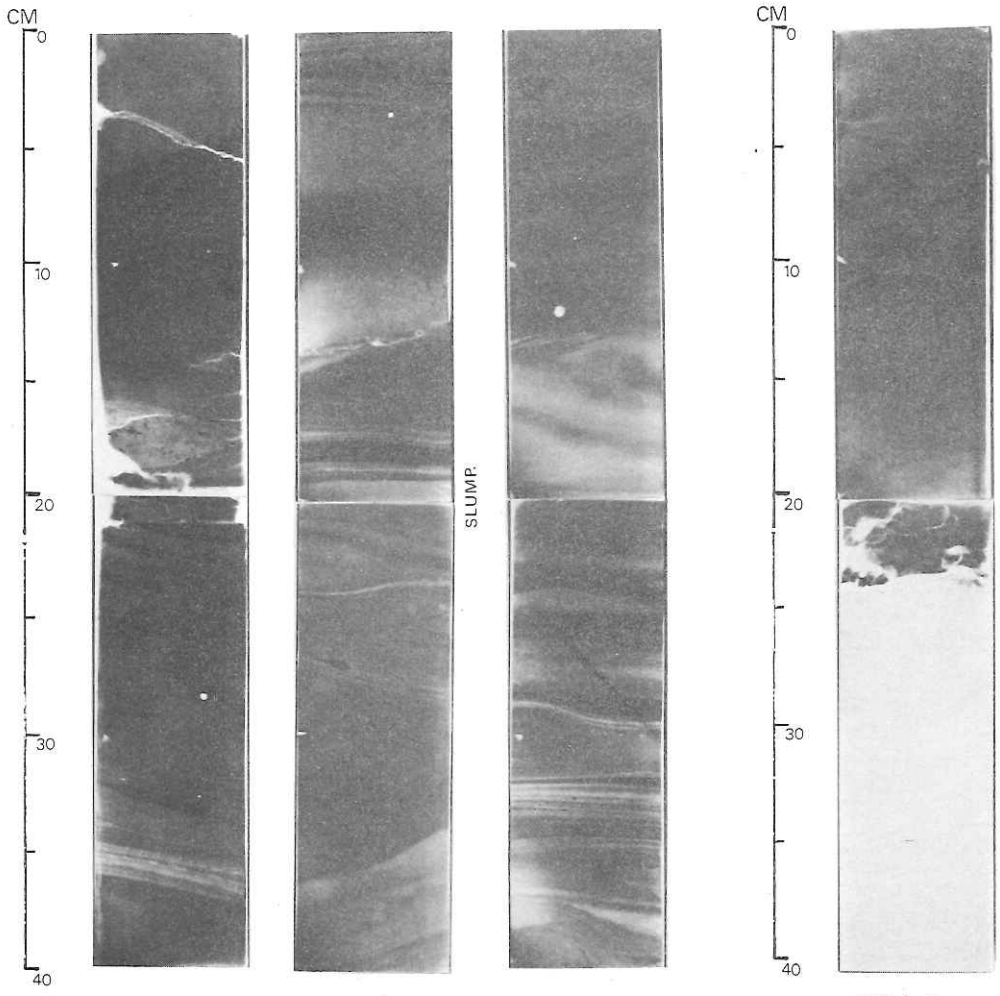
CM
0
10
20
30
40
SLUMP
840-880
880-920
920-960
CM
0
10
20
30
40
960-bottom

ST 16

ST 16

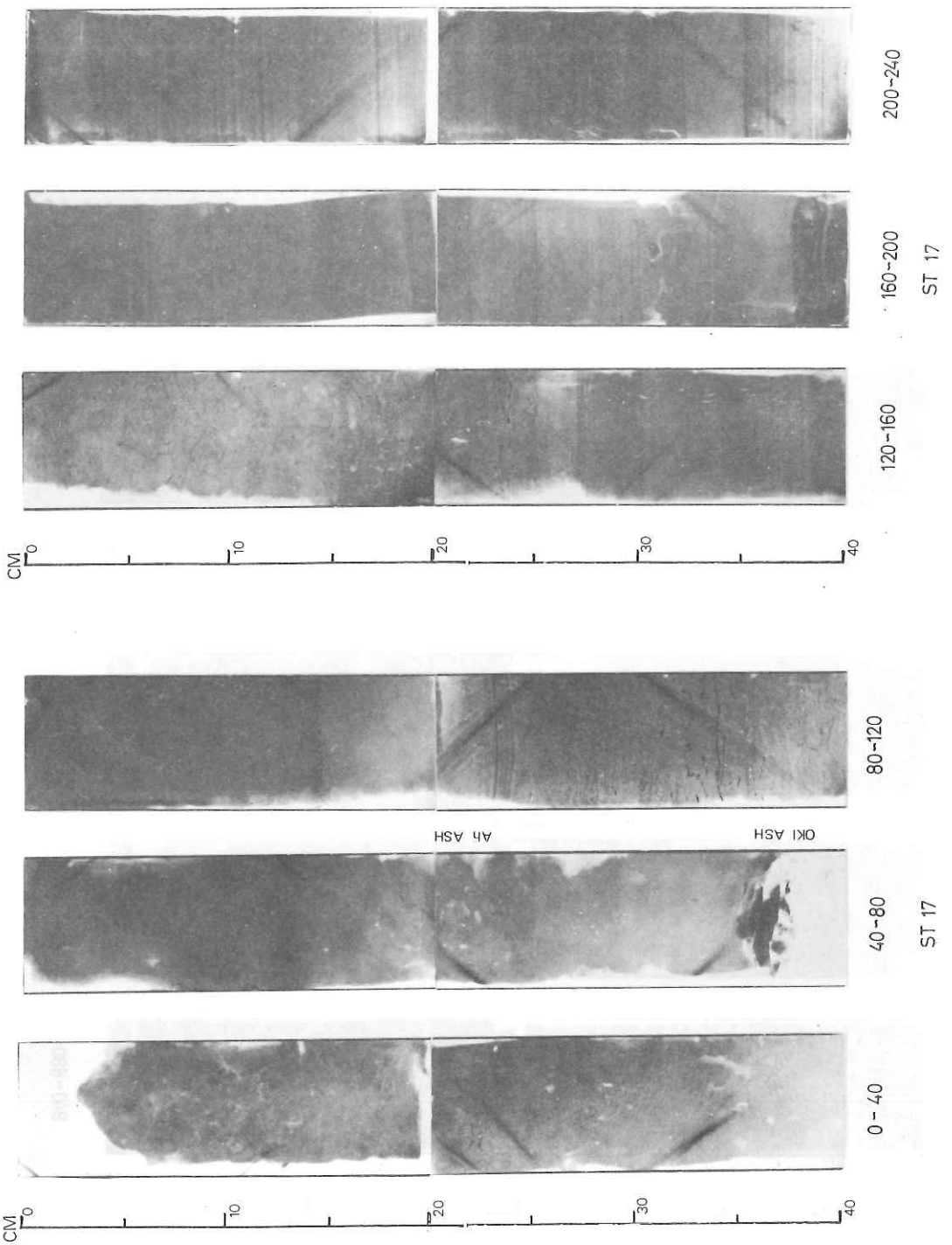
CM
0
10
20
30
40
0 - 40
40~80
80~120
120~160
160~200
200~240
ST 17
ST 17
Ah ASH
OKI ASH

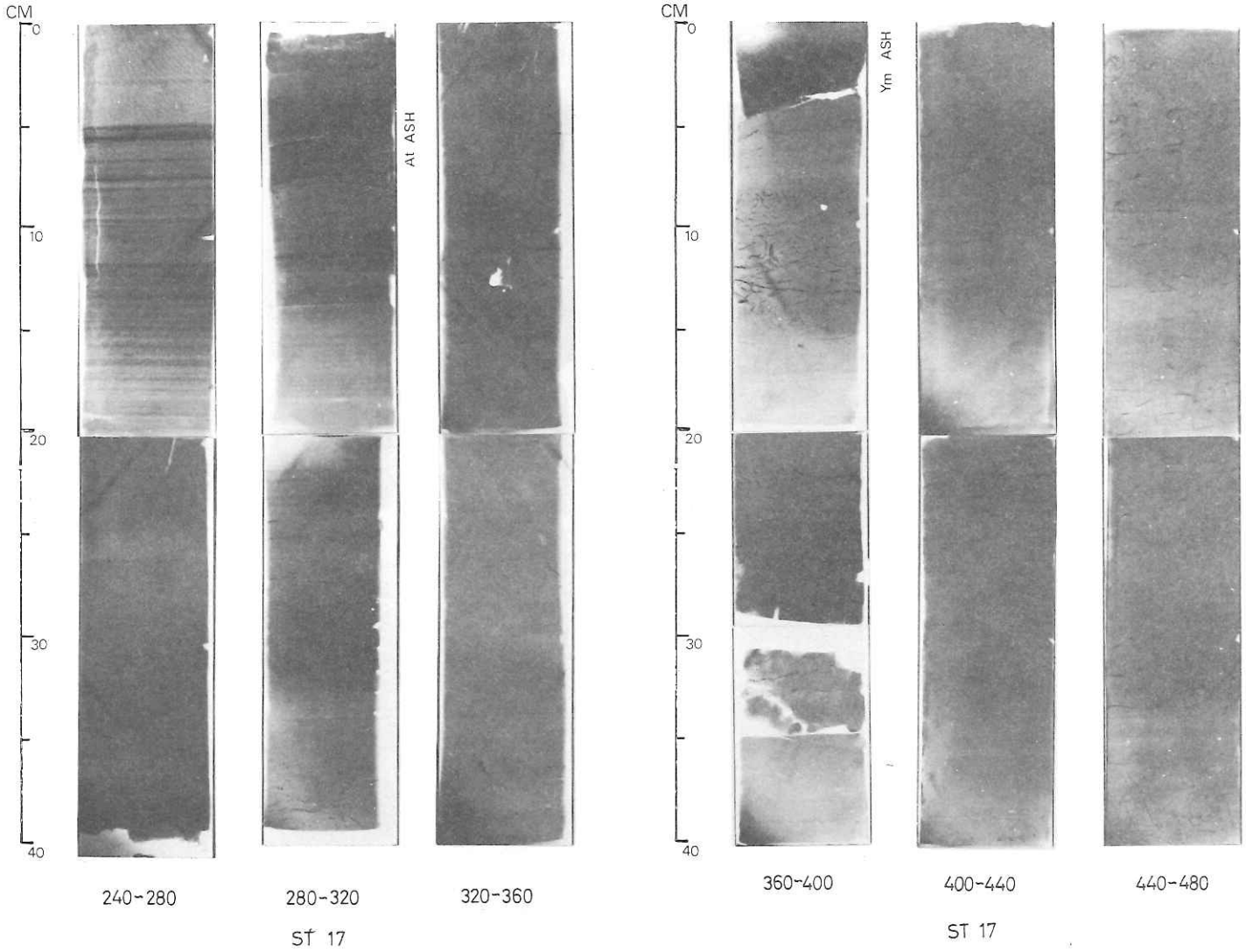
CM
0
10
20
30
40
At ASH
240-280
280-320
320-360
ST 17
CM
0
10
20
30
40
Ym ASH
360-400
400-440
440-480
ST 17

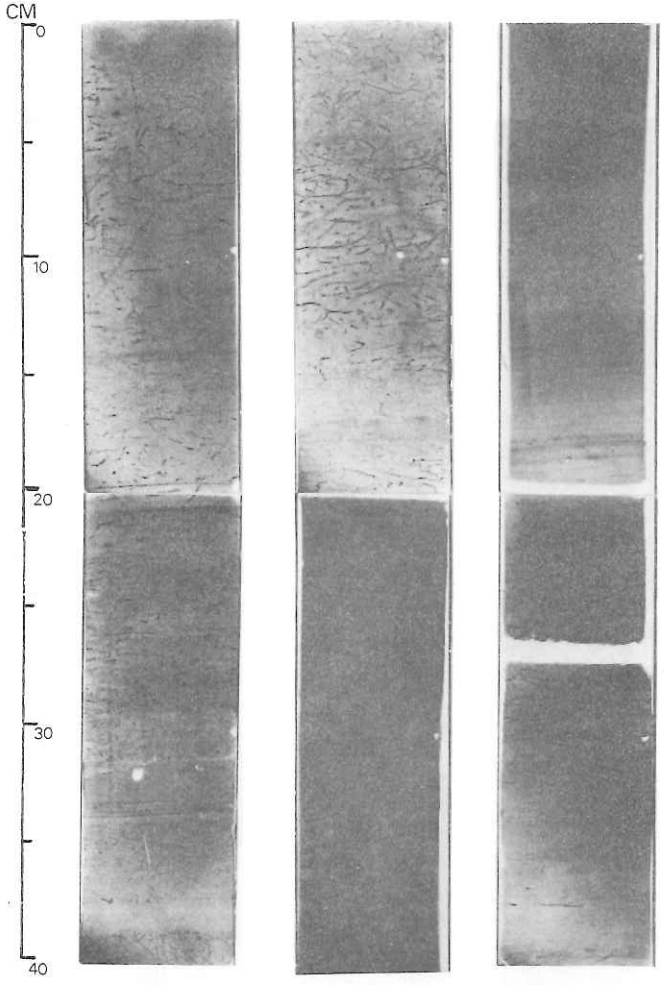
CM
0
10
20
30
40
480-520
520-560
560-600
ST 17

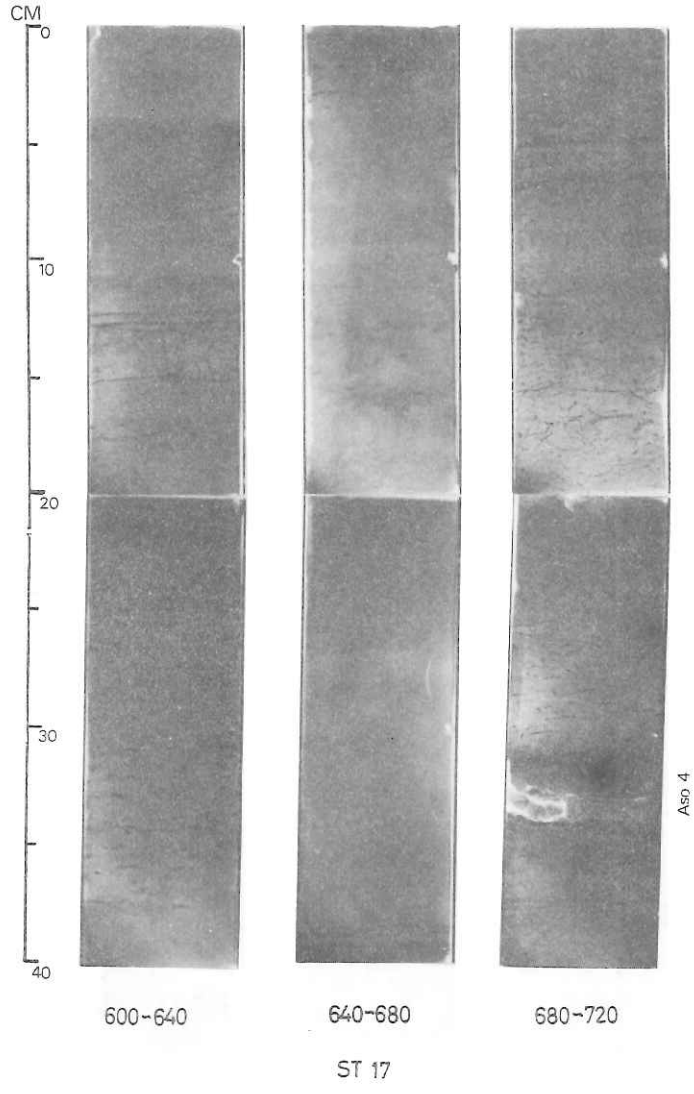
CM
0
10
20
30
40
600-640
640-680
680-720
ST 17
Aso 4

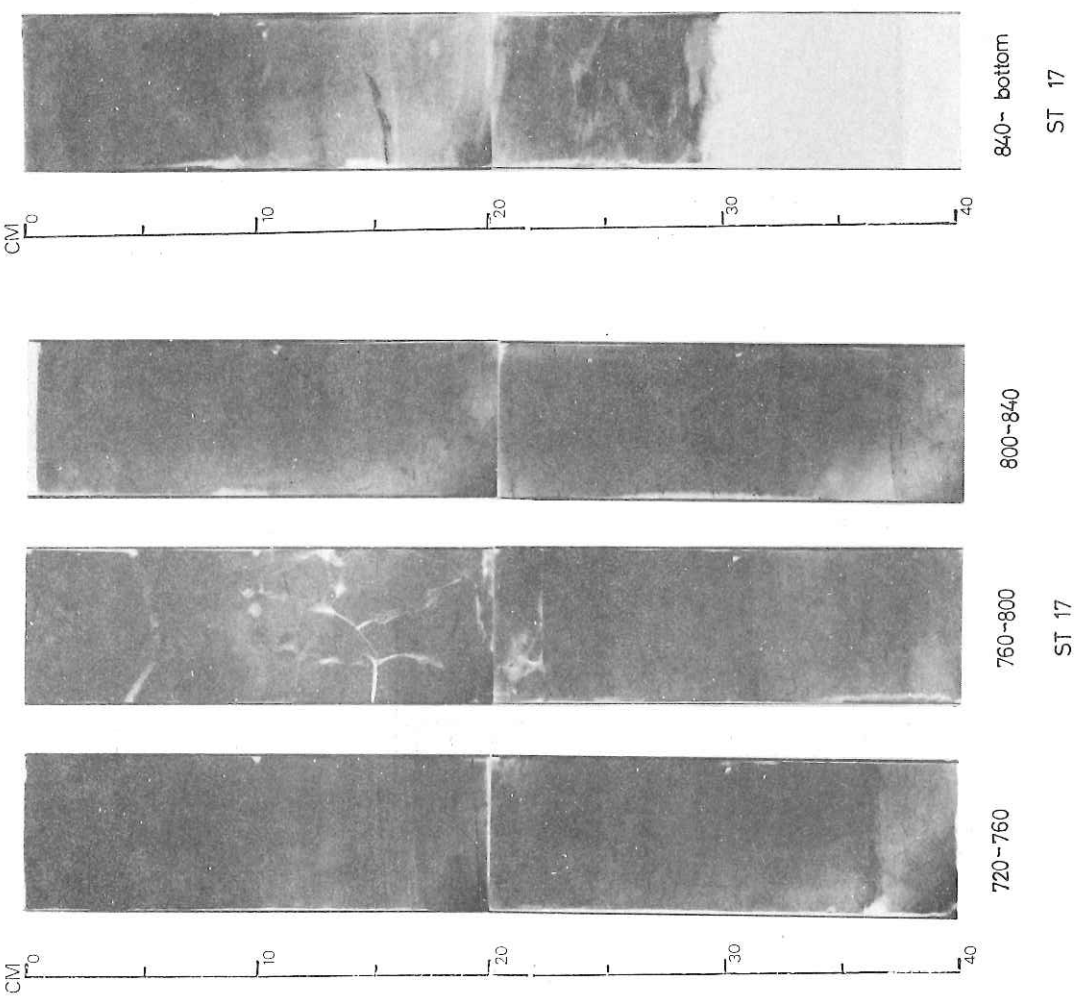
CM
0
10
20
30
40
720-760
760-800
800-840
840- bottom
ST 17
ST 17

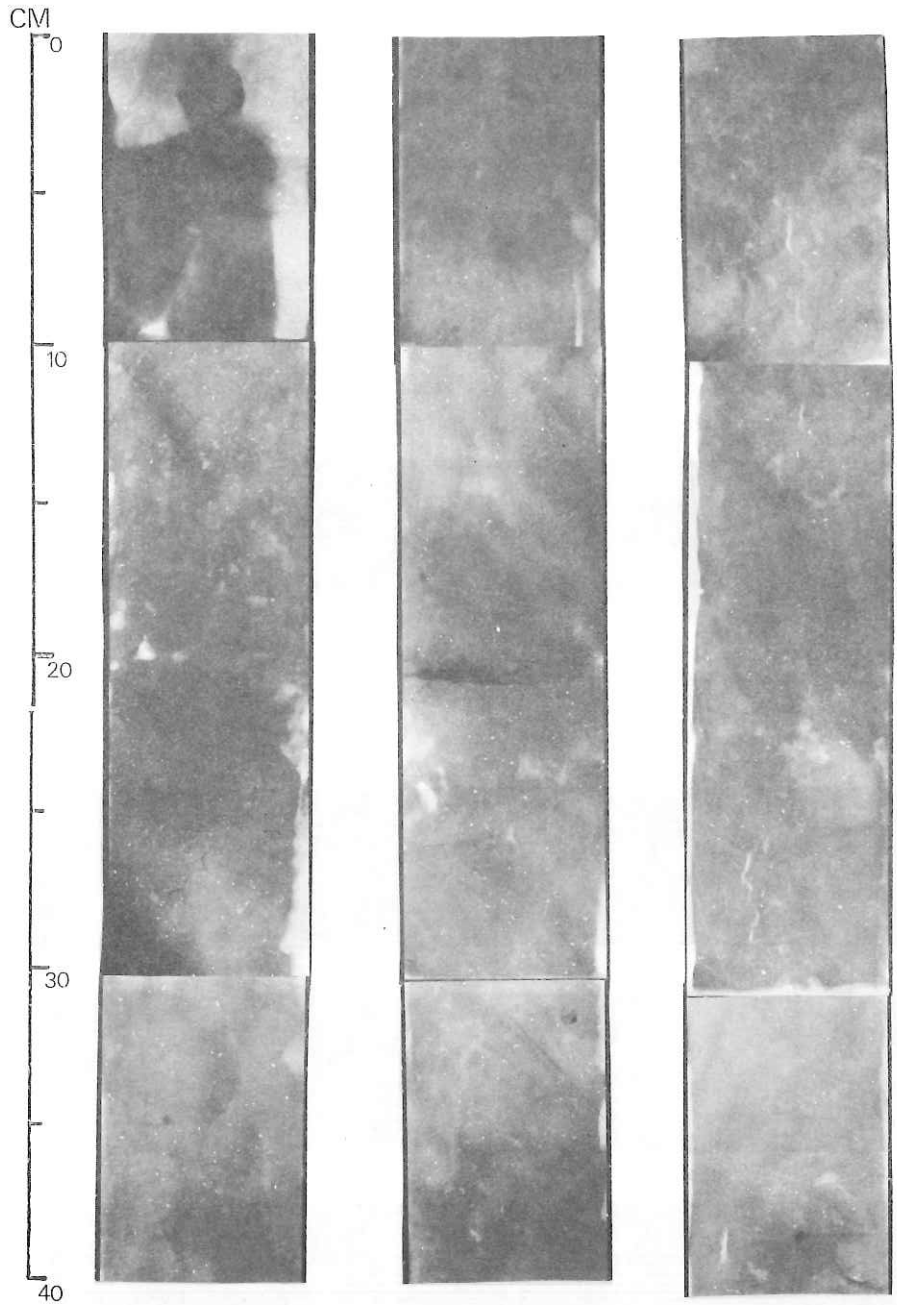

ST 23

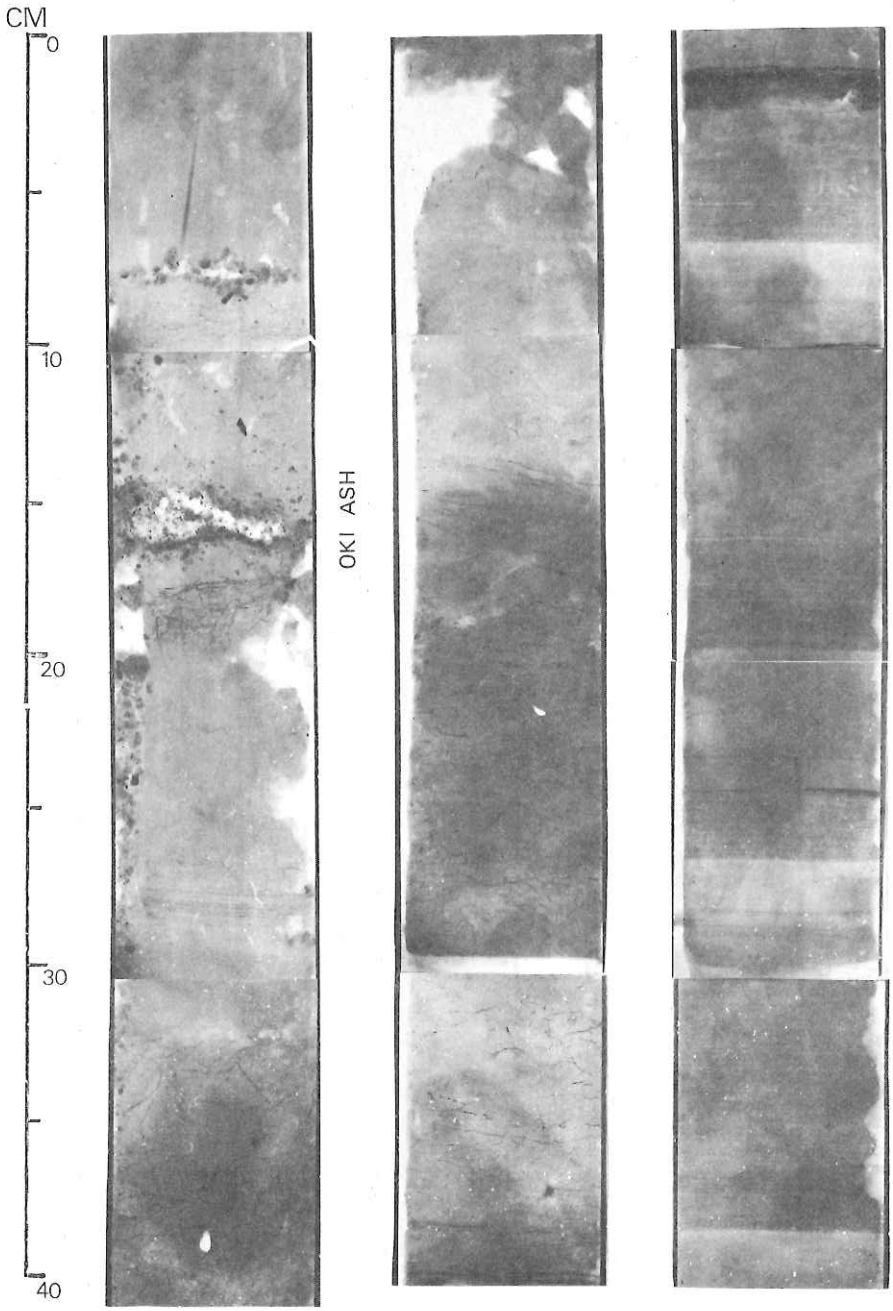

ST 23

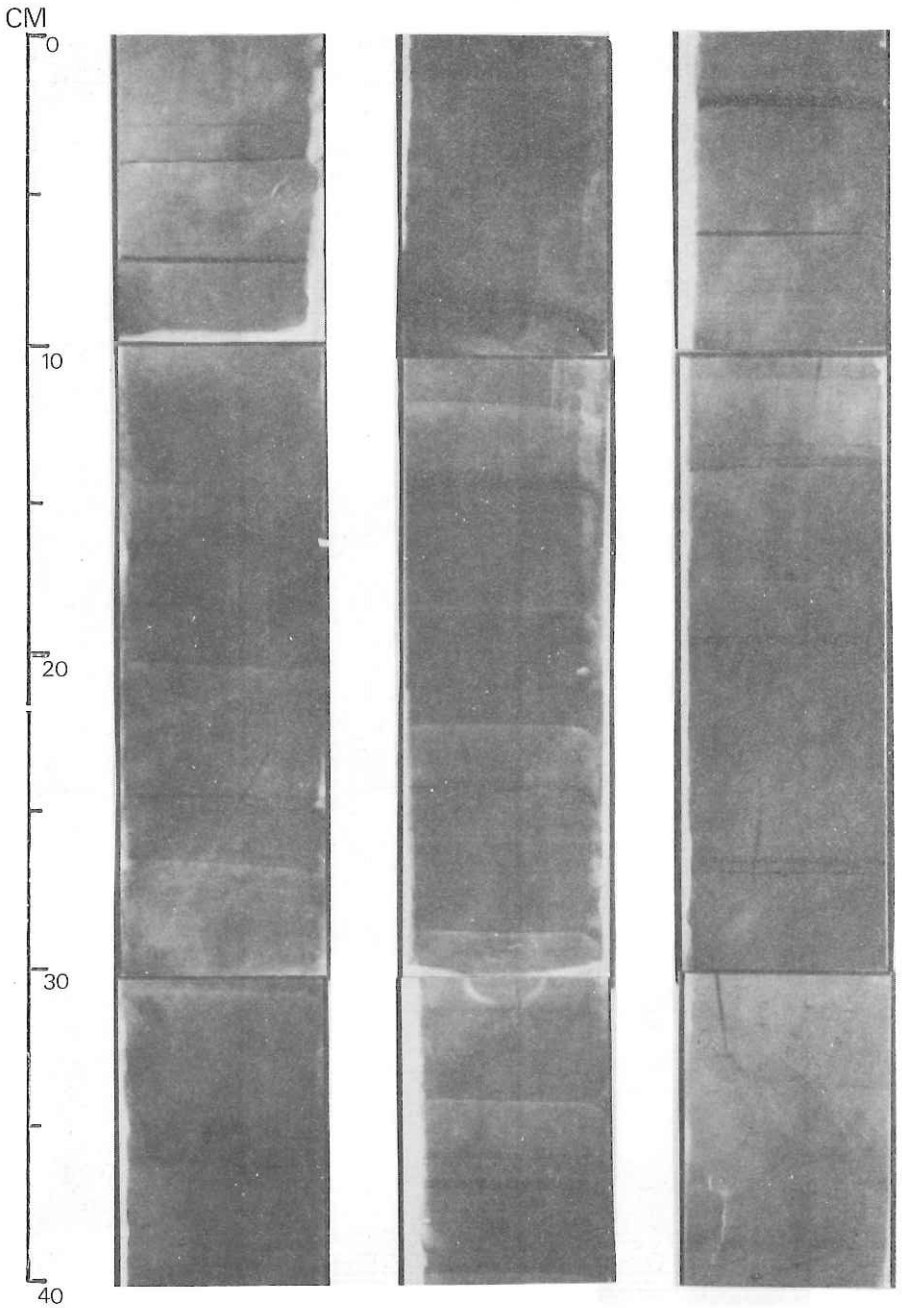

ST 23

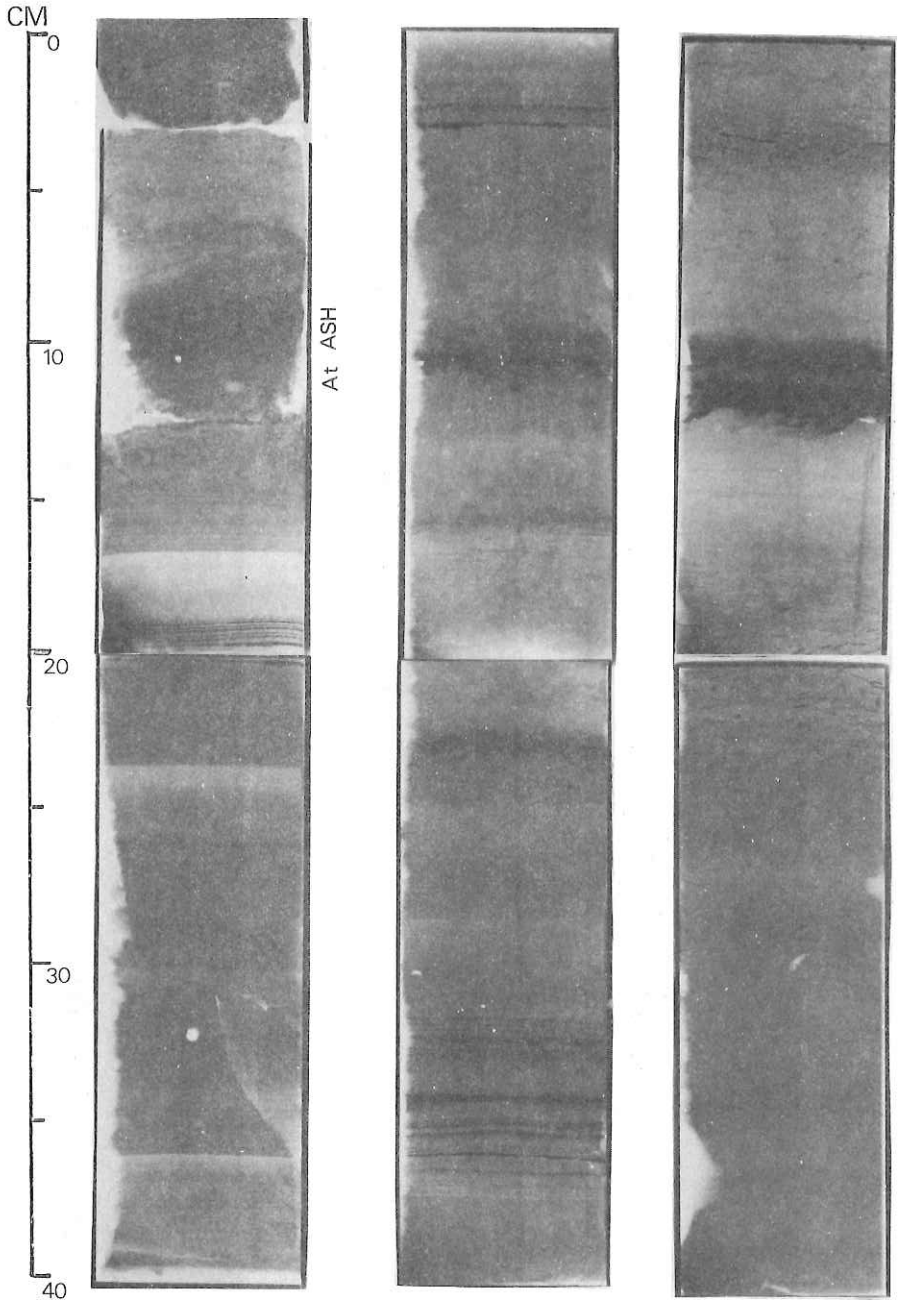

ST 23

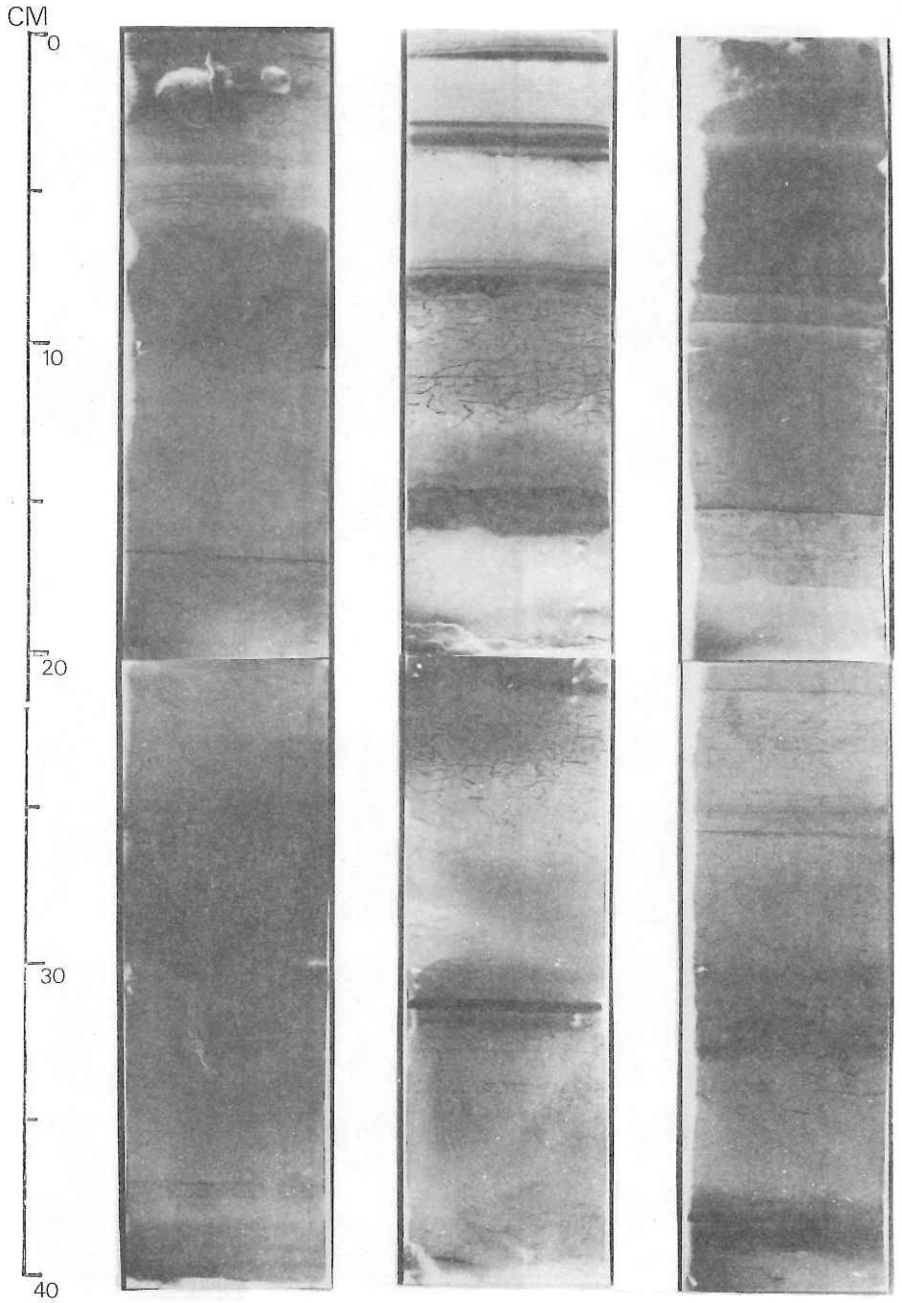

ST 23

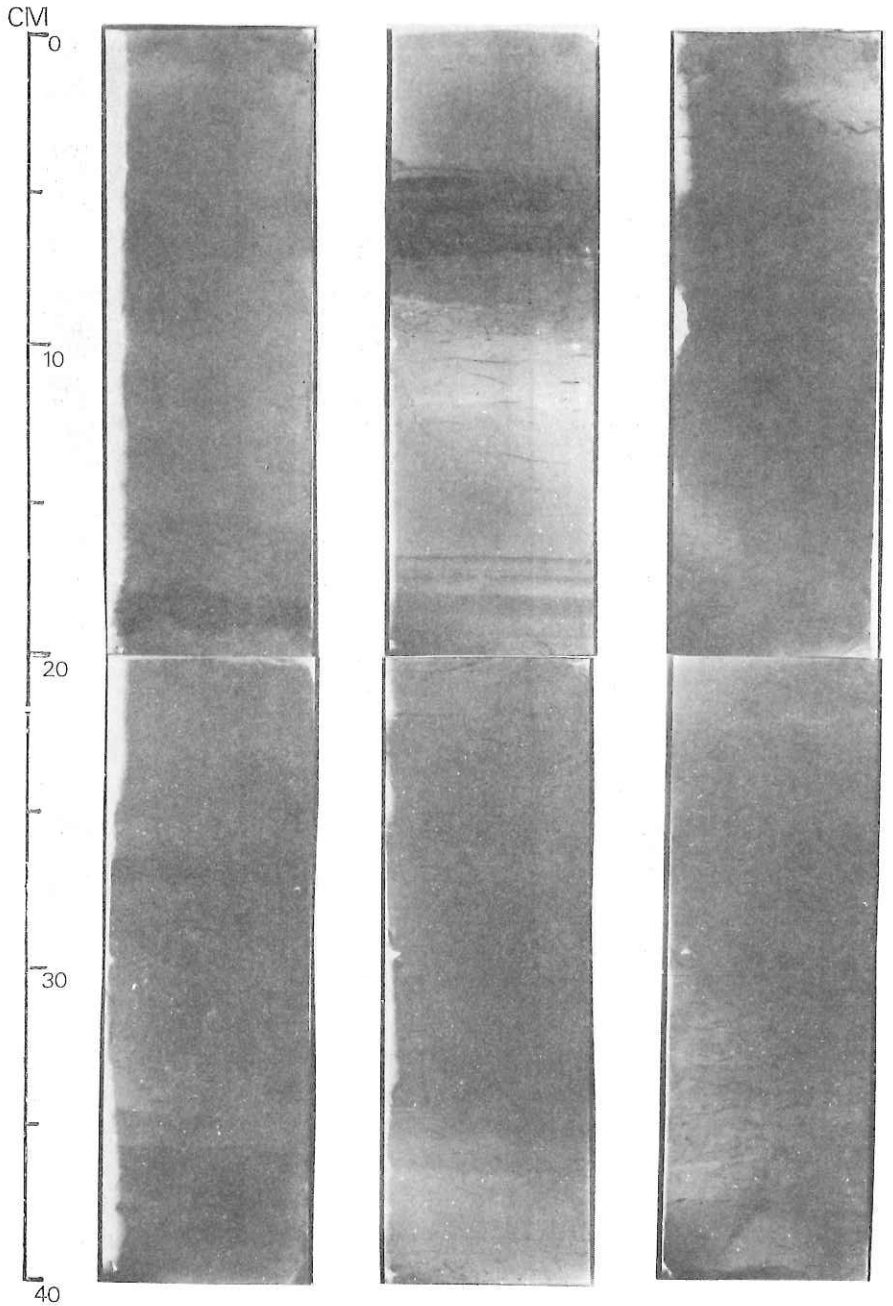

ST 23

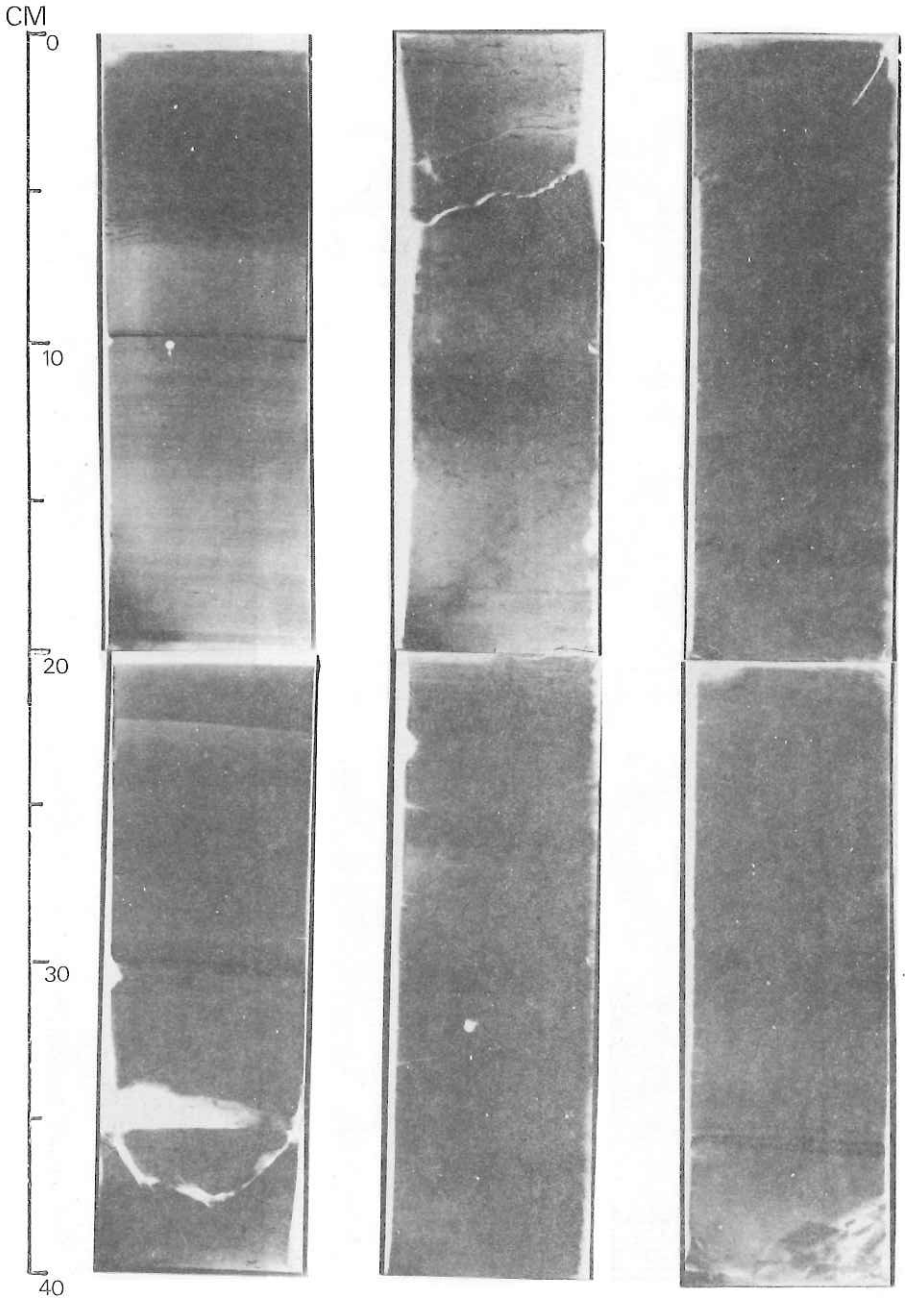

ST 23

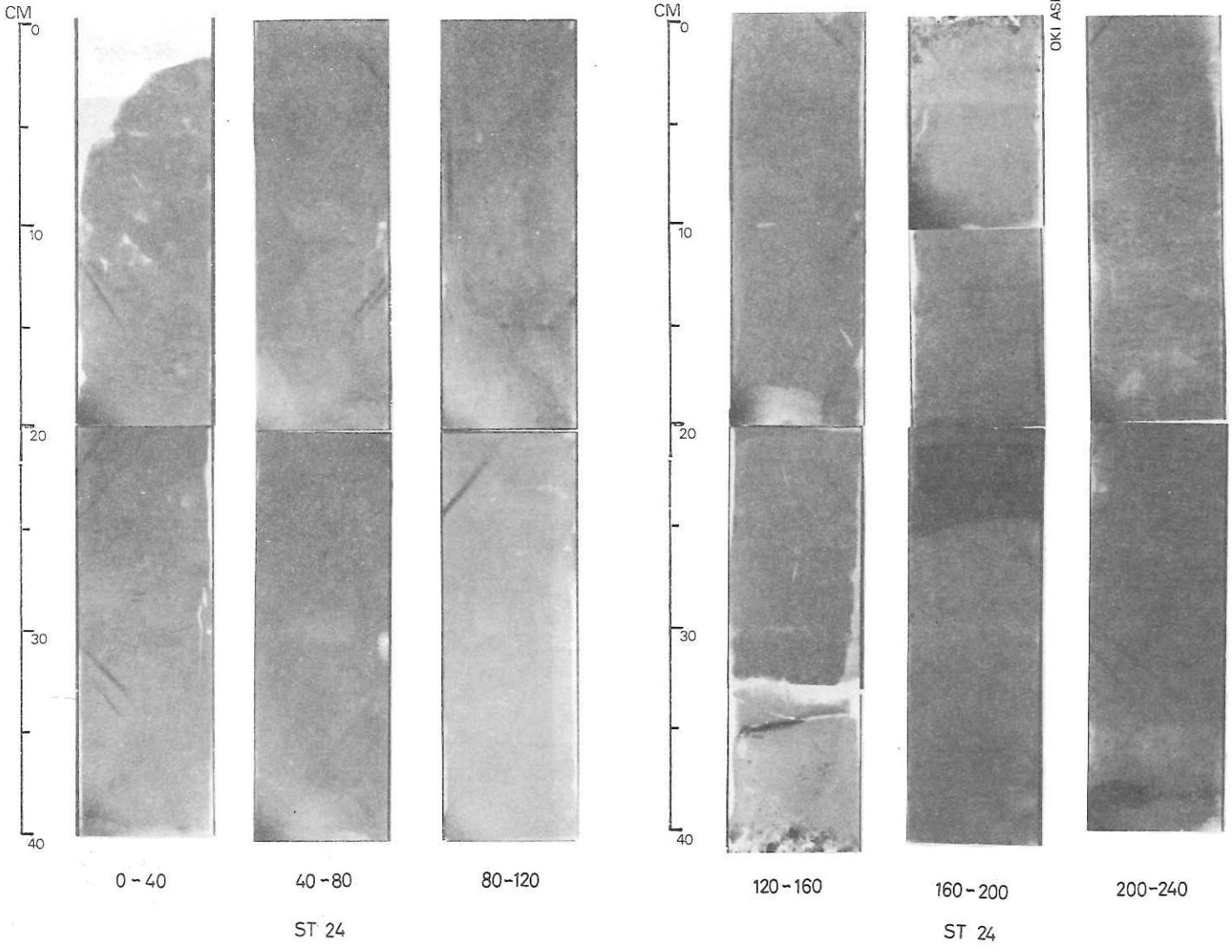
CM
0
10
20
30
40
OKI ASH
0 - 40
40 - 80
80-120
120 - 160
160 - 200
200-240
ST 24
ST 24

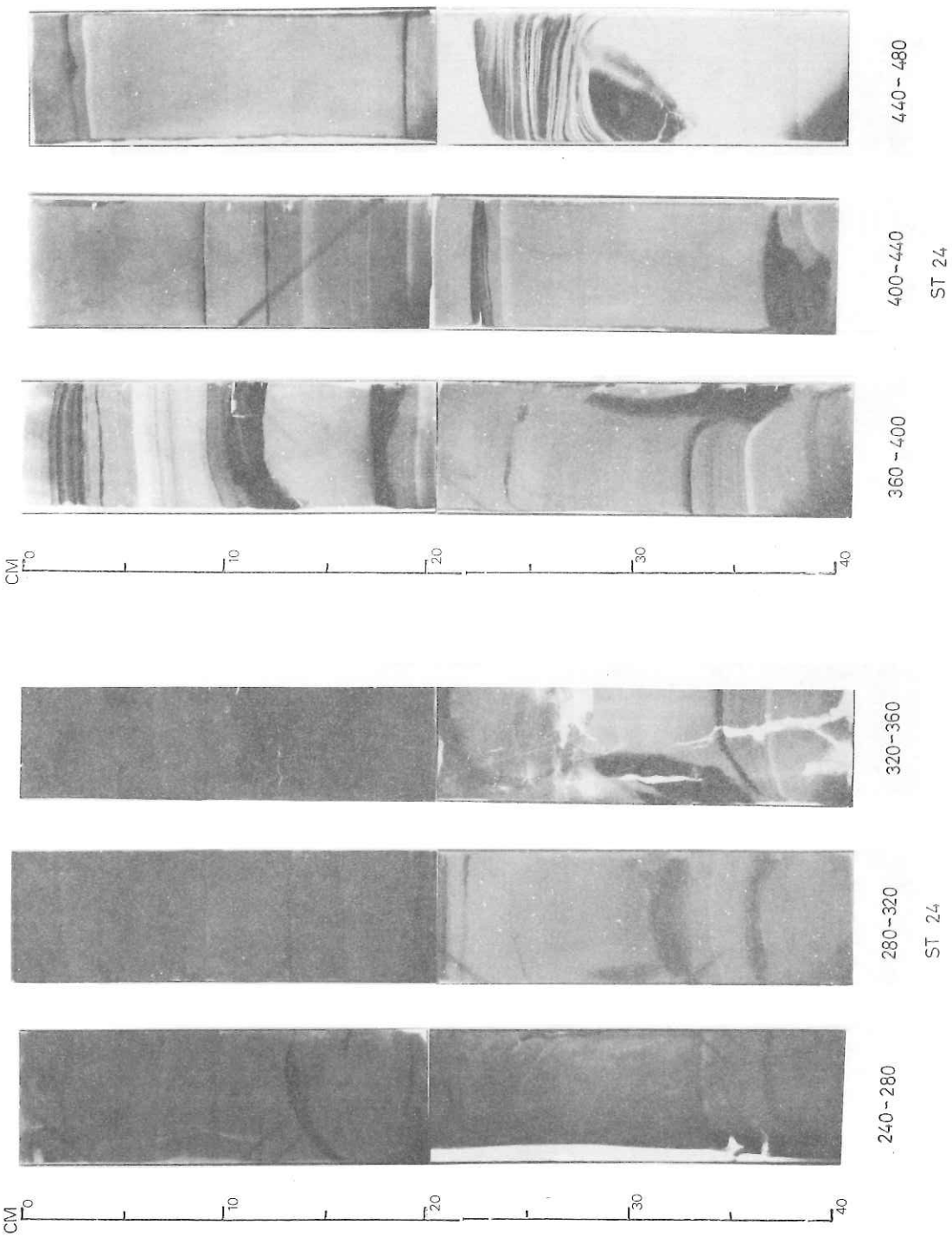
CM
0
10
20
30
40
240-280
280-320
320-360
360-400
400-440
440-480
ST 24
ST 24

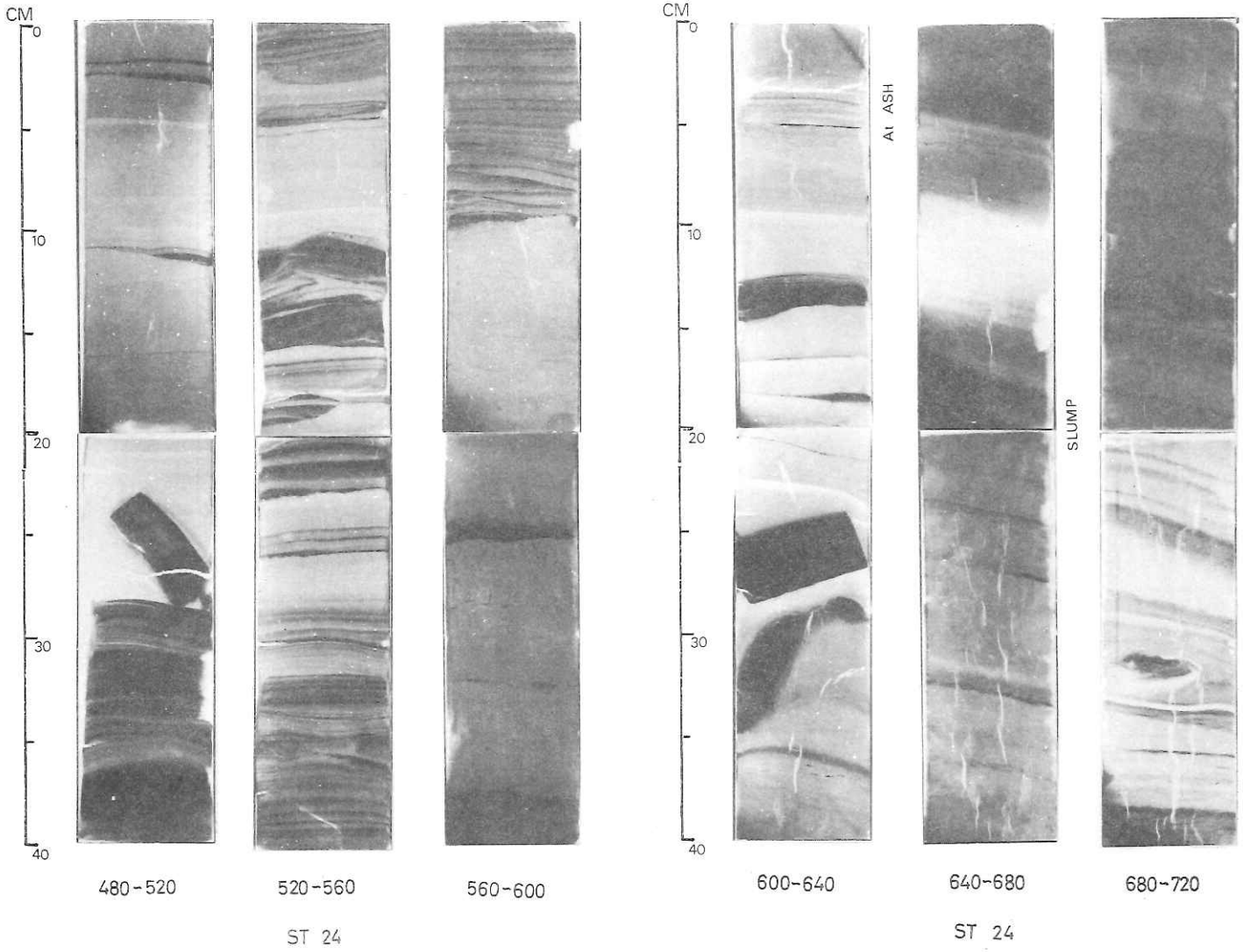
CM
0
10
20
30
40
480-520
520-560
560-600
ST 24
CM
0
10
20
30
40
At ASH
SLUMP
600-640
640-680
680-720
ST 24

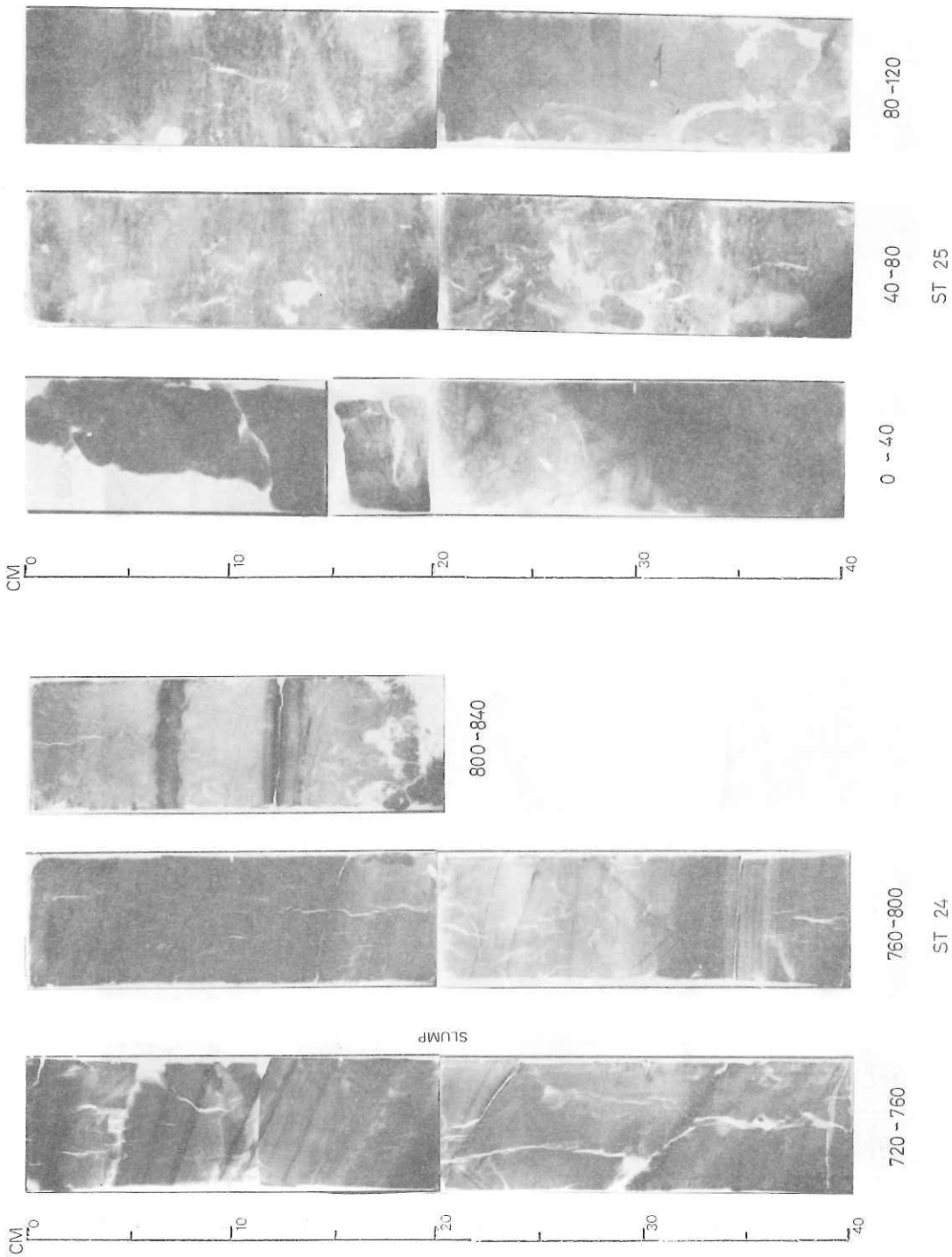
CM
0
10
20
30
40
0 - 40
40-80
80-120
ST 25
SLUMP
720 - 760
760-800
800-840
ST 24

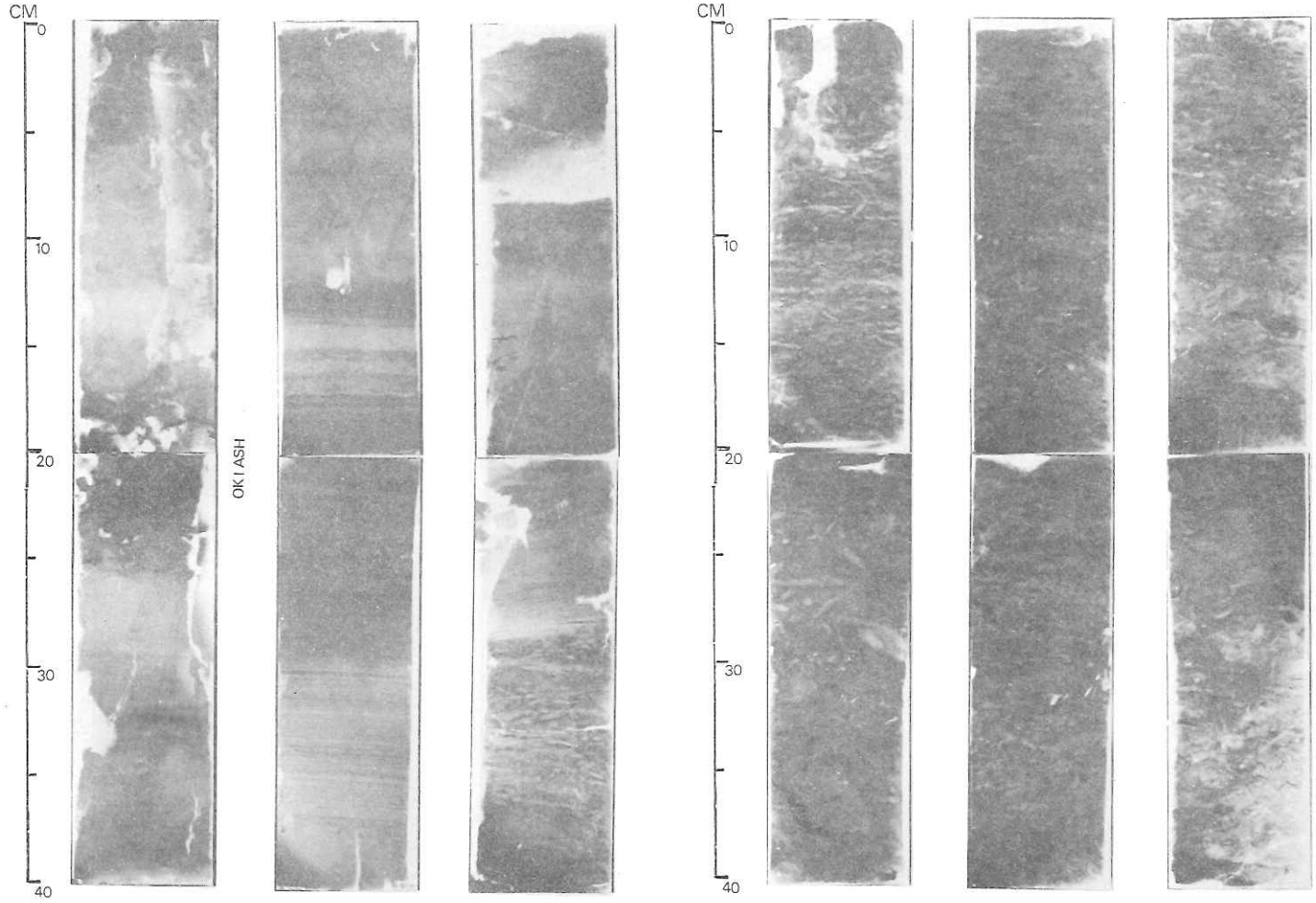
CM
0
10
20
30
40
OKI ASH
120-160
160-200
200-240
ST 25
CM
0
10
20
30
40
240-280
280-320
320-360
ST 25

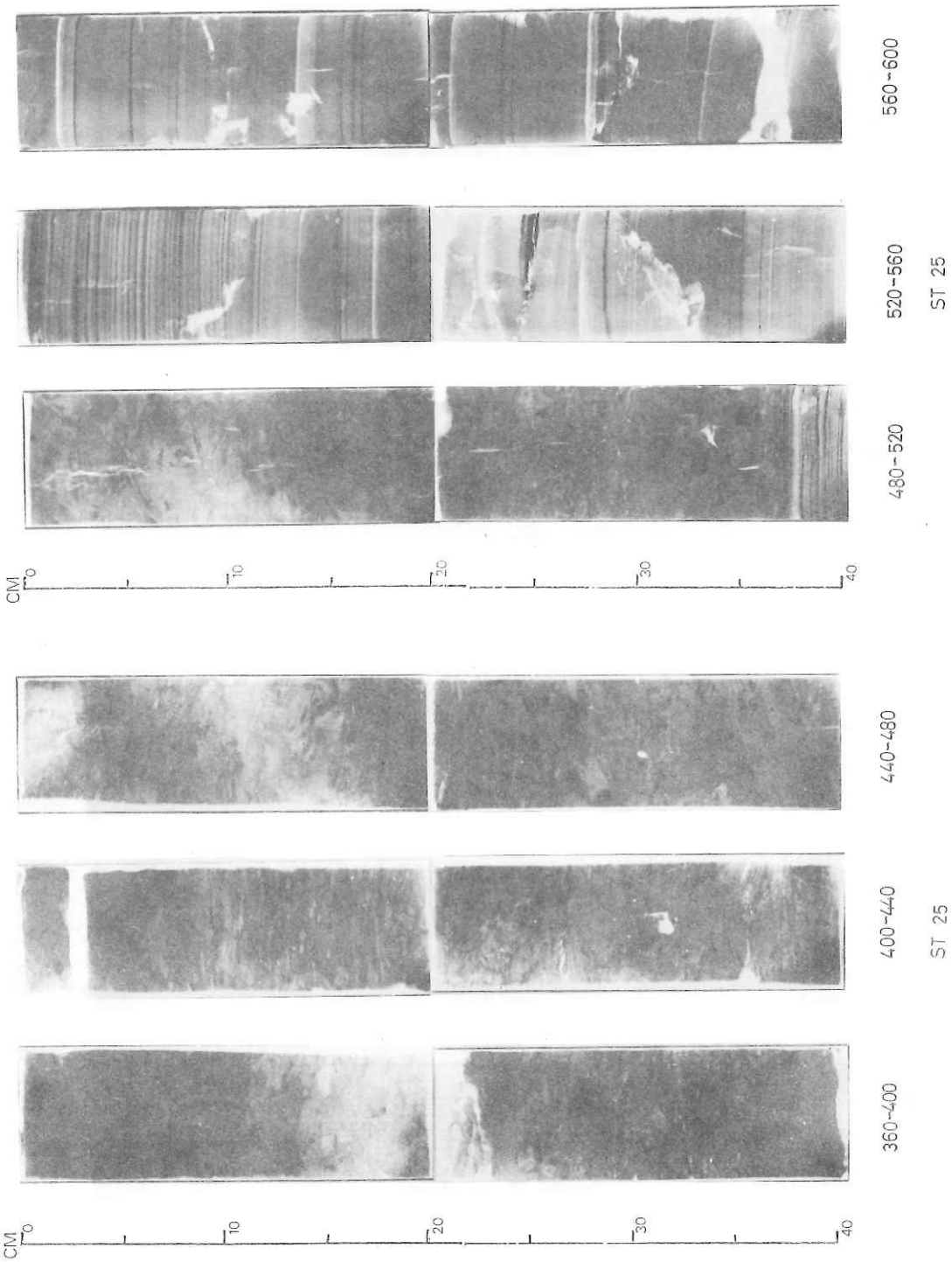
360-400
400-440
440-480
ST 25
CM
0
10
20
30
40
480-520
520-560
560-600
ST 25
CM
0
10
20
30
40

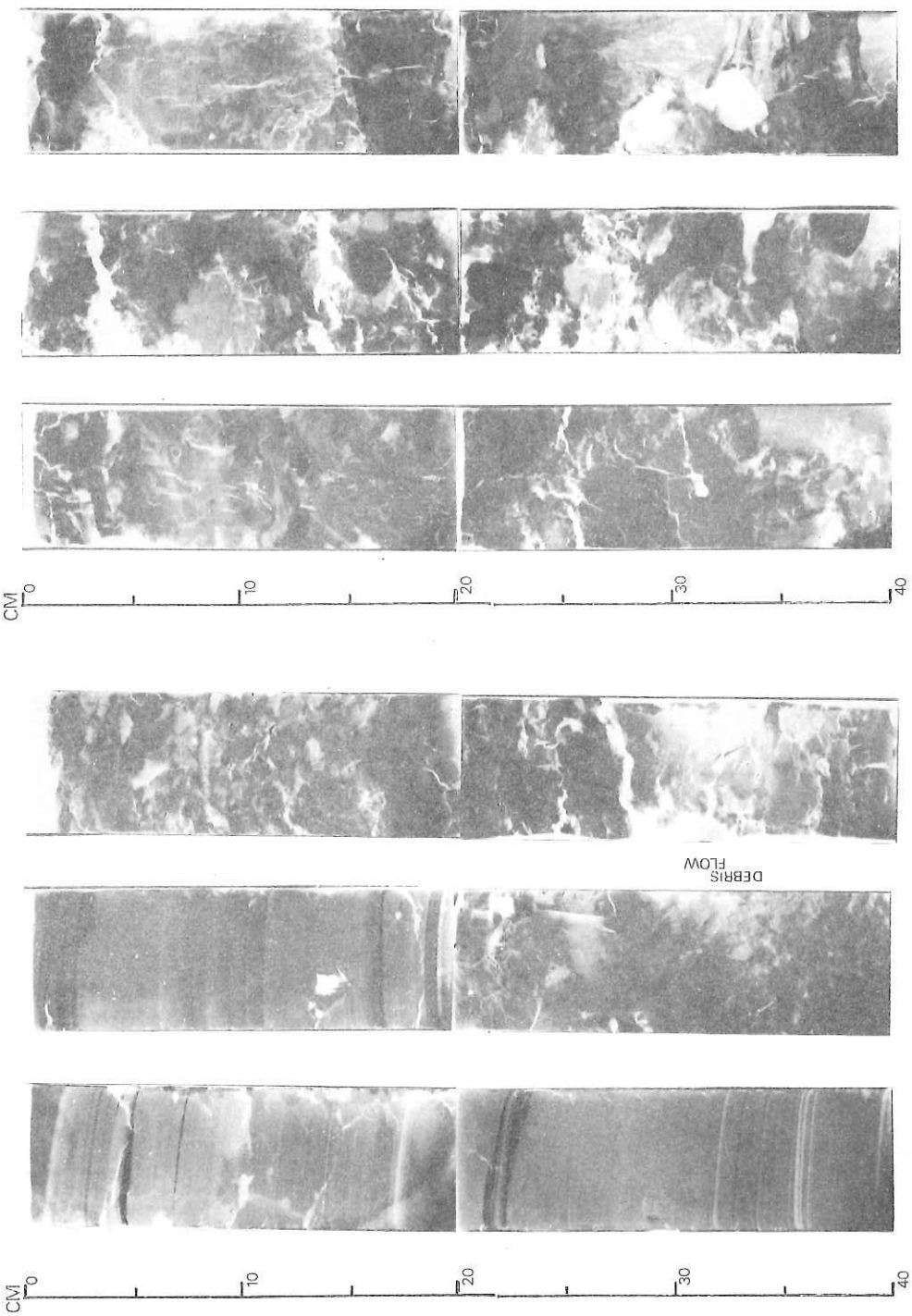
CM
0
10
20
30
40
600-640
640-680
680-720
720-760
760-800
800-840
ST 25
ST 25
DEBRIS FLOW

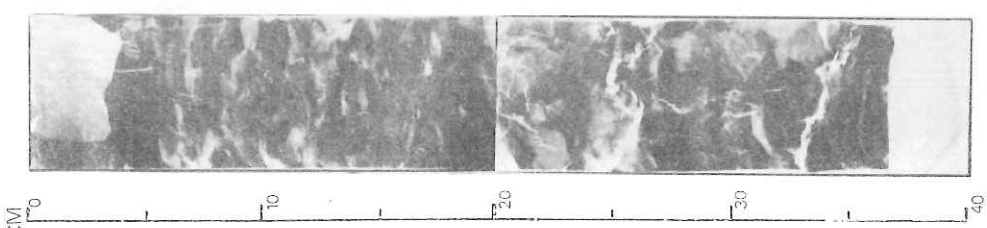
CM
0
10
20
30
40
840-bottom
ST 25

7-7. INTERSTITIAL WATER STUDIES

T. MASUZAWA

Interstitial waters of deep-sea sediments were studied for five cores collected from Yamato (KH82-4-15, -16, -17, and -19) and Tsushima (82-4-23) basins of the Sea of Japan during the KH 82-4 Cruise. Immediately after the collection of core samples, interstitial waters were squeezed air-tightly with a nine-chambered mechanical squeezer (Masuzawa et al.,1980) at a simulated temperature of bottom waters (1 $\pm$ 1°C). Just after squeezing, pH, redox potential (Eh), and hydrogen sulfide of interstitial waters were determined for cores of KH82-4-19 and 23. The pH and Eh values were measured in a closed system with a flow-type pH-Eh cell at 25.0°C. A part of the interstitial water was acidified with hydrochloric acid for the analyses of sulfate and major and minor cations, and the residual interstitial water was stored in a refrigerator. Other chemical species were analyzed at the laboratory on land. Analytical methods were the same as those reported previously (Masuzawa and Kitano, MS).

Bottom waters were collected by T.Oba at the same time of piston coring with a 2.7 liters NISKIN-type PVC sampler, which was fixed just above the pilot corer, and were analyzed similarly.

Table 7-7-1 lists the analytical results of bottom and interstitial waters for alkalinity (Alk), sulfate (SO_4), ammonium (NH_4-N), phosphate (PO_4-P), dissolved silica (SiO_2), hydrogen sulfide (H_2S), pH, and Eh. As clearly seen from T.7-7-1, sulfate reduction is proceeding actively in the sediments of the five stations studied here. A clear discontinuity of interstitial water composition is observed at 100 cm below the top of the core of KH82-4-19. A living organism was found there when the core was described megascopically.

Major and minor cations will be analyzed in future. Diagenetic reactions occuring in these sediments will be clarified and their effects on the chemical compositions of sediments will be discussed.

REFERENCES

Masuzawa,T., Kanamori,S., and Kitano,Y., 1980. The reversible effect of temperature on the chemical composition of interstitial water of marine sediment. J.Oceanogr.Soc.Japan,36,68-72.

Masuzawa,T. and Kitano,Y., MS. Interstitial water chemistry in deep-sea sediments from the Japan Sea. Submitted to J.Oceanogr.Soc.Japan.

TABLE 7-7-1. Chemical composition of interstitial waters

KH 82-4, Stn.15 (36°44.3'N, 133°33.6'E; 1095 m)

Depth (cm)	Alk (meq/kg)	SO_4	NH_4-N	PO_4-P	SiO_2	H_2S	pH(25°C)	Eh(25°C) (V)
		(←		mmol/kg		→)		
Error	±0.02	±0.3	±0.005	±0.002	±0.005	±0.01	±0.03	±0.01
BW[1)]	-	-	-	-	-	-	-	-
15- 18	3.00	27.5	0.08	0.014	0.55	-	-	-
25- 28	3.39	27.8	0.14	0.015	0.58	-	-	-
35- 38	3.91	27.4	0.17	-	0.58	-	-	-
45- 48	4.52	28.0	0.23	0.020	0.62	-	-	-
65- 68	-	25.7	-	-	-	-	-	-
85- 88	6.90	24.4	0.41	0.029	0.63	-	-	-
105-108	7.75	25.4	0.47	0.029	0.60	-	-	-
120-123	7.95	24.6	0.59	0.029	0.57	-	-	-
140-143	9.21	24.2	0.68	0.035	-	-	-	-
160-163	10.02	24.4	0.73	0.035	0.56	-	-	-
180-183	11.08	23.9	0.77	0.035	0.52	-	-	-
200-203	12.39	22.2	-	-	-	-	-	-
260-263	17.13	18.3	1.19	0.065	0.51	-	-	-
280-283	17.81	16.7	1.39	0.066	0.51	-	-	-
320-323	19.90	15.3	1.39	-	0.49	-	-	-
380-383	-	12.7	-	-	-	-	-	-
440-443	26.74	9.6	1.88	0.102	0.47	-	-	-
500-503	29.40	5.4	2.30	0.106	0.43	-	-	-
560-563	25.80	3.8	2.44	0.091	0.43	-	-	-
640-643	31.19	1.9	2.69	0.098	0.43	-	-	-
737-740	33.77	1.9	3.05	0.124	0.41	-	-	-
800-803	36.51	0.8	3.39	-	0.41	-	-	-
880-883	37.82	1.2	3.47	0.167	-	-	-	-
960-963	39.65	1.4	4.13	0.177	0.37	-	-	-

1) bottom water

2) not detected

3) bottom water of Stn. 24

KH 82-4, Stn.16 (37°00.2'N, 133°54.2'E; 1740 m)

Depth (cm)	Alk (meq/kg)	SO_4	NH_4-N	PO_4-P	SiO_2	H_2S	pH(25°C)	Eh(25°C) (V)
		(←		mmol/kg		→)		
BW	2.26	27.1	0.00$_1$	0.001	0.08$_4$	-	7.95	+0.30
5- 8	2.63	28.4	-	-	0.42	-	-	-
15- 18	3.19	-	0.09	0.016	0.52	-	-	-
25- 28	3.58	27.0	0.12	0.014	0.54	-	-	-
35- 38	4.18	27.8	0.16	0.017	0.56	-	-	-
45- 48	4.69	27.0	-	-	-	-	-	-
55- 58	5.16	26.3	0.25	0.025	0.57	-	-	-
65- 68	5.40	25.2	0.26	0.023	0.55	-	-	-
85- 88	6.06	-	-	-	0.53	-	-	-
95- 98	6.44	24.9	0.33	0.027	0.52	-	-	-
120-123	7.47	23.5	0.42	-	0.50	-	-	-
140-143	7.95	23.9	0.48	0.029	0.45	-	-	-
160-163	-	23.7	0.55	0.031	0.40	-	-	-
180-183	8.94	22.4	0.58	0.033	0.38	-	-	-
220-223	11.17	21.8	0.71	0.042	0.41	-	-	-
260-263	12.55	20.8	0.79	-	-	-	-	-
320-323	-	19.3	0.93	0.060	0.47	-	-	-
380-383	16.48	17.4	1.04	0.061	0.44	-	-	-
440-443	19.51	15.2	1.28	0.070	0.41	-	-	-
620-623	24.55	8.6	1.62	0.092	0.44	-	-	-
680-683	27.86	6.9	1.81	0.111	-	-	-	-
740-743	30.58	5.8	1.93	0.112	0.41	-	-	-
800-803	31.54	3.4	2.03	0.114	0.43	-	-	-
840-843	33.19	3.0	2.05	0.117	0.43	-	-	-
900-903	-	1.9	-	-	0.45	-	-	-

KH 82-4, Stn.17 (37°15.5'N, 134°16.2'E; 2455 m)

Depth (cm)	Alk (meq/kg)	SO_4	NH_4-N	PO_4-P	SiO_2	H_2S	pH(25°C)	Eh(25°C) (V)
		(←		mmol/kg		→)		
BW	2.33	27.3	0.00_1	0.000_5	0.08_3	-	7.82	+0.30
3- 6	2.68	27.7	0.03_5	0.014	0.44	-	-	-
10- 13	3.14	28.0	-	0.017	0.46	-	-	-
15- 18	3.41	27.6	0.06_0	0.022	0.48	-	-	-
20- 23	3.63	-	0.07_1	0.023	0.53	-	-	-
25- 28	3.81	-	0.08_9	0.022	0.53	-	-	-
30- 33	3.96	27.6	0.10	0.022	0.54	-	-	-
35- 38	4.24	-	0.12	0.026	0.51	-	-	-
40- 43	4.37	26.3	0.13	0.023	0.50	-	-	-
45- 48	4.80	-	0.14	0.026	0.50	-	-	-
50- 53	4.86	26.4	0.15	0.027	0.51	-	-	-
55- 58	5.03	-	0.16	0.027	0.51	-	-	-
70- 73	5.25	26.3	0.18	0.029	0.48	-	-	-
80- 83	6.10	25.1	0.24	0.021	0.44	-	-	-
90- 93	6.23	24.3	0.25	0.031	0.44	-	-	-
100-103	6.27	24.8	0.28	0.017	0.43	-	-	-
110-113	7.35	23.3	0.30	0.031	0.40	-	-	-
120-123	7.00	23.7	0.33	0.028	0.36	-	-	-
130-133	8.17	-	0.34	0.033	0.35	-	-	-
140-143	8.53	23.7	0.35	0.030	0.34	-	-	-
150-153	8.06	-	0.37	0.021	0.33	-	-	-
160-163	7.81	23.5	0.40	0.014	0.36	-	-	-
180-183	7.55	21.9	0.44	0.019	0.36	-	-	-
220-223	10.34	21.9	-	0.022	0.34	-	-	-
240-243	11.08	21.1	0.56	0.033	0.36	-	-	-
260-263	12.10	19.8	0.61	0.037	0.38	-	-	-
320-323	14.37	18.2	0.74	0.053	0.42	-	-	-
380-383	16.83	15.8	0.78	0.062	0.42	-	-	-
440-443	18.47	14.5	0.99	0.062	0.41	-	-	-
500-553	19.81	12.4	1.06	0.062	-	-	-	-
560-563	19.94	10.3	1.16	0.065	0.43	-	-	-
680-683	22.96	6.9	1.39	-	0.40	-	-	-
740-743	26.99	3.8	1.45	0.072	0.35	-	-	-
800-803	28.62	-	1.55	0.065	0.35	-	-	-
840-843	28.39	3.0	-	-	0.42	-	-	-

KH 82-4, Stn.19 (38°29.1'N, 134°34.6'E; 3010 m)

Depth (cm)	Alk (meq/kg)	SO_4	NH_4-N	PO_4-P	SiO_2	H_2S	pH(25°C)	Eh(25°C) (V)
		(←		mmol/kg		→)		
BW	2.23	27.6	0.00_0	0.001	0.08_2	ND[2)]	7.73	+0.33
0- 12	4.59	25.6	0.21	0.010	0.30	ND	-	-
12- 16	7.48	-	0.25	0.028	0.38	ND	8.08	+0.33
20- 24	8.80	-	0.35	0.039	0.40	ND	8.24	+0.33
31- 35	8.43	23.8	0.31	0.042	0.46	ND	-	-
40- 44	7.57	-	0.30	0.040	0.46	ND	8.10	+0.32
50- 54	7.96	-	0.26	0.032	0.44	ND	8.17	+0.32
60- 64	7.70	23.0	0.27	0.024	0.39	ND	8.10	+0.32
70- 74	12.38	-	0.51	0.052	0.41	0.02	8.34	+0.28
80- 84	12.38	-	0.54	0.051	0.39	ND	-	-
90- 94	10.69	21.1	0.46	0.050	0.43	ND	8.19	+0.28
100-104	2.77	27.0	0.02_5	0.006_2	0.43	ND	-	-
110-114	2.83	27.4	0.02_9	0.006_7	0.42	ND	7.75	+0.32
120-124	3.43	27.4	0.04_6	0.012	0.40	ND	-	-
130-134	3.83	27.3	0.03_8	0.020	0.43	ND	8.17	+0.31
140-144	3.93	26.7	0.06_2	0.018	0.47	ND	-	-
150-154	4.24	26.7	0.07_2	0.019	0.45	ND	8.32	+0.30
160-164	4.33	26.7	0.08_6	0.016	0.44	ND	-	-
180-184	4.83	26.0	-	0.017	0.48	-	8.28	+0.29
202-206	5.29	25.6	0.14	0.026	0.48	ND	8.00	+0.24
220-224	5.55	25.6	0.15	0.022	0.49	ND	-	-
240-244	6.19	25.2	0.18	0.023	0.47	ND	8.15	+0.05
260-264	6.37	24.4	0.18	-	0.46	ND	-	-
280-284	6.83	-	0.23	0.032	0.49	ND	8.02	+0.02
300-304	7.18	24.5	0.20	0.034	0.50	ND	-	-
340-344	8.06	23.8	0.28	0.038	0.48	0.02	8.13	-0.05
380-384	8.56	22.8	0.32	-	0.45	0.01	-	-
420-424	9.01	22.4	0.35	0.039	0.41	0.02	8.04	-0.09
460-464	10.22	21.8	0.44	0.045	0.40	0.01	-	-
501-505	11.25	20.5	0.48	0.049	0.45	0.02	8.00	-0.08
560-565	13.83	19.7	0.54	0.052	0.45	0.37	8.07	-0.15
640-644	16.30	17.2	0.69	0.062	0.43	0.59	-	-
680-684	17.16	16.4	0.75	0.063	0.46	0.60	7.95	-0.14
740-744	19.79	15.4	0.89	0.068	0.45	1.39	-	-
780-784	21.01	13.0	0.92	0.073	0.44	-	8.02	-0.15
820-824	24.12	11.7	1.04	0.082	0.44	1.12	-	-
850-854	25.19	12.1	1.05	0.088	0.43	0.66	7.93	-0.15

KH 82-4, Stn.23 (36°48.4'N, 131°34.9'E; 2080 m)

Depth (cm)	Alk (meq/kg)	SO_4	NH_4-N	PO_4-P	SiO_2	H_2S	pH(25°C)	Eh(25°C) (V)
		(←		mmol/kg		→)		
BW[3)]	2.24	27.2	0.00_0	0.000	0.09_0	ND	7.95	+0.33
10- 14	3.43	27.1	0.04_5	0.006	0.49	ND	8.19	+0.28
20- 24	3.95	26.6	0.08_2	0.020	0.56	ND	-	-
30- 34	4.08	26.0	0.11	0.015	0.54	ND	8.14	+0.27
40- 44	4.66	26.2	0.13	0.020	0.55	ND	8.21	+0.27
50- 54	5.04	25.6	0.17	0.023	0.54	ND	-	-
60- 64	5.72	25.3	0.20	0.023	0.54	ND	8.26	+0.26
70- 74	6.28	25.3	0.23	0.032	0.53	ND	8.28	+0.25
80- 84	6.43	25.4	0.26	-	-	ND	-	-
90- 94	6.88	24.7	0.29	0.036	0.51	ND	-	-
100-104	7.19	24.7	0.32	0.039	0.53	ND	8.10	+0.25
120-124	7.60	24.2	-	0.032	0.52	ND	-	-
130-134	7.73	24.1	0.38	0.035	0.49	ND	8.08	+0.26
140-144	8.79	23.0	0.34	0.040	0.50	ND	-	-
150-154	9.05	23.4	-	-	0.45	ND	8.17	+0.27
180-184	10.38	-	0.51	0.049	0.45	-	8.32	+0.25
190-194	11.04	21.8	0.56	0.056	0.48	0.01	8.17	+0.04
220-224	11.58	20.7	0.60	0.054	0.50	0.01	-	-
240-244	12.55	20.3	0.63	0.064	0.52	0.05	8.19	+0.10
280-284	14.70	18.7	0.75	0.074	0.52	0.13	8.26	-0.06
300-304	15.62	18.2	0.83	0.076	0.52	0.46	-	-
340-344	17.89	16.8	0.92	0.081	0.53	0.33	8.15	-0.09
380-384	19.53	15.1	1.09	0.087	0.54	0.88	-	-
460-464	24.37	11.8	1.25	0.101	0.55	1.25	-	-
500-504	25.79	10.2	1.27	0.106	0.51	-	7.86	-0.12
530-534	27.48	9.7	1.41	0.110	0.52	1.65	-	-
560-564	28.64	8.7	1.46	0.108	0.52	-	-	-
600-604	31.17	7.0	1.59	0.101	0.55	2.1_8	8.06	-0.27
660-664	33.47	4.8	1.71	0.121	0.53	3.0_5	-	-
720-724	35.50	2.6	1.82	0.119	0.55	4.7_8	7.84	-0.18
780-784	37.61	1.4	1.93	0.131	0.57	4.0_0	-	-
830-834	40.12	0.9_3	2.16	0.148	0.57	3.9_5	7.93	-0.20

7-8. AN ATTEMPT TO USE URANIUM AND THORIUM ISOTOPES FOR DETERMINATION OF THE ACCUMULATION RATE OF SEDIMENT IN THE SEA OF JAPAN

A. OMURA

The final aim of this study is to know the accumulation rate of sediment deposited in the Sea of Japan during Late Pleistocene. Such an accumulation rate will be helpful to determine the ages of some marker-tephras, Aira-Tn, Yamato, Aso-4 and so on, which are extensively found in subbottom sediments of the Sea of Japan.

Sediment samples were taken at about 50 cm interval from two piston cores (P-15 & -17) collected at Stations KH 82-4-15 and -17 during this cruise. In the present study, the C-3 core sample was also used to methodize the uranium and thorium isotopic analysis, prior to examining the core samples collected during this cruise. The C-3 piston core was collected during KH 79-3 cruise at a locality of 37°03.5'N Lat. and 134°42.6'E Long. and at the water depth of 935 m. The core sediment seems to be lithologically similar to those in P-15 and -17 cores.

The sediment was treated with hot hydrochloric acid which liberates the thorium that is absorbed on detrital particles or resides in authigenic phases. The principal detrital materials like quartz and feldspars are not dissolved by this procedure. The separation and purification method of uranium and thorium isotopes are schematically summarized in Fig. 7-8-1. Alpha-particle spectrometry was employed, using a multi-channel pulse height analyzer with silicon solid-state detectors.

The preliminary results on isotopic analysis are shown in Table 7-8-1.

The P-15 and -17 core samples will hereafter be analyzed by the same manner and compared with each other in the isotopic composition with respect to uranium and thorium in leachable fractions.

Table 7-8-1. Uranirm and Thorium Isotopic Compostition in Sediments of C-3 Piston Core.

Depth (cm)	U (ppm)	Th (ppm)	Activity Ratio		
			$^{234}U/^{238}U$	$^{230}Th/^{232}Th$	$^{230}Th/^{234}U$
0 ~ 2	2.66 ± 0.06	5.68 ± 0.26	1.06 ± 0.03	1.15 ± 0.07	0.746±0.037
49~51	5.03 ± 0.19	8.58 ± 0.26	1.14 ± 0.04	1.07 ± 0.04	0.517±0.025
199~201	4.24 ± 0.19	9.00 ± 0.15	1.13 ± 0.05	1.24 ± 0.02	0.751±0.034
299~301	7.07 ± 0.26	8.99 ± 0.22	1.13 ± 0.04	1.01 ± 0.03	0.362±0.016
499~501	14.7 ± 0.3	6.61 ± 0.24	1.13 ± 0.02	3.57 ± 0.13	0.456±0.014
599~601	1.71 ± 0.05	8.93 ± 0.19	1.14 ± 0.04	1.13 ± 0.03	1.65 ± 0.06
699~701	3.73 ± 0.17	8.11 ± 0.19	1.06 ± 0.05	1.54 ± 0.04	1.01 ± 0.05
799~801	16.1 ± 0.3	6.39 ± 0.19	1.13 ± 0.02	4.84 ± 0.14	0.548±0.015
899~901	18.4 ± 0.5	7.64 ± 0.40	1.10 ± 0.02	4.49 ± 0.23	0.547±0.022

The weight of sample is defined as that leachable by HCl.

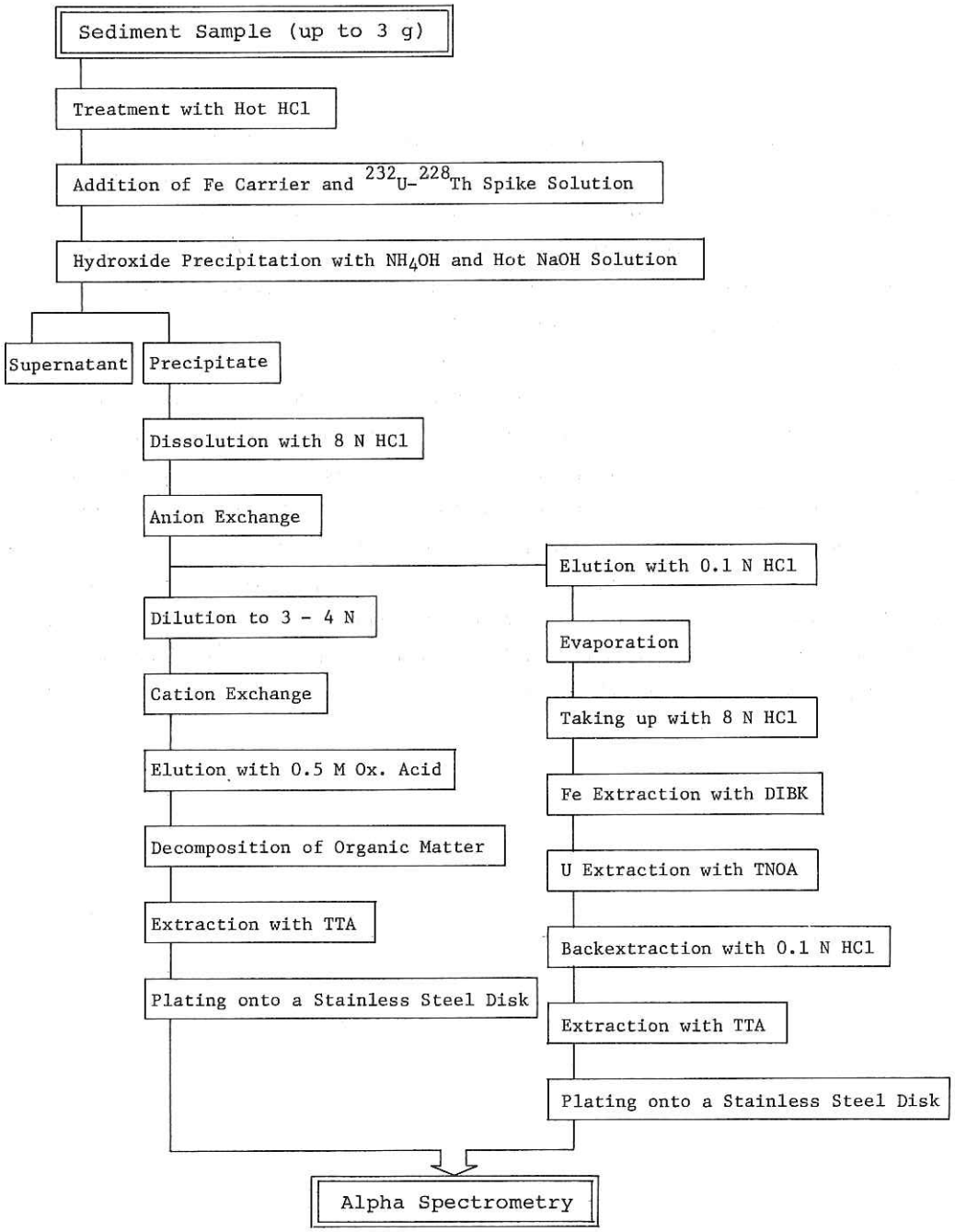

Fig. 7-8-1. Analytical Scheme for Uranium and Thorium Isotopes in Sea-Bottom Sediments.

7-9. OXYGEN ISOTOPIC ANALYSIS

T. OBA

Two cores taken from the northern and southern parts of the Tsushima Strait (KH 82-4-14 and 23) were chosen to investigate the paleoceanographic conditions of the both sides of the strait. Oxygen isotope of planktonic and benthic foraminiferal tests in these cores was anlyzed using a micro-mass spectrometer at the Department of Earth Science, University of Yamagata. The preliminary result is shown in Fig. 7-9-1.

The analysis of the planktonic foraminiferal tests in the core 23, which is located at the northern part of the strait, gives much the same pattern of oxygen isotopic curve that was observed in the two cores taken from Oki bank in the Sea of Japan and examined by Oba et al. (1980). On the other hand, the result of the core 14, which is located at the southern part of the strait, shows a completely different pattern of the oxygen isotopic curves from that of the core 23, except for the uppermost one meter of both cores. This indicates that the paleoceanographic conditions of the northern and southern parts of the Tsushima Strait were completely different from each other during the last glacial period.

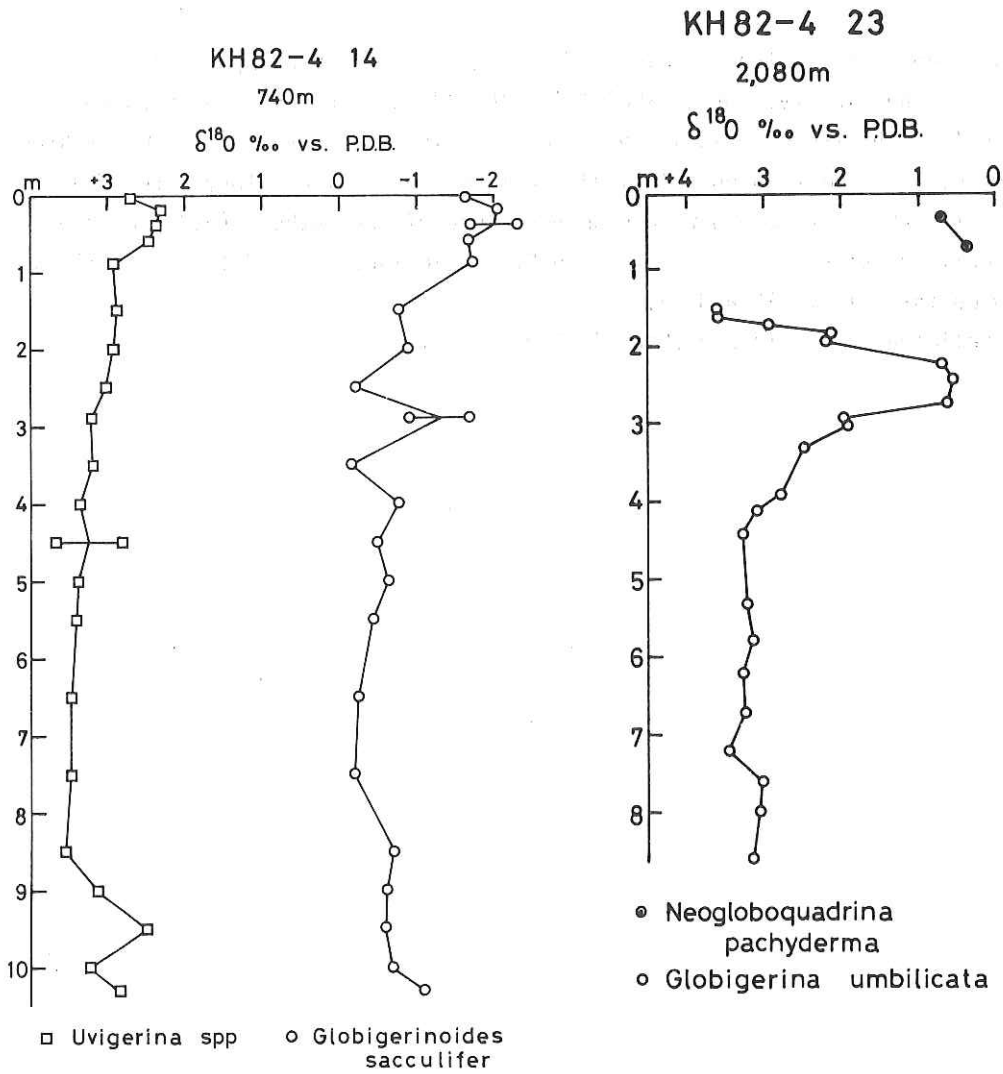

Fig. 7-9-1 $\delta^{18}O$ contents of planktonic (circle) and benthic (square) foraminiferal tests in two cores.

7-10. FORAMINIFERA

H. KITAZATO and T. OBA

Coiling ratio of the *Neogloboquadrina pachyderma* (Ehrenberg) *s.l.* was examined in five cores (KH82-4-15,-16,-17,-23, and-25). Samples were taken from the whole cores at every ten centimeter interval and were treated with the usual micropaleontological procedure in the laboratory, Residuals above the 250 mesh screen were examined. One of the authors (H.K.) examined the coiling ratio of *N. pachyderma* in St. 15,16, and 17, and the other (T.O.) studied that of St. 23 and 25.

Preliminary results are shown in Fig. 7-10-1.

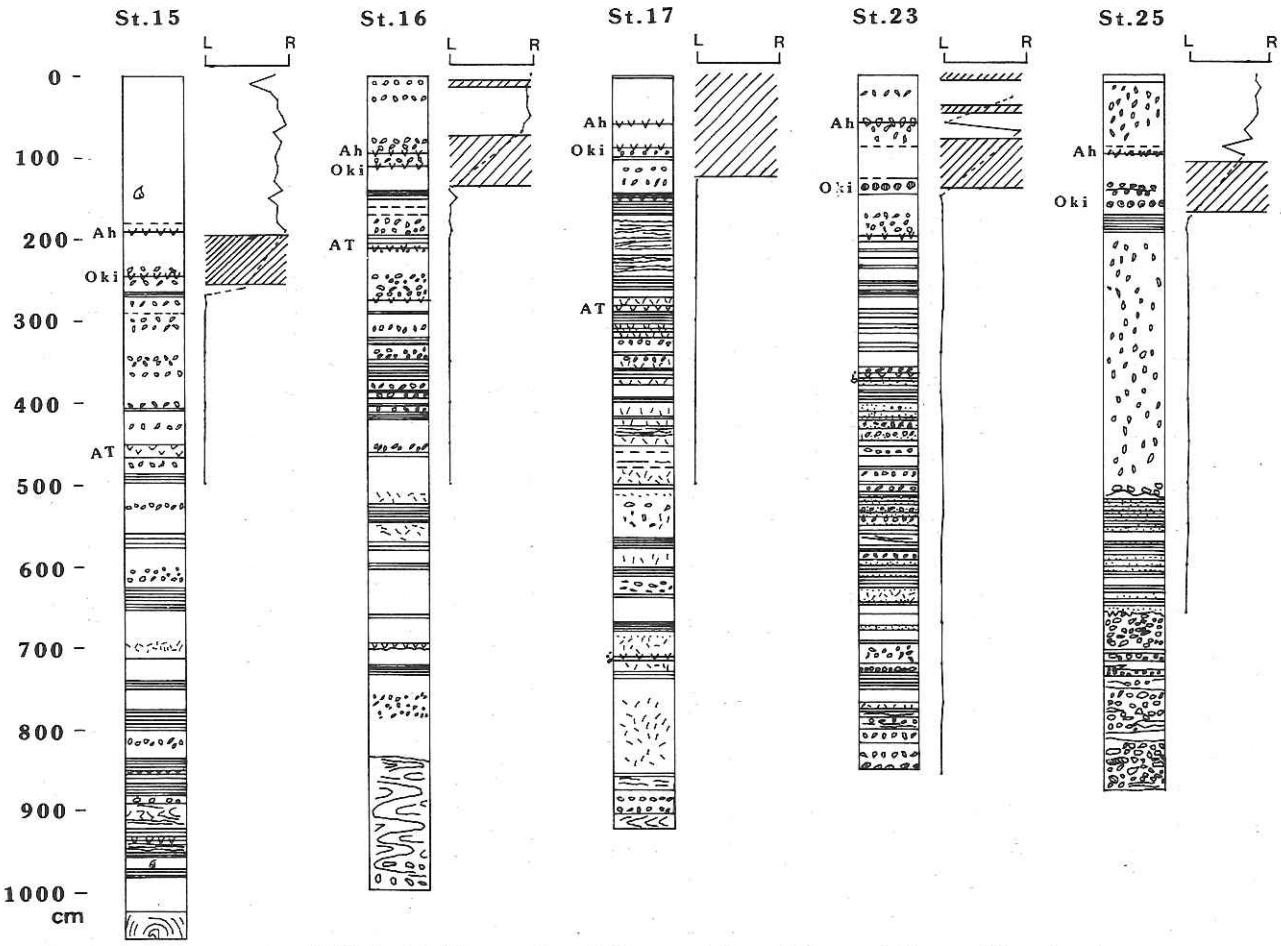

Fig. 7-10-1. Coiling ratio of the *Neogloboquadrina pachyderma* (Ehrenberg) in the cores. Shaded parts show the barren formaminiferal horizons.

7-11. CALCAREOUS NANNOFOSSILS

N. OHYAMA

The calcareous nannofossils from the thirteen cores were examined. The aims of this study are to know the geologic age of five cores from the Pacific Ocean and to detect the latest Quaternary paleoenvironment of the Sea of Japan using the cores from the East China Sea and the Sea of Japan.

Materials and Methods of this study

The samples were taken at about 5-20 cm intervals in each core. The sample was placed in the polyethylene bottle and water was added. The capped bottle was shaked and put into the ultrasonic shaker for five second to disaggregate the materials. After heavier particles were settled, two or three drops of suspension were placed on a cover glass (24mm x 24mm). It was dried on a hot plate and mounted on a slide glass with Entellan-new. The slide was examined by binocular optical polarizing microscope OPM of 1500 magnification. For the scanning electron microscope SEM examination, a few drops of the suspension were placed on a cover glass and dried naturally. It was coated with gold in the ion spatter and examined.

The cores from the Pacific were examined by both OPM and SEM to find the calcareous nannofossil biostratigraphic events, and only OPM was used for those from the East China Sea and the Sea of Japan. On each slide, over 200 individuals of nannofossils were counted. The abundances of three environmentarily characteristic species are shown in Fig. 7-11-1. These three species are *Coccolithus pelagicus* (Wallich) Schiller (cold water species), *Gephyrocapsa oceanica* Kamptner (warm water species) and *Braarudosphaera bigelowi* (Gran & Braarud) Deflandre (shallow marine species).

Preservation

Preservation states of the calcareous nannofossils are as follows; G: good, M; moderate, P: poor and B: barren. The specimens in cores from

the Pacific and the East China Sea are preserved in good to moderate conditions. However, the preservation of the specimens in the cores from the Sea of Japan are moderate to poor. Further, the nannofossils are barren by obliteration in many horizons of the cores collected in deeper sea.

Result

A) Pacific Ocean

Nannofossil events were found in only KH 82-4-7 core. The last occurrence datum of *Pseudoemiliania lacunosa* (Kamptner) Garter is at 278 cm and the first occurrence datum of *Emiliania huxleyi* (Lohmann) Hay & Mohler is at 140 cm of the core. In KH 82-4-1,-2,-5 and-6, *E. huxleyi* is dominant throughout the cores and the reworked Tertiary species of nannofossils is comprised sporadically. *E. huxleyi* occurs from the lowest part of the KH 80-3-8 core and becomes dominant above a depth of 340 cm from the top.

B) The East China Sea and Sea of Japan

In KH 80-3-14 core, the variable nannofossils are abundant and well preserved, so it seems to be under the Tsushima warm current all the time. The cores from the Sea of Japan, except for KH 80-3-17 and -19 which were collected from deeper sea than others, have the same tendency. There are barren parts around the Oki tuff and the assemblage is differnt between the above and below. Below the barren parts, both *G. oceanica* and *C. pelagicus* occur successively and in the above *G. oceanica* occurs again but *C. pelagicus* is scarce. It indicates that the strong inflow of Tsushima warm current into the Sea of Japan at the time, and the warm current should have increased after the event.

REFERENCES

Geitzenauer, K. R., Roche, M. B., and McIntyre, A., 1976. Modern Pacific Coccolith Assemblages: Derivation and Application to Late Pleistocene Paleotemperature Analysis. in Cline, R. M., and Hays, J. D., Investigation of Late Quaternary paleoceanography and paleoclimatology: Geol. Soc. Amer.Mem.145, 423-448.

Nishida, S. 1979 Atlas of Pacific nannoplankton. NOM (News of Osaka Micropaleontologists), Spec. Pap., 3, 1-22.

Okada, H. and Honjo, S. 1973 Distribution of oceanic coccolithopholids in the Pacific. Deep-Sea Res., 20, 355-374.

Takayama, T. 1972 A note on the distribution of *Braarudosphaera bigelowi* (Gran and Braarud) Defrandre in the bottom sediments of Sendai Bay, Japan. Trans. Proc. Paleontol. Soc. Japan, N. S. 87, 429-435.

Takayanagi, Y., Takayama, T., Sakai, T, Oda M., and Kato, M., 1979 Late Cenozoic Micropaleontologic Events in the equatorial Pacific sediments. Tohoku Univ., Sci, Rep., 2nd ser. (Geol.), 49, 71-87.

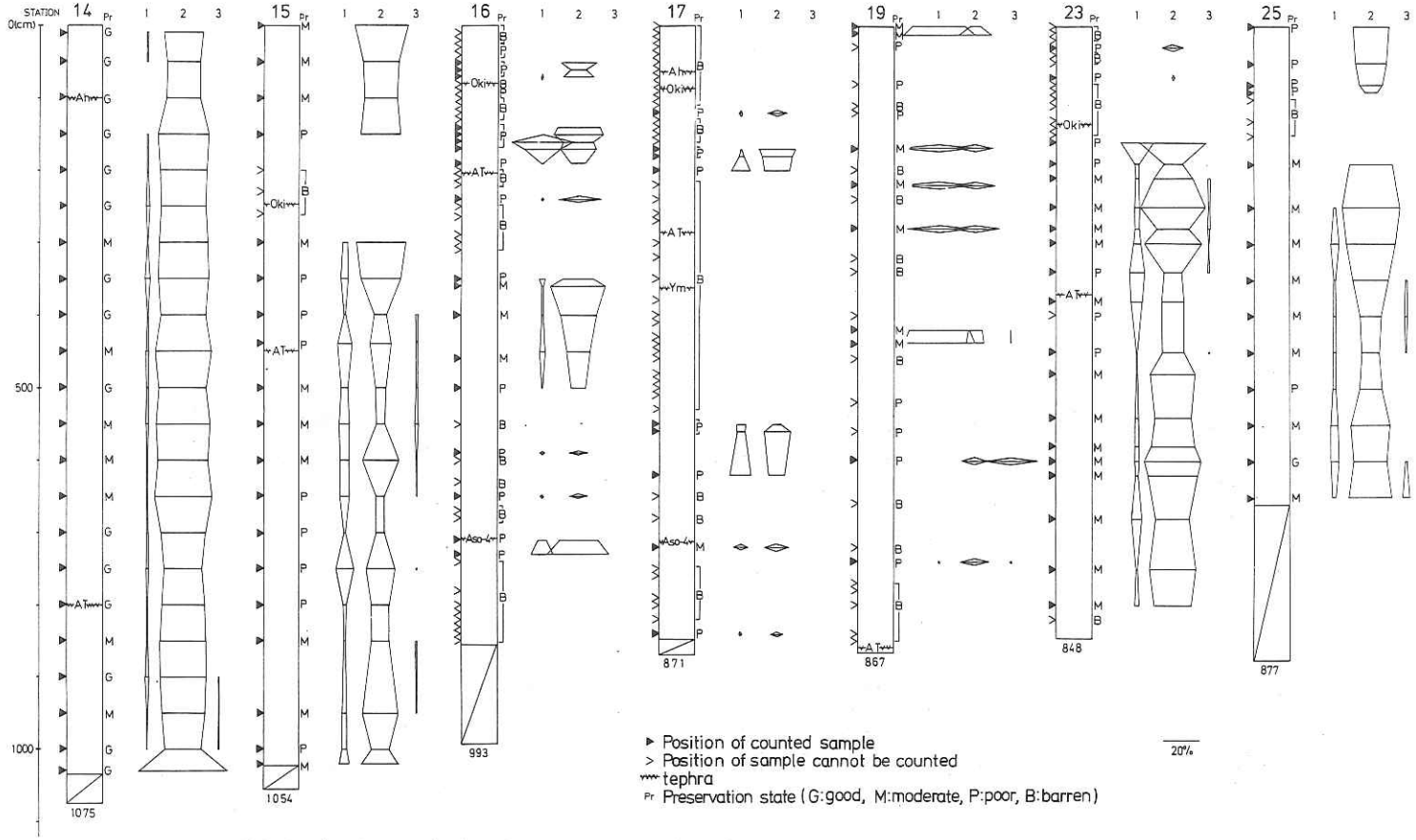

Relative abundances of selected calcareous nannofossil species and preservation states of calcareous nannofossils
1: *Coccolithus pelagicus*, 2: *Gephyrocapsa oceanica*, 3: *Braarudosphaera bigelowi*.

Fig. 7-11-1. Abundance of three characteristic species of calcareous nannofossils.

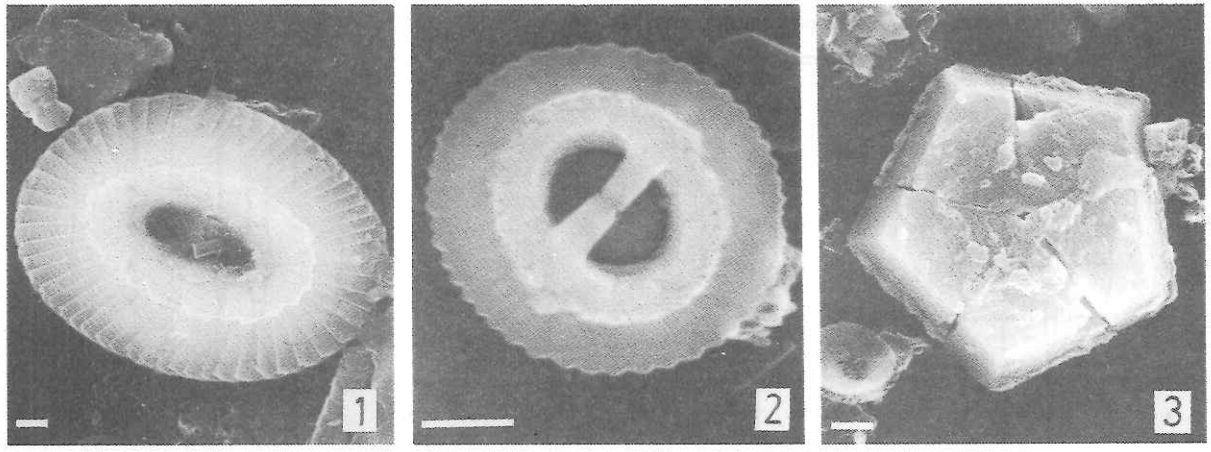

SCALE BAR = 1 μ

Fig. 7-11-2. 1. *Coccolithus pelagicus* (Wallich) Schiller
sample KH 82-4-23, 599-600 cm, distal view.
2. *Gephyrocapsa oceanica* Kamptner
sample KH 82-4-8, 449-450 cm, distal view.
3. *Braarudoshaera bigelowi* (Gran & Braarud) Deflandre
sample KH 82-4-25, 549-550 cm, proximal view.

7-12. DIATOMS IN THE PISTON CORES

Y. TANIMURA

Diatoms in the upper parts of piston cores were examined to elucidate the historical change of diatom floras and those paleoceanographic implications in the Sea of Japan since 18,000 Y BP. Prior to the examination with optical and electron microscopes, raw materials were cleaned as follows:
i) Sediment samples, taken at about 10 - 20 cm intervals, were placed in 15 ml centrifuge tube with 2-3 drops of hydrogen peroxide, and the contents were exposed to UV radiation for about 6 hours to decompose organic materials. ii) Each tube was filled with water, and fine-grained materials in suspension were removed by centrifugation (1,200 rpm, 5 min.). iii) The residue obtained by this process was stored in the plastic vial with a mixture of acetic acid and formalin.

Piston core KH 82-4-16 983 cm long, was taken from the northeast off Oki Islands at a depth of 1,745m. In total 22 samples, taken at about 10 cm intervals, were used for the examination. All of these samples yield well preserved diatom valves.

One of the most abundant species in the samples from the core is *Thalassionema nitzschioides* Grunow, and it forms about 25 to 65% of the total. Stratigraphical changes of *T. nitzschioides* and those of diatom taxa selected as the indicator of oceanographic conditions in Tanimura (1981) are shown in Fig. 7-12-2. Conspicuous difference of diatom floras was observed between the upper layers of the core and the lower. *Pseudoeunotia doliolus* (Wall.) Grunow, *Thalassiosira oestrupii* (Ostf.) Proškina-Lavrenko and *Melosira sulcata* (Ehr.) Kützing occur with high frequency on the upper part (from 80 cm to the top of the core). On the contrary, and abundant or common occurrence of *M. sulcata*, *Denticulopsis seminae* (Simonsen et Kanaya) Simonsen, *Thalassiosira trifulta* Fryxell et Hasle (*Thalassiosira* sp. 1; Tanimura, 1981) and *Thalassiosira nordenskioeldii* Cleve was recognized in the lower part of the core.

The surface water of the Sea of Japan is classified into two masses of the warm- and cold-currnt regions by their physical characters (Moriyasu, 1972). The upper layer of the surface water in the warm-current region is influenced by the low saline water brought from the East China Sea.

The diatom flora in the modern sediments of the sea is characterized by an abundant occurrence of *P. doliolus*, *T. oestrupii* and *M. sulcata* in the warm-current region, and that of *D. seminae*, *T. nordenskioeldii* and *T. trifulta* in the cold-current region. Particularly, *M. sulcata* in the sediments is restricted to the southern part of the sea under influence of low saline water brought from the East China Sea (Tanimura, 1981).

The relationship between the abiotic property of surface water and the geographical distrubution of *P. doliolus*, *T. oestrupii*, *M. sulcata*, *D. seminae*, *T. nordenskioeldii* and *T. trifulta* in the modern sediments of the sea indicates that the stratigraphical distribution of these species in the core suggest the following oceanographic conditions;

1) The diatom flora in the upper layers of the core was probably formed under the similar oceanographic conditions of the present warm-current region of the sea.

2) The diatom flora in the lower part of the core indicates stronger influence of the low saline water from the East China Sea and of cold water than that of the upper part.

However, the origin of the low saline water in a period of the last glacial low stand sea level is far beyond the deduction on the data in the present study.

These floral changes are also recognized in the cores KH 82-4-15 and -17 within the intervals from 200 to 160 cm and from 80 to 60 cm measured from the top. Furthermore, the ^{14}C age of aforementioned event, assigned by the relationship between the stratigraphic position of tephra(Akahoya ash, Oki ash and Aira Tn ash) and it's ^{14}C age, roughly coincides among the three cores (6,000 - 9,000 Y BP.).

FLORAL REFERENCES

Denticulopsis seminae (Simonsen et Kanaya) Simonsen, 1979: p. 65. Syn., *Denticula seminae* Simonsen et Kanaya, 1961: p. 503, pl. 1, figs. 26-30. (Fig. 7-12-1-3)

Melosira sulcata (Ehr.) Kützing, 1844: Hustedt, 1928, Kieselalg., Teil I, p.276, fig. 119a. (Fig. 7-12-1)

Pseudounotia doliolus (Wall.) Grunow, 1880: Hustedt, 1932, Kieselalg., Teil II, p. 259, fig. 737. (Fig. 7-12-1-5)

Thalassionema nitzschioides Grunow, 1881: Hustedt, 1932, Kieselalg., Teil II, p. 244, fig. 725; Cupp, 1943, p. 182, fig. 133. (Fig. 7-12-1-6)

Thalassiosira nordenskioeldii Cleve, 1875: Hustedt, 1928, Kieselalg., Teil. I, p. 321, fig. 157. (Fig. 7-12-1-7)

Thalassiosira oestrupii (Ostf.) Proškina-Lavrenko, 1956: Hasle, 1960, p.8, pl. 1, figs. 5-7, 11. (Figs. 7-12-1-4a, 4b)

Thalassiosira trifulata Fryxell et Hasle, 1979: p. 16-19, pl. 1-5. (Figs. 7-12-1-1, -2a, -2b)

REFERENCES

Cupp, E.E., 1943, Marine plankton diatoms of the West Coast of North America. Scripps Inst. Oceanogr. Univ. Calif., Bull., 5, no.1, 1-238.

Fryxell, G.A. and Hasle, G.R., 1979, The genus *Thalassiosira*: *T. trifulta* sp. nova and other species with tricolumnar supports on the strutted processes. Nova Hedwigia, Beiheft 64, 13-40

Hasle, G.R., 1960, Phytoplankton and ciliate species from the tropical Pacific. Skrif. det Norske Videnskaps-Akademi, Oslo, Matemt. Natutv. KI., no.2. 1-50.

Hustedt, F., 1927 *et seq.*, Die kieselalgen Deutschland, Oesterreichs und der Schweiz mit Berucksichting der ubrigen Lander Europas sowie der angrenzenden Meeresegebite. In Dr. Rabenhorst s Kryptogamen-Flora von Deutschland, Oesterreichs und der Schweiz, v. 7, Teil I, Teil II, 1758 p., Leipzig.

Moriyasu, S., 1972, Hydrography of the Japan Sea. Kaiyo Kagaku,(Marine Science), 4, no. 3, p. 27-33.

Simonsen, R., 1979, The diatom system: Ideas on phyrogeny. Bacillaria, 2, 9-71.

Simonsen, R. and Kanaya, T., 1961, Notes on the marine species of diatom genus *Denticula* Kutz. Inst. Revue ges. Hydrobiol., 46, no. 4, 498-503.

Tanimura, Y., 1981, Late Quaternary diatoms of the Sea of Japan. Tohoku Univ., Sci. Rep., 2nd ser. (Geol.), 51, nos. 1-2, 1-37.

Fig. 7-12-1. Photomicrographs of diatoms contained in the present cores

(Scale bar = 10 μm)

1. *Thalassiosira trifulta* Fryxell et Hasle. Sample KH82-4-16, 169-170 cm.
2a, b. *Thalassiosira trifulta* Fryxell et Hasle. Sample KH82-4-16, 159-160 cm, inside views.
   a. Arrows point to central strutted processes and submarginal labiate process.
   b. Central strutted processes, x 15000.
3. *Denticulopsis seminae* (Simonsen et Kanaya) Simonsen. Sample KH82-4-16, 109-110 cm, inside view.
4a, b. *Thalassiosira oestrupii* (Ostf.) Proškina-Lavrenko Sample KH82-4-16, 9-10 cm.
5. *Pseudoeunotia doliolus* (Wall.) Grunow. Sample KH82-4-16, 9-10 cm.
6. *Thalassionema nitzxchioides* Grunow. Sample KH82-4-16, 9-10 cm.
7. *Thalassiosira nordenskiceldii* Cleve. Sample KH82-4-16, 149-150 cm.
8. *Melosira sulcata* (Ehr.) Kützing. Sample KH82-4-16, 149-150 cm.

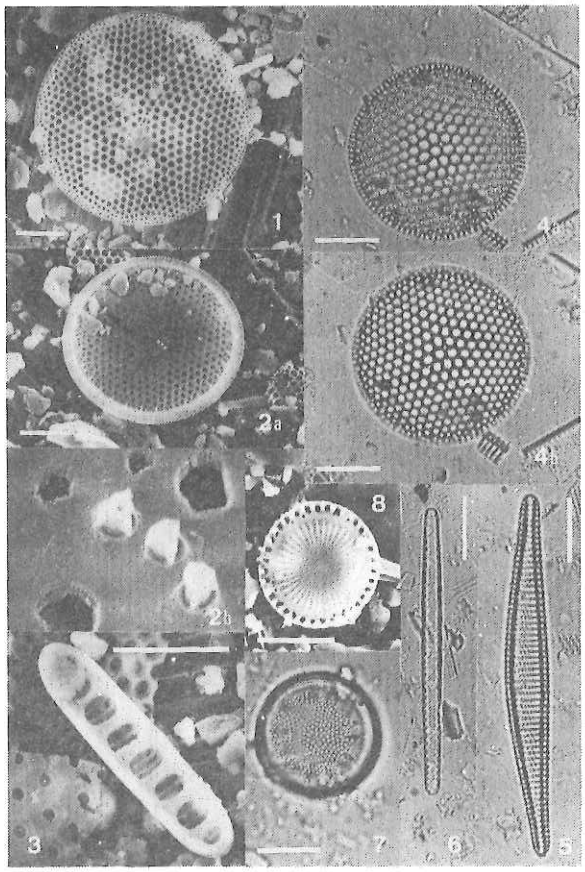
1
2a
2b
3
4a
4b
8
7
6
5

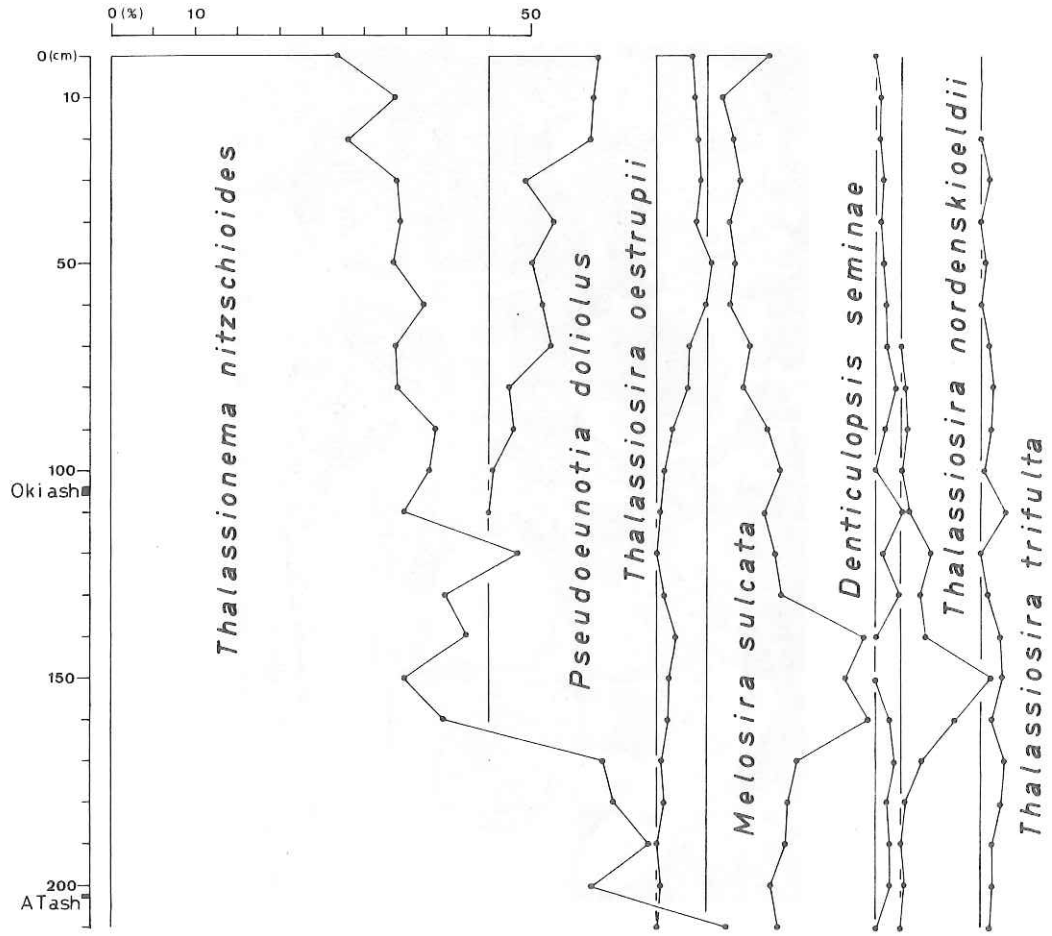

Fig. 7-12-2. Frequency distributions of selected diatom species in the upper part of the core KH 82-4-16.

7-13. FLUCTUATIONS OF THE SILICOFLAGELLATE FLORA IN KH 82-4 CORE

H. KOBAYASHI

INTRODUCTION

Five cores were examined to determine the vertical distributions of *Dictyocha mandrai* Ling and of the total populations of the species coming under the genus *Distephanus* Stöhr since the last glacial age in the Sea of Japan and the East China Sea. The former species abundantly occurs in the middle latitude upwelling regions. On the contrary, the distribution of the latter genus in deep-sea bottom sediments is restricted in the cold water regions (Poelchau, 1976). This study aims to deduce the paleoceanographic changes in the Sea of Japan and the East China Sea on the basis of fluctuations of these silicoflagellate flora.

MATERIALS AND METHODS OF STUDY

Only one core (KH 82-4-14) was taken from the East China Sea near the Koshikijima Islands and the other four cores (-15, -16, -17 and -23) were taken from the Sea of Japan (the Yamato and Tsushima basins).

Sediment samples of 1 cm in thickness were examined at intervals of 10 to 30 cm. The laboratory procedures and microscopic observations were as follows;

1) A sediment sample was boiled with 15% hydrogen peroxide (H_2O_2) in a 200 ml beaker to remove organic matter.
2) After boiling for about 10 min, the beaker was filled with water and kept for about 5 hr at room temperature.
3) A few drops of the residue were placed on a 18 x 24 mm cover glass with Pleurax. Two slides were prepared for each sample.
4) Under optical microscope the slide was transected until counting up to 200 specimens. In case of the total count was less than 200, another slide was additionally examined.
5) D_m and D_s ratios, which are the proportion of *Dictyscha mandrai* and that of *Distephanus* to the total count, respectively, were proposed in this study.
6) The total population of silicoflagellates contained in two slides is shown as Ab (Fig. 7-13-2).

RESULTS

A summary of the results of this study is illustrated in Fig. 7-13-2. Among the examined cores, a remarkably high peak of the D_m ratio (30 to 55 %) was recognized in the four cores from the Sea of Japan. The high content (>30 %) of *Dictyocha mandrai* in the North Pacific bottom sediments was found in the areas of the Alaskan Gyre and of the western Pacific under the Kuroshio Extension (Poelchau, 1976). The first appearance datum has been estimated to be middle Pleistocene in age in Japanese landsections in the Choshi district on the Pacific side (Kobayashi, 1981). However, the occurrence is confined to the upper part of the studied intervals except for KH 82-4-14 core. In relation to the tephrochronologic correlation, the maximum peak of D_m ratio appears to be isochronous and coincides with the minimum point of D_s ratio in the cores. In addition, the next minimum point of D_s ratio was also characteristically found slightly below the above mentioned biohorizon in the cores of the Sea of Japan without containing *Dictyocha mandrai*. A third minimum point of D_s ratio was recognized in all the cores studied. The minimum point is located at just above the Aira Tn Ash (AT). Furthermore, just above it, a large abundance peak of silicoflagellates was recognized in the five cores. An abundance (>200) of silicoflagellates continues from the top to slightly above the maximum peak of D_m ratio only in the cores from the Sea of Japan.

I would like to thank Professor Yokichi Takayanagi and Dr. Kunihiro Ishizaki, Associate Professor of the Institute of Geology and Paleontology, Tohoku University for their critical reading of the manuscript.

REFERENCES

Arai, F., Oba, T., Kitazato, H., Horibe, Y., Machida, H., 1981. Late Quaternary tephrochronology and paleo-oceanography of the Japan Sea. Quat. Research, 20(3), 209-230 (in Japanese with English abstract).

Kobayashi, H., 1981. Late Cenozoic silicoflagellate biostratigraphy in the Choshi district, Pacific Coast, Japan (M. Sc. thesis). Chiba University.

Oba, T., Horibe, Y. and Kitazato, H., 1981. Analysis of the paleoenvironment since the last glacial age based on two cores from the Japan Sea. Kokogaku-to-Shizen-Kagaku (Archaeology and Natural Science), no.13, 31-49 (in Japanese with English abstract).

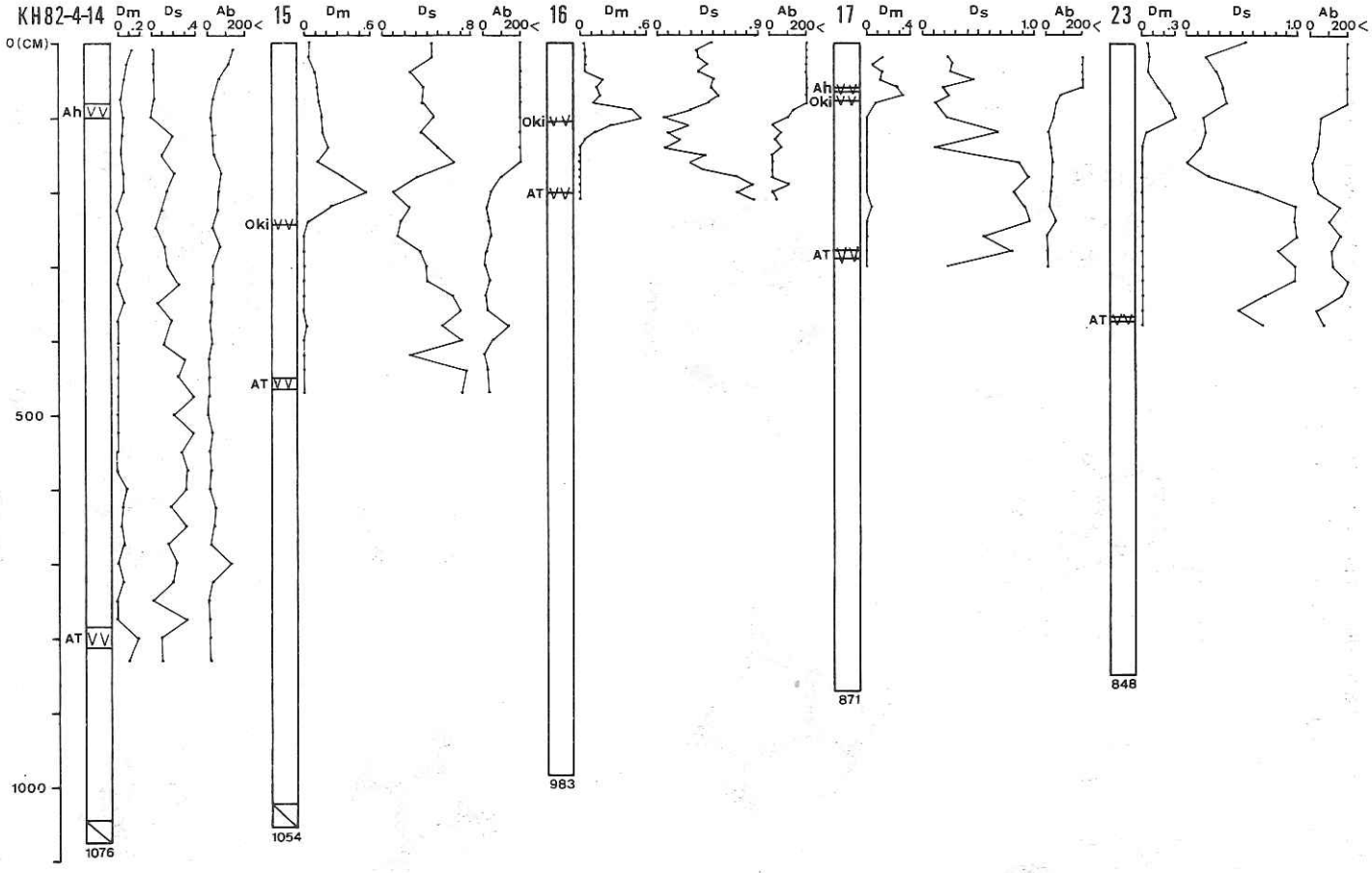

Fig. 7-13-2. Total population of silicoflagellates and proportions of *Dictyocha mandrai* and *Distephanus* with depths of the cores. Horizons of identified tephras are also shown.

Poelchau, H. S., 1976. Distribution of Holocene silicoflagellates in North Pacific sediments. Micropaleont., 22(2), 164-193.

Tanimura, Y., 1981. Late Quaternary diatoms of the Sea of Japan. Sci. Rep. Tohoku Univ., 2nd ser. (Geol.), 51, 1-37.

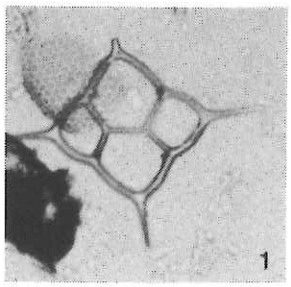

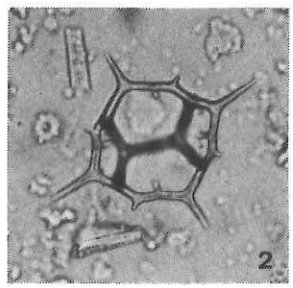

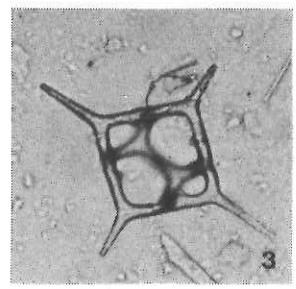

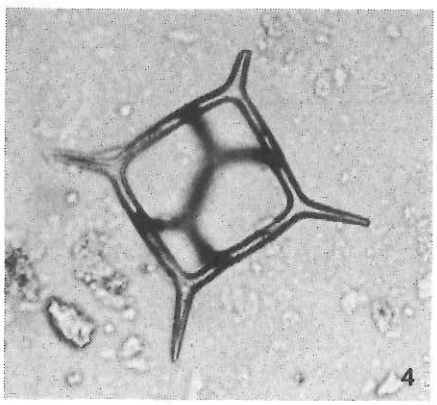

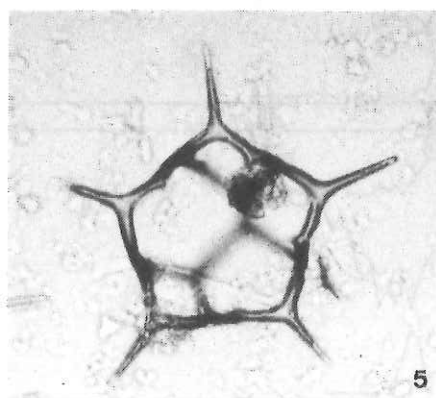

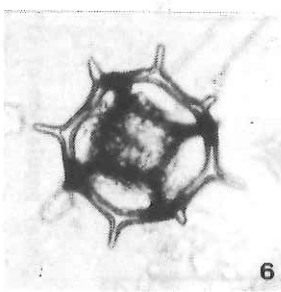

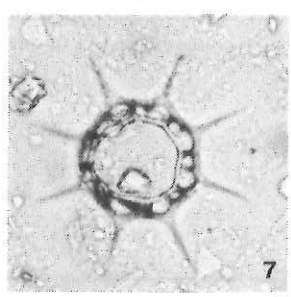

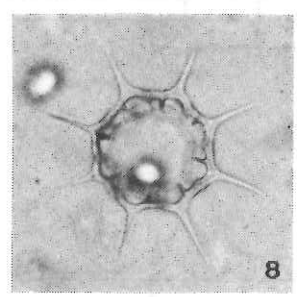

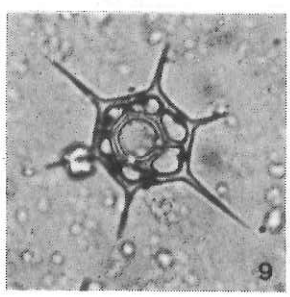

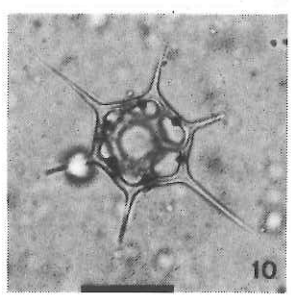

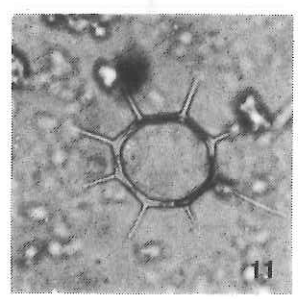

Fig. 7-13-1.
Silicoflagellates obtained on the Cruise KH 82-4.
(All 800x magnification, scale bar = 20 μ)

1 *Dictyocha calida* Poelchau
Sample KH 82-4-15, 98-100 cm (L56/3)

2 *Dictyocha mandrai* Ling
Sample KH 82-4-14, 9-10 cm (D38/1)

3 *Dictyocha messanensis* f. *messanensis* Haeckel
Sample KH 82-4-23, 259-260 cm (U55/2)

4 *Dictyocha messanensis* f. *spinosa* Lemmermann
Sample KH 82-4-14, 174-175 cm (Z51/0)

5 *Dictyocha pentagona* (Schulz)
Sample KH 82-4-14, 14-15 cm (X56/4)

6 *Distephanus octangulatus* Wailes
Sample KH 82-4-15, 98-100 cm (P48/0)

7, 8 *Distephnus octonarius* Deflandre
Sample KH 82-4-23, 259-260 cm (D46/4)

9,10 *Distephanus speculum* (Ehrenberg)
Sample KH 82-4-14, 374-375 cm (M38/1)

11 *Octactis pulchra* Schiller
Sample KH 82-4-14, 174-175 cm (G55/3)

7-14. TEPHROCHRONOLOGY IN THE SEA OF JAPAN AND THE NORTHERN EAST CHINA SEA

H. MORIWAKI, T. FURUTA and F. ARAI

Many late Pleistocene and Holocene tephras have been known in the sediments from the Sea of Japan. Most of them have already been identified by the petrographic characteristics, particularly by the refractive indices of glass and some phenocrysts (Arai et al., 1981; Machida et al., 1981). Several tephra layers mainly composed of volcanic ashes are found in the piston cores of this cruise, which were collected in the Yamato and Tsushima basins of the Sea of Japan and in the area off the Koshiki Islands in the northern East China Sea. The stratigraphic, lithologic and petrographic characteristics of those tephras were described on ship, and the refractive indices of glass shards and some phenocrysts, and chemical composition of glass shards by microprobe were determined in the laboratory for those piston core tephras.

As a result, petrographic characteristics and refractive indices of glass shards made it possible to identify the following five marker ashes: Kikai-Akahoya ash (KH82-4-14(1), -17(1)), U-Oki ash (-15(1), -16(1), -17(2), -23(1)), Aira-Tn ash (-15(2), -16(2), -17(3), -19(1)·(2)·(3),-23(2)), Yamato ash (-16(3), -17(4)), and Aso-4 ash (-16(4), -17(5), -23(3)), younger to older(Table 7-14-1).

Concerning chemical composition, major elements were determined with the microprobe, and results were listed in Table 7-14-2. Alkali concentrations are important for the correlation of the Sea of Japan tephras. For microprobe work on volcanic glass shards, however, the major problem is the uncontrolled volatilization of sodium, which is governed by probe current, beam diameter and counting period. We controlled the volatilization of sodium on the following analytical condition: probe current; 2×10^{-8}A, beam diameter ; 15-20 μm, accelerating voltage; 15kv and counting period; 20 seconds. Though the variation of sodium concentration is slightly recognized between correlated tephras probably owing to volatilization, there are significant differences of the concentration between uncorrelated tephras.

The correlation of the tephra layers by the refractive indices is supported by the chemical composition of glass shards. There are significant differences

for chemical composition among five marker tephras. One of the most remarkable features is the difference of alkali (K_2O + Na_2O)concentration. The alkali concentration of U-Oki and Yamato ash is high: 12-13 wt%. Those ashes are derived from the Ulreung Island of Korea. In contrast, that of other tephras derived from the Japanese Islands is low; less than 9 wt%. It is fairly hard to distinguish U-Oki from Yamato ash by alkali concentration, and other chemical composition of these tephras are very similar. This similarity may suggest that these tephras were derived from the same volcano, i.e. the Ulreung Island.

The chemical compositions among the Japanese marker tephras are significantly different from each other. For example, the alkali concentration of Aso-4 is ca. 8.5 wt%, but that of Kikai-Akahoya and Aira-Tn ash ranges ca. 6 -6.5 wt%.

The other remarkable feature is the difference of transition metal oxides contents, as represented by total FeO. These oxides should control the refractive index of glass. As shown in Tables 7-14-1 and -2, glasses higher content of FeO* have higher refractive index. There may be the following relationship between refractive index and the content of transition metal oxides;

$$R = \frac{7}{1000}M + 1.492 \pm 0.005$$

where R is refractive index, and M is content of total transition metal oxides.

The ash of KH82-4-15(3) is not correlated with any other tephras collected in this cruise. Much lower alkali concetration (K_2O+Na_2O= 5.39 wt%) of this ash than that of U-Oki and Yamato ash indicates that this ash was not clearly derived from the Ulreung Island. Because this ash contains biotite, it seems to be derived from the volcanoes of San'in district, i.e., Sanbe and Daisen volcanoes.

References

Arai F., Oba T., Kitazato Y., Horibe Y. and Machida H., 1981, Late Quaternary tephrochronology and paleo-oceanography of the sediments of the Japan Sea. Quaternary Res., 20, 209-230.

Machida H., Arai F. and Moriwaki H., 1981, Two Korean tephras, Holocene markers in the Sea of Japan and the Japan Islands. Kagaku, 51, 562-569 (in Japanese)

Table. 7-14-1. Petrographic characteristics of abyssal tephra in the Sea of Japan

(1) core sample No.	(2) Subbottom depth(cm)	(3) max. dia of tephra clasts (mm)	(4) volcanic glass Type	(4) R.I. range <modal> (mean)	(5) phenocrysts charact. minerals R.I.	(6) note & correlation
KH82-4-14						
1	85-90	0.3	bw>pm	1.508-1.515 (1.509-1.512)		Kikai-Akahoya ash
2	780-812	1.0	bw>pm	1.499-1.501 <1.500>		Aira-Tn ash
KH82-4-15						
1	242-244	0.6	pm (fib-sp) (cl-pc)	1.519-1.524	af; ho, bi af n_1=1.522-1.524	U-Oki ash
2	450-464.5	1.0	bw (cl)	1.499-1.501 <1.500>		Aira-Tn ash
3	936-936.5		pm (fib-str) (cl)	1.495-1.497 <1.496>	bi	probably derived from Sanbe volcano
KH82-4-16						
1	104-106	0.3	pm (wh-pc)	1.518-1.523	af; cpx af n_1=1.522-1.524	U-Oki ash
2	202-203	0.2	bw>pm (str) (cl)	1.499-1.501 <1.500>	opx, cpx	Aira-Tn ash
3	275-279.5	0.6	pm (sp-fib) (wh)	1.521-1.523	af; bi, ho, cpx af n_1=1.522-1.524	Yamato ash

4	700-702	1.0	bw, pm (pc-cl)	1.508-1.512 <1.510>	pl; opx, ho, cpx ho n_2=1.686-1.688 <1.687> opx γ=1.700	Aso-4 ash
KH82-4-17						
1	60-65	0.4	bw (pc)	1.508-1.518 (1.508-1.512)	pl	Kikai-Akahoya ash
2	76-78	0.3	pm (wh-pc)	1.518-1.523 (1.519-1.523)	af; bi af n_1=1.522-1.524 <1.523>	U-Oki ash
3	280-290	0.3	bw (cl)	1.499-1.501 <1.500>		Aira-Tn ash
4	364-366	0.5	pm, sc (wh)	1.522-1.524 <1.523>	af; bi af n_1=1.523±	Yamato ash
5	711-714	1.2	bw(pc-cl), pm(wh)	1.508-1.512 (1.509-1.511) <1.510>	pl; opx, ho, cpx ho n_2=1.686-1.688 opx γ=1.700	Aso-4 ash
KH82-4-19						
1	797-797.5	0.3	bw>pm	1.499-1.523		Aira-Tn ash (reworked)
2	811-811.5	0.6	bw>pm	1.499-1.501 <1.500>		*do.*
3	864-869	0.6	bw>pm (cl)	1.499-1.501 <1.500>	pl	Aira-Tn ash

KH82-4-23						
1	135-137	5.0	pm (sp) (wh)	1.518-1.523	af af n_1=1.523	U-Oki ash (?) rounded pumice
2	368-848	0.6	bw>pm (cl)	1.499-1.501	opx, cpx opx γ=1.732±	Aira-Tn ash
3	847-848	1.2 (pm)	bw(cl-pc), pm(wh)	1.508-1.512 (1.509-1.511)	pl; opx, ho opx γ=1.700± ho n_2=1.687±	Aso-4 ash
KH82-4-25						
1	245-245.5	15	pm (wh)	1.518-1.523	af af n_1=1.523±	rounded pumice
2	260-271	10	pm (wh)	1.518-1.523	af af n_1=1.523±	rounded pumice

Notes

Column (4) : R.I, refractive index; pm, pumiceous glass; bw, bubble-walled glass; sc, scoriaceous glass; sp, spongy pumiceous glass; fib, fibrous pumiceous glass; str, striped pumiceous glass; cl colorless; pc, pale colored; wh, white.

Column (5) : R.I, refractive index; characteristic minerals are arranged in decreasing order. af, alkali feldspar; pl, plagioclase; ho, hornblende; opx, orthopyroxene; cpx, clinopyroxene; bi, biotite; qt, quartz.

Table 7-14-2. Average glass composition of piston core tephras by EPMA.

sample core	No.	depth(m)	SiO_2	TiO_2	Al_2O_3	FeO*	MgO	CaO	MnO	K_2O	Na_2O	Total	N	Correlation
KH82-4-14	1	85-90	73.56	0.53	13.11	2.41	0.15	2.09	0.08	2.67	3.29	98.23	19	Kikai-Akahoya ash
	2	780-812	75.00	0.12	11.76	1.18	0.13	1.06	0.04	3.16	3.36	95.85	27	Aira-Tn ash
KH82-4-15	1	242-244	60.97	0.42	19.65	3.13	0.25	1.35	0.18	6.52	5.94	98.43	14	U-Oki ash
	2	450-464.5	75.98	0.12	11.86	1.20	0.13	1.06	-	3.16	2.65	96.24	35	Aira-Tn ash
	3	936-936.5	73.44	0.03	12.92	0.41	0.07	0.57	0.09	3.70	1.69	92.73	23	?
KH82-4-16	1	104-106	62.11	0.48	20.48	2.68	0.25	1.50	0.15	6.63	4.95	99.25	22	U-Oki ash
	2	202-203	75.48	0.14	11.75	1.10	0.14	0.95	0.03	3.10	2.87	95.57		Aira-Tn ash
	3	275-279.5	60.63	0.48	18.89	3.10	0.24	1.32	0.16	6.33	6.42	97.59		Yamato ash
	4	700-702	69.24	0.41	14.29	1.50	0.38	1.09	0.09	4.08	4.32	95.45	23	Aso-4 ash
KH82-4-17	1	60-65	73.78	0.51	12.93	2.39	0.49	2.00	0.07	2.76	3.54	98.48	22	Kikai-Akahoya ash
	2	76-78	60.31	0.49	19.55	2.63	0.26	1.49	0.13	6.65	6.85	98.39	26	U-Oki ash
	3	280-290	74.40	0.12	11.72	1.17	0.13	1.03	0.04	3.23	3.17	95.04	33	Aira-Tn ash
	4	364-366	59.52	0.41	19.00	3.00	0.24	1.41	0.17	6.27	6.72	96.73	11	Yamato ash
	5	711-714	69.97	0.40	14.42	1.50	0.37	1.11	0.10	4.29	4.39	96.57	30	Aso-4 ash
KH82-4-19	1	797-797.5	74.86	0.14	11.76	1.18	0.14	1.06	0.04	3.13	3.17	95.49	26	Aira-Tn ash (reworked)
	2	811-811.5	75.56	0.13	11.88	1.17	0.13	1.05	0.04	3.14	3.25	96.37	38	"
	3	864-869	76.40	0.12	11.62	1.18	0.13	1.01	0.12	3.03	3.02	96.60	30	Aira-Tn ash
KH82-4-23	2	368-374	75.25	0.12	11.84	1.22	0.13	1.06	0.04	3.16	3.33	96.17	27	Aira-Tn ash
	3	847-848	70.01	0.39	14.34	1.52	0.36	1.08	0.09	4.29	4.25	96.36	20	Aso-4 ash

note: N; Number of glass shards

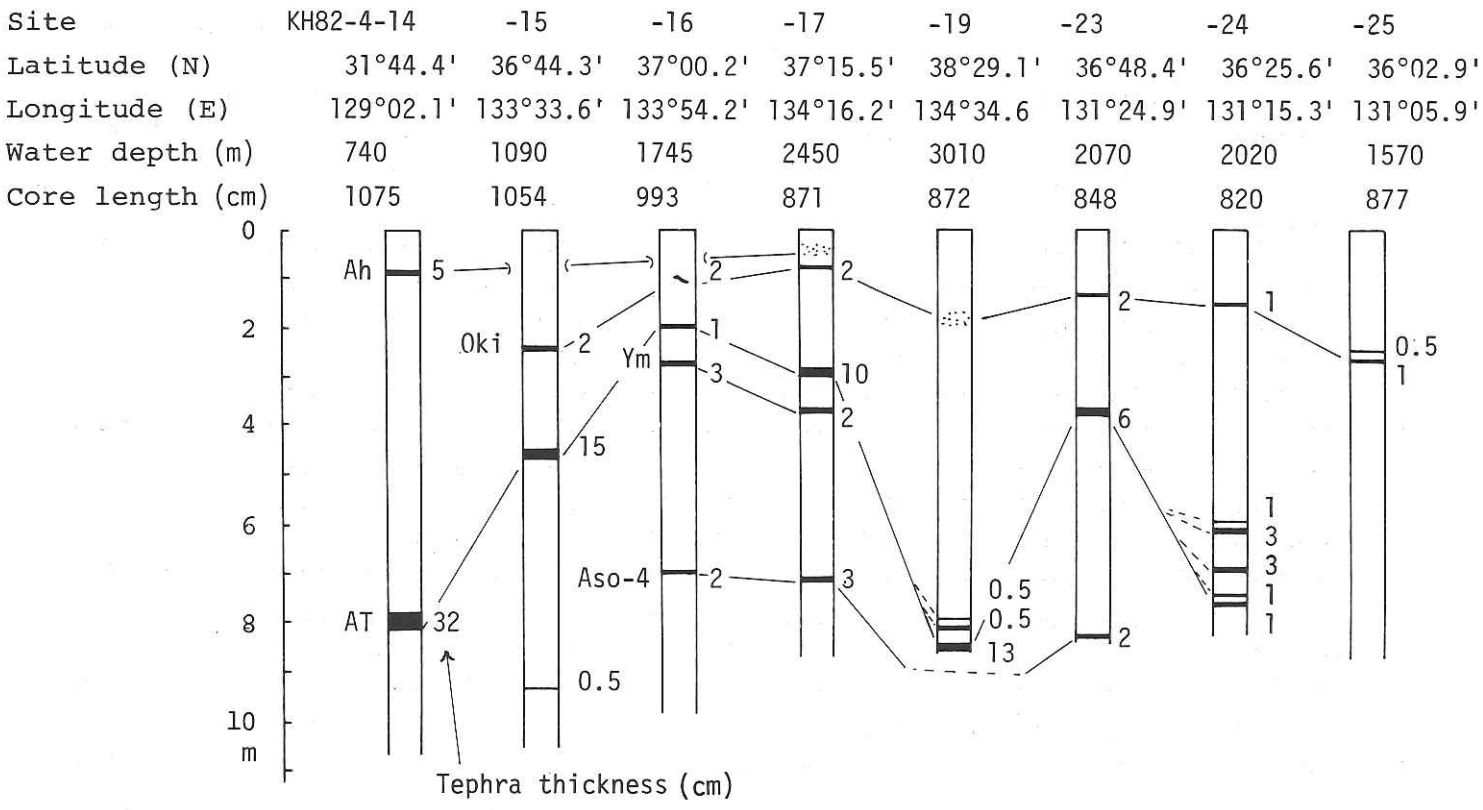

Fig. 7-14-1. Intercore correlation of tephra layers based on petrographic and chemical analyses.

8. DREDGE HAULS

8-1. OPERATION LOGS.

Date July 26, 1982 Ship Hakuho Maru KH 82-4 Station No. 3
Location Ogasawara fore-arc seamount
Weather clear(typhoon nearby) Wind 8m/s, N80°E Sea swell large
Bottom Topography South flank of seamount
Type of Dredge Nalwalk chain-bag Add.Wt. 150kg+chain
Time lowered 13 h 34 m Uncorr. Water Depth 2750 m
Initial Time on Bottom 14 h 27 m Uncorr. Water Depth 2730 m
Wire Length 2832 m Wire Angle
Ship Position Lat. 26°08.8'N Long. 142°59.2'E
Direction of Haul 342° Ship Speed 1~1.2 kt. (till h m)
Speed Wire-in 0.3 m/min (from 18 h 30 m) Winch No. 5
Final Time on Bottom 17 h 45 m Uncorr. Water Depth 1970 m
Wire Length 2500 m Wire Angle 30~40°
Ship Position Lat. 26°11.1'N Long. 143°01.3'E
Time Surfaced 18 h 30 m
Dredged Materials About 50 boulder to pebble gravels, sediments (7 liter)

Date July 26, 1982 Ship Hakuho Maru KH 82-4 Station No. 4
Location Ogasawara fore-arc seamount
Weather clear-partly cloudy Wind Sea swell
Bottom Topography near south crest
Type of Dredge Nalwalk chain-bag Add.Wt. 150kg+chain
Time lowered 18 h 40 m Uncorr. Water Depth 1690 m
Initial Time on Bottom 19 h 11 m Uncorr. Water Depth 1630 m
Wire Length 1855 m Wire Angle 10~15°
Ship Position Lat. 26°10.8'N Long. 143°02.9'E
Direction of Haul 345° Ship Speed 0.9 kt. (till h m)
Speed Wire-in 0.35 m/min (from 21 h 53 m) Winch No. 5
Final Time on Bottom 22 h 30 m Uncorr. Water Depth 1150 m
Wire Length 1249 m Wire Angle 10~15°
Ship Position Lat. 26°12.2'N Long. 143°03.8'E
Time Surfaced 22 h 54 m
Dredged Materials About 300 boulder to pebble gravels (Ultramafic rock, gabbro, dolerite, basalt, amphibolite, siltsone, sandstone, breccia, scoria, pumice), sediments (0.5 liter)

Date Aug. 02, 1982 Ship Hakuho Maru KH 82-4 Station No. 9
Location Amami Plateau, SE part
Weather cloudy Wind 10m/s, S Sea low swell
Bottom Topography crest of a seamount
Type of Dredge Nalwalk chain-bag Add.Wt. 150kg+chain
Time lowered 23 h 56 m Uncorr. Water Depth 1950 m
Initial Time on Bottom 00 h 36 m Uncorr. Water Depth 1670 m
Wire Length 1800 m Wire Angle 5°
Ship Position Lat. 27°55.1'N Long. 133°00.7'E
Direction of Haul Ship Speed 0.6 kt. (till h m)
Speed Wire-in 15 m/min (from 01 h 03 m) - Winch No. 5
Final Time on Bottom 01 h 49 m Uncorr. Water Depth 1470 m
Wire Length 1500 m Wire Angle
Ship Position Lat. 27°55.5'N Long. 133°00.9'E
Time Surfaced 02 h 18 m
Dredged Materials Sediments (4 g)

Date Aug. 03, 1982 Ship Hakuho Maru KH 82-4 Station No. 11
Location Amami Plateau, SW part
Weather cloudy-partly clear Wind 3m/s, 215° Sea calm, low swell
Bottom Topography middle slope of a ridge of Amami plateau
Type of Dredge Nalwalk chain-bag Add.Wt. 150kg+chain
Time lowered 23 h 52 m Uncorr. Water Depth 2730 m
Initial Time on Bottom 00 h 43 m Uncorr. Water Depth 2770 m
Wire Length 2847 m Wire Angle 15-20°
Ship Position Lat. 27°59.4'N Long. 132°09.7'E
Direction of Haul 0° Ship Speed 1-2 kt. (till h m)
Speed Wire-in 18 m/min (from 02 h 59 m) Winch No. 5
Final Time on Bottom 03 h 24 m Uncorr. Water Depth 2600 m
Wire Length 2600 m Wire Angle
Ship Position Lat. 28°00.1'N Long. 132°07.7'E
Time Surfaced 04 h 08 m
Dredged Materials Soft sediments (2 liter)

Date Aug. 04, 1982 Ship Hakuho Maru KH 82-4 Station No. 12
Location Amami Plateau
Weather cloudy, occasional shower Wind 3-6m/s, 220° Sea calm, low swell
Bottom Topography Upper part of northern slope of a linear ridge running E-W
Type of Dredge Nalwalk chain-bag Add.Wt. 150kg+chain
Time lowered 05 h 08 m Uncorr. Water Depth 2050 m
Initial Time on Bottom 05 h 49 m Uncorr. Water Depth 2030 m
Wire Length 2140 m Wire Angle 15°
Ship Position Lat. 28.08.3'N Long. 132°07.3'E
Direction of Haul 0° Ship Speed 1.2 kt. (till h m)
Speed Wire-in 21 m/min (from 06 h 45 m) Winch No. 5
Final Time on Bottom 07 h 03 m Uncorr. Water Depth 1910 m
Wire Length 1910 m Wire Angle 0°
Ship Position Lat. 28°07.6'N Long. 132°07.1'E
Time Surfaced 07 h 35 m
Dredged Materials 5 Mn-nodules with lithic inclusion, trondhjemite, basalt(?), siltstone, sandstone, sediments (30 g)

Date Aug. 15, 1982 Ship Hakuho Maru KH 82-4 Station No. 20
Location Kita-Yamato Tai
Weather rain, close to low Wind 13m/s, S Sea wavy, low swell
Bottom Topography crestal slope
Type of Dredge Nalwalk chain-bag Add.Wt. 150kg+chain
Time lowered 16 h 08 m Uncorr. Water Depth 670 m
Initial Time on Bottom 16 h 21 m Uncorr. Water Depth 680 m
Wire Length 700 m Wire Angle 15∿20°
Ship Position Lat. 39°49.3'N Long. 133°45.9'E
Direction of Haul 0° Ship Speed 2.2 kt. (till h m)
Speed Wire-in m/min (from h m) Winch No. 5
Final Time on Bottom 16 h 32 m Uncorr. Water Depth 495 m
Wire Length m Wire Angle
Ship Position Lat. 39°50.8'N Long. 133°46.0'E
Time Surfaced h m
Dredged Materials About thirty pebbles and sand grains

Date Aug. 15, 1982 Ship Hakuho Maru KH 82-4 Station No. 21
Location Kita-Yamato Tai
Weather Wind 13m/s, ENE Sea swell
Bottom Topography near crest
Type of Dredge Nalwalk chain-bag Add.Wt. 150kg+chain
Time lowered 22 h 00 m Uncorr. Water Depth 630 m
Initial Time on Bottom 22 h 11 m Uncorr. Water Depth 430 m
Wire Length 478 m Wire Angle 0°
Ship Position Lat. 39°53.1'N Long. 133°49.9'E
Direction of Haul 270° Ship Speed kt. (till h m)
Speed Wire-in m/min (from h m) Winch No. 5
Final Time on Bottom 22 h 25 m Uncorr. Water Depth 450 m
Wire Length 460 m Wire Angle 0°
Ship Position Lat. 39°53.6'N Long. 133°49.5'E
Time Surfaced 22 h 25 m
Dredged Materials

8.2. POSITION OF DREDGE HAULS

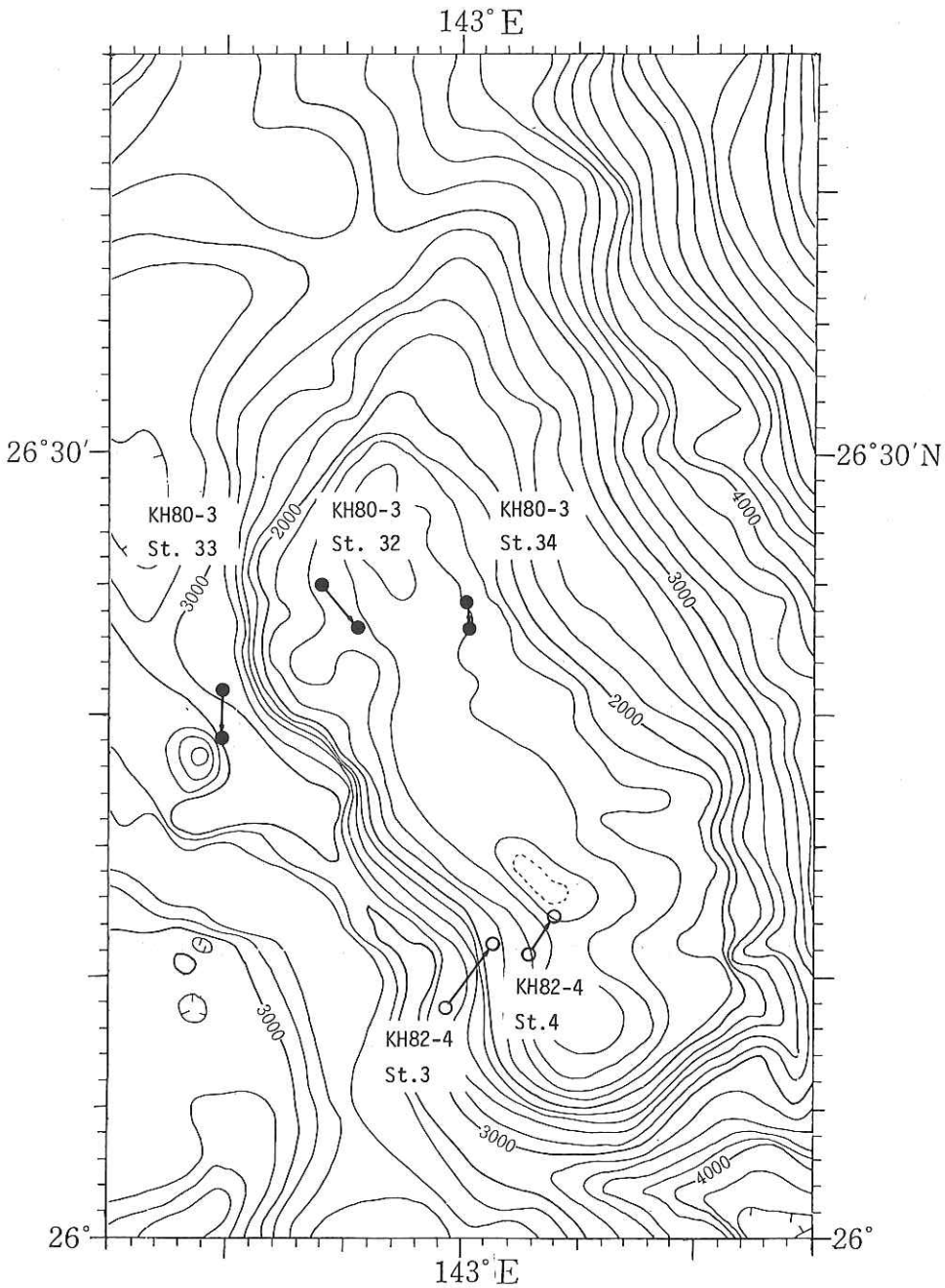

Fig. 8-2-1. Location of dredge hauls in Ogasawara fore-arc region.
Hollow circle: this cruise, Solid circle: KH 80-3.

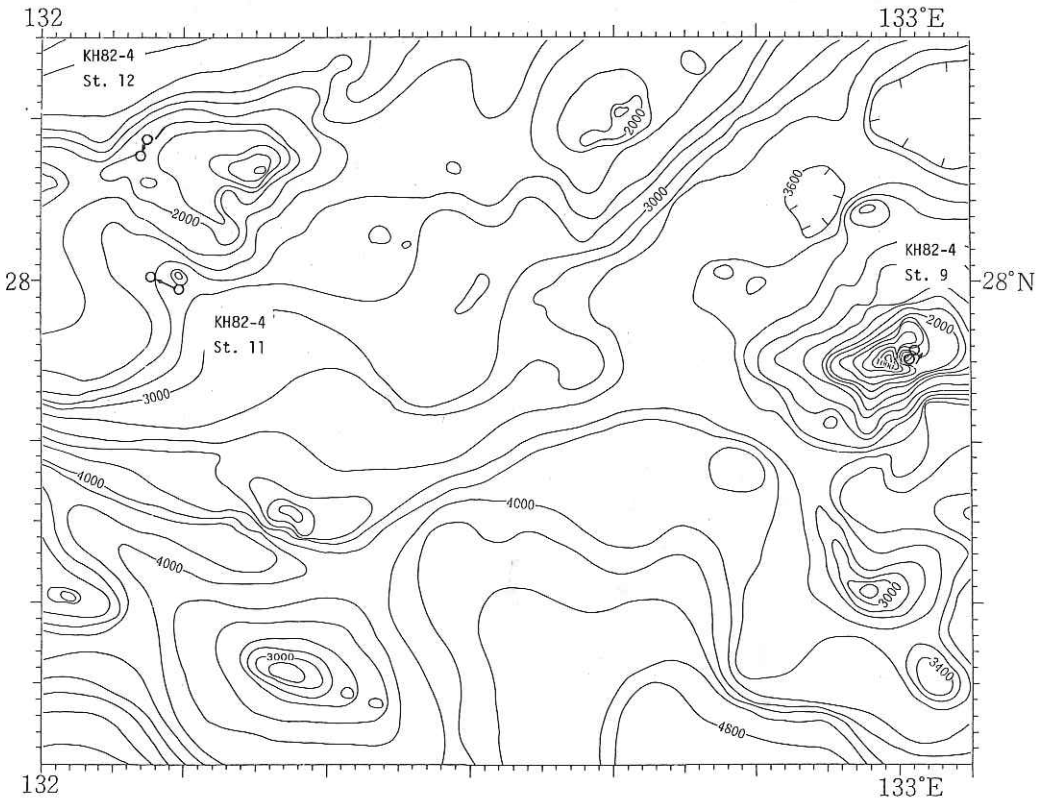

Fig. 8-2-2. Location of dredge hauls on the Amami Plateau (KH 82-4).

8-3. DESCRIPTION OF SAMPES FROM OGASAWARA FORE-ARC SEAMOUNT OR "OGASAWARA PALEOLAND"

T.ISHII, K.KONISHI, J.NAKA, K.FUTAKUCHI and H.OHARA

More than four hundred rocks including harzburgite, dunite, gabbro, dolerite, basalt (of which assemlage is that of the so-called ophiolite) and volcaniclastic rocks were dredged in this cruise from the Ogasawara fore-arc seamount (Fig 8-2-1), where about six hundred rocks including boninite, serpentinite, gabbro, basalt, andesite and many volcaniclastic rocks had been dredged during KH80-3 cruise (Ishii et al.,1981). Each sample was described in table 8-3-1. Lithologic distribution was summarized in Fig. 8-3-1. In the table, roundness is described after Powers' system (Powers,1953). The nomenclature of igneous rocks are described mainly after Strekeisen's systematics (Strekeisen,1976,1979).

The present samples were mainly dredged from near the crest (about 1100 m deep, site number 4) of the seamount (30x50 km in dimension) with 1800 m high north of 26°N latitude. The dredged samples contain many subrounded to rounded gravels of sedimentary rocks as well as igneous rocks including relatively fresh basaltic, doleritic and gabbroic rocks. It is very difficult to consider that these gravels were ice raft products or detrital products from some provenances. The above characteristics suggest that the rounded gravels were in situ wave erosion products inshore, that is, the present Ogasawara fore-arc seamount was exposed above the sea surface. This land shall be called "Ogasawara paleoland".

Observation of more than three hundred polished thin sections, with careful attention focused on orthopyroxene and olivine pseudomorphs and other relict textures, have revealed the following; (1) harzburgite is most predominant and dunite is subordinate in the ultramafic rocks, (2) lherzolite is not observed, which is predominant in the oceanic lithosphere, (3) some harzburgites show commonly characteristic texture of foliation and lineation observed in the ultramafic tectonite, which may be a refractory residue of primary mantle material, (4) harzburgite doesn't show porphyroclastic textures, which is common in the ultramafic tectonite of the oceanic lithosphere, (5) metagabbro and metadolerite were derived from (two-) pyroxene gabbro and (two-) pyroxene dolerite, respectively, (6) some pyroxene gabbros contain inverted pigeonite of both Stillwater and Kintoki-san types as a Ca-poor pyroxene phase, and (7) a basalt lava contains groundmass pigeonite.

The ophiolites are generally considered to be oceanic lithosphere that originated at a midoceanic ridge and were tectonically emplaced along continental margins. The above observations (1, 2 and 4) suggest that this "ophiolite", if so, would have been formed by magmatism in other enviromnents. It may be

expected according to the above observations (1, 2, 5, 6 and 7) that the ophiolite was formed by arc volcanism. Detailed petrological and geochemical investigations have been in progress to understand the petrogenesis of the ophiolite.

REFERENCES

Ishii, T., Konishi, K. and Omura, A., 1981. Prelim. Rep. KH80-3 pp. 105-163, Ocean Res. Inst. Univ. of Tokyo.

Powers, M. C., 1953. J. Sed. Pet. 23, 117-119.

Strekeisen, A., 1976. Earth-Science Reviews, 12, 1-33.

Strekeisen, A., 1979. Geology, 7, 331-335.

ACKNOWLEDGEMENTS

We thank Drs. K. Ozawa, M. Otsuki and H. Tokuyama for their discussion and suggestion in optical observations on thin rections. Thanks are due to Mrs. Akemi Hatanaka for her help in preparation of more than three hundred polished thin sections and to Miss Yoshiko Moriwaki in typewriting.

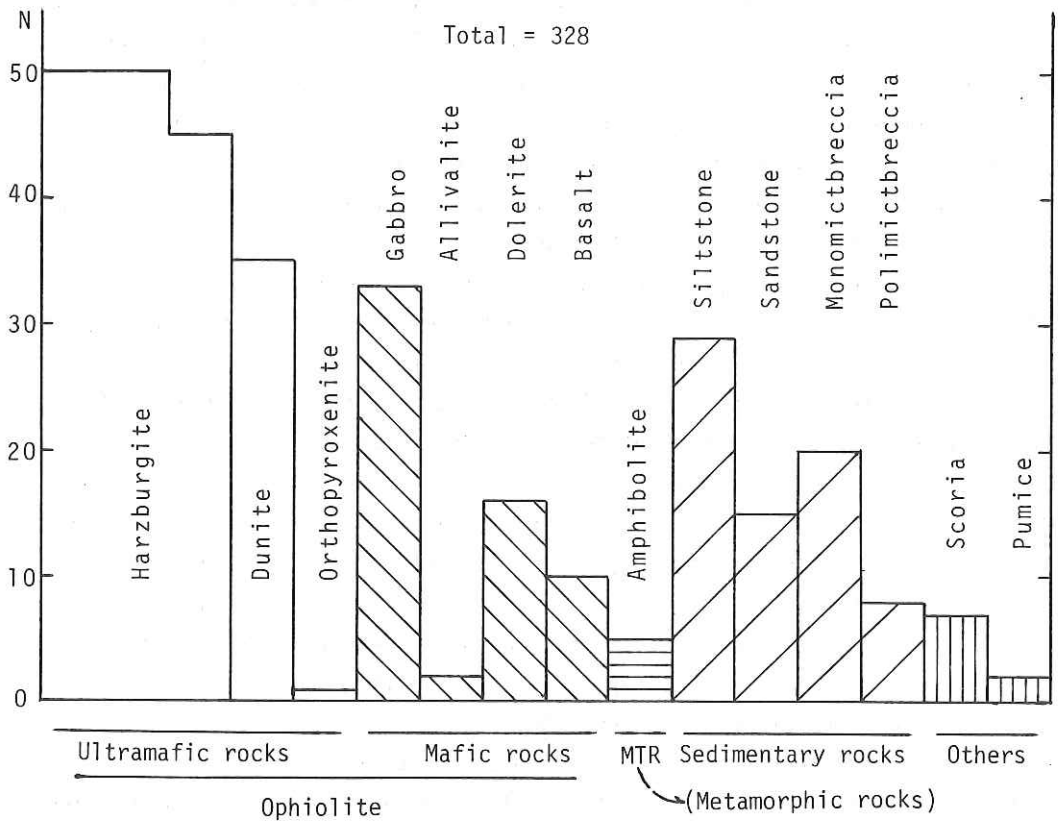

Fig. 8-3-1. Lithologic distribution of dredged sample.

Table 8-3-1. List of dredged materials.

Sample No.	Diameter(mm) L	M	S	Round-ness	Wt(g)	Mn-coat-ing(mm)	Lithology & Remarks
03-01	358	208	124	0.50	6460	0-2.4	tuffaceous lithic wacke, K,P,S,
02	298	245	152	0.60	10150	0-1.6	" B,K,M,P
03	297	204	125	0.60	5650	0-F	" B,K,
04	236	147	66	0.70	2600	F	" B,K,P
05	113	67	58	0.50	275	F	" I,P
06	129	95	44	0.50	690	F	" L,P
07	68	56	36	0.50	210	0-F	" M,P
08	57	45	19	0.40	81	0-2.4	" M,
09	100	87	50	0.55	255	0-F	" L,M,P
10	77	67	30	0.45	84	0-1.1	" B,L,M
11	107	76	51	0.55	335	N	" B,M
12	68	44	36	0.45	135	0-0.9	" M,P
13	77	56	49	0.45	98	0-1.3	" M
14	86	52	49	0.50	117	0-1.4	" M,P
15	101	56	35	0.45	129	0-0.4	" M,P
16	178	108	53	0.45	490	0-4.2	" M,P
17	140	80	52	0.45	435	0-F	" M,P
18	85	79	42	0.55	200	N	" B,L,M,P
19	90	67	35	0.60	182	0-F	" L,M,P
20	44	31	25	0.55	17	N	" C,P
21	52	47	25	0.55	35	N	" C,M
22	61	55	46	0.55	70	0-1.4	" M,S
23	59	33	31	0.45	36	0-1.5	" M,S
24	95	50	26	0.45	68	0-3.8	" M,S
25	67	43	39	0.50	65	N	" L,M
26	70	45	40	0.55	56	N	" L,M
27	54	40	38	0.45	40	0-F	" B
28	58	55	47	0.45	57	0-F	" B,P,S
29	62	56	39	0.60	81	N	" M
30	82	74	24	0.50	77	0-1.5	" M
31	71	60	24	0.45	71	F	" C,M
32	43	34	23	0.50	20	N	" B
33	80	42	27	0.60	51	0-3.9	" M
34	93	50	29	0.50	94	0-F	" M
35	111	102	49	0.35	340	0-1.4	" C,M
36	90	67	30	0.40	110	0-F	" B,M

Sample No.	Diameter(mm) L	M	S	Roundness	Wt(g)	Mn-coating(mm)	Lithology & Remarks
03-41	160	92	47		225	F	siltstone M
42	95	76	35		210	F	" B,M,P
43	105	65	46		180	F	" M
44	82	43	32		71	-	" B,L,P
45	93	34	32		75	O-F	" M
46	79	49	37		89	O-F	" M
47	53	45	32		46	N	" M
48	43	35	28		31	N	"
51	255	195	135	0.55	4450	F	"mudstone", debris flow deposit
61	76	33	32	0.40	60	O-1.3	"siltstone", calcareous, B
71	89	47	46	0.45	150	O-F	scoria (black)
72	20	15	12	0.50	1	N	" (dark gray)
81	58	52	51	0.80	150	N	gabbro (brecciated?)
91					4500		sediments
92					2850		"
93					2350		"
94					390		"
95					750		pebbles
96					530		"

Note F: film
N: none

B: bored
C: coarse grained
I: bioturbated
K: block
L: lithic or mineral inclusion
M: mottled
P: pumice inclusion
S: poorly sorted

Sample No.	Diameter(mm) L	M	S	Round-ness	Wt(g)	Mn-coat-ing(mm)	Lithology & Remarks
04-001	180	152	135	0.36	3080	F-2	harzburgite
002	127	115	97	0.40	1500	0-1.0	"
003	135	80	75	0.35	760	0.4-0.5	"
004	120	100	80	0.30	755	F	"
005	122	96	60	0.40	730	F	" (Cr-spinel poor)
006	119	95	68	0.30	590	F	" (Cr-spinel rich)
007	115	78	59	0.40	575	F	"
008	99	96	75	0.40	530	0-F	"
009	104	100	74	0.35	715	F	"
010	102	88	70	0.40	495	0-F	"
011	83	78	74	0.30	365	F	"
012	86	79	46	0.35	370	F	"
013	84	57	38	0.25	240	F	"
014	92	70	61	0.30	360	F	" (Cr-spinel rich)
015	76	52	46	0.35	220	F	"
016	79	62	38	0.30	210	F	"
017	80	53	48	0.40	220	0-0.5	" (Cr-spinel rich)
018	72	72	44	0.35	195	F	dunite
019	91	56	40	0.50	230	F	harzburgite
020	72	51	42	0.25	142	F	"
021	78	63	36	0.40	187	F	"
022	70	54	43	0.20	180	F	"
023	74	53	31	0.35	116	0-F	dunite (Cr-spinel rich)
024	63	57	43	0.30	160	F-1	hargburgite
025	53	51	41	0.40	89	F	"
026	60	48	32	0.30	87	N	"
027	57	37	34	0.34	87	N	"
051	140	115	82	0.70	2030	F	pyroxene gabbro (cpx, opx, ol)
052	151	77	74	0.50	895	F	" (cpx, opx)
053	111	108	69	0.40	850	F	" (cpx, opx, Cr-spinel)
054	107	89	64	0.60	760	F	" (cpx, opx)
055	111	70	63	0.45	535	F	" (cpx, opx, ol)
056	95	75	46	0.50	445	F	" (cpx, opx, Cr-spinel)
057	122	97	37	0.30	395	N	" (cpx, opx)
058	96	61	56	0.30	295	F	metagabbro (green-hornblende)

Sample No.	Diameter(mm) L	M	S	Round-ness	Wt(g)	Mn-coating(mm)	Lithology & Remarks
04-059	92	90	41	0.30	345	0-F	pyroxene gabbro (cpx, ol, opx)
060	92	73	44	0.55	365	0-F	" (cpx, opx, ol)
061	88	67	42	0.40	181	N	" (cpx, opx, Cr-spinel)
062	78	49	47	0.60	172	F	" (cpx, ol)
063	77	68	40	0.60	280	F	" (cpx, opx, ol, Cr-spinel)
101	188	133	61	0.45	1415	0-1	harzburgite
102	153	123	74	0.35	1465	F	dunite
103	145	102	76	0.45	1050	0-1	harzburgite
104	143	79	62	0.45	760	F	"
105	144	97	71	0.40	1185	F	dunite (Cr-spinel rich)
106	167	99	53	0.35	935	0-2	"
107	162	107	56	0.40	1005	0-1	harzburgite
108	103	85	81	0.40	930	1-2	" (relatively fresh)
109	132	112	78	0.25	980	0-1.5	"
110	125	110	108	0.40	950	F	" (orthopyroxene layer)
111	124	115	73	0.35	800	F	"
112	118	95	60	0.40	690	0-1	"
113	112	90	59	0.35	570	F	"
114	123	78	60	0.45	810	F	"
115	107	74	59	0.35	365	F	"
116	113	65	59	0.30	490	F	dunite
117	112	65	59	0.40	400	0-1	harzburgite
118	99	87	58	0.45	550	F-2	"
119	109	88	71	0.40	480	N	"
120	103	80	56	0.40	449	F	" (relatively fresh)
121	91	68	45	0.45	335	F	dunite
122	95	74	73	0.50	570	F	harzburgite
123	107	96	66	0.40	555	F	"
124	107	72	43	0.35	470	F	"
125	91	65	54	0.50	420	F	"
126	98	71	59	0.50	480	F	"
127	105	69	53	0.50	375	0-1	" (Cr-spinel poor)
128	108	65	51	0.25	370	F	"
129	112	91	59	0.35	595	F	dunite
130	94	83	46	0.35	400	F	harzburgite

Sample No.	Diameter(mm) L	M	S	Round-ness	Wt(g)	Mn-coat-ing(mm)	Lithology & Remarks
04-131	130	72	70	0.45	455	F-0.5	harzburgite
132	89	69	48	0.35	325	N	dunite
133	62	55	38	0.10	150	N	harzburgite (orthopyroxene rich)
134	98	64	58	0.40	212	F	"
135	85	76	55	0.35	342	F	"
136	96	78	53	0.50	340	0-1	"
137	93	62	51	0.25	285	F	"
138	93	72	44	0.30	190	F	"
139	76	76	48	0.30	300	F	"
140	99	89	53	0.40	405	0-1	"
141	80	73	63	0.45	328	F	"
142	96	59	57	0.30	300	F	"
143	101	54	52	0.35	255	F	"
144	98	65	47	0.40	325	F	"
145	94	78	56	0.25	380	F-2	"
146	88	66	53	0.40	275	F	dunite
147	85	70	50	0.35	258	N	harzburgite
148	85	82	40	0.35	305	F	dunite (Cr-spinel rich)
149	88	68	42	0.30	245	F	harzburgite
150	94	77	46	0.40	320	0-1	dunite
151	78	56	50	0.35	230	F	harzburgite
152	88	88	56	0.30	330	F	"
153	81	53	49	0.40	195	F	"
154	86	62	49	0.40	215	F	"
155	90	77	46	0.30	228	0-1	dunite
156	67	65	46	0.35	200	F	harzburgite
157	72	69	43	0.40	172	0-F	"
158	76	62	43	0.30	186	F	"
159	69	51	45	0.30	150	F	"
160	79	47	44	0.25	183	F	"
161	81	53	50	0.35	192	F	"
162	74	70	47	0.35	177	F	"
163	77	59	54	0.15	175	N	"
164	80	67	41	0.35	236	0-0.4	"
165	84	56	50	0.40	210	F	dunite (Cr-spinel rich)

Sample No.	Diameter(mm) L	M	S	Round-ness	Wt(g)	Mn-coat-ing(mm)	Lithology & Remarks
04-166	81	65	45	0.30	205	F	harzburgite
167	75	51	43	0.40	135	F-0.5	"
168	69	61	58	0.15	145	N	dunite (Cr-spinel rich)
169	82	72	40	0.20	195	F	"
170	75	57	41	0.40	134	0-F	"
171	72	60	37	0.35	155	F	" (Cr-spinel rich)
172	57	51	45	0.40	120	0-0.5	harzburgite
173	58	50	32	0.25	93	0-F	"
174	78	76	54	0.30	290	0-F	"
175	93	72	51	0.35	270	F	dunite (Cr-spinel rich)
176	83	58	51	0.35	185	F	harzburgite
177	82	64	37	0.55	178	0-1.0	"
178	91	56	43	0.40	116	0-1.0	"
179	81	51	39	0.30	202	F	"
180	72	66	48	0.40	205	0-1.0	"
181	81	64	43	0.40	185	0-1.5	dunite
182	73	55	35	0.40	140	0-1.0	" (Cr-spinel rich)
183	78	57	44	0.30	225	0-F	harzburgite
184	69	55	43	0.35	144	0-F	dunite
185	76	68	35	0.30	193	0-F	" (Cr-spinel rich)
186	77	68	48	0.30	256	F	harzburgite
187	78	59	45	0.35	200	F	"
188	66	55	54	0.35	155	F	dunite (Cr-spinel rich)
189	76	69	35	0.35	190	F	harzburgite
190	72	63	34	0.35	140	F-1.0	"
191	87	48	28	0.20	132	0-F	"
192	69	60	35	0.35	137	F-0.7	"
193	66	45	32	0.15	82	0-2.5	"
194	65	56	46	0.45	137	F-1.5	"
195	79	56	33	0.30	110	0-3.0	"
196	77	59	29	0.35	113	F	dunite (Cr-spinel rich)
197	68	46	41	0.40	92	F	"
198	64	58	41	0.35	127	F	harzburgite
199	58	43	42	0.25	115	0-1.0	"
200	77	53	44	0.30	155	F	"

Sample No.	Diameter(mm) L	M	S	Roundness	Wt(g)	Mn-coating(mm)	Lithology & Remarks
04-201	54	51	40	0.30	93	N	harzburgite
202	73	69	52	0.20	212	F	"
203	62	54	34	0.30	99	F	"
204	57	56	44	0.25	109	F	"
205	65	41	33	0.20	89	0-2.5	" (Cr-spinel rich)
206	74	55	53	0.25	168	F	" (Cr-spinel poor)
207	76	65	40	0.30	180	F	"
208	66	55	43	0.40	157	0-1.0	"
209	80	45	40	0.30	127	F	"
210	77	75	39	0.35	210	F	"
211	72	62	54	0.35	195	F	"
212	80	54	41	0.35	176	0-F	"
213	65	63	53	0.35	191	0-F	" (Cr-spinel poor)
214	77	58	45	0.35	162	F-1	dunite (Cr-spinel rich)
215	68	67	61	0.40	175	0-0.8	harzburgite (Cr-spinel rich)
216	75	61	46	0.35	182	F	"
217	61	59	53	0.35	160	F	"
218	67	62	43	0.35	163	F	"
219	74	64	57	0.30	219	F	" (relatively fresh)
220	66	58	48	0.30	169	F	"
221	68	53	43	0.35	140	F	"
222	63	60	42	0.35	134	F	"
223	69	56	42	0.35	120	F	"
224	70	53	25	0.40	113	0-F	"
225	69	66	51	0.30	185	F	dunite (Cr-spinel rich)
226	76	63	47	0.35	200	F	harzburgite
227	61	49	34	0.35	120	F	"
228	67	57	37	0.35	191	F	orthopyroxenite (fresh)
229	71	59	48	0.30	134	F	harzburgite
230	74	59	23	0.35	92	0-F	dunite
231	54	42	27	0.25	70	F	harzburgite
232	55	44	42	0.30	83	F	"
233	60	53	28	0.35	92	F	"
234	57	44	34	0.25	83	F	"
235	61	58	31	0.40	105	F-0.5	"

Sample No.	Diameter(mm) L	M	S	Round-ness	Wt(g)	Mn-coat-ing(mm)	Lithology & Remarks
04-236	50	43	38	0.35	79	F	dunite (Cr-spinel rich)
237	56	44	39	0.25	105	0-F	harzburgite
238	67	37	37	0.20	81	0-F	"
239	49	32	22	0.25	31	F	" (?)
240	46	37	35	0.25	33	0-F	dunite (?)
241	55	35	15	0.15	31	0-F	harzburgite
242	37	29	10	0.35	14	0-F	"
243	52	42	34	0.30	65	F	dunite (Cr-spinel rich)
244	61	47	31	0.45	103	0-F	"
245	47	34	23	0.25	44	F	harzburgite
246	61	53	34	0.45	116	0-F	"
247	57	47	40	0.30	91	F	" (Cr-spinel poor)
248	43	34	21	0.35	24	0-F	" (orthopyroxene rich)
249	25	21	12	0.20	(6+)	N	"
250	40	32	27	0.30	32	0-F	" (Cr-spinel poor)
251	53	40	37	0.30	63	F	dunite (?)
252	57	27	27	0.35	57	0-F	" (Cr-spinel rich)
253	53	44	32	0.15	45	F	harzburgite
254	56	36	29	0.30	63	N	"
301	195	143	121	0.40	5340	F	pyroxene gabbro (cpx, opx)
302	185	107	68	0.30	1750	F	" (cpx, pig, ol)
303	113	83	82	0.25	720	F	" (cpx, opx)
304	132	117	77	0.35	1130	F	" (cpx, ol, opx)
305	154	108	52	0.50	1050	F	allivalite (ol, Cr-spinel)
306	108	86	79	0.55	940	F	pyroxene gabbro(cpx, opx)
307	101	84	67	0.30	560	F	" (cpx, ol, pig)
308	112	87	54	0.40	570	F	" (" , " , ")
309	91	78	68	0.35	450	F	" (" , " , ")
310	104	64	57	0.35	450	0-F	" (cpx, pig, ilmenite)
311	83	65	44	0.40	282	F	" (cpx, ol, opx)
312	75	50	23	0.35	136	F	allivalite (ol, cpx)
313	71	58	40	0.35	182	F	pyroxene gabbro (cpx, pig)

Sample No.	Diameter(mm) L	M	S	Round-ness	Wt(g)	Mn-coat-ing(mm)	Lithology & Remarks
04-321	230	155	62	0.30	2670	F	pyroxene gabbro (cpx)
322	163	121	115	0.35	2400	F-1.0	metadolerite (green-hornblende)
323	155	130	100	0.25	1380	F-2.0	" (")
324	176	123	43	0.25	900	F-1.0	" (")
325	166	69	68	0.35	740	0-1.0	" (")
326	147	125	26	0.25	490	0-1.5	" (")
327	103	86	48	0.30	530	F	" (")
328	106	67	65	0.30	336	0-F	" (")
329	94	68	27	0.35	264	F	" (")
330	76	60	41	0.35	220	F	" (")
331	72	62	45	0.30	172	F	" (")
332	102	43	28	0.30	122	0-F	" (")
333	84	74	32	0.40	272	0-F	pyroxene gabbro (cpx, opx)
334	61	60	37	0.40	169	F	" (cpx, ol, opx)
335	73	60	38	0.35	151	F	metadolerite (green-hornblende)
336	94	65	19	0.35	101	0-2.0	" (")
337	96	56	21	0.35	140	0-F	metadolerite (?)
338	100	53	29	0.25	210	F	pyroxene gabbro (cpx, anorthositic)
341	165	131	55	0.35	1600	F	metadolerite (green-hornblende)
342	114	76	70	0.35	910	F	metabasalt (green-hornblende)
343	146	88	44	0.30	435	F	" (")
344	123	60	54	0.25	425	0-F	" (")
345	93	88	60	0.40	540	0-F	basalt (pigeonite in groundmass)
346	80	68	56	0.20	455	F	metabasalt (green-hornblende)
347	110	55	47	0.25	276	F	amphibolite (?)
348	77	64	46	0.35	252	F	metabasalt (pillow lava?)
349	80	49	42	0.40	202	F	" (porphyritic)
350	82	63	39	0.30	218	F	" (green-harnblende)
351	82	62	36	0.35	215	F	" (Cr-spinel)
352	92	42	42	0.30	148	F	" (green-hornblende)
353	62	48	48	0.35	152	F	metadolerite (green-hornblende)

Sample No.	Diameter(mm) L	M	S	Roundness	Wt(g)	Mn-coating(mm)	Lithology & Remarks
04-401	116	102	58	0.40	800	F	pyroxene gabbro (cpx)
402	112	87	65	0.40	710	F	" (cpx, opx, Cr-spinel)
403	134	95	47	0.40	740	F	" (cpx)
404	92	62	45	0.35	325	F	amphibolite
405	61	56	41	0.35	167	F	pyroxene gabbro (cpx rich)
411	124	57	47	0.30	392	F	amphibolite (?)
412	126	90	21	0.15	196	F	amphibolite
413	117	73	44	0.35	458	F	"
451	106	79	60	0.30	280	N	scoria (aegirin augite)
452	70	47	37	0.30	60	N	" (")
453	63	52	37	0.35	53	N	"
454	75	53	43	0.15	64	N	"
455	56	53	42	0.35	43	N	"
456	50	42	34	0.20	32	N	"
457	50	34	28	0.40	19	N	"
461	102	77	54	0.35	240	N	pumice (hornblende)
462	68	60	33	0.20	57	N	"
501	176	122	56	0.10	1165	N	breccia (harzburgite)
502	137	87	76	0.20	710	O-F	" (")
503	126	72	41	0.20	510	N	" (")
504	83	87	65	0.30	470	F	" (serpentinite, metabasalt)
505	108	82	48	0.25	355	F	" (metabasalt)
506	49	30	20	0.35	37	N	" (serpentinite)
507	98	59	55	0.40	320	F	" (gabbro, mineral clasts)
508	72	56	53	0.30	195	F	" (gabbro, basalt, chart?)
509	96	78	66	0.50	438	N	" (serpentinite?)
510	108	62	53	0.15	239	F	" (gabbro, basalt)
511	79	76	48	0.25	246	N	" (serpentinite)
512	72	52	38	0.40	180	F	" (gabbro)
513	78	57	33	0.20	133	N	" (harzburgite)

Sample No.	Diameter(mm) L	M	S	Round-ness	Wt(g)	Mn-coat-ing(mm)	Lithology & Remarks
04-514	63	41	30	0.35	52	F	breccia (basalt, mineral clasts)
515	74	48	33	0.15	83	F-1	" (" , " " , gabbro)
516	61	42	38	0.35	105	N	" (basalt)
517	77	39	27	0.35	96	F	" (serpentinite)
518	76	62	51	0.35	250	F	" (metadorelite)
519	73	55	42	0.25	164	N	" (metabasalt)
520	71	54	45	0.40	200	O-F	" (serpentinite)
521	61	48	44	0.30	119	O-F	pgroxene gabbro(cpx, opx, ol)
522	61	48	27	0.25	80	O-F	breccia (dunite)
523	74	58	38	0.20	135	O-F	" (metagabbro)
531	101	85	49	0.50	242	O-F	breccia (siltstone, sandy)
532	56	37	23	0.50	27	O-7	" (siltstone)
533	120	79	37	0.50	245	O-F	" (siltstone, sandy)
534	44	28	19	0.45	21	O-F	" (serpentinite)
551	297	107	88	0.45	3450	O-1	sandstone(fine) P
552	280	150	125	0.60	2150	N	" (fine) B,I,P
553	180	117	54	0.50	1130	O-F	" (silty) P,
554	162	148	70	0.55	1120	N	" (") I,P
555	157	142	72	0.50	970	N	siltstone(sandy) B,I
556	140	107	80	0.50	1020	N	" (") P
557	153	112	65	0.50	770	O-F	" (") B,I
558	114	93	60	0.45	385	O-F	" (") B,I
559	117	97	68	0.60	560	N	" (") I,P
560	134	107	42	0.40	435	N	" (") B,I
561	107	81	62	0.50	385	N	sandstone(silty) B,I
562	115	95	52	0.55	355	O-F	" (") I
563	124	64	44	0.60	258	F	" (") B,I
564	110	97	78	0.45	515	O-F	" (") B,I,P
565	109	99	45	0.55	280	N	" (") I,L
566	104	82	49	0.55	275	N	siltstone(sandy) B,I,P
567	91	80	48	0.50	235	N	sandstone(silty) B,L(S,MB),P
568	97	56	47	0.50	178	N	" (") B,P

Sample No.	Diameter(mm) L	M	S	Round-ness	Wt(g)	Mn-coat-ing(mm)	Lithology & Remarks
04-569	87	45	22	0.55	76	N	coarse sandstone(silty), P,SB
570	89	60	49	0.65	159	F	siltstone (sandy) I,L(S)
571	91	46	21	0.45	77	N	" (") I,
572	102	62	39	0.50	193	0-F	" (") B,
573	82	66	49	0.40	120	0-F	" (") B,L(S)
574	82	47	30	0.50	74	0-F	" (") B,L(A)
575	68	54	42	0.35	115	F	siltstone L,SS
576	74	65	37	0.55	111	N	" (sandy) A,I
577	82	71	40	0.45	128	0-F	sandstone (silty) I,P
578	84	57	47	0.65	145	N	siltstone (sandy) A,I
579	74	57	37	0.55	96	N	" (") A,B,I,PS
580	72	56	42	0.40	115	0-F	" (") I,P
581	70	60	47	0.35	92	0-0.5	" (") B,I,P
582	76	59	42	0.50	104	0-F	clastic monomict breccia
583	62	46	30	0.45	47	N	siltstone (sandy) L
584	74	47	30	0.50	59	0-F	" (sandy patch) I,L
585	68	63	52	0.40	115	0-F	" (sandy) (lamination)
586	77	52	24	0.45	89	N	" (sandy) I
587	58	39	39	0.45	55	N	sandstone (silty) PS
588	51	47	24	0.60	38	0-F	siltstone
589	52	40	33	0.35	30	0-F	clastic monomict breccia (sand size)
590	51	42	30	0.45	34	0-F	sandstone (silty) I,PS
591	53	40	36	0.40	37	0-0.3	" (") I,PS
592	54	35	30	0.35	37	N	" (") P,PS
593	40	34	29		20	0-F	siltstone (sandy) (breccia?)
594	37	21	21		11	N	" (") I,P
595	31	28	19		10	N	sandstone (")(tuffaceous) P
596	34	20	16		7	N	" (silty) L,PS
601					475		mud (with pebbles) 10YR4/2

Note

F : film
N : none
ol : olivine
cpx: Ca-rich clinopyroxene
opx: orthopyroxene
pig: inverted pigeonite

A: scoria inclusion
B: bored
C: coarse grained
I: bioturbated
L: lithic inclusion
M: mottled

P: pumice inclusion
S: serpentinite inclusion
MB: mud breccia
PS: pooly sorted
SB: silty breccia
SS: slide stracture

8-4. IGNEOUS ROCKS DREDGED FROM SITES KH82-4-3 AND-4

J. NAKA and S. UEHARA

INTRODUCTION

During the cruise KH 82-4, volcaniclastic and pyroclastic rocks, ultrabasic rocks, gabbro, dolerite and basalt, the last four of which can be referrableto an ophiolitic assemblage, were obtained from a fore-are seamount of the Ogasawara Islands (KH82-4-3 and -4). These samples were roughly classifiedinto several groups on the ship. In this preliminary report, we will describe petrography of these igneous rocks. For this purpose,54(fifty four) samples were selected and their texture, mineral composition of bulk samples and bulk chemical composition (except for ultrabasic rocks) were examined by microscope, X-ray diffractometor and X-ray microprobe analyser.

X-ray diffraction patterns were recorded with a Rigaku RAD-IIA diffractometor using filtered Cu-Kα radiation and a standard aluminium sample holder. A scanning speed of 4°(2θ)/min., and a chart speed of 20mm/min. were used to analyses the mineral composition of bulk samples.

Rock glasses were prepared by direct fusion method of Fukuyama and Sakuyama (1976) for the analysis of bulk chemical compostion. The analyses were preformed by X-ray microprobe analyser, JEOL model JXA5A which was operated under the following condition : specimen current and accelerating voltage was kept at 20nA and 15kV on pure MgO, respectively. Data correction procedure followed Bence and Albee (1968), and α-factor by Nakamura and Kushiro (1970) was used. Standards were used series of synthetic oxides for Mg, Fe, Al, Ni, Cr, Mn, and Ti, wollastonite for Si and Ca, albite for Na and adularia for K.

RESULTS

The results of analyses of mineral composition of bulk samples were shown in Table 8-4-1. and bulk chemical compositions in Table 8-4-2.

A. Ultrabasic rocks (04-001, 002,003,004,006,007,019,022,059,101,102,103,105, 106,107,114,116,119,132,163,169,170)

The ultrabasic rocks are more or less serpentinized but in most samples their primary minerals and texture are preserved. In appearance, they are dark and brownish green and yellowish, reddish and dark brown. The brownish green samples (001-004) contain small amounts of relic olivine, orthopyroxene and clinopyroxene. Some of the yellowish brown samples (101-103) comprise large amounts of olivine and orthopyroxene (totally about 50%), and the rest yellowish brown samples (105-107,114,116,119,132) contain small amounts of relict olivine and clinopyroxene. The dark brown samples (059,521) have large amounts of relict olivine and clinopyroxene. On the other hand, the dark green (006,007,019,022) and reddish brown (163,169,170) samples are perfectly serpentinized. Magnetite and chromite are contained in most samples.

Olivine is replaced mostly by serpentine minerals, rarely with a small amount of actinolite along the periphery. Pyroxene is also replaced mainly by serpentine minerals (bastite) but sometimes by talc.

Based on the original texture, relict minerals and pseudomorphs, these ultrabasic rocks are originally referrable to dunite (105,106,116,119,132), harzburgite (001,002,004,007,019,022,103), lherzolite (003,101,102,107,114) and wehrlite (059,521).

B. Basic rocks (03-81,04-051,052,053,057,063,301,302,304,305,306,311,321,322, 323,325,329,338,341,342,343,345,349,401,403,404,512)

All of basic rocks have undergone alteration or metamorphism (zeolite facies - amphibolite facies) to some degree. However, excepting 04-404, they do not exhibit schistosity and their original texture is well preserved. The following samples are referable to gabbro and show a poikilitic and ophitic texture : 04-051,052,053,057,063,301,302,304,305,306,311,512,03-81. Based on bulk chemical composition (8-4-2), 04-302 and 305 are included in ultrabasic rock, however these samples exhibit a poikilitic and ophitic texture and are leucoclatic, so that these are regarded as gabbro. In these gabbroic rocks, olivine, clinopyroxene, Ca rich plagioclase and spinel are seen as relict minerals. Clinopyroxene commonly shows exsolution lamella. Olivine and pyroxene pseudomorphs also can be seen in some samples. Olivine is replaced by serpentine minerals, chlorite and actinolite and pyroxene by green hornblende, actinolite, chlorite and white mica. Plagioclase is partially altered into prehnite, zeolites (analcime and natrolite) and

epidote (clinozoisite). Based on the relict minerals and pseudomorphs, gabbros are classified into leuco-trochtolite (305), leuco-olivine gabbro (302), olivine gabbro (306) and gabbro (the others).

Dolerite including microgabbro with a ophtic texture are represented by the following : 04-321,322,323,325,329,338,341,342,343,349. Most of dolerite are much more altered as compared with gabbro, and some of them are almost entirely composed of pseudomorphs. Clinopyroxene and Ca rich plagioclase are seen as relict minerals, and olivine, pyroxene and plagioclase pseudomorphs are recognized. Olivine is replaced by actinolite and chlorite, pyroxene by mainly zeolite (analcime and natrolite).

The sample of No.04-404 can be distinguished from the above-mentioned rocks by having a intersertal texture and is referable to basalt. Clinopyroxene and Ca rich plagioclase phenocryst are seen as relict minerals. In the groundmass Ca rich plagioclase and a opaque mineral (magnetite ?) are recognized as relict minerals. Green hounblende, chlorite and clay minerals are found as altered or metamorphosed minerals in the groundmass.

* The sample 04-404 exhibits a clear schistosity. This sample comprises mainly green hornblende and Ca rich plagioclase and these two minerals seen as metamorphic minerals. This sample is regarded as schistose basic amphibolite.

C. Scoria (03-71,04-451,452) and pumice (04-461)

Fresh scoria and pumice are obtained toghther with basic and ultrabasic rocks of ophiolitic assemblages at the station 3 and 4. In these rocks, glass is well preserved and a little amount of plagioclase phenocryst are scattered in a glass.

* Halite was detected by X-ray diffraction analysis in 04-461 and 452. It is rather common in 04-461, but absent in 03-71 and 04-451. The difference of amount of Na_2O between bulk sample and natural glass is greatest in 04-461 and is smallest in 03-71 and 04-451, so that this halite is considered to have derived from sea water.(8-4-2).

ACKNOWLEDGEMENT

Analysis of bulk chemical compositions and sample preparation were made

at Kochi University. We would like to thank Prof. T. Suzuki and Mr. S. Yoshikura of Kochi University for thier kind help and valuable advice in the analysis.

REFERENCES

Bence, A. E. and Albee, A. L., 1968. Empirical correction factors for the electron microanalysis of silicate and oxied. J. Geol., 76, 382-403.

Fukuyama, H. and Sakuyama, M.,1976. Major element analysis of rocks by electron microprobe analyser. J. Geol. Soc. Jap., 82, 345-346.

Nakamura, y. and Kushuro, I., 1970. Compositonal relations of coexisting orthopyroxene, pigeonite and augite in a tholeiitic andesite from Hakone Volcano. Contr. Mineral. Petrol., 26, 265-275

TABLE 8-4-1. Mineral compositions of bulk samples

	Plagioclase	Natrolite	Analcime	Lizardite	Clinochrysotile	Orthochrysotile	Antigorite	Talc	Chlorite	White Mica	Prehnite	Amphibole	Clinopyroxene	Orthopyroxene	Olivine	Clinozoisite	Spinels	Halite
04-001				++	++									+			+	
002				++	++				+					+	+			
003				++	+												+	
004				++										+				
006				++	++												+	
007				++	++												+	
019				++	+												+	
022				++	+												+	
059				++									+	+		+		
101				++	+									+	+			
102				++											+			
103				++	+									+			+	
105				++	++													
106				++	++													
107				++	+				+						+			
114				++	+									+	+			
116				++	+		+							+	+			
119				++	++										+			
132				++	+	+								+				
163				++									+		+			
169				++	++													
170				++	++													
521				+										++	++			
03-81	++									+			+					
04-051	++												+	+				
052	++	+								+			++					
053	++										+			++				

	Plagioclase	Natrolite	Analcime	Lizardite	Clinochrysotile	Orthochrysotile	Antigorite	Talc	Chlorite	White Mica	Prehnite	Amphibole	Clinopyroxene	Orthopyroxene	Olivine	Clinozoisite	Spinels	Halite
04-057	++								+				++					
063	++	+							+			+	++					
301	++								+			++	+					
302	++	+							++	+		+						
304	++	+							+	+		+						
305	++								+		+							
306	++	+							++			+	++					
311	++	+							+	+			++					
321	++	+	+						+			+	++					
322		++	++						+			++						
323	+		++						+			++						
325		++							+			++						
329									+			++						
338	++												++					
341			++						+			++				+		
342	+		+						+			++						
343			++						+			++						
345	++								+			++	+					
349	++		+						++	+		++						
401	++								+			+	+					
403	++								+	+		+	+					
404	++											++						
512	++								+	+		+						
03-71	++																	
04-451	++																	
452	+																	+
461	+																	++

Note: ++: major concentrations, +: minor concentrations

TABLE 8-4-2. Bulk chemical compositions of basic rocks, scoria and pumice

	03-71	03-71**	03-81	04-051	04-052	04-053	04-057	04-063	04-301
SiO_2	58.03	61.58	50.08	48.93	49.18	49.37	49.41	49.12	48.09
TiO_2	0.83	0.77	0.45	0.22	0.20	0.23	0.62	0.32	0.22
Al_2O_3	16.34	17.97	15.65	19.31	19.22	16.21	15.55	17.45	16.57
Cr_2O_3	0.00	0.00	0.00	0.08	0.08	0.02	0.07	0.01	0.10
FeO*	6.24	5.46	7.26	5.41	6.23	6.24	8.76	5.98	5.25
MnO	0.27	0.23	0.17	0.14	0.17	0.14	0.14	0.13	0.17
NiO	0.00	0.00	0.00	0.02	0.00	0.02	0.01	0.00	0.04
MgO	1.93	1.09	10.06	9.55	9.41	11.39	8.75	10.53	11.96
CaO	3.96	3.42	13.25	15.29	13.75	13.08	12.70	13.98	13.88
Na_2O	6.32	6.06	2.38	1.47	2.01	1.87	2.45	2.56	1.78
K_2O	3.08	3.68	0.30	0.01	0.03	0.56	0.12	0.07	0.17
Total	97.00	100.26	99.63	100.43	100.28	99.13	98.58	100.24	98.23

	04-302	04-304	04-305	04-306	04-311	04-321	04-322	04-323	04-325
SiO_2	44.11	50.35	44.47	45.56	45.78	48.00	47.50	51.26	47.93
TiO_2	0.15	0.24	0.02	0.02	0.10	0.15	0.73	0.66	0.81
Al_2O_3	24.88	17.29	28.21	20.49	21.41	20.20	14.92	16.40	16.76
Cr_2O_3	0.00	0.06	0.01	0.11	0.06	0.06	0.03	0.00	0.00
FeO*	5.71	5.74	2.35	4.11	5.21	4.87	11.31	10.46	10.66
MnO	0.10	0.16	0.05	0.07	0.10	0.10	0.25	0.17	0.19
NiO	0.06	0.01	0.06	0.08	0.02	0.05	0.00	0.01	0.02
MgO	10.24	8.83	8.75	14.19	10.54	8.91	9.18	6.71	9.67
CaO	11.94	12.77	15.76	13.60	14.13	14.50	7.39	6.35	7.09
Na_2O	1.86	3.15	0.89	1.13	1.08	2.02	4.40	5.78	5.34
K_2O	0.07	0.46	0.00	0.03	0.19	0.49	0.32	0.14	0.09
Total	99.12	99.06	100.57	99.39	98.62	99.35	96.03	97.94	98.56

	04-329	04-338	04-341	04-342	04-343	04-345	04-349	04-401	04-403
SiO_2	47.72	48.74	48.84	53.25	48.45	49.72	47.00	50.30	50.41
TiO_2	0.94	0.12	0.70	0.83	1.03	0.67	0.07	0.20	0.29
Al_2O_3	9.68	17.99	15.55	14.10	13.84	12.95	22.46	16.98	17.00
Cr_2O_3	0.00	0.15	0.00	0.02	0.01	0.00	0.07	0.03	0.08
FeO*	13.76	2.34	9.38	10.82	13.11	10.29	3.70	5.22	6.42
MnO	0.36	0.07	0.23	0.18	0.26	0.23	0.02	0.12	0. 10
NiO	0.07	0.05	0.04	0.04	0.05	0.01	0.05	0.05	0.05
MgO	18.43	10.30	13.15	7.88	13.29	13.15	11.94	10.09	12.16
CaO	7.32	17.75	8.75	11.70	5.53	5.95	11.08	16.36	12.21
Na_2O	0.88	1.23	3.40	2.78	3.90	4.74	2.34	1.54	2.12
K_2O	0.16	0.55	0.10	0.07	0.48	0.16	0.68	0.05	0.30
Total	99.32	99.38	100.14	101.67	99.95	97.87	99.41	100.94	101.05

	04-404	04-451	04-451**	04-452	04-452**	04-461	04-461**	04-512	JB-2
SiO_2	47.22	64.15	65.61	60.56	63.49	70.90	77.68	49.37	53.66
TiO_2	0.43	0.62	0.55	0.88	0.79	0.19	0.10	0.14	1.22
Al_2O_3	19.25	16.67	16.51	15.81	16.93	14.33	12.12	18.31	15.09
Cr_2O_3	0.08	0.00	0.02	0.00	0.00	0.00	0.00	0.22	0.00
FeO*	6.54	4.83	4.43	6.85	5.74	1.67	1.26	2.78	13.43
MnO	0.04	0.23	0.18	0.27	0.23	0.09	0.04	0.05	0.23
NiO	0.04	0.00	0.00	0.00	0.00	0.00	0.00	0.04	0.00
MgO	9.35	2.00	0.92	1.60	1.06	0.58	0.12	11.02	4.94
CaO	14.26	3.59	2.30	3.19	2.44	1.96	1.06	17.02	9.69
Na_2O	1.78	4.78	4.95	6.16	5.16	4.88	2.09	1.55	2.11
K_2O	0.00	3.97	4.84	3.35	4.07	2.74	2.91	0.30	0.32
Total	98.99	100.66	100.31	98.67	99.91	97.34	97.38	100.80	100.69

total iron as FeO **natural glass

8-5. SERPENTINES DREDGED FROM KH82-4

S.UEHARA and J. NAKA

INTRODUCTION

Serpentinized ultramafic rocks collected from the ocean floor have been described by many investigators(e.g., Aumento and Loubat, 1971). However, very few works have been carried out on the crystal chemistry of serpentine-group species in these rocks, particularly on serpentines dredged from arc-trench gap. During the cruise KH82-4, many serpentinized ultramafic rocks were dredged from the fore-arc seamount of the Ogasawara Islands. In this report we will describe the mineralogical properties of serpentine minerals in these rocks.

MATERIALS AND EXPERIMENTAL

Serpentine minerals described in this report were dredged from the fore-arc seamount of the Ogasawara Islands. A rapid scan of X-ray diffractometer was made(4°, 2θ/min.) on thirty serpentinized ultramafic rocks for preliminary identification, and five completely or nealy completely serpentinized rocks and one less serpentinized rock were selected for the following experiments(Table 8-5-1). The samples were analysed by electron microprobe, X-ray powder diffraction, and transmission electron microscopy.

Chemical analyses were made by electron microprobe analyser, JEOL model JXA5A, which was operated under the following condition: specimen current and accelerating voltage were kept at 20nA on pure Fe_2O_3 and 15kV, respectively. Data correction was made by the method of Bence and Albee(1968), and α-factor by Nakamura and Kushiro(1970) was used. Standards used were a series of synthetic oxides for Mg, Fe, Al, Ni, and Cr, and synthetic $CaSiO_3$ for Si.

X-ray powder diffraction pattern were recorded with a Rigaku RAD-IIA diffractometer using filtered Cu$K\alpha$ radiation and a standard aluminium sample holder. A scanning speed of 1/8°/min. and a chart speed of 5mm/min. were used to measure d-spacings and to determine the polymorph of serpentine minerals.

Eleltron optical observations were made with a JEOL JEM-200B of HVEM LAB., Kyushu University, operated at 200kV. The crushed samples were disaggregated by ultrasonic treatment in distilted water. Drops of suitably diluted suspensions were placed on microgrids and examined in the electron microscope.

RESULTS

Serpentine species were identifided by the typical reflection lines of each species(Whittaker and Zussman, 1956). Whole-rock powders analysed by X-ray diffraction gave the patterns indicating to be mixtures of lizardite and chrysotile(Fig. 8-5-1). The amount of both polymorphs varies from specimen to specimen. However, in specimen 04-003 and 04-019, lizardite is predominant. Specimen 04-006 contains a considerable quantity of clinochrysotile. The basal spacings, as one serpentine layer, were determined by the average of d(002) and d(004) for specimens 04-006, 04-019, and 04-003, and of d(001) and d(002) for 04-002 and 04-170. The values of b were determined by d(060). The d(001) and b values obtained are as follows:

specimen No.	04-006	04-019	04-002	04-003	04-170	04-004	
d(001)	7.320	7.310	7.320	7.315	7.346	7.319	Å
b	9.213	9.208	9.220	9.211	9.217	9.214	Å.

TEM photographs are shown in Fig. 8-5-2 Specimens 04-003 and 04-019 contain more amount of platy serpentine(lizardite) than the others. Antigorite is not detected by X-ray powder diffraction, but a small amount of antigorite is sparse in specimens 04-002, 04-003, and 04-019 under the electron microscope. Specimen 04-170 contains short fibrous particles.

Tables 8-5-2,-3 &-4 give the electron microprobe analyses and cationic proportions for mesh-textured, opx-bastite, and vein serpentines. The analyses indicated that the serpentines examined are chemicaly more or less inhomogeneous, particulary in Fe and Mg. Chemical differences among the differently textured serpentines(bastite, mesh, and vein) are found paticularly in Cr and Al contents. The Cr_2O_3 content of opx-bastite ranges from 0.79 to 1.34%, whereas that of mesh-textured pseudomorphs ranges from 0.00 to 0.06%. The Al_2O_3 content of mesh-textured serpentine is low(0.00-1.18%), and bastites show slightly high contents(0.72-2.08%). This result is concordant with that of Dungan(1979), but the Ogasawara opx-bastite has higher Cr_2O_3 content compared with those of his opx-bastite and of the

Mid-Atrantic Ridge opx-bastite(Prinz et al.,1976).

In a specimen, the chemical difference in the same textured serpentine is very small except for veinlets. The differences between mesh-textured and bastite serpentines are recognized not only in Cr and Al contents, but also in Fe.

REFERENCES

Aumento, F. and Loubat, H., 1971. The Mid-Atlantic Ridge near 45°N, 16, serpentinized ultramafic intrusions, Can. J. Earth Sci., 8, 631-663.

Bence, A. E. and Albee, A. L, 1968. Empirical correction factors for the electron microanalysis of silicates and oxides, J. Geol., 76, 382-403.

Dungan, M. A., 1979. A microprobe study of antigorite and some serpentine pseudomorphs, Can. Mineral. 17, 771-784.

Nakamura, Y. and Kushiro, I., 1970. Compositional relations of coexisting orthopyroxene, pigeonite and augite in a tholeiitic andesite from Hakone Volcano, Contr. Mineral. and Petrol., 26,265-275.

Prinz, M., Keil, K., Green, J. A., Reid, A. M., Bonatti, E., and Honnorez, J., 1976. Ultramafic and mafic dredged samples from the equatorial mid-Atlantic ridge and fracture zone, J. Geophys. Res., 81, 4087-4103.

Whittaker, E. J. W., and Zussman, J., 1956. The characterization of serpentine minerals by X-ray diffraction, Mineral. Mag., 31,107-126.

Table 8-5-1. Samlpes examined

Specimen No.	Description	
	Colour and texture	Constituent minerals
04-002	Nearly completely serpentinized harzburgite, dark green to pale green bastite in a brown to pale green matrix with fine dark green veins.	Lizardite and clinochrysotile with small amounts of talc, spinel, olivine, and orthopyroxene.
04-003	Nearly completely serpentinized lherzolite, yellowish green bastite in a pale green matrix with fine brack veins.	Lizardite with minor clinochrysotile and a small amount of spinel.
04-004	Partly serpentinized harzburgite, yellow to pale green bastite in a brown to pale green matrix with fine dark veins.	Lizardite, clinochrysotile, and orthopyroxene with small amounts of olivine and spinel.
04-006	Completely serpentinized harzburgite, light green bastite in black to dark green matrix.	Lizardite and clinochrysotile with a small amount of spinel.
04-019	Completely serpentinized harzburgite, greenish brown with fine black veins.	Lizardite with minor clinochrysotile and a small amount of spinel.
04-170	Weathered serpentinite, brown with light green veins.	Poorly crystallized serpentine.

Table 8-5-2. Microprobe analysis of mesh-textured serpentines

Specimen No.	04-002					04-003	
Analysis No.	4	5	6	7	8	1	2
SiO_2	40.37	41.81	41.98	42.18	40.12	42.09	42.20
Al_2O_3	0.00	0.07	0.07	0.07	0.12	0.09	0.08
FeO*	4.08	3.29	3.99	3.48	5.13	2.23	3.46
MgO	40.40	40.18	38.94	40.33	38.96	42.95	41.70
Cr_2O_3	0.00	0.00	0.00	0.00	0.06	0.04	0.00
NiO	0.44	0.25	0.20	0.26	0.56	0.18	0.29
Total	85.29	85.60	85.18	86.37	84.90	87.57	87.55
Number of cations on the basis of fourteen oxygens							
Si	3.91	3.99	4.04	4.00	3.92	3.92	3.94
Al	0.00	0.01	0.01	0.01	0.01	0.01	0.01
Cr	0.00	0.00	0.00	0.00	0.01	0.00	0.00
Fe	0.33	0.26	0.32	0.28	0.42	0.17	0.27
Mg	5.83	5.72	5.58	5.69	5.68	5.96	5.82
Ni	0.03	0.02	0.02	0.02	0.04	0.01	0.02
Total	10.10	10.00	9.97	10.00	10.08	10.07	10.06

Specimen No.	04-003				04-004		
Analysis No.	6	7	9	10	10	11	12
SiO_2	42.24	42.64	41.83	41.51	40.60	41.01	40.40
Al_2O_3	0.08	0.06	0.06	0.09	0.18	0.15	0.13
FeO*	2.46	2.41	1.99	2.28	3.69	3.84	3.98
MgO	42.36	42.07	44.19	44.01	40.40	39.97	39.93
Cr_2O_3	0.00	0.00	0.00	0.00	0.03	0.06	0.01
NiO	0.12	0.16	0.08	0.14	0.16	0.14	0.18
Total	87.26	87.34	88.15	88.03	85.06	85.17	84.63
Number of cations on the basis of fourteen oxygens							
Si	3.95	3.97	3.87	3.85	3.92	3.95	3.93
Al	0.01	0.01	0.01	0.01	0.02	0.02	0.02
Cr	0.00	0.00	0.00	0.00	0.00	0.00	0.00
Fe	0.19	0.19	0.15	0.18	0.30	0.31	0.32
Mg	5.90	5.84	6.06	6.09	5.82	5.74	5.79
Ni	0.01	0.01	0.01	0.01	0.01	0.01	0.01
Total	10.06	10.02	10.13	10.14	10.07	10.03	10.07

Table 8-5-2. -continued.

Specimen No.	04-006				04-019		
Analysis No.	2	3	4	5	1	2	3
SiO_2	41.59	40.64	41.60	40.87	41.74	41.11	41.12
Al_2O_3	0.53	0.39	0.50	0.81	0.80	0.84	0.77
FeO*	2.04	1.80	1.80	2.31	4.03	3.26	2.25
MgO	40.87	41.05	40.82	40.68	39.93	39.80	40.70
Cr_2O_3	0.00	0.00	0.00	0.00	0.00	0.00	0.00
NiO	0.36	0.36	0.12	0.30	0.29	0.19	0.16
Total	85.39	84.25	84.94	84.97	86.78	85.20	85.00
Number of cations on the basis of fourteen oxygens							
Si	3.96	3.93	3.97	3.92	3.95	3.95	3.94
Al	0.06	0.04	0.06	0.09	0.09	0.10	0.09
Cr	0.00	0.00	0.00	0.00	0.00	0.00	0.00
Fe	0.16	0.15	0.14	0.19	0.32	0.26	0.18
Mg	5.80	5.91	5.81	5.82	5.63	5.69	5.81
Ni	0.03	0.03	0.02	0.02	0.02	0.01	0.01
Total	10.01	10.06	10.00	10.04	10.01	10.01	10.03

Specimen No.	04-019		04-170		
Analysis No.	4	8	1	2	3
SiO_2	40.28	43.68	41.75	42.65	42.69
Al_2O_3	1.18	0.49	0.35	0.32	0.34
FeO*	2.61	2.53	4.82	4.75	4.81
MgO	40.74	40.00	37.15	37.26	37.60
Cr_2O_3	0.00	0.00	0.02	0.02	0.00
NiO	0.26	0.16	0.31	0.28	0.32
Total	85.07	86.86	84.40	85.28	85.76
Number of cations on the basis of fourteen oxygens					
Si	3.87	4.07	4.07	4.10	4.09
Al	0.13	0.05	0.04	0.04	0.04
Cr	0.00	0.00	0.00	0.00	0.00
Fe	0.21	0.20	0.39	0.38	0.39
Mg	5.83	5.56	5.39	5.34	5.36
Ni	0.02	0.01	0.02	0.02	0.03
Total	10.06	9.89	9.91	9.88	9.90

*Total Fe as FeO.

Table 8-5-3. Microprobe analysis of opx-bastites

Specimen No.	04-002	04-004						04-006		
Analysis No.	10	1	2	3	4	5	6	6	7	8
SiO_2	43.56	41.14	41.26	40.85	40.37	40.56	41.46	40.95	40.01	40.01
Al_2O_3	1.26	0.81	0.76	0.94	0.78	0.79	0.72	1.77	1.86	2.08
FeO*	5.54	8.06	8.31	8.44	7.98	8.05	7.87	2.68	3.18	3.11
MgO	36.76	36.65	36.12	34.89	36.10	36.21	36.83	40.24	39.48	39.68
Cr_2O_3	0.79	0.99	0.80	0.97	0.95	0.98	0.96	1.07	1.12	1.34
NiO	0.19	0.31	0.35	0.35	0.34	0.34	0.28	0.35	0.34	0.34
Total	88.10	87.96	87.60	86.46	86.52	86.93	88.12	87.05	85.99	86.57
Number of cations on the basis of fourteen oxygens										
Si	4.07	3.93	3.96	3.98	3.93	3.93	3.95	3.85	3.83	3.80
Al	0.14	0.09	0.09	0.11	0.09	0.09	0.08	0.20	0.21	0.23
Cr	0.06	0.08	0.06	0.07	0.07	0.08	0.08	0.08	0.09	0.10
Fe	0.43	0.64	0.67	0.69	0.65	0.65	0.63	0.21	0.25	0.25
Mg	5.12	5.22	5.17	5.06	5.23	5.22	5.23	5.64	5.63	5.62
Ni	0.01	0.02	0.03	0.03	0.03	0.03	0.02	0.03	0.03	0.03
Total	9.83	9.98	9.98	9.94	10.00	10.00	9.99	10.01	10.04	10.03

*Total Fe as FeO.

Table 8-5-4. Microprobe analysis of vein serpentines

Specimen No.	04-002			04-003		04-004			04-006
Analysis No.	15	16	17	5	8	13	14	15	1
SiO_2	40.17	41.45	41.22	40.22	40.77	40.55	40.77	40.29	42.47
Al_2O_3	0.31	1.51	0.07	0.26	0.28	0.31	0.31	0.34	0.52
FeO*	7.37	8.31	4.30	4.78	4.73	8.73	8.59	8.46	1.92
MgO	36.73	32.87	40.14	38.84	40.78	37.01	38.35	37.46	43.65
Cr_2O_3	0.00	0.00	0.00	0.00	0.00	0.00	0.00	0.00	0.00
NiO	0.67	0.77	0.37	0.32	0.32	0.36	0.33	0.28	0.29
Total	85.25	84.91	86.10	84.42	86.88	86.96	88.35	86.83	88.85
Number of cations on the basis of fourteen oxygens									
Si	3.95	4.08	3.95	3.94	3.88	3.93	3.89	3.91	3.89
Al	0.04	0.18	0.01	0.03	0.03	0.04	0.04	0.04	0.06
Cr	0.00	0.00	0.00	0.00	0.00	0.00	0.00	0.00	0.00
Fe	0.61	0.69	0.34	0.39	0.38	0.71	0.69	0.69	0.15
Mg	5.39	4.83	5.73	5.67	5.79	5.35	5.46	5.42	5.96
Ni	0.05	0.06	0.03	0.03	0.03	0.03	0.03	0.02	0.02
Total	10.04	9.84	10.06	10.06	10.11	10.06	10.10	10.08	10.08

*Total Fe as FeO

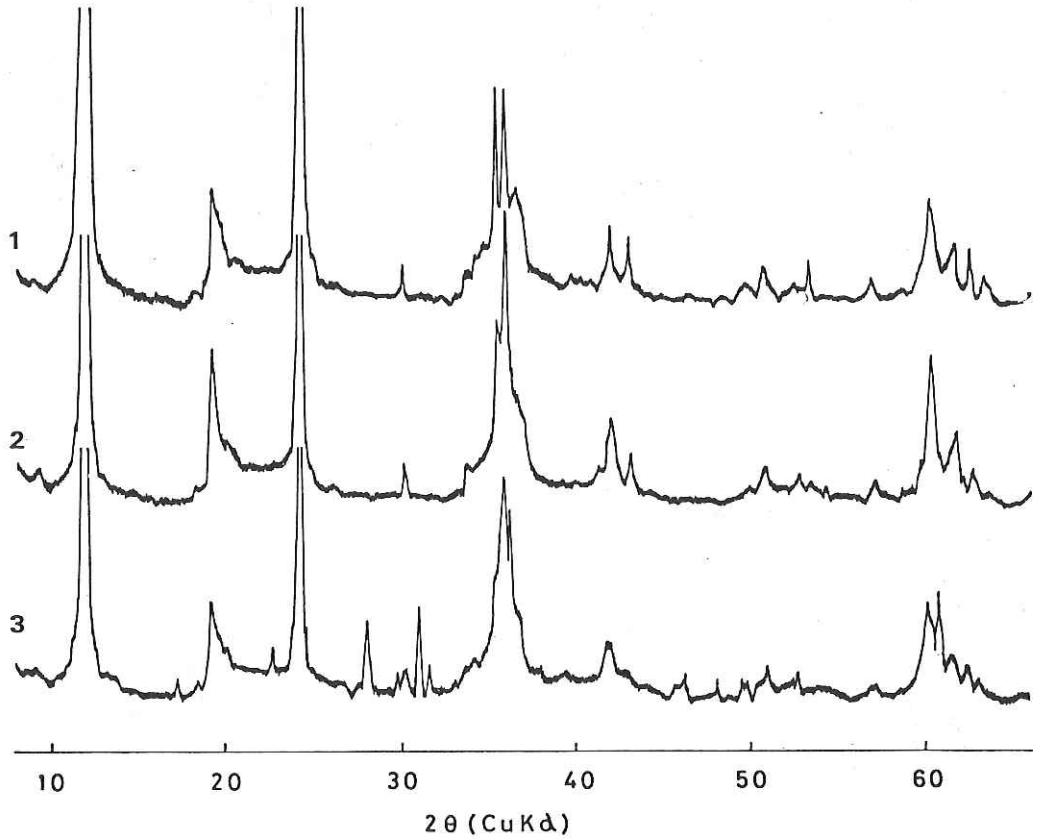

Fig. 8-5-1. X-ray powder patterns. 1:specimen 04-006. 2:specimen 04-019. 3:specimen 04-004.

04−003

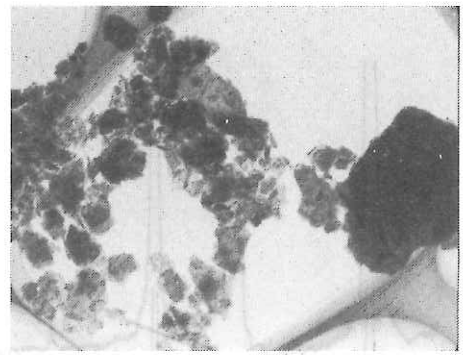

04−019

04−006

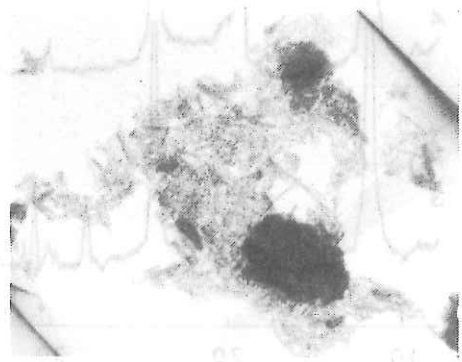

04−170

04−006

04−170

Fig. 8-5-2. Transparent electron microscope photographs.
Bar indicates 1 μm.

8-6. DESCRIPTION OF SAMPLES FROM AMAMI PLATEAU

K.KONISHI, T.ISHII, J.NAKA, H.OHARA and K.FUTAKUCHI

All the nodules and clasts recovered from the Amami Plateau have a considerable thickness of ferro-manganese encrustation ranging from 3 to 10 cm and suggest a lengthy period of their submarine exposure. Besides one pebble of acidic plutonic rock (trondhjemite) forming a nucleus of a rounded nodule (12-04). Angular pebbles of the similar lithology and rounded pebbles of andesite (?) form a conglomeratic substratum on which a thick crust has grown (12-01, 02).

Should the provenance of these rocks be close to or on the site of ferro-manganese encrustation, they may vindicate the previous interpretation that the Amami Plateau represents a remnant of an old island arc system.

Table 8-6-1 List of dredged materials.

Sample No.	Diameter(mm) L	M	S	Round-ness	Wt(g)	Mn-coat-ing(mm)	Lithology & Remarks	
09-01					3.2		foraminifera ooze	
02					0.4		shell fragments	
03					0.4		pumice and scoria	
04					0.1		lithic fragments	
11-01					2750		soft sediment	
05					90		coarse sand with pebbles	
12-01	423	300	102	0.35	12460	NC,KT	Mn-nudule	LI (diorite?)
02	318	183	94	0.45	5230	NC,KT	"	LI (" ?)
03	307	164	102	0.55	5250	NC,KT	"	LI (basalt?)
04	133	116	114	0.85	1750	31.5-56.0	trondhjemite	(tonalite)
05	187	73	72	0.45	995	0.4-3.7	calcareous siltstone, bored	
06	148	130	83	0.40	1135	NC, KT	Mn-nodule	LI(coarse sandstone)
07	144	115	85	0.55	1210	NC	"	LI
08	63	58	44	0.60	115	4-10	calcareous sandstone	
09	56	51	47	0.80	115	14-23.5	basalt(?)	
10	64	51	23	0.40	75	0-1	siltstone	
21					30		soft sediment, calcareous ooze	

Note KT: knobby on top NC: no core LI: lithic inclusion

8-7. DREDGE RESULT AT SITE KH 82-4-20 in KITA-YAMATO-TAI

Y. OGAWA

Dredge was hauled twice at site KH 82-4-20, but samples were recovered only once, where the wire just on the main bucket was cut. This chapter describes the result of microscopic observation of 13 thin sections which include typical rock types about thirty pebbles and sand grains recovered by this dredge haul.

This site is located 39°50'N, 133°50'E,, and is situated on the SE flank of the Kita-Yamato Bank, from 580m to 674m in depth. Pebbles and sand grains were recovered within foraminifer rich sands, and range from one centimeter to a few milimeters in diameter. They are roughly divided into two kinds genetically ; one is angular fragments of pumice, probably derived form the Japanese island arc, and the other is generally rounded grains of hard rocks, probably in situ ones (refer Honza, 1979). The latter is further divided into igneous rocks and sedimentary rocks. Igneous rocks are mostly tonalite without K-feldspar, granite with K-feldspar and dacite or rhyolite of porphyritic texture. Most of them are more or less altered, and chlorite replaced the mafic minerals. Sometimes cataclastic deformation of various fashion is common. Some rocks are mylonitic and rarely schistose.
The general amount of each rock type is shown in Fig. 1. But on account of samples being small, to decide the rock name is not critical. Interesting specimen is pebble of no. 8-1, which bears coarse sandstone grains that are made of quartz and feldspar fine grains. This pebble has recorded three stages of decomposition, originally a granitic rock.

In general, pebbles and sands of the dredged samples indicate that there are granitic rocks (including tonalite and granite), dacitic or rhyolitic volcanic or hypabyssal rocks, clastic rocks and metamorphic rocks around the Kita-Yamato Bank. Some pebbles are possibly ice- rafted (erratic) ones, but this idea is fairly doubtfull (refer Honza, 1979). The result is roughly coincident to that of GH 78-2 of Geological Survey of Japan (Honza(ed.), 1979), in which Yuasa et al. (1979) reported mylonite, hornblende-actinolite-albite-quartz schist and fine sandstone from the Kita-Yamato Bank. Honza(1979) discussed the origin of the Japan Sea and concluded that the Kita-Yamato Bank

together with the Yamato Bank and the Oki Bank is the remnant rise or ridge when the main Japanese island arc drifted apart from the Eurasian continent. To give a certain criticism to this idea, the result of the dredge of our cruise was too poor.

REFERENCE

Honza, E. (ed.) (1979) Geological Investigation of the Japan Sea. April -June, 1978. Geological Survey of Japan. 99pp.

Honza, E. (1979) Sediments, structure and origin of Japan Sea-Concluding remark- in Honza (ed.) (1979), P. 89-93.

Yuasa, M., Kanaya, H., & Terashima, S. (1979) Rocks and sediments. in Honza, E. (ed.) (1979) p.54-60.

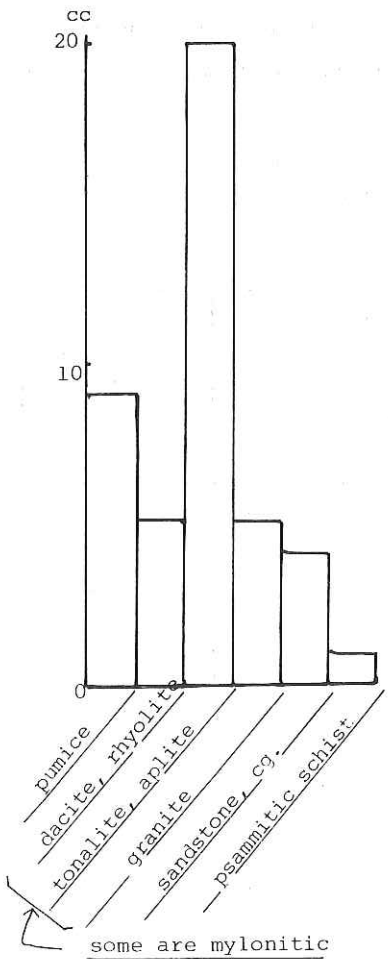

Fig.8-7-1. Volume (cc ca.) of dredge samples collected at site KH 82-4-20.

9. Camera

9-1. SEA TRIAL OF SMALL-SIZED DEEP SEA CAMERA SYSTEM

J. HASHIMOTO

The small-sized deep sea camera is under development at the Japan Marine Science and Technology Center (JAMSTEC). A series of its sea trials was carried out during the HAKUHO-MARU cruise KH-82-4. The camera system basically consists of a camera, a strobe, a release, buoys and a radio beacon (Fig. 9-1-1). The camera is actuated by timer. The strobe is synchronized by a shutter through penetrative connectors. The developed release is actuated by timer, too. Three operations of the free-fall camera system were carried out during this cruise, as shown in operation logs (Table 9-1-1.) . As a result of sea trials, recoveries of the system were successful, but deep sea photography was unsuccessful. The reason for unsuccess is that there was defect in the take-up function of the camera and it makes the film jammed at halfway.

Table 9-1-1. OPERATION

DATE	July 25,1982	July 28,1982	July 30,1982
TIME	10:18 - 12:40	08:27 - 10:32	09:12 - 11:01
LOCATION	Ogasawara Ridge	Shikoku Basin	Shikoku Basin
SHIP POSITION	28°50.6'N,141°15.0'E	27°49.6'N,139°29.1'E	28°23.7'N,132°46.3'E
DEPTH	4020 m	3300 m	2630 m
DESCENDING SPEED	Approx. 1.0 m/sec.	Approx. 1.0 m/sec.	Approx. 1.0 m/sec.
ASCENDING SPEED	Approx. 1.2 m/sec.	Approx. 1.1 m/sec.	Approx. 1.1 m/sec.

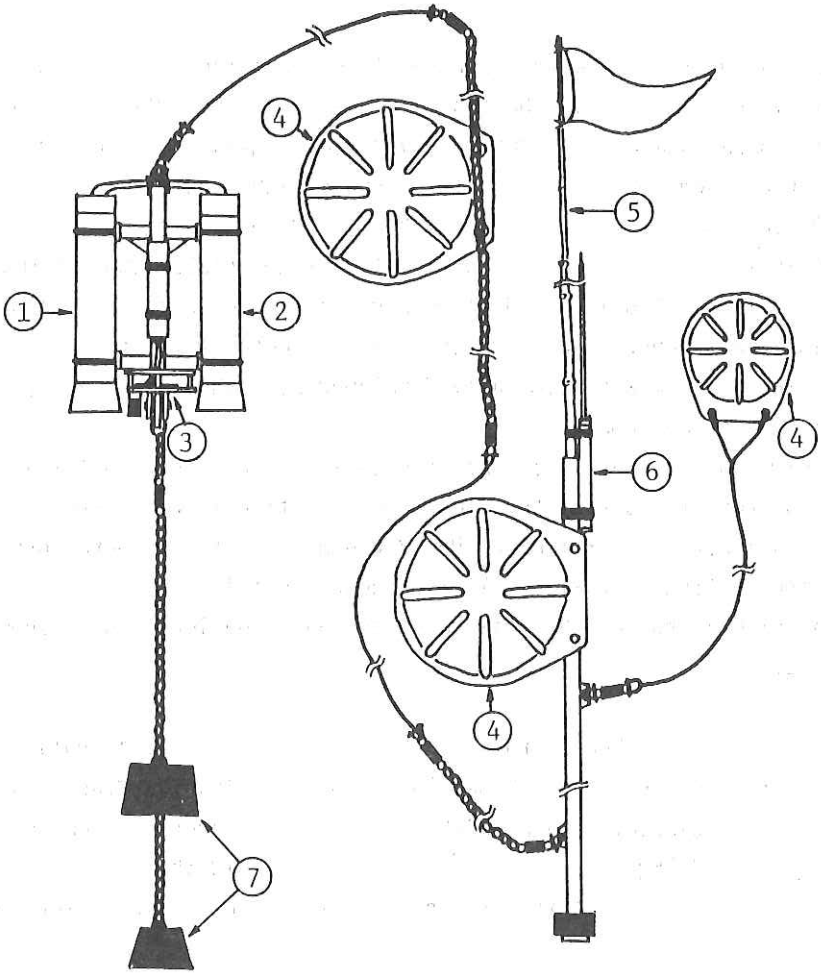

1 ; CAMERA 2 ; STROBE 3 ; RELEASE 4 ; BUOY
5 ; FLAG ROD 6 ; RADIO BEACON 7 ; WEIGHT

Fig. 9-1-1. Illustration of small-sized deep sea camera

9-2. WIRED GLASS SPHERE DEEP SEA CAMERA

M. WATANABE and T. ISHII

Deep sea camera system was prepared to observe the ocean bottom materials, especially in rocky area. The system consists of the following four units.

1)Camera sphere — moter-drived 35mm camera with time controller.
2)Flash sphere — two stroboscopic light sources.
3)Sonar pinger — EG and G Model 220 sonar pinger.
4)Frame — stainless steel frame (1350x1300x1000mm, 100kg).

Camera plus controller, and flash were contained in individual pressure-resistant glass sphere. Both spheres are connected with optical fiber cable. This system was originally developed by Hashimoto et al. (1975) as a free-fall deep sea camera.

In this cruise, the system was mounted in a stainless steel fram with a sonar pinger for repeated use of the camera in operation in rocky areas. The whole system was lowered and raised by No. 3 winch. The first operations during KH80-3 cruise (Ishii et al. 1981) were unsuccessful.

After KH80-3 cruise, this camera system has been improved as shown in the following.

	KH80-3 cruise	KH82-4 cruise
Glass spheres	Benthos Inc. Model 2040-13H ϕ=33cm, 1.14cm thick 7.7kg with relatively rough surface	Toshiba Glass Inc. ϕ=36cm, 1.5cm thick 12.5kg with smooth surface
Time controller	storage battery National Inc. LC-156, 6volt	dry cell battery 1.5 voltx4
Flash controller	storage batterly National Inc. LC-156, 6volt	dry cell battery 1.5 voltx4
Additional weight	iron weight 80(20x4)kg	lead weight (made to order) 160(20x2x4)kg

As shown in operation logs (table 9-2-1), four-operations of deep sea photography were attempted by this system during the cruise. Representative photographs of the ocean bottom in the each operation site are shown in Fig. 9-2-1 to 9-2-8 (cf. Okada et al. 1980).

On-off remote swith of time controller was originally designed to be operated with magnet through the glass sphere. This swith system did not work in this cruise, because original glass sphere was replaced by thicker one. It is very difficult to know exact distance between camera and ocean bottom using the present pinger + syncroscope monitering system. This camera system has still some problems which should be improved as shown previously.

REFERENCES

Hashimoto, J., Hattori, M., Natori,K. and Aoki, T., 1978. A self-buoyand free-fall deep sea camera system using submersible glass spheres (In Japanese). Jamstectr 3., 24-28.

Ishii, T., Watanabe, M. and Furuta, T., 1981. First trial use of a Q.I. deep-sea camera. Preliminary report of the Hakuhō-maru cruise KH 80-3 (Ocean Research Institute, University of Tokyo), 200-202

Okada, H., Ohta , S. and Niitsuma, N., 1980. Lebensspuren photographed on the deep-sea floor of Suruga Bay, Central Japan. Geosci. Repts. Shizuoka Univ., 7, 97-102.

ACKNOWLEDGMENTS

The authors are much grateful to Mr. J. Hashimoto and Mr. M. Hattori, Japan Marine Science and Technology Center, and Dr. S. Ohta, Univ. of Tokyo, for their suggestions and discussions on the improvenent and operation of this system. Thanks are due to Dr. S. Ohta for his comments on the lebensspuren and benthos photographed on the deep-sea floor.

TABLE 9-2-1. OPERATION LOGS OF DEEP SEA CAMERA

Date	August 3, 1982	August 14, 1982
Station No.	KH82-4-10B	KH82-4-19
Location	Amami Plateau	NW of Yamato Basin
Weather	fine	fine
Sea	low swell	low swell
Bottom topography	flat	flat
Water depth	3060m	3100m
Ship position (start)	28°25.5′N 132°28.1′E	38°28.1′N 134°35.9′E
(finish)	28°24.3′N 132°28.5′E	38°27.2′N 134°36.4′E
Film & Film length	triX(150frame) +sakura400(100frame)	triX(250frame)
Lens focussed	2.0m	2.0m
Iris	11	11
Shutter speed	1/60sec	1/60sec
Shutter interval	10 sec	10 sec
Add. wt.	160(20x2x4)kg	160(20x2x4)kg
Speed wire-out	0.8m/sec	0.8m/sec
Shutter set time	19^h40^m-20^h22^m	22^h06^m-22^h48^m
Time lowered	18^h30^m	20^h56^m
Initial time on bottom	19^h33^m (20m from bottom)	21^h51^m (40m from bottom)
Time surfaced	21^h00^m	23^h30^m
Result	Fig. 9-2-1 and 2	Fig. 9-2-3 and 4
Remarks	Combined with heat flow meas. No. 10A.	Combined with piston coring No. 19 and heat flow meas. No. 19.

Date	August 15,1982	August 17. 1982
Station No.	KH82-4-20	KH82-4-25
Location	Kita-Yamato Tai	Tsushima Basin
Weather	fine	fine
Sea	low swell	low swell
Bottom topography	flat	flat
Water depth	700m	1550m
Ship position (start)	39°47.4′N 133°47.3′E	36°01.6N 131°04.5′E
(finish)	39°47.9′N 133°47.0′E	36°01.4N 131°03.7′E
Film & Film lengh	triX(250 frame)	sakura400 (150 frame)
Lens focussed	1.5 m	1.5m
Iris	11	11
Shutter speed	1/60 sec	1/60 sec
Shutter interval	10 sce	10 sec
Add, wt.	160(20x2x4)kg	160(20x2x4)kg
Speed wire-out	0.8m/sec	0.8m/sec
Shutter set time	19^h45^m-20^h30^m	20^h45^m-21^h10^m
Time lowered	19^h42^m	20^h05^m
Initial time on bottom	20^h40^m(20m from bottom	20^h40^m(20m from bottom)
Time surfaced	21^h30^m	21^h30^m
Result	Fig. 9-2-5 and 6	Fig. 9-2-7 and 8
Remarks	Combined with dredge hauls No. 20.	Combined with piston coring No. 25 and heat flow meas. No. 25.

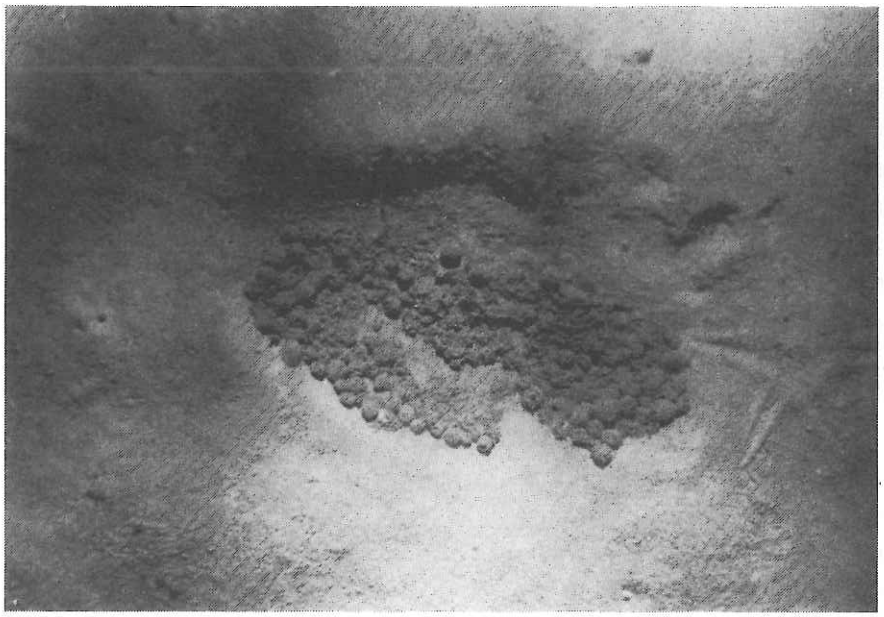

Fig. 9-2-1. Bottom photographs taken at Station KH82-4-10B. Unidentified structure (center) and "sitzmark"of an asteroid (right) on soft sediment.

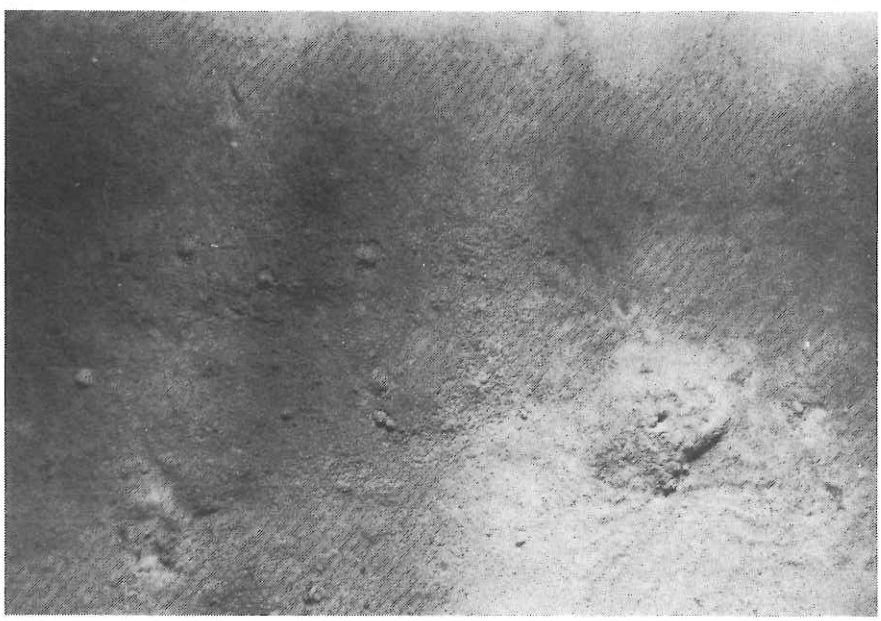

Fig. 9-2-2. Bottom photographs taken at Station KH82-4-10B. A track of a holothurian (?) (center) and radial traces of bonellid worms (right) on soft sediment.

Fig. 9-2-3. Bottom photographs taken at Station KH82-4-19. A polynoid polychaete (left), trails of molluscs (?) (top), and amphipods or isopods (bottom) on soft sediment.

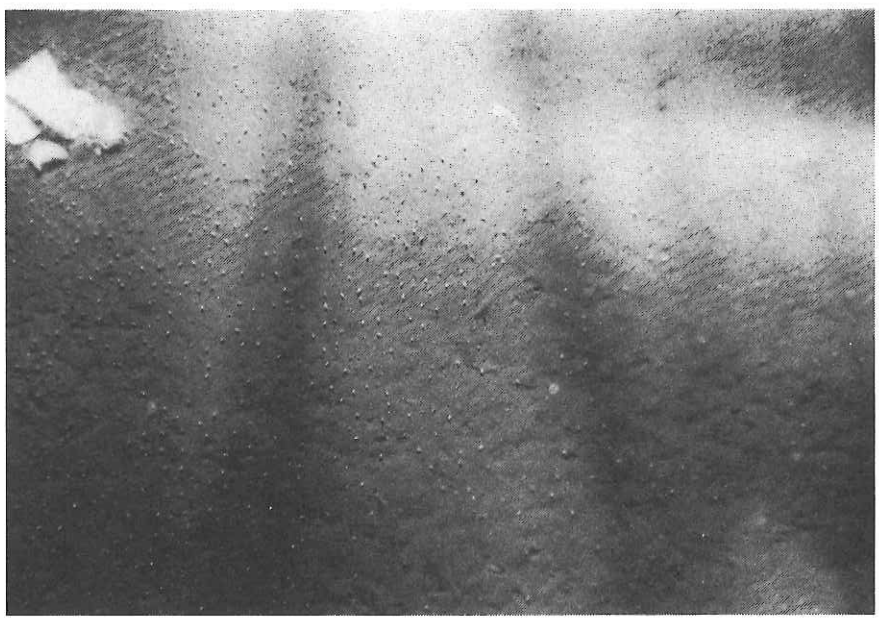

Fig. 9-2-4. Bottom photographs taken at Station KH82-4-19. Carcass of a squid (left), polynoid polychaete (top), and aggregate of amphipods or isopods (allover) on soft sediment.

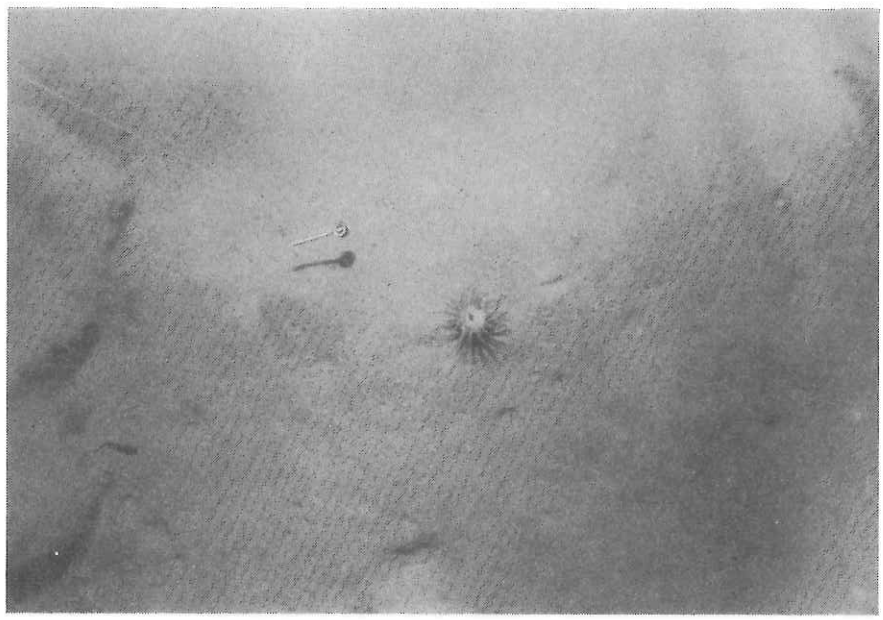

Fig. 9-2-5. Bottom photographs taken at Station KH82-4-20. A sea anemone (center), an asteroid, *Crossaster papposus* LINNAEVS (left), and a fish (left) on soft sediment.

Fig. 9-2-6. Bottom photographs taken at Station KH82-4-20. Structures of biological origin (?) (top) and human artefacts (?) (center) on soft sediment.

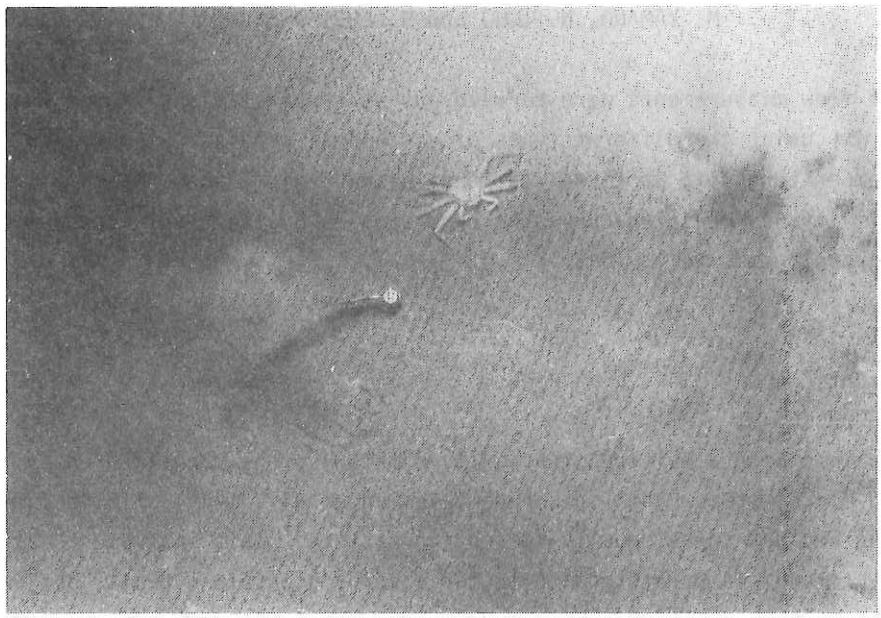

Fig. 9-2-7. Bottom photographs taken at Station KH82-4-25. A crab, *Chionoecetes japonicus* RATHBUN (center) and trail of a bnccinid gastropod (center) on soft sediment.

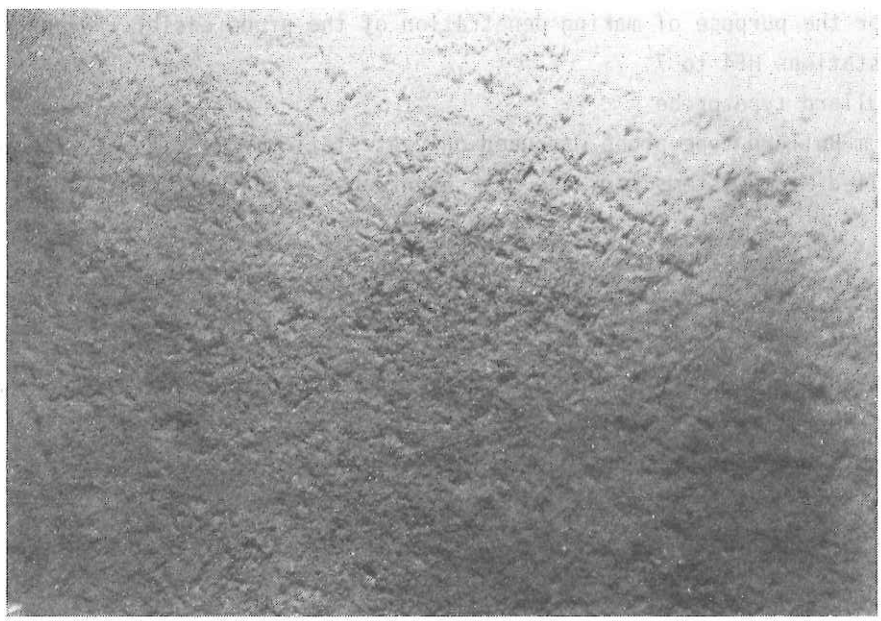

Fig. 9-2-8. Bottom photographs taken at Station KH82-4-25. Foot prints of a crab, *Chionoecetes japonicus* RATHBON (allover) on soft sediment.

10. HEAT FLOW MEASUREMENTS

M. YAMANO, N. FUJII and H. FUJISAWA

Heat flow measurements were carried out at seven stations listed in Table 10-1 using two differnt types of geothermal probes. We obtained good temperature data at three stations in the Sea of Japan. Thermal conductivity was measured on piston core samples by the needle probe method (von Herzen and Maxwell, 1959).

Instruments

(1) POGO Probe

We mainly used a multipenetration type (POGO) probe manufactured by Applied Microsystems Ltd. in Canada (Hyndman et al., 1979). It is 2 m or 6 m long and has seven equally-spaced thermistors. This instrument has the ability to send temperature data to the ship by acoustic signals, but we did not use this ability since the data recorder for the acoustic transmission was out of order. In-situ thermal conductivity measurement by calibrated heat pulse was unsuccessful because of unstable heat generation.

A weight system which can slide along the probe was developed by the crew for the purpose of making penetration of the probe easier. We used it at stations HF4 to 7.

(2) Bullard type probe

A 3 m Bullard type probe was used only at station HF2. It was also made by Applied Microsystems Ltd. and has seven equally-spaced thermistors.

Results at each station and Discussions

HF1

We used the 2 m POGO probe. The data recorder stopped just before the first penetration due to water leakage into the pressure housing, so that we could not measure temperature in the sediment.

HF2

The Bullard type probe was used. It seems that the probe was partially

pulled out about 4 minutes after the penetration. In the end one or two thermistors were in mud. The estimated temperature gradient is about 50 mK/m and average of thermal condictivity is 0.81W/m K. A heat flow value, about 40 mW/m^2, might be calculated from these data but it is not reliable one.

HF3

We lowered the 6 m POGO probe and hit the bottom three times. The probe did not penetrate into the sediment on the first hit and only one thermistor penetrated on the second and the third hits. Thus geothermal gradient was not obtained.

HF4

The 2 m POGO probe was used. Again sea water leaked into the pressure housing and the data recorder stopped.

As it was revealed that a defect in sealing of the 2 m probe is responsible for the water leakage, we used the 6 m probe at stations HF5 to 7.

HF5

Six thermistors penetrated into the sediment on both hits. The temperature profiles are shown in Fig.10-1. It is recognizable that the two profiles are very similar and the temperature gradient gradually decreases with depth. Although thermal conductivity was not measured at this station, heat flow can be calculated using the conductivity values at HF6 (Table 10-1). This assumption seems reasonable since the thermal conductivities of the sediments around this site are reported to be 0.7 to 0.8 W/m K (Yoshii, 1979).

HF 6

At this station and station HF7 we tried to shift the position of the probe by drifting after the first penetration. Six thermistors penetrated and the temperature profiles resemble those at HF5 as can be seen in Fig 10-1. Thermal conductivity was measured at interval of 1 m. The obtained conductivity varies around 4 m from the surface.

HF7

Five of the thermistors penetrated on both hits but there is a small difference between the two temperature profiles. Temperature garadient

decreases with depth as in the case of HF5 and 6 and this tendency is more pronounced at 7-A. Thermal conductivity was measured at intervals of 1 m as well. An increase in conductivity is observed around 2 m from the surface.

The temperature profiles obtained by multiple-penetration are similar (Fig.10-1), which suggests high reliablity of temperature data and uniform heat flow around these sites. Temperature gradient, thermal conductivity and calculated heat flow in the Sea of Japan area are complied in Table 10-2. The variation of thermal conductivity seems to be consistent with decrease of thermal gradient with depth as calculated heat flow is nearly constant. At HF7-B station the heat flow is higher in the lower part but the difference is within the limits of errors considering uncertainty of thermal conductivity. The averaged heat flow values on each penetration are presented in Table 10-1. The errors of these values are estimated to be 10 to 15 mW/m^2. They mainly come from uncertainty of thermal conductivities.

Many heat flow measurements have been made in the Sea of Japan area (Fig.10-2). Our new data roughly agree with the former measurements by shorter (2 m long) probes, 91 to 111 mW/m^2, 78 to 90 mW/m^2 and 82 to 90 mW/m^2 around stations HF5, 6 and 7 respectively, and the overall mean in the Sea of Japan, 92 W/m^2 (Sclater et al., 1980), confirming the high heat flow in this area. As heat flow in the marginal basins is thought to reflect their ages (e.g. Sclater et al., 1980), these values imply that the ages of the Yamato Basin and the Tsushima Basin are about 25 Ma.

We obtained good penetration (4 to 5 m) at stations HF5 to 7. It must be attributed mainly to the soft sediments in the Sea of Japan but the sliding weight may have contributed. We are planning to improve the weight system for the next opportunity.

References

Hyndman, R.D., E.E. Davis, and J.A. Wright, The measurement of marine geothermal heat flow by a multipenetration probe with digital acoustic telemetry and insitu thermal conductivity, Marine Geophys. Res., 4, 181-205, 1979.

Sclater, J.G., C. Jaupart, and D. Galson, The heat flow through oceanic and continental crust and the heat loss of the earth, Rev. Geophys. Space Phys., 18, 269-311, 1980.

von Herzen, R., and A.E. Maxwell, The measurement of thermal conductivity of deep-sea sediments by a needly-probe method, J. Geophys. Res., 64, 1557-1563, 1959.

Yoshii, T., Compilation of geophysical data around the Japanese Islands (I), Bull. Earthquake Res. Inst. Univ. Tokyo, 54, 75-117, in Japanese with English abstract, 1979.

Table 10-1. Heat flow stations

Area	Station		North Latitude	East Longitude	Uncorrected Water Depth, m	Probe	Heat Flow, mW/m^2
Bonin Trough	St. 2	HF1-A	28°28.5'	141°21.0'	4010	2m POGO	
		B	28°27.9'	141°20.7'	4120		
	St. 6	HF2	27°55.6'	142°18.5'	4100	Bullard	
Amami Plateau	St.10	HF3-A	28°26.3'	132°27.7'	3040	6m POGO	
		B	28°26.0'	132°27.7'			
		C	28°25.8'	132°27.7'	3030		
Ryukyu Trench	St.13	HF4-A	29°45.1'	131°17.9'	3390	2m POGO	
		B	29°45.0'	131°18.2'			
		C	29°45.4'	131°18.3'	3430		
Yamato Basin	St.17	HF5-A	37°15.4'	134°15.6'	2430	6m POGO	98
		B	37°15.5'	134°15.4'	2430		100
	St.19	HF6-A	38°28.5'	134°35.2'	3010	6m POGO	102
		B	38°28.4'	134°35.4'	3010		99
Tsushima Basin	St.25	HF7-A	36°02.4'	131°04.7'	1550	6m POGO	92
		B	36°01.9'	131°04.5'	1520		102

Table 10-2. Heat flow data in the Sea of Japan

Station	N*	Subbottom Depth, m	Gradient, mK/m	Conductivity, W/m K	Heat Flow, mW/m^2
HF5-A	6	0-4	123-138	0.74**	91-102
		4-5	119	0.84**	100
HF5-B	6	0-4	125-137	0.74**	93-101
		4-5	122	0.84**	104
HF6-A	6	0-4	128-140	0.74	95-104
		4-5	124	0.84	104
HF6-B	6	0-4	127-143	0.74	94-106
		4-5	115	0.84	97
HF7-A	5	0-2	113-117	0.78	88- 91
		2-4	88-102	1.00	88-102
HF7-B	5	0-2	121-123	0.78	94- 96
		2-4	101-117	1.00	101-117

* numbers of thermistors in mud

** assumed values

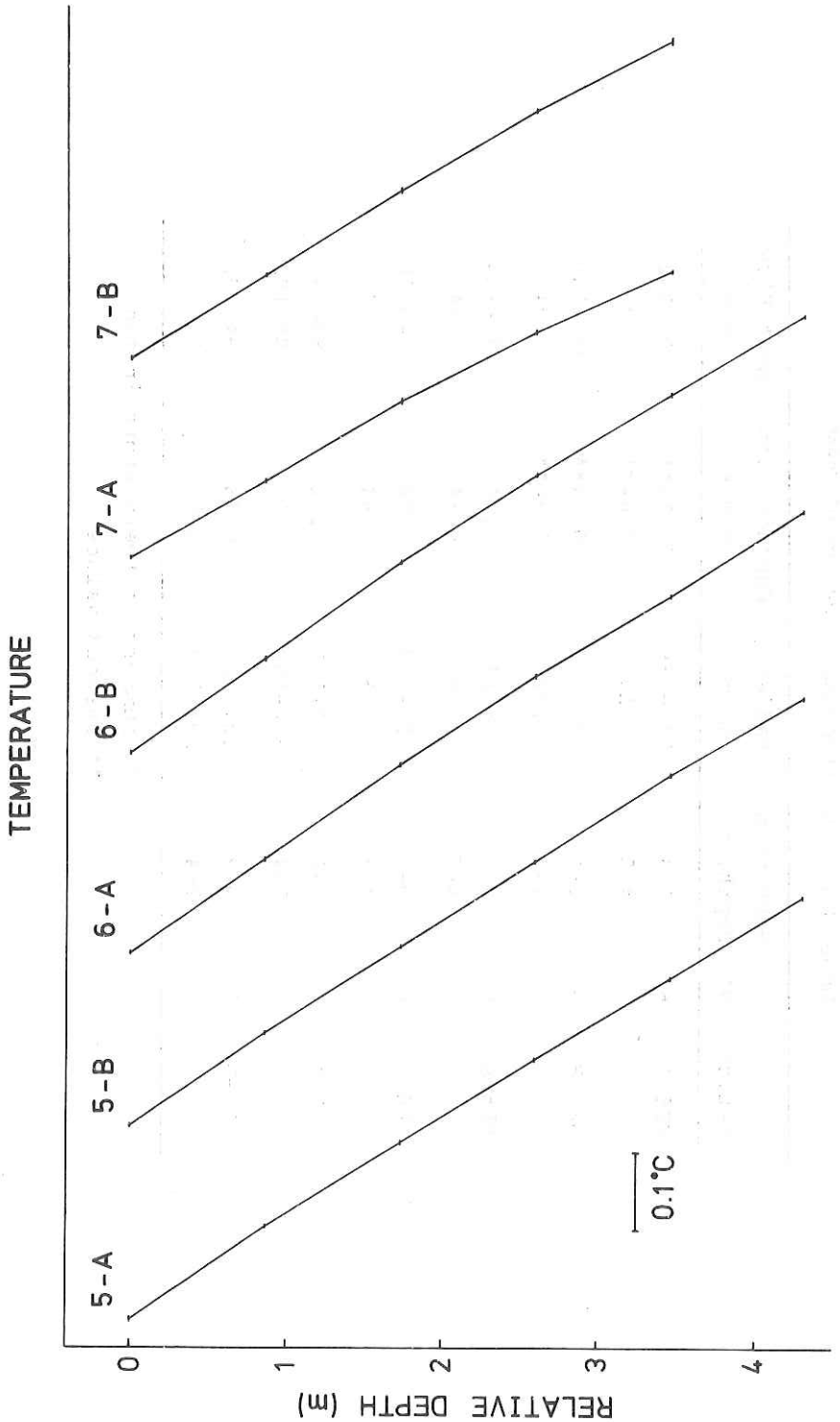

Fig. 10-1. Temperature profiles measured at sites HF 5,6 and 7.

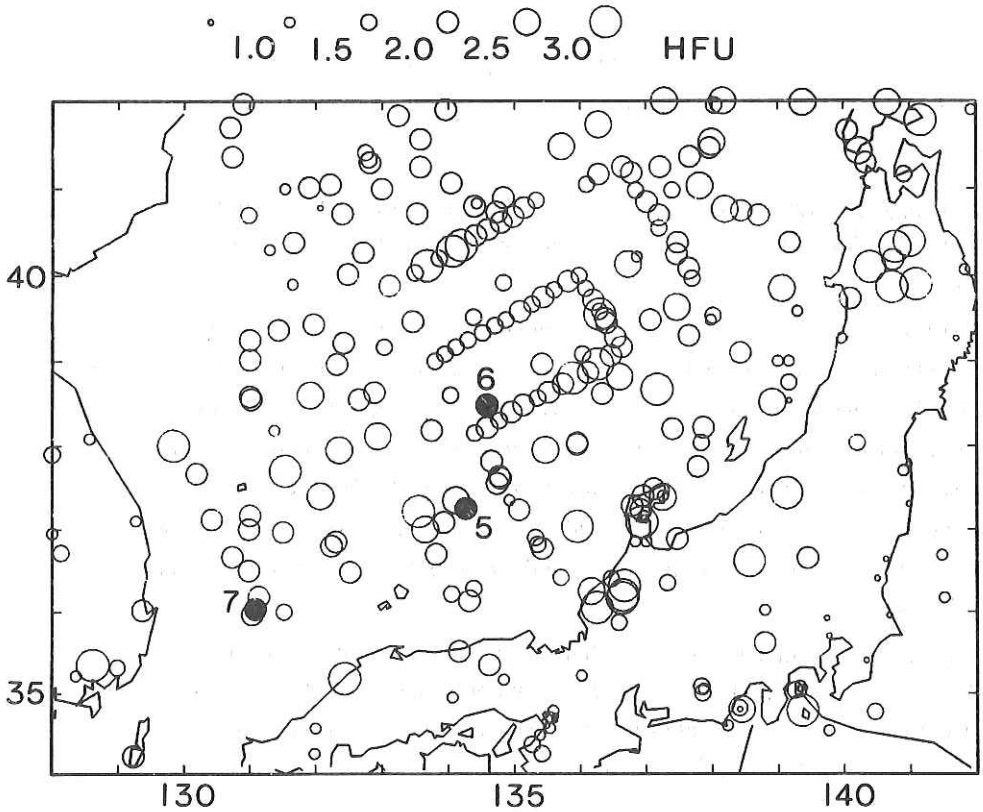

Fig. 10-2. Map of heat flow values in the Sea of Japan area (modified from Yoshii,1979). Unpublished values by Lamont-Doherty Geological Observatory and Earthquake Research Institute are added to the compilation by Yoshii (1979). The shaded circles represent the data obtained on this cruise.
1 HFU = 42 mW/m^2.

11. SEISMIC PROFILING AND NATURAL MICROEARTHQUAKES OBSERVATION BY AN OBS TRIPARTITE ARRAY ON THE AMAMI PLATEAU

K. SUYEHIRO, A. NISHIZAWA
and H. SHIMIZU

A tripartite OBS array was deployed on the Amami Plateau to investigate the velocity structure underneath and the seismicity in its vicinity.

Instruments : Pop-up type OBSs developed at Geophysical Institute, University of Tokyo and Laboratory for Ocean Bottom Seismology were used as signal receivers. The OBS is equipped with vertical and horizontal sensors, amplifiers, a cassette tape recorder, a time code generator, and batteries for power supply, which are housed in a glass sphere. High-and low-gain vertical and middle-gain horizontal sensors signals and BCD coded time signal are recorded on a DAR tape at a tape speed of 0.13 mm/s.

Bolt 1500C airgun with wave shape kit and 9 ℓ air chamber which belongs to O. R. I., University of Tokyo was used as the artificial seismic source for this experiment. The airgun was fired at 30 s interval at 70-100 kg/cm^3 pressure.

Experiment: The OBSs were deployed at locations as given in Table 11-1, Fig. 11-1 and operated for about 3 1/2 days (Jul. 30 - Aug. 3, 1982). All three OBSs were successfully recovered and the data have been analyzed.

The airgun profiles were shot as given in Table 11-2.

Microearthquakes: During the recording period of about 90 hours, events were registered by OBSs at a rate of about one per hour. S-P times could be read for about 1/3 to 1/2 of these events and are shown in Fig. 11-1. It is evident from Fig. 11-2 that there are no nearby events and the activity peaks at about 25 s S-P time.

Calculation of apparent velocities and azimuths indicates that all the events are on the Ryukyu Trench side of the array. Considering the sensitivity of the OBSs, this means that the West Phillipine Basin is aseismic for events as small as M=2.0 within at least 300 km distance range.

Most events seem to have occurred on the landward side of the trench, which agrees with reliable solutions of I. S. C. or J. M. A. However, there were events which occurred on the oceanic side of the trench. Fig. 11-3 shows epicenters determined by this experiment. Note the events at the western edge of the Amami Plateau. Large circles are determined from S-P times and azimuths and triangles from conventional hypocenter determination method. As all these events occurred outside our array, focal depths cannot be determined accurately. This type of events have not been detected by land networks and requires longer on-site observation to reveal its nature in detail.

Refraction profiling: The airgun signals recorded on OBS cassette tapes were all digitized at a sampling speed of 100/s. After time corrections, the data were digitally processed (time reduction, filtering, and stacking) and record sections were plotted out. Fig. 11-4 shows an example section at P-1 for Profile 1. Shot-receiver distances were determined from direct water arrivals.

More data analysis is necessary before drawing any conclusion as to the Amami Plateau's origin being continental or oceanic. However, a layer with seismic velocity, 5.2-5.5 km/s, which seems to be thicker than 4 km is found from both profiles at all OBSs.

TABLE 11-1. OBS LOCATIONS

OBS	LATITUDE	LONGITUDE	WATER DEPTH
P-1	28°20.9' N	132°52.5' E	2610 m
P-2	28° 3.2'	132°33.2'	2930
P-3	28°27.3'	132°27.6'	3045

TABLE 11-2. SEISMIC PROFILES

PROFILE 1 (28°27.1'N, 132°27.8'E)-(28°18.3', 132°3.8')
Aug.1 13:30 -20:00

PROFILE 2 (27°55.0'N, 132°35.2'E)-(28°12.5', 132°30.3')
Aug. 2 00:45 -05:00

Note: Profile 1 crosses P-1 and P-3, and Profile 2 crosses P-2

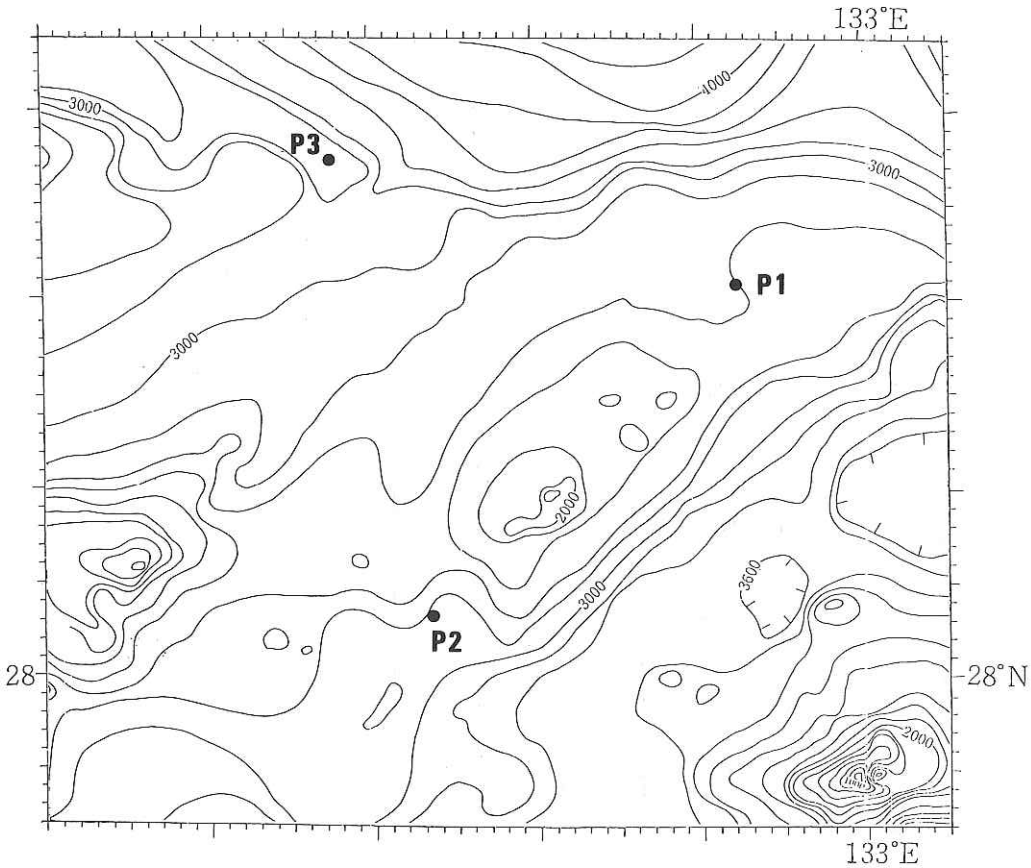

Fig. 11-1. Location of a tripartite OBS array on the Amami Plateau.

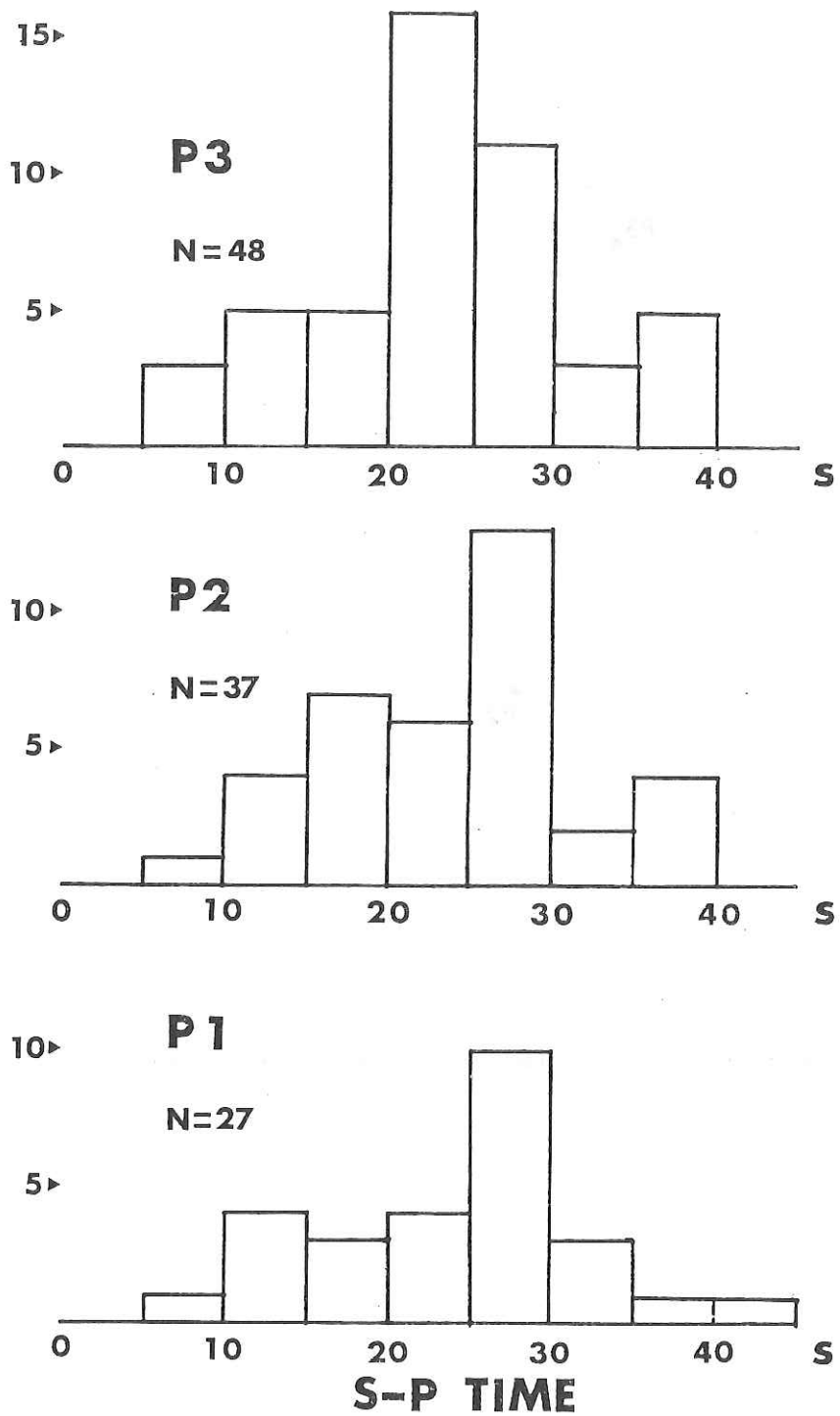

Fig. 11-2. Histogram of S-P time.

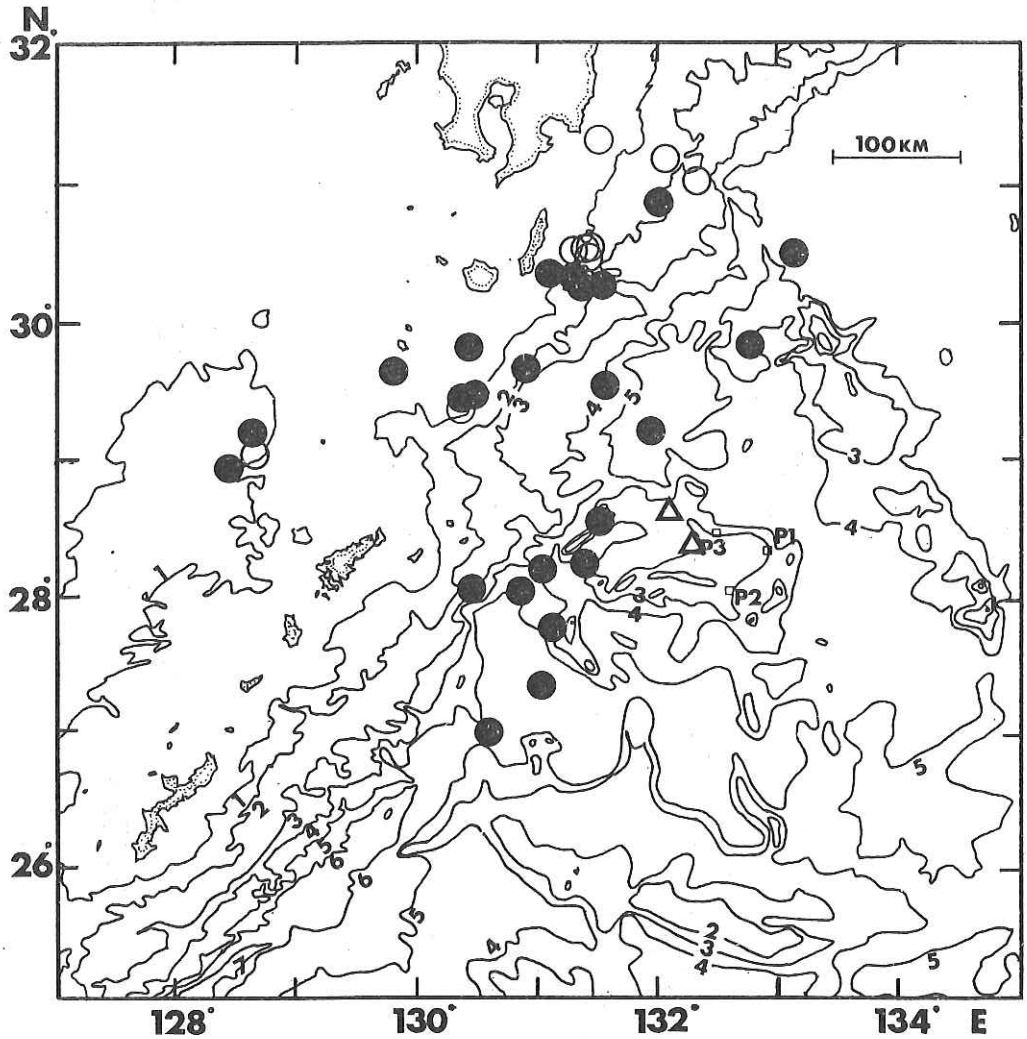

Fig. 11-3. Distribution of epicenters determined by this experiment.

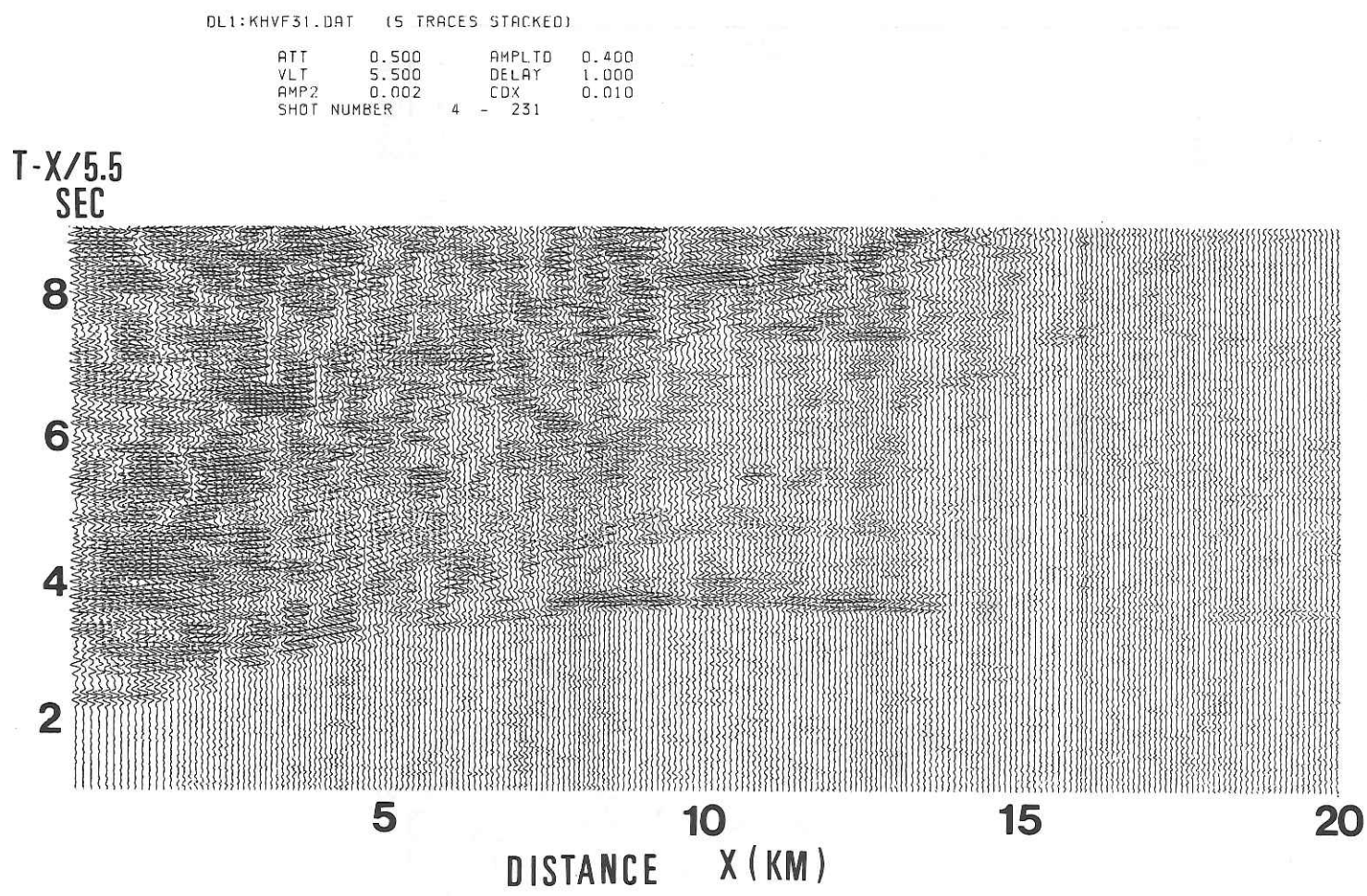

Fig. 11-4. A refraction profile P-1 after processings.

12. SEISMIC PROFILER RECORDS BY SINGLE-CHANNEL REFLECTION

T. ASANUMA, H. AMAMIYA, N. OHYAMA,
K. SUYEHIRO*, H. SHIMIZU*, A. NISHIZAWA*,
T. MATSUMOTO**, T.TANAKA**, M. YAMANO**,
Y. MATSUBARA**, LUI Zhong Chen, and A. BRAVO**

Seismic reflection records were observed along tracks shown in Fig. 12-1 using a single-channel seismic profiler with air-guns. During the multichannel recording the second or third channel was used as a monitor. All the observed records were stored in magnetic tapes as well as a chart recorder.

Quite a good record was obtained while curising at a speed of 5 knots, although the records were slightly noisy at a speed of 10 knots. Further analyses of recorded signals are planned particularly for the Ryukyu trench and Yamato-Tai.

Airguns used were 1500C (with air capacity of about 10ℓ) and 1900C (about 2ℓ) manufactured by Bolt Inc.

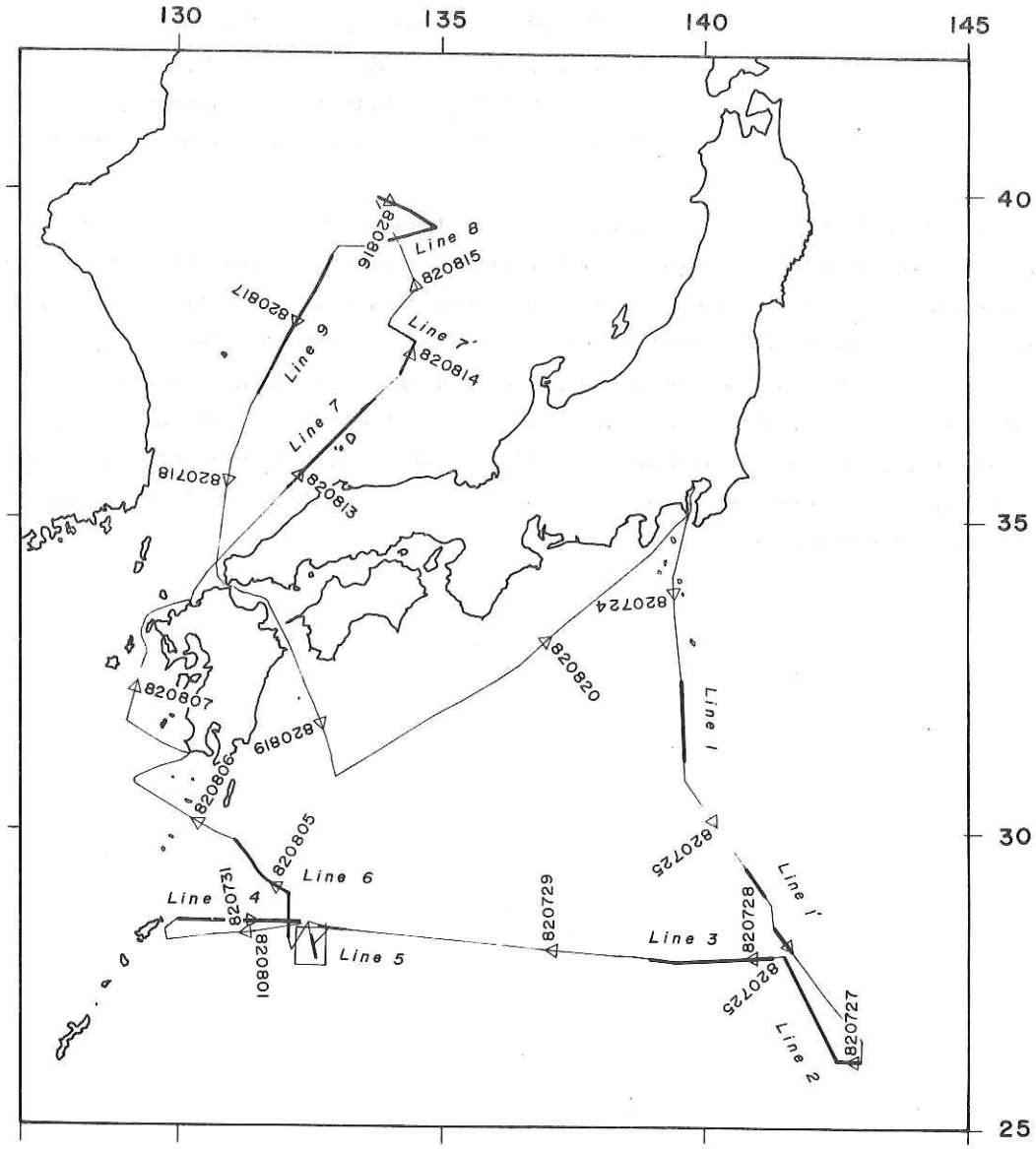

Fig. 12-1. Ship's tracks for single-channel seismic reflection observation.

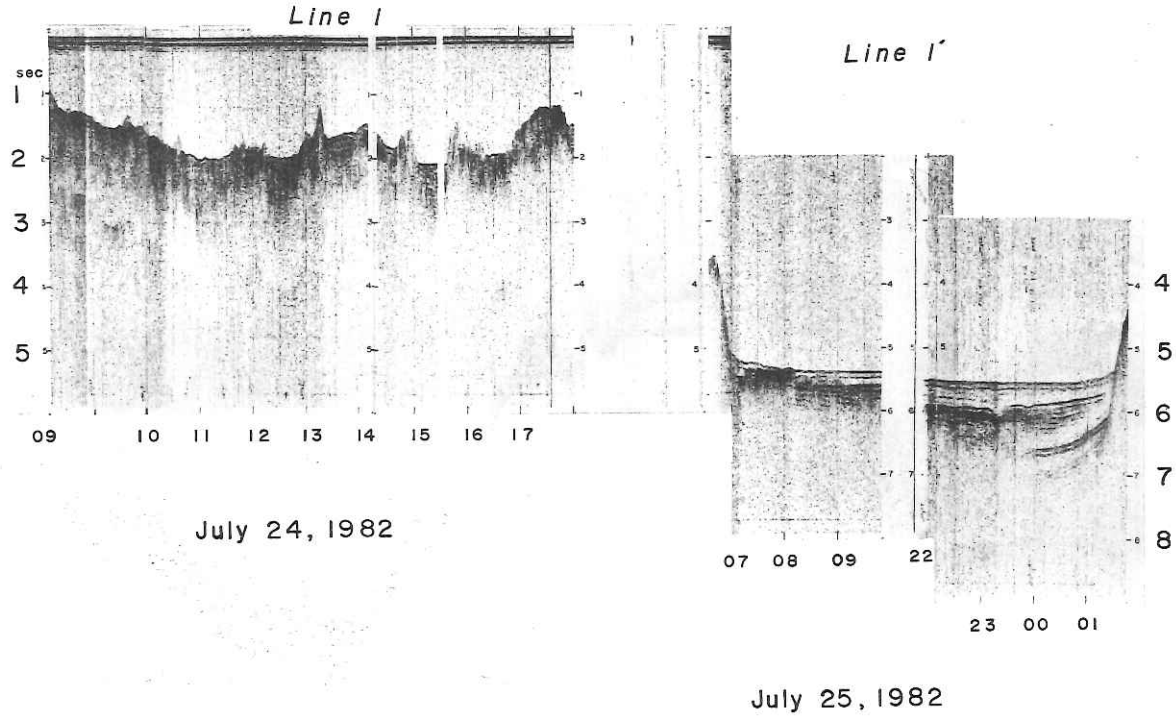

Fig. 12-2. Seismic profiler records obtained on board KH 82-4 cruise.

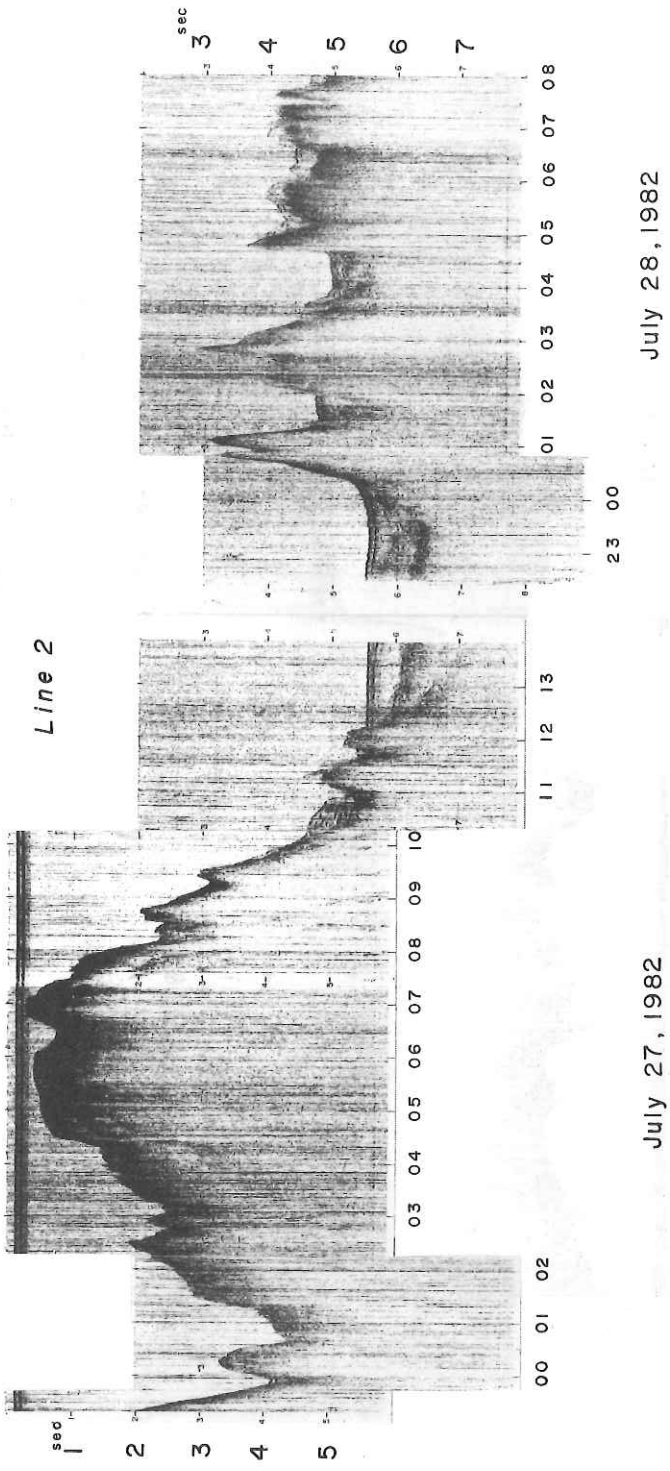
Line 2
sec
1
2
3
4
5
00 01 02 03 04 05 06 07 08 09 10
11 12 13
July 27, 1982
sec
3
4
5
6
7
23 00 01 02 03 04 05 06 07 08
July 28, 1982

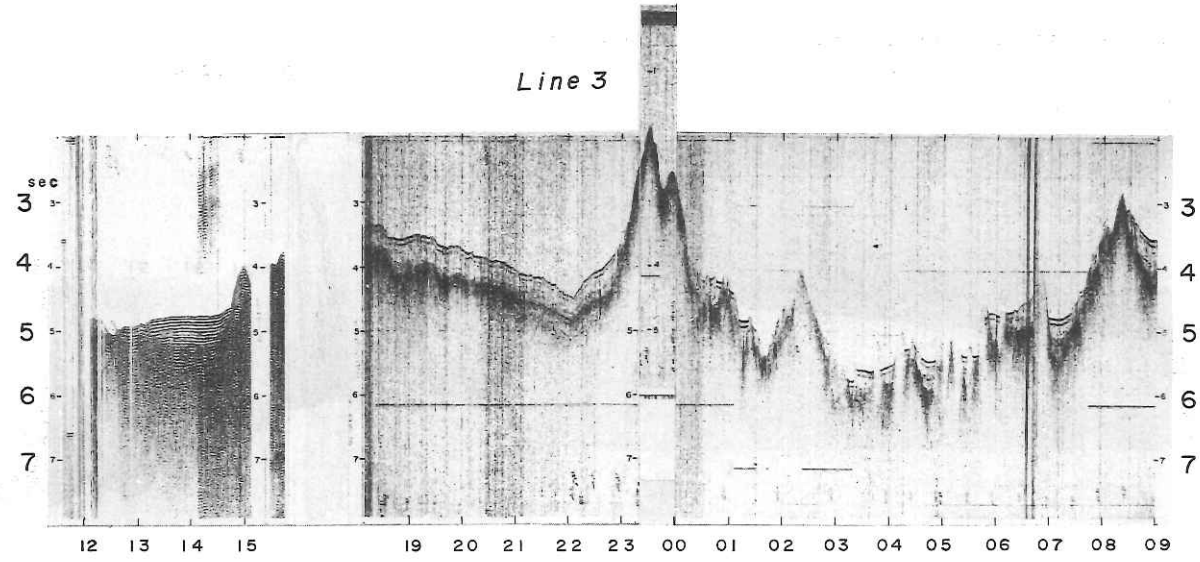
Line 3
sec
3
4
5
6
7
12 13 14 15
19 20 21 22 23 00 01 02 03 04 05 06 07 08 09
July 28, 1982
July 29, 1982
July 30, 1982

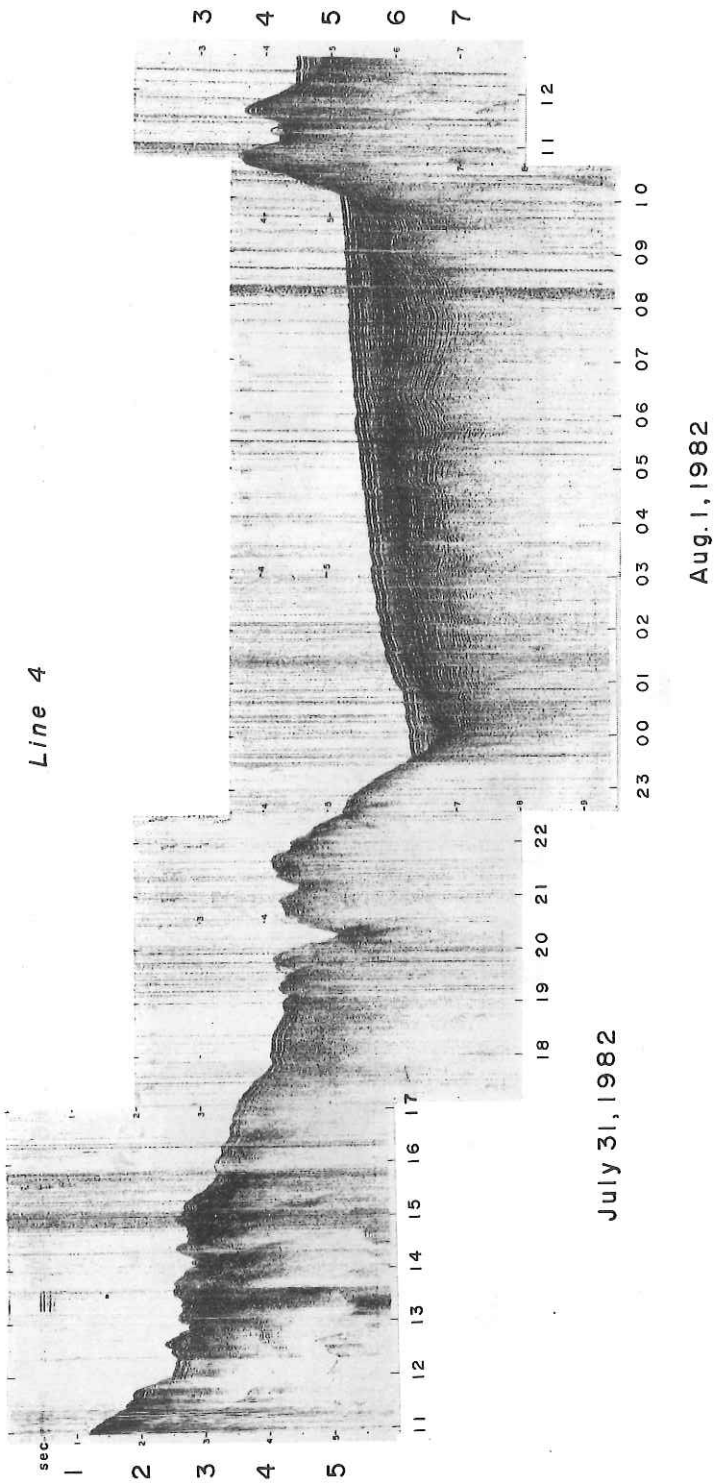
Line 4
July 31, 1982
Aug. 1, 1982
sec.

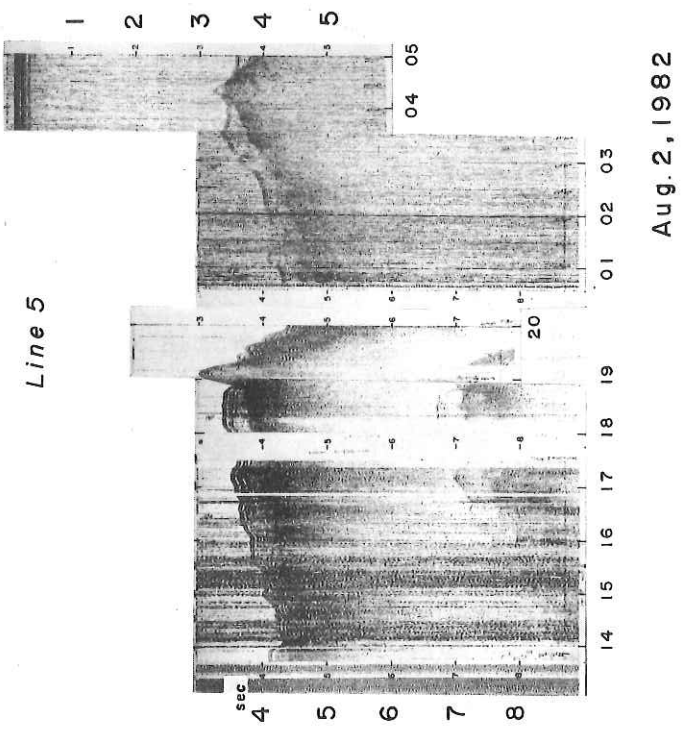
Line 5
Aug. 2, 1982
sec

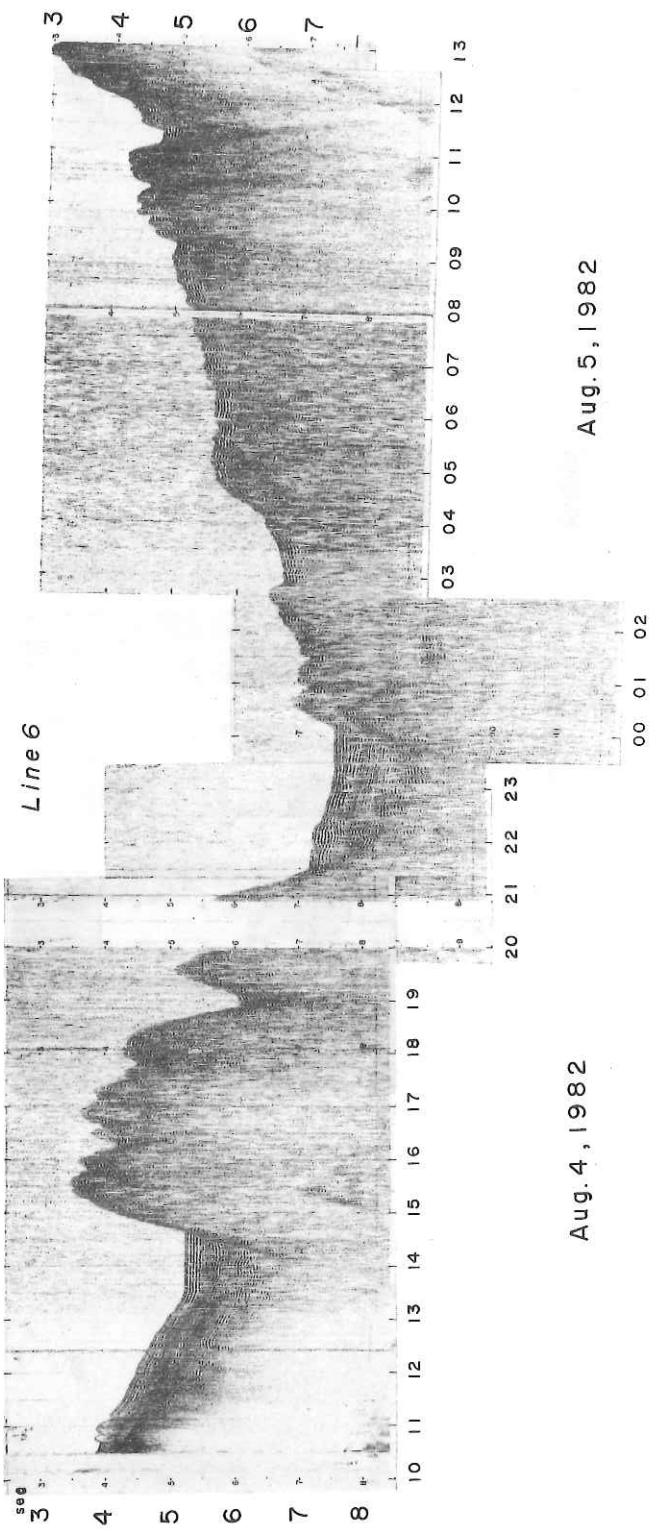
Line 6
sec
Aug. 4, 1982
Aug. 5, 1982

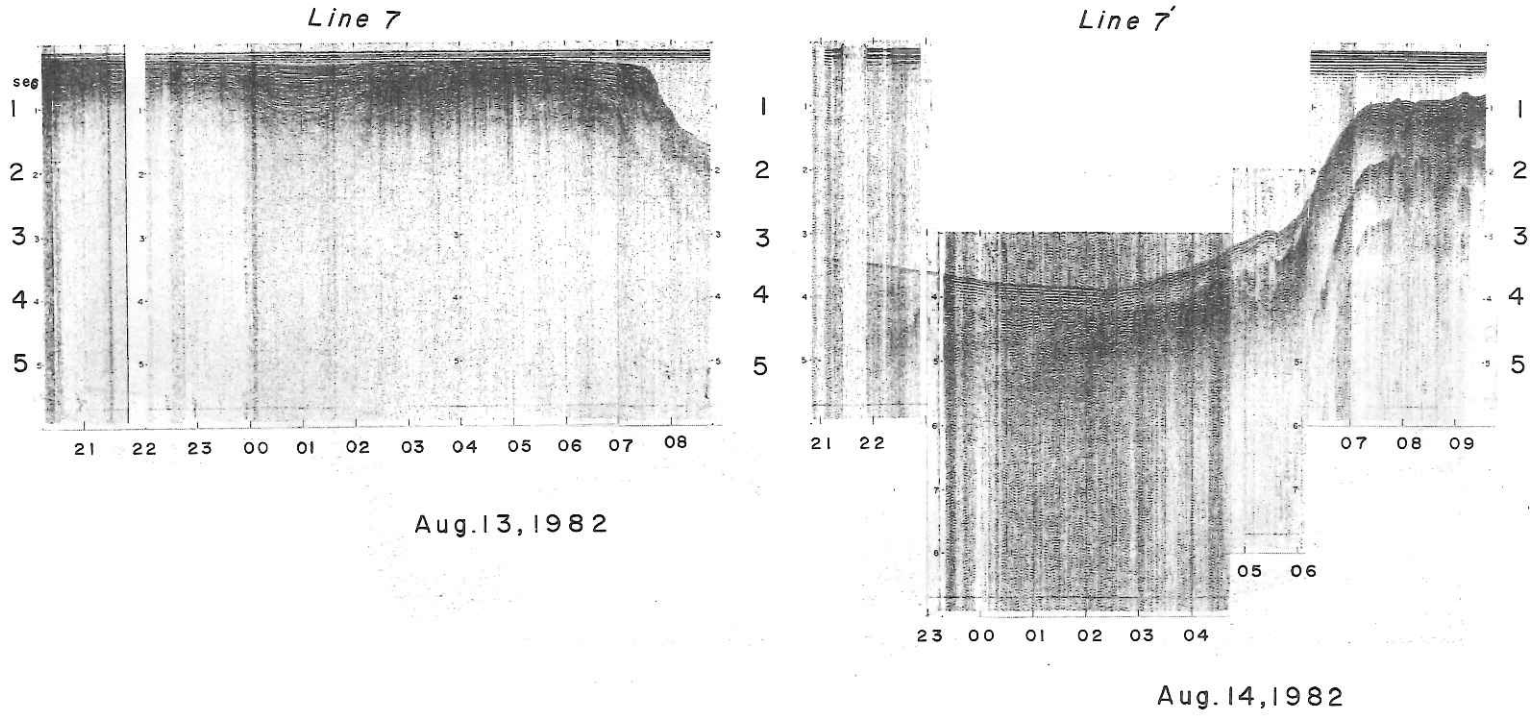
Line 7
sec
1
2
3
4
5
21 22 23 00 01 02 03 04 05 06 07 08
Aug.13,1982
Line 7'
1
2
3
4
5
21 22
07 08 09
05 06
23 00 01 02 03 04
Aug.14,1982

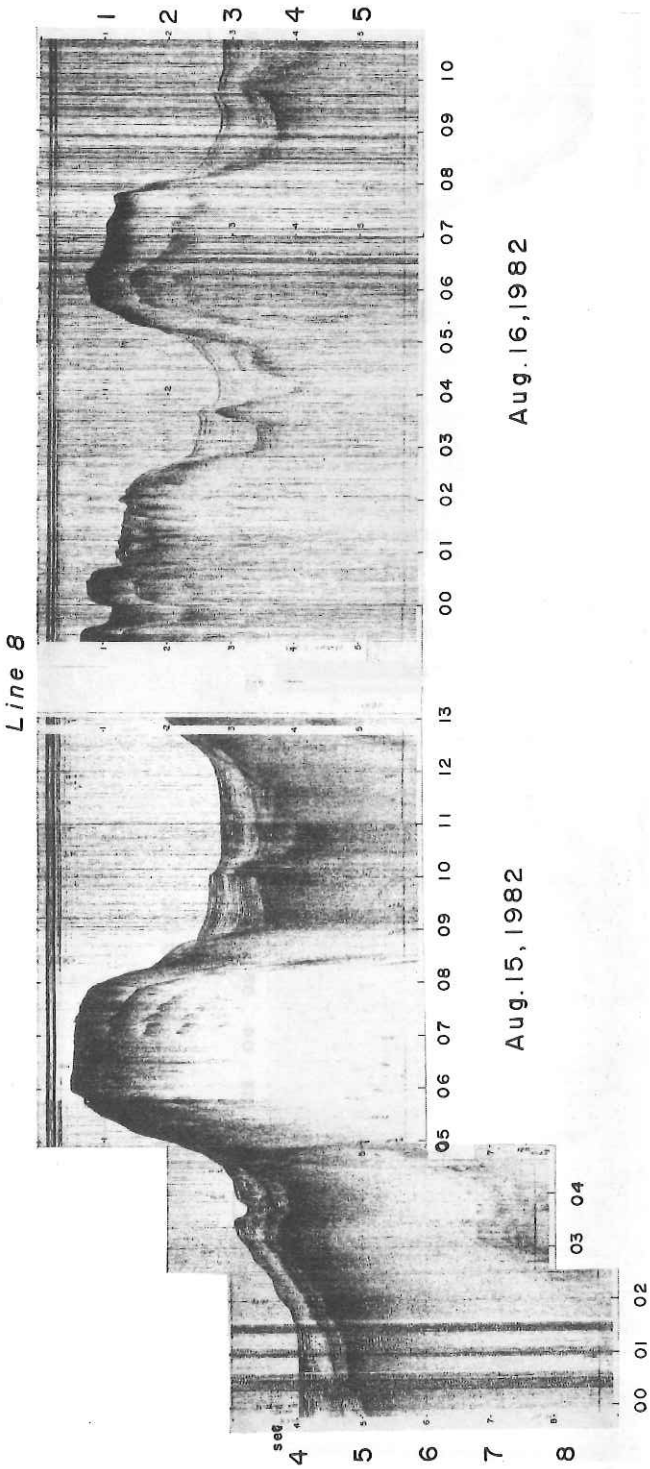
Line 8
Aug.15,1982
Aug.16,1982
sec

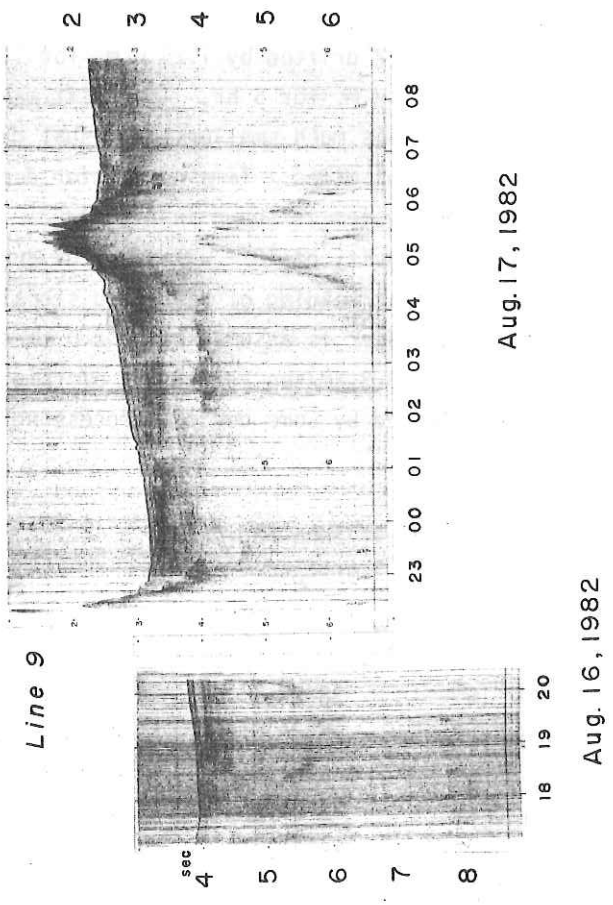
Line 9
sec
4
5
6
7
8
18
19
20
Aug. 16, 1982
23
00
01
02
03
04
05
06
07
08
Aug. 17, 1982
2
3
4
5
6

13. SEISMIC SONO-RADIO BUOY OBSERVATION

T. ASANUMA, H. AMAMIYA and N. OHYAMA

A reverse-method sono-radio buoy observation was done on a flat top (D.= 2800 m) of the Amami Plateau (Fig. 13-1). To avoid drifting of sono-radio buoy out of the top region by wind and current, the buoy was anchored by about 60 kg weight using fishing line made of thin (2.5mmφ) rayon string which is free from resistance to the current.

It was found that a bucy SB-2 drifted by 1.25 n.m. for 11 hr of deployment but SB-2R drifted by only 0.4 n.m. for 5 hr. The drift may be due to slipage of weight on the bottom but it is much smaller than usual drift of floating buoy amounting to a few nautical miles. Time needed for deployment of the anchor was only 30 min. The system is shown in Fig. 13-2.

A large airgun with air capacity of 10 ℓ was used for shots. The records obtained have some noise so that reading of refracted signals is not easy. If velocity of the uppermost layer is assumed to be 2.0 km/sec, velocity of the next layer is estimated to be 3.3 km/sec. Thickness of this layer and velocity of the lower layers are obtained by some degital processing such as stacking.

KH-82-4 Sono radiobuoy
1982-8-2

				DEPTH	WATER TEMP. °C
Sono buoy-2	07^h16^m	28°24.5'	132°38.8'	2,955m	27.0
abeam	08^h10^m	28°24.0'	132°38.3'	2,850	27.6
end	10^h10^m	28°21.5'	132°48.6	2,630	27.5
sono buoy-2R	10^h57^m	28°21.8'	132°49.2	2,630	27.4
abeam	11^h24^m	28°21.7'	132°48.8	2,620	
end	13^h45^m				
Sono buoy 2 repeat	13^h55^m				
abeam	14^h24^m				
end	15^h30^m	28°22.3	132°45.5	2,680	
2R on Deck	17^h53^m	28°21.1	132°48.5	2,650	
2 on Deck	20^h33^m	28°23.4	132°38.6	2,800	

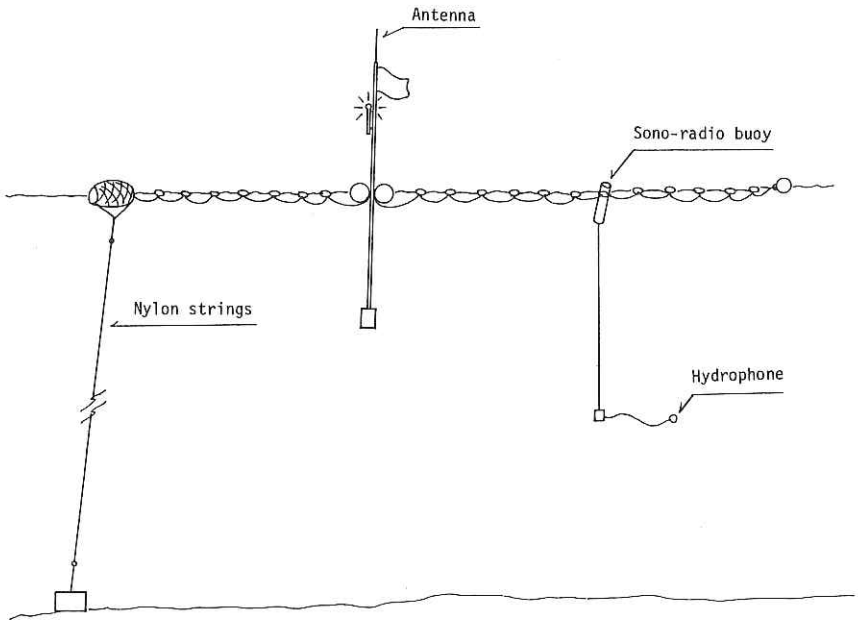

Fig. 13-1. Sono-radio buoy observation on the Amami Plateau.

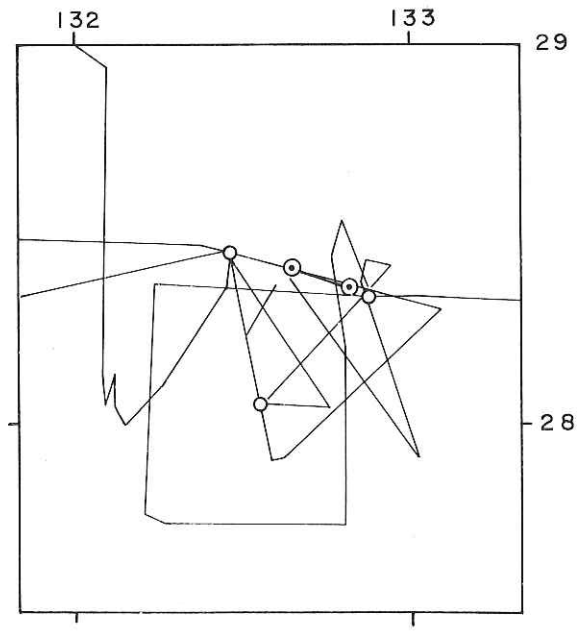

Fig. 13-2. Anchored sono-radio buoy system used in this cruise.

14. MULTICHANNEL SEISMIC REFLECTION SURVEY AROUND THE AMAMI PLATEAU

H. TOKUYAMA and KONG YOUNG SAE

A multichannel seismic reflection survey was carried out during KH 82-4 around the Amami Plateau. Fig 14-1 shows a layout of the multichannel seismic survey system which was accomplished during KH 82-4. The system is composed of the following blocks; I) Sound source block, II) Hydrostreamer cable block, III) Amplifier block, IV) Recording block, and V) Depth/Distance indicator block (Fig. 14-2).

SEISMIC INTERPRETATION OF THE AMAMI PLATEAU AREA

The Amami Plateau is irregularly shaped without much elongation and bounded, on north side, by a deep depression which is situated between the plateau and the Kyushyu Palau Ridge on east side. On its south an elongated basin exists to segregate the Daito Ridge. Western side of the plateau is proximal to the Ryukyu Trench.

The plateau is topographically rough with numerous peaks and thick sediment fills among these peaks up to 1.3 seconds in two way travel time.

From multichannel seismic reflection profiles, five acoustic units are identified at the Amami Plateau. Line KH 82-4-14 starts at 28°10.9N, 132°15.0 E (S.P. 0001) and ends at 28°56.2N, 132°05.8E (S.P. 1688) (Fig. 14-3, Fig.14-4). The stratigraphic sequence at S.P. 110 is identified with Unit A, Unit B, Unit D and Unit E in decending order (Fig. 14-5). Unit A, about 0.2 seconds thick, is acoustically transparent. Unit B, about 0.2 seconds thick, is also acoustically transparent. Reflector which defines Units A and B is not continuously identified. Unit D, about 0.6 seconds thick, is characterized by well-stratified, high frequency reflectors. Unit E is acoustic basement. Unit C, about 0.9 seconds thick, is identified between Units B and D at S.P. 260 (Fig. 14-5). The unit is considered as turbiditic deposits, mainly

because of characterized by low frequency stratified reflectors. The unit terminates updip progressively against surface of more inclined Unit Dt at S.P. 150 and 260. Line 82-4-14 intersects with Line 82-4-10 at S.P. 668, which is located at the foot of bathymetrical peak of the Amami Plateau, and stratigraphic sequence is similar to that of S.P. 260, except that Unit C thickens up to 1.3 seconds in two way travel time (Fig. 14-6). Toward the north Units A, B, C lap out against Unit D at S.P. between 700 and 790, although Units D and E are traced as far as northern bathymetrical peak (Fig. 14-7). Unit D, about 0.8 seconds thick, is exposed on southern slope of the peak underlaid by Unit E (Fig. 14-7). Toward the summit of the peak, Unit D gradually decreases in thickness and transparent veneer, which probably corresponds to Unit A, directly overlays Unit E without Unit D at S.P. 930 (Fig. 14-7).

Line KH-82-4-15 starts at 28°56.0N, 132°06.5E (S.P. 0001) ends at 29 49. 1N, 131 06.4E (S.P. 2888) (Fig. 14-8). The stratigraphic sequence at the axis of the Ryukyu Trench is identified with Unit T, Unit C, and Unit D in decending order at S.P. 440 (Fig 14-9). Units C and D are continuously traced from the Amami Plateau. Thickness of Unit C is about 0.5 seconds thick, is distinguished from Units A and B based on characteristic high frequency reflectors. Transition from Units A and B to Unit T is gradual so that relation of depositional sequences between Units A and B and Unit T is ambiguous. Unit T is considered as mixed strata which consist of transported sediments along trench axis, probably from the north, and Units A and B. Boundary between trench axis and lower inner trench slope is bounded by topographic high of Unit D (Fig. 14-9). Units C and D continuously traced from the Amami Plateau are not identified on landward side of the high. Unit C terminates progressively against Unit D. On the other hand, Units O and F are identified in decending order at S.P.720(Fig. 14-9). Unit O, about 1.4 second thick, is sedimentary mass of lower inner trench slope of the Ryukyu Trench. That the unit is charaterized by hyperbolic difraction at S.P. between 570 and 1060 suggests development of thrust faults (Fig. 14-8). Unit F is characterized by low freqrency reflector, definitely distinguished from Units C and D based on acoustic nature. It is assumed that there is significant acoustic impedance difference at the boundary between upper and lower units. The unit is traced

as far as 50 km on landward side of the topographic high, taking with graben structures at the interval of approximately 5 to 7 km. These graben structures are often observed in oceanic crust of outer trench slope (Hilde et al, 1978 and Iwabuchi 1980) and subducting oceanic crust beneath sedimentary masses of lower inner trench slope (Tokuyama et al., 1981). Consequently Unit F is assumed to correspond with oceanic layer 2A. Remarkable reflector is identified in graben structure between S.P. 750 and 900 (Fig. 14-10). The reflector is represented by drawing line from horst to horst in single graben structure and appears to be straight extension of top surface of oceanic layer 2A. Similar reflector has been reported from subducting Pacific plate at the Japan Trench (Tokuyama et al., 1981). Thrust faults prevailing in Unit O seem to converge with both the reflector and top surface of Unit F in the lower part (Fig. 14-10). Therefore, the reflector and top surface of Unit F act as master slip plane, through which the Philippine plate subducts beneath aht Ryukyu Arc. Unit T are off-scraped from subducting plate by thrust slices and added to lower inner trench slope. This suggests that Unit O mainly consists of off-scraped sediments.

Sedimentary mass of inner trench slope is devided into two units at S.P. between 1060 and 1900 (Fig. 14-8). Upper unit 0.3 to 0.35 seconds thick, is acoustically transparent and considered as mainly pelagic sediment. Lower unit is acoustically chaotic without significant reflectors. It is ambiguous whether the unit is highly deformed unit O or other strata. The chaotic unit abruptly terminates at S.P. 1900 and different unit emerges. The unit is characterized by stratified reflectors inclining to the west at S.P. between 1900 and 2000. Further to the west, dip of the unit gradually decreases and becomes almost flat at S.P. between 2120 and 2190 (Fig.14-8). The unit is considered as the Shimajiri Formation Pliocene to Late Miocene in age, which distributes mainly Okinawa Island. Boundary between chaotic sedimentary mass and the Shimajiri Formation is defined by several thrust faults. Schematic structure along line KH 82-4-15 is summarized in Fig. 14-11.

Line KH 82-4-10 starts at 28 28.9N, 130 07.5E (S.P. 0001) and ends at 28 27.8N, 132 27.8E (S.P. 4633) from Kikai Island to the Amami Platear in E-W running direction (Fig. 3, Fig. 12). The line crosses line KH 82-4-14 at S.P. 4161. Stratigraphic sequence at S.P. 4120 is quite similar to that of line KH 82-4-14 (Fig. 14-13). It can be identified with Unit A (0.2 seconds

thick), Unit B (0.2 seconds thick), Unit C (about 1.2 seconds thick), Unit D (about 0.7 seconds thick), and Unit E. Units A and B successively change into Unit T toward trench axis, similar to line KH 82-4-15. Unit C terminates downdip progressively against Unit D at S.P. between 2460 and 2600, however, Unit D is continuously traced westward as far as lower inner trench slope beyond trench axis (Fig. 14-14). Unit F, subducting oceanic layer 2A, is not kentified beneath sedimentary mass of lower inner trench slope differing from line KH 82-4-15. Unit D abruptly terminates by westward dipping thrust fault at S.P. 1835. That Unit D originally derived from the Amami Plateau is continuously traced westward beyond bathymetrical axis of the Ryukyu Trench leads to the conclusion that Unit D has been accreted on inner trench slope. Tectonic plate boundary between the Ryukyu Island Arc and the Philippine plate is overriding the landward side of the Ryukyu Trench axis due to collision of the Amami Plateau with the Ryukyu Island Arc (Fig. 15-15). Schematic structure along line KH 82-4-10 is summarized in Fig. 14-16.

Shallow earthquakes are reported in the Amami Plateau (Suyehiro et al., 1982). Distribution of epicenters of shallow earthquakes seems to be aligned in approximately N 70°W and is equivalent to southeastern extension of the Tokara depression in the Ryukyu Island Arc (Konishi, 1963). Trend of the alignment appears consistent with subducting direction of the Philippine plate beneath the Ryukyu Island Arc (Seno, 1978). Multichannel seismic profile of line KH 82-4-15 indicates subduction of the Philippine plate beneath Ryukyu Island Arc. On the contrary, multichannel seismic profile of line KH 82-4-10 suggests collision of the Amami Plateau with the Ryukyu Island Arc without subducting evidence of the Philippine plate. Although focal mechanism of shallow earthquakes is ambiguous, this tectonic setting may introduce strike-slip fault, whose trend is approximately parallel with subducting direction of Philippine plate. Therefore, shallow earthquakes might be caused by collision of the Amami Plateau with the Ryukyu Island Arc.

Kikai Island is located at western extention of line KH 82-4-10. The island is uplifting at rate of approximately 1.5 ~ 1.8 m/1000 yr. (Konishi et al., 1974). The Shimajiri Formation in the island, more than 5 km thick, overlays pre-tertiary basement which forms sedimentary basin (Kimura, personal communication, 1982). The rapid uplift of the island might be caused by collision of the Amami Plateau with Ryukyu Island Arc.

Crustal structure of the Amami Plateau is reported by Suyehiro et al. (1982). They identified 4 layers in the Amami Plateau based on P-wave velocity by using O.B.S.. They are 1.8 km/s, 2.7 km/s, 3.3 km/s, and 5.5 km/s layers in decending order. By correlating with multichannel seismic profile, we can identify the layers of 1.8 km/s, 2.7 km/s, 3.3 km/s and 5.5 km/s with units A, B, D and E, respectively (Fig. 14-5). Igneous rocks are reported from crest of peak at station of GDP-11-7, which is located on southern side of line KH 82-4-14 (Shiki et al., 1975). As mention above, Unit E is overlaid by veneer of Unit A on crests of peaks. Therefore, we can suppose that igneous rocks are dredged from Unit E. An age of hornblende bearing tonalite among dredged hauls was determined to be 75.1 Ma by using K-Ar method (Matsuda et al., 1975). This evidence suggests that Unit E consists of mainly igneous rocks in Late Cretaceous age.

Nummulite boninnensis of middle Eocene was collected from western peaks at station of GDP-11-9 together with basaltic rocks. Unit D is apparently exposed on slope of peaks as mentioned above, so that *Nummulite boninnensis* was dredged from Unit D. Unit C is correlated with the strata which is identified in the Kita Daito Basin (Tokuyama,in prep.). The strata are underlaid by Middle Eocene volcaniclastic distal sediments supplied from the Kyushu Palau Ridge and overlaid by Early to Late Oligocene volcaniclastic distal sediments supplied from the Kyushu Palau Ridge. The available data demonstrate that Unit D is Middle Eocene in age and Unit C are redeposited strata supplied from Unit E and mainly Unit D after Middle Eocene volcanic epoch on the Kyushu Palau Ridbe. Units A and B are pelagic sediments possibly after Late Eocene.

REFERENCES

Hilde, T. W. C. and G. F. Sharman, 1978: Fault structure of the decending plate and its influence of the subduction process (Abstract). Proc. AGU Meeting, Dec., 1978.

Iwabuchi, Y., 1980: Topography of trenches in the adjecent seas of Japan. Marine Geodesy, 4, 121-140.

Konishi, K., 1963: Pre-Miocene basement complex of Okinawa, and the tectonic belts of the Ryukyu Islands. Sci. Rept. Kanazawa Univ., 8, 2, 569-602.

Matsuda, J., K. Saito, and S, Zashu, 1975: K-Ar ages and Sr isotopic study of the ignous rock fragments in the manganese nodules dredged form the Western Philippine Sea and the Amami Plateau. Preprint. Geological Problems in the Philippine Sea, Annu. Meet. Geol. Soc. Jap., 99-101

Seno, T., 1977: The instataneous rotation vector of the Philippine Sea plate relative to the Eurasian plate. Tectonophys., 42, 209-226.

shiki. T., H. Aoki, and Y. Misawa, 1975: Geological results of recent studies of the Philippine Sea. Mar. Sci., 7, 454-460.

Suyehiro, K., A. Nishizawa, and H. Shimizu, 1982: Seismic Activity near the axis of the Ryukyu Trench by using O.B.S. (Abstract). Seism. Soc. Japan, 2,47.

Tokuyama, H., H. Kagami, Y. Kong, C. Igarashi, and N. Nasu, 1982: The recent results from the multi-channel seismic profiling across the Japan Trench and Nanki Trough. Modern Sea Bottom Research II, Proceedings of Symposium -2, 73-80.

Figs. 14-4, -8, -12 are reproduced as a foldout in the attached envelope.

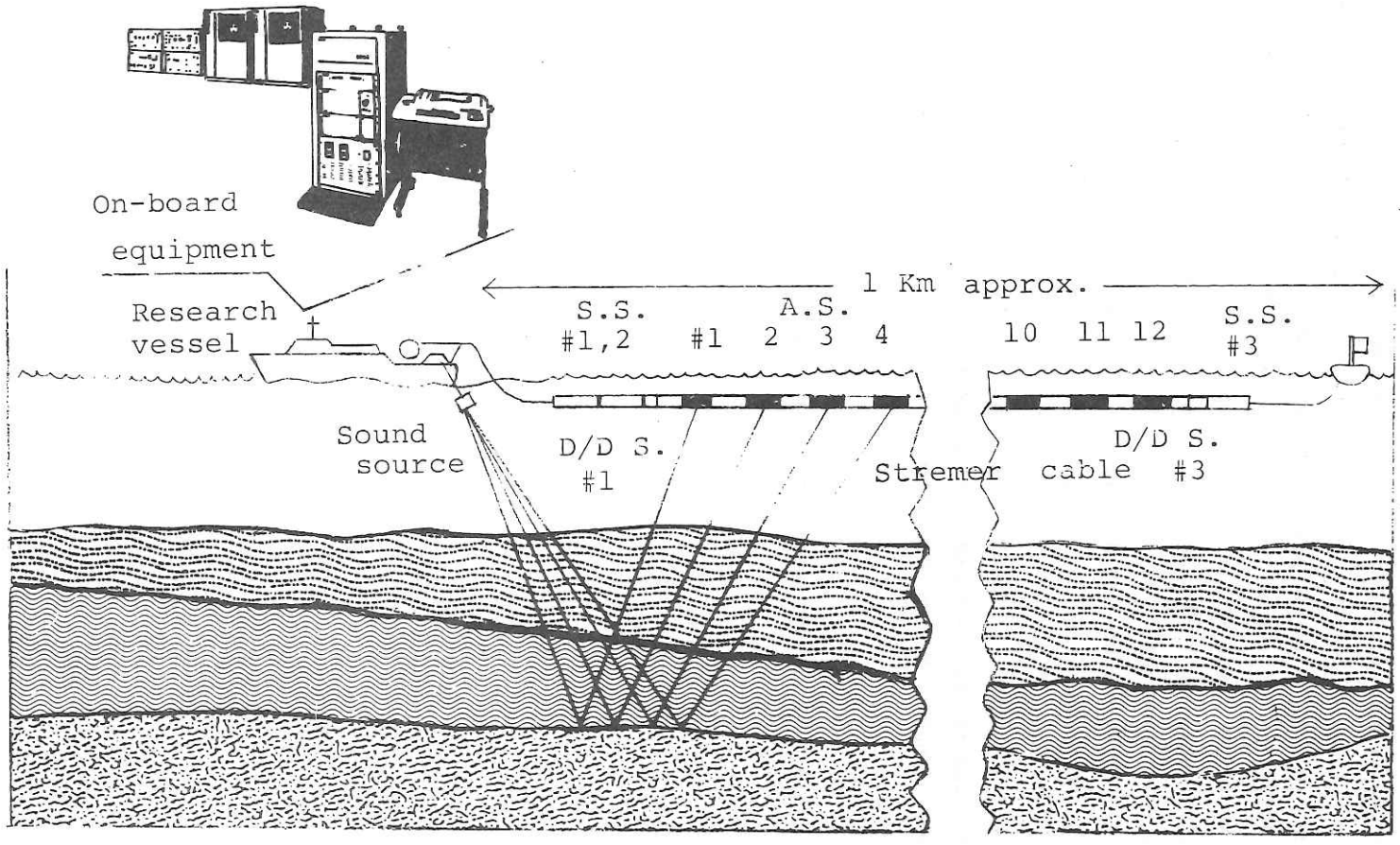

Fig. 14-1. Layout of the multichannel seismic survey system.

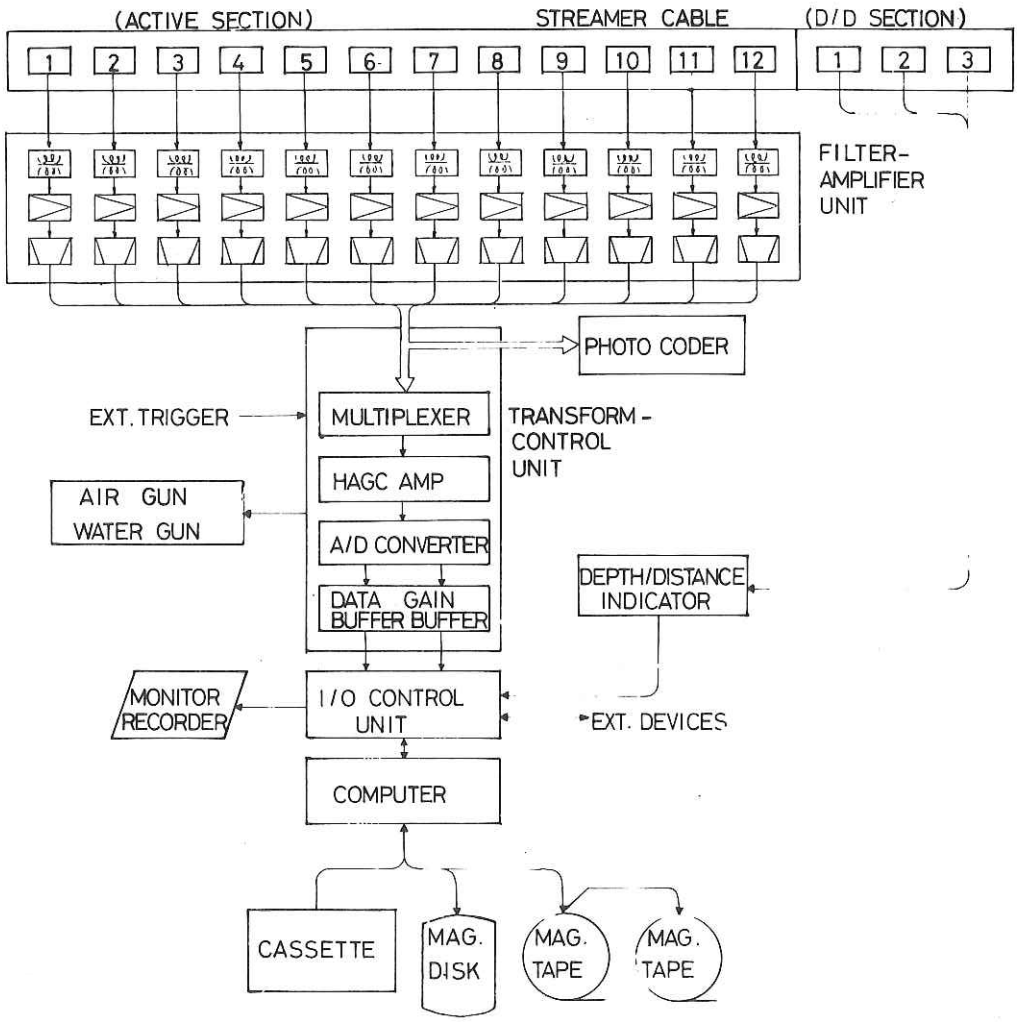

Fig. 14-2. Block diagram of multichannel seismic survey system.

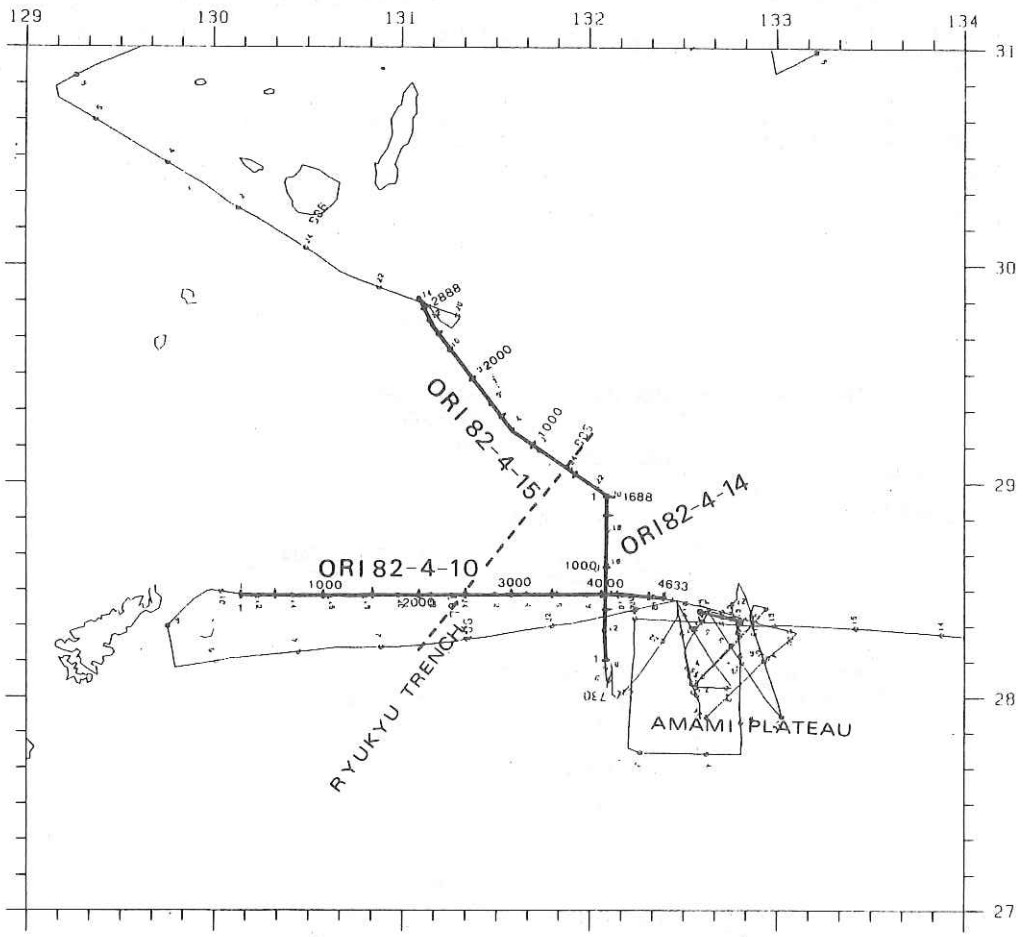

Fig. 14-3. Track line of the multichannel seismic profile.

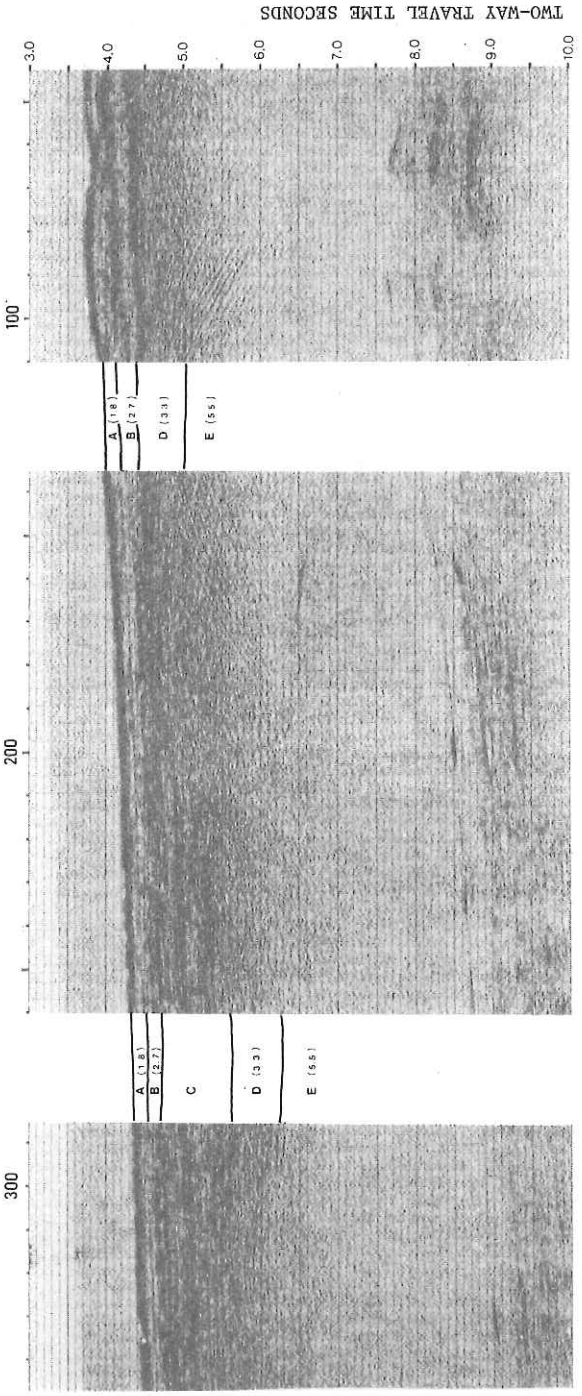

Fig. 14-5. Processed multichannel seismic profile of the line KH-82-4-14 (s.p. 43-347)

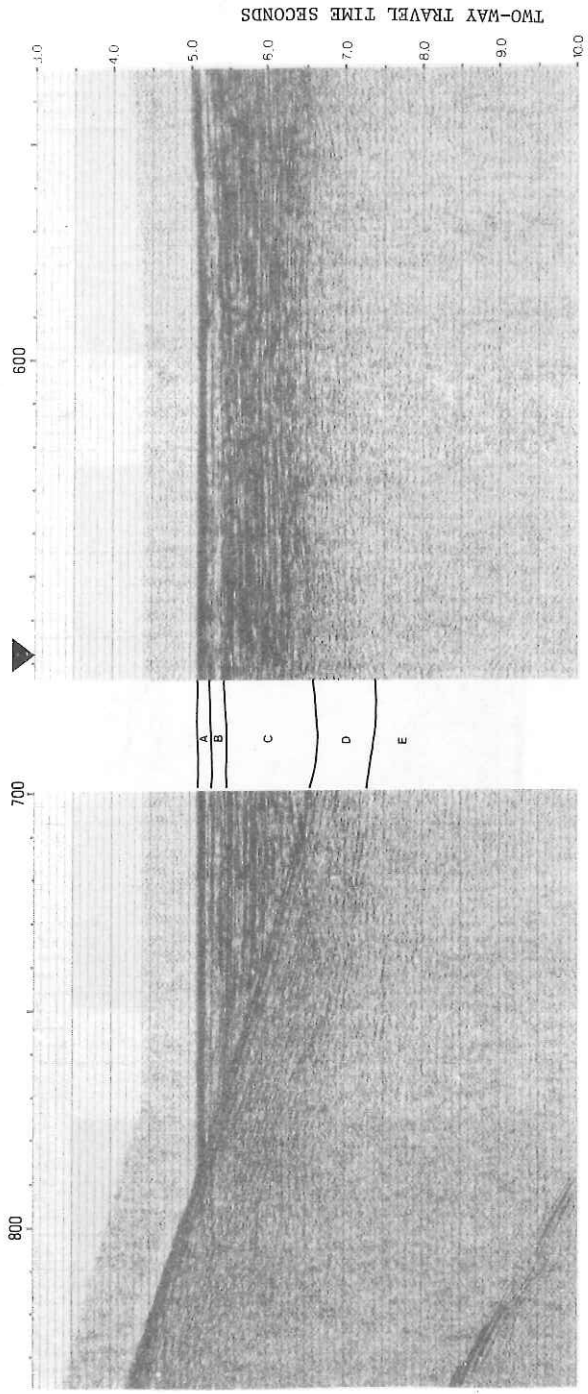

Fig. 14-6. Processed multichannel seismic profile of the line KH-82-4-14 (s.p. 533-837)

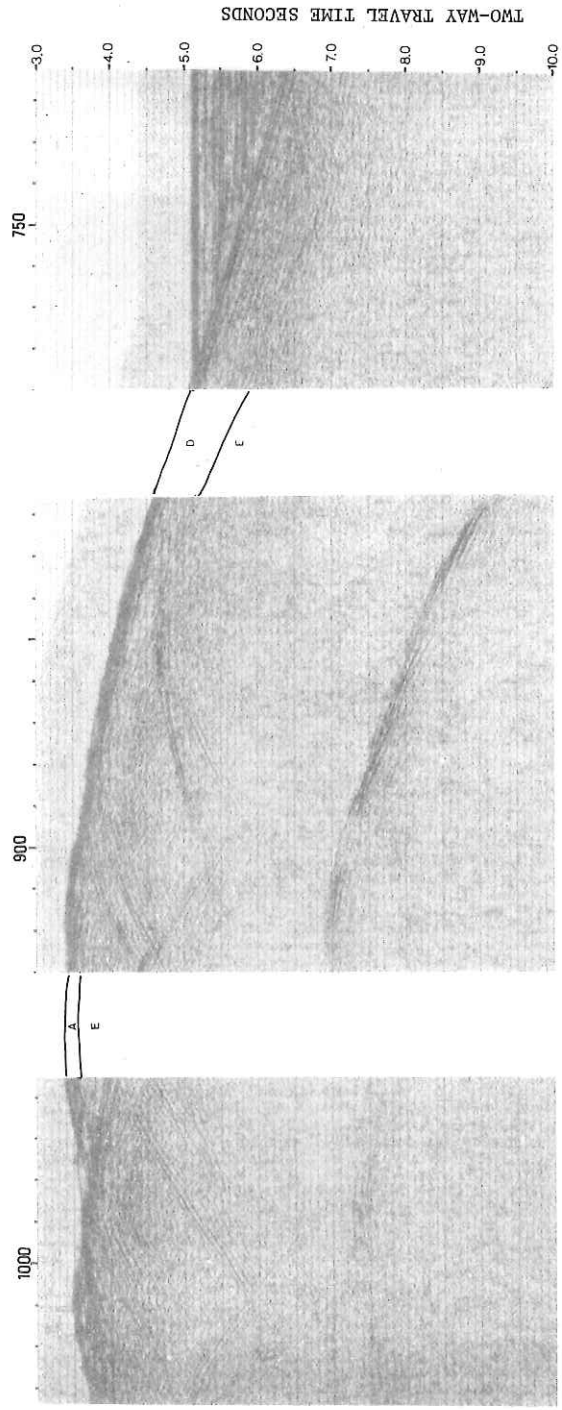

Fig. 14-7. Processed multichannel seismic profile of the line KH-82-4-14 (s.p. 713-1033)

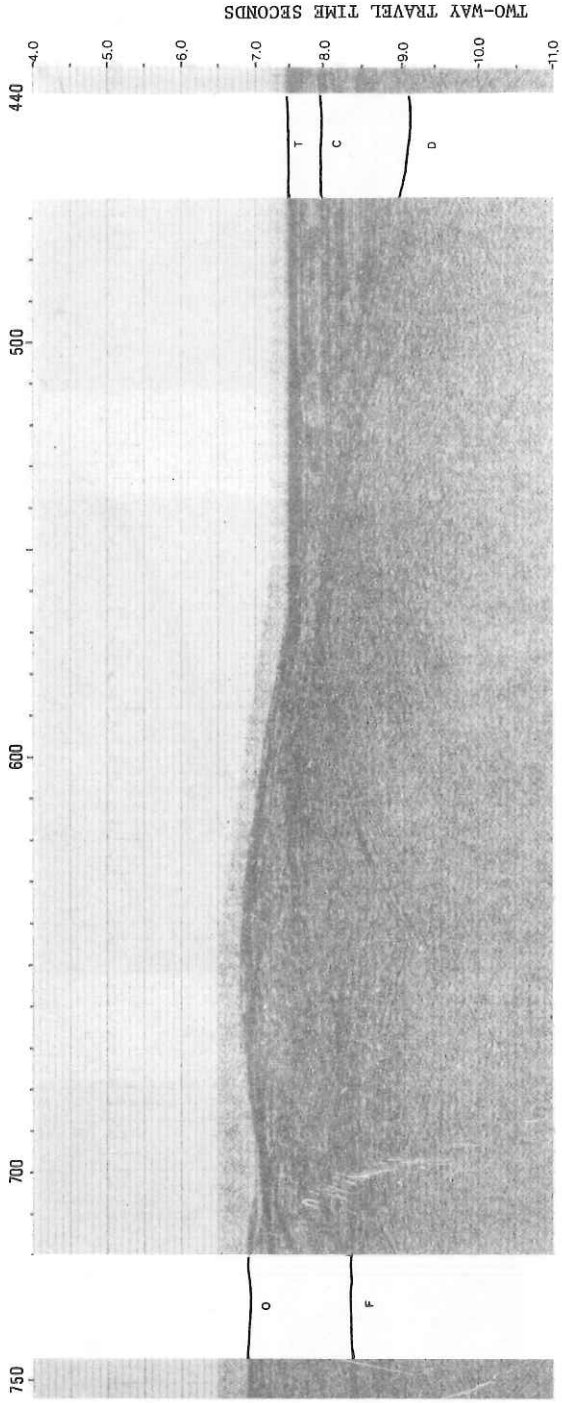

Fig. 14-9. Processed seismic multichannel seismic profile of the line KH-82-4-15 (s.p. 433-754)

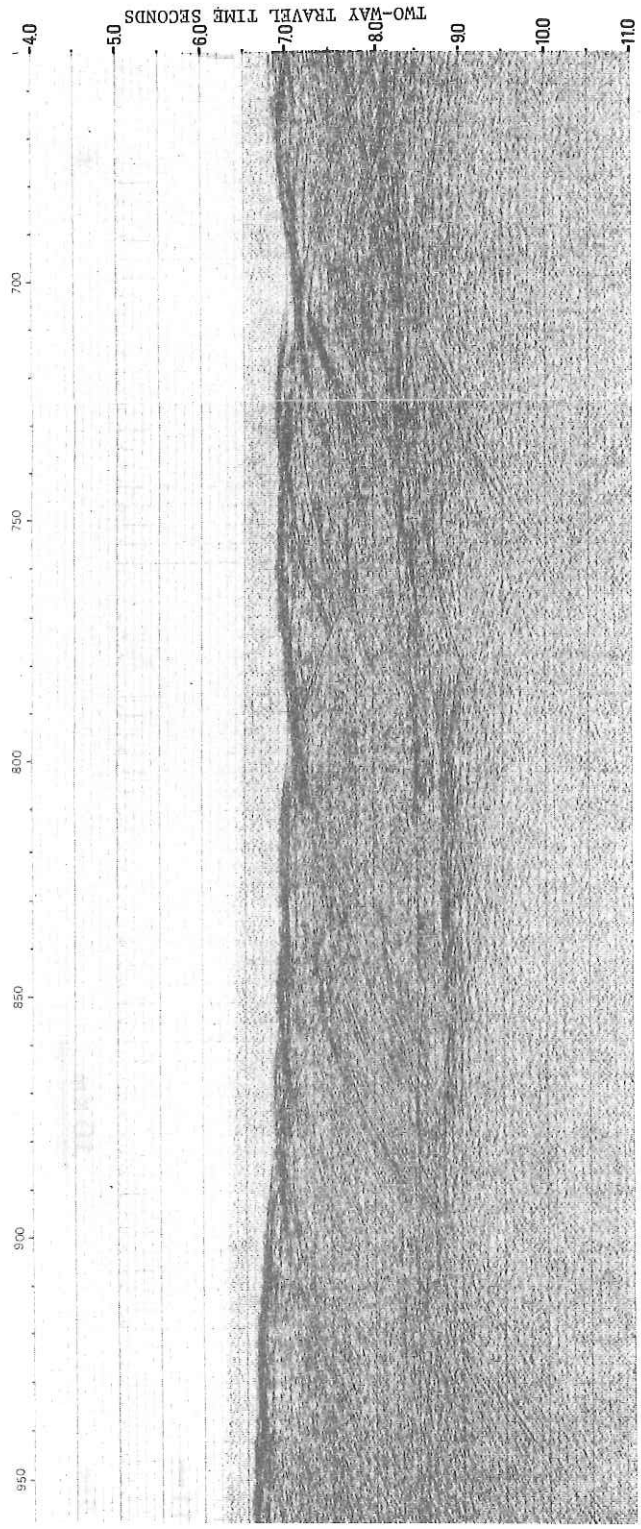

Fig. 14-10. Processed seismic multichannel seismic profile of the line KH-82-4-15 (s.p. 700-950)

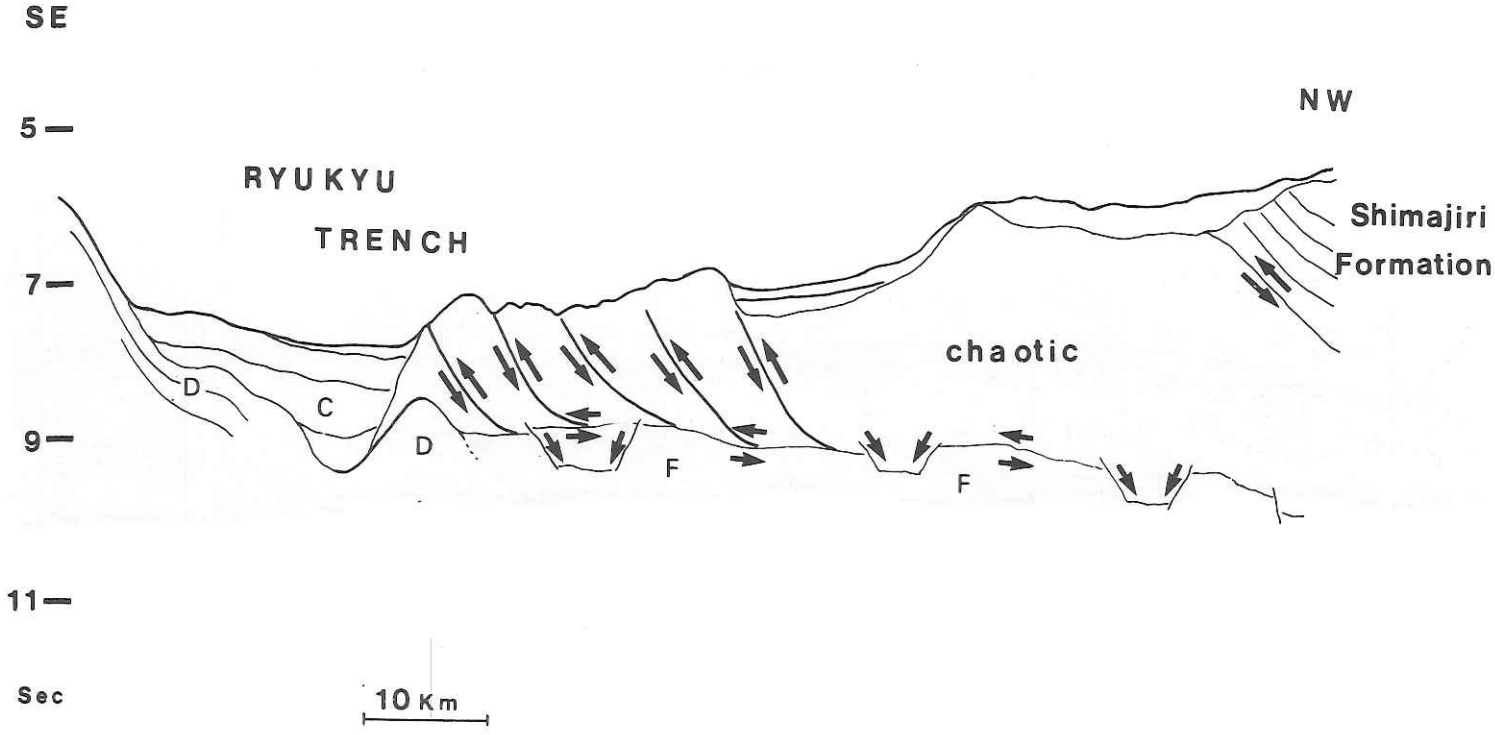

Fig. 14-11. Processed seismic multichannel seismic profile of the line KH-82-4-10

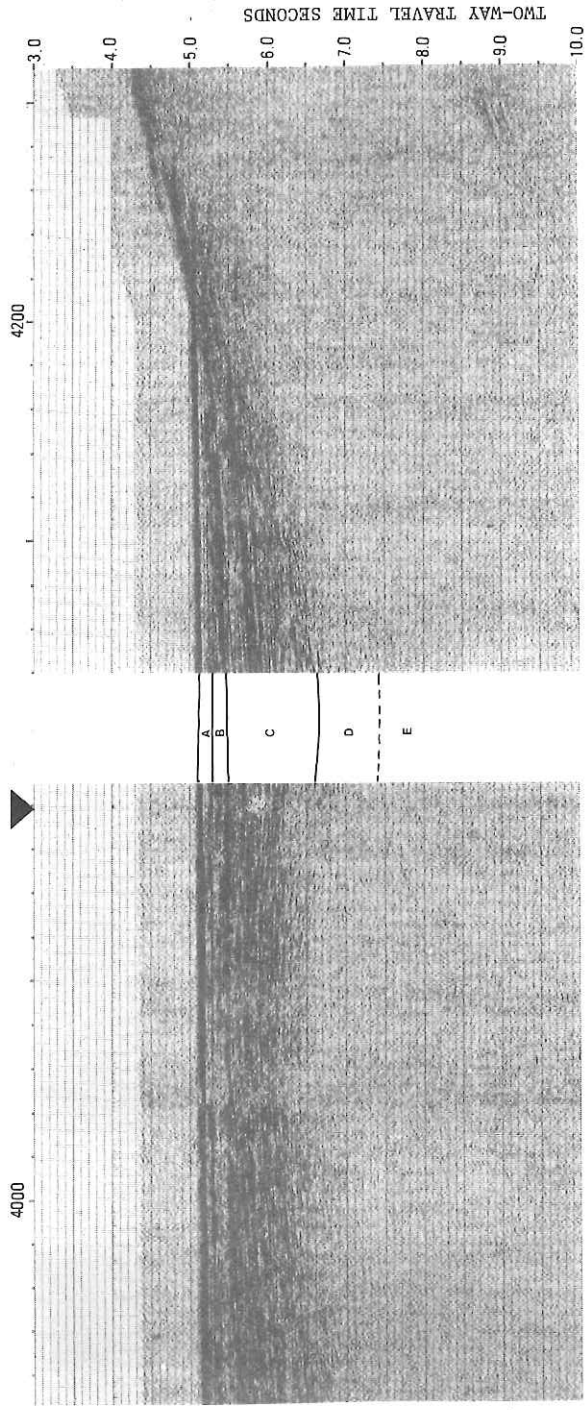

Fig. 14-13. Processed seismic multichannel seismic profile of the line KH-82-4-10 (s.p. 3952-4258)

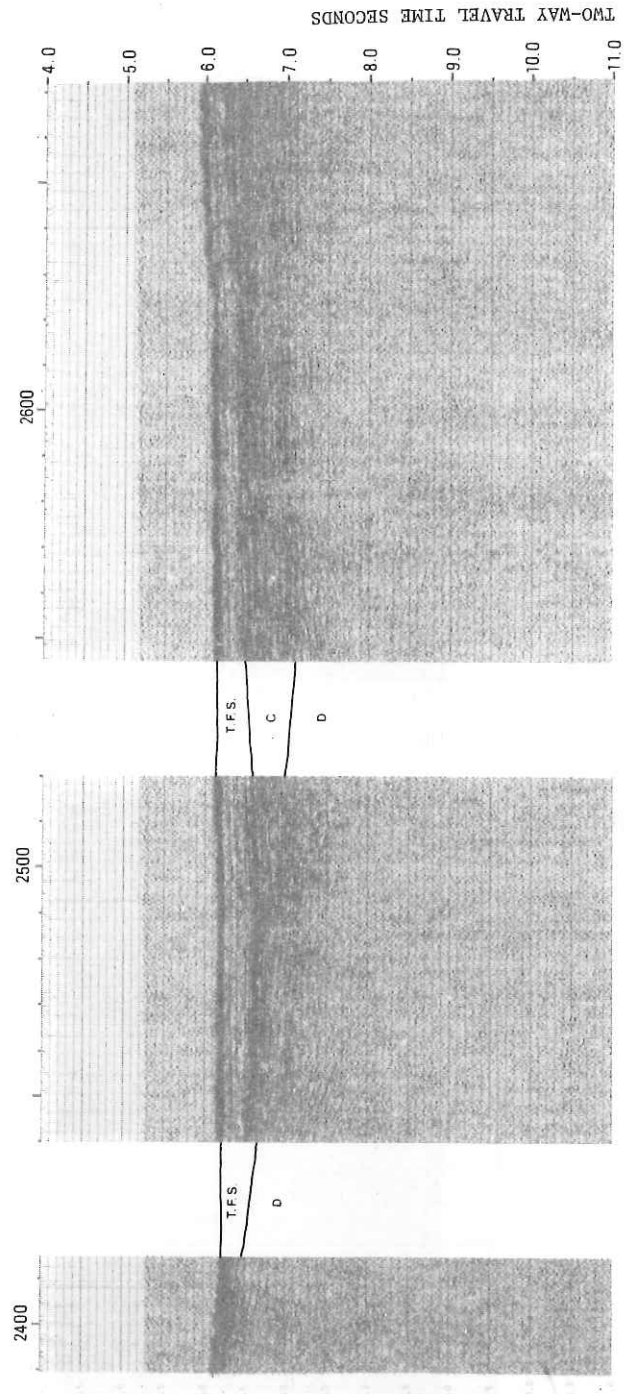

Fig. 14-14. Processed seismic multichannel seismic profile of the line KH-82-4-10 (s.p. 2389-2671)

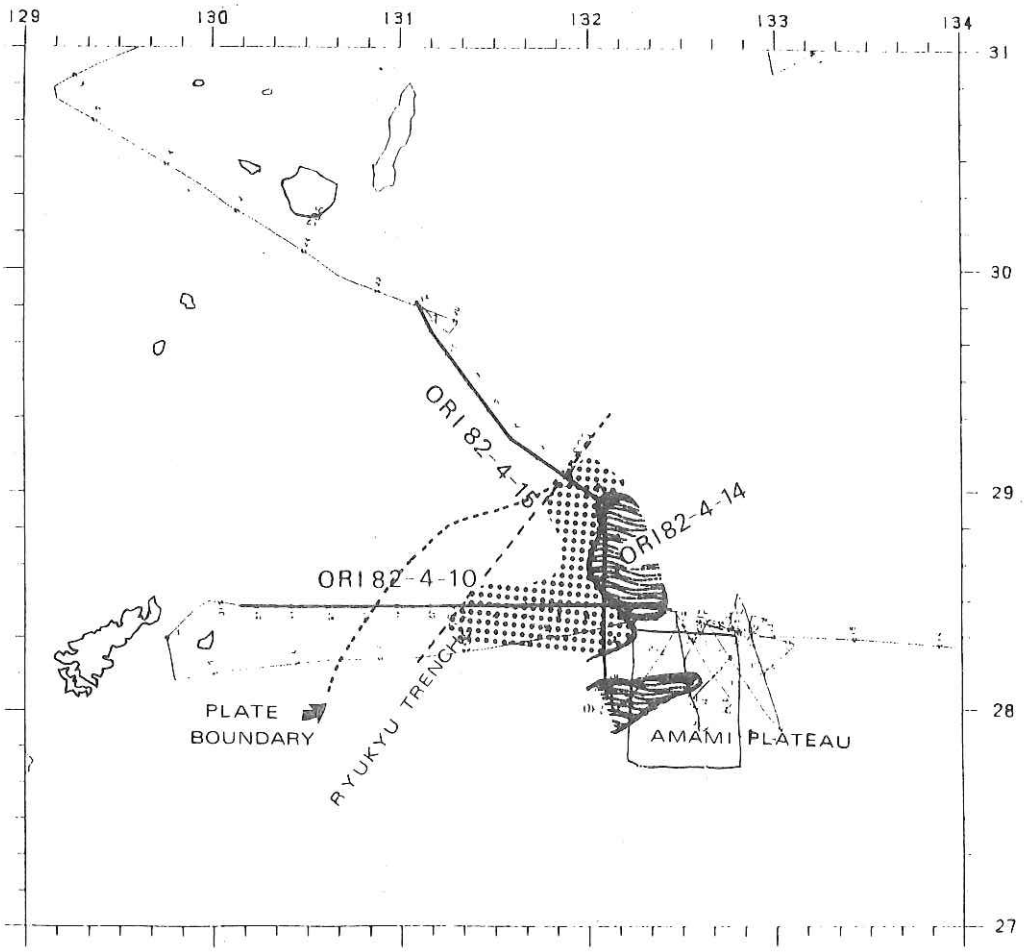

Fig. 14-15. Plate boundary between the Ryukyu Island Arc and the Philippine plate.

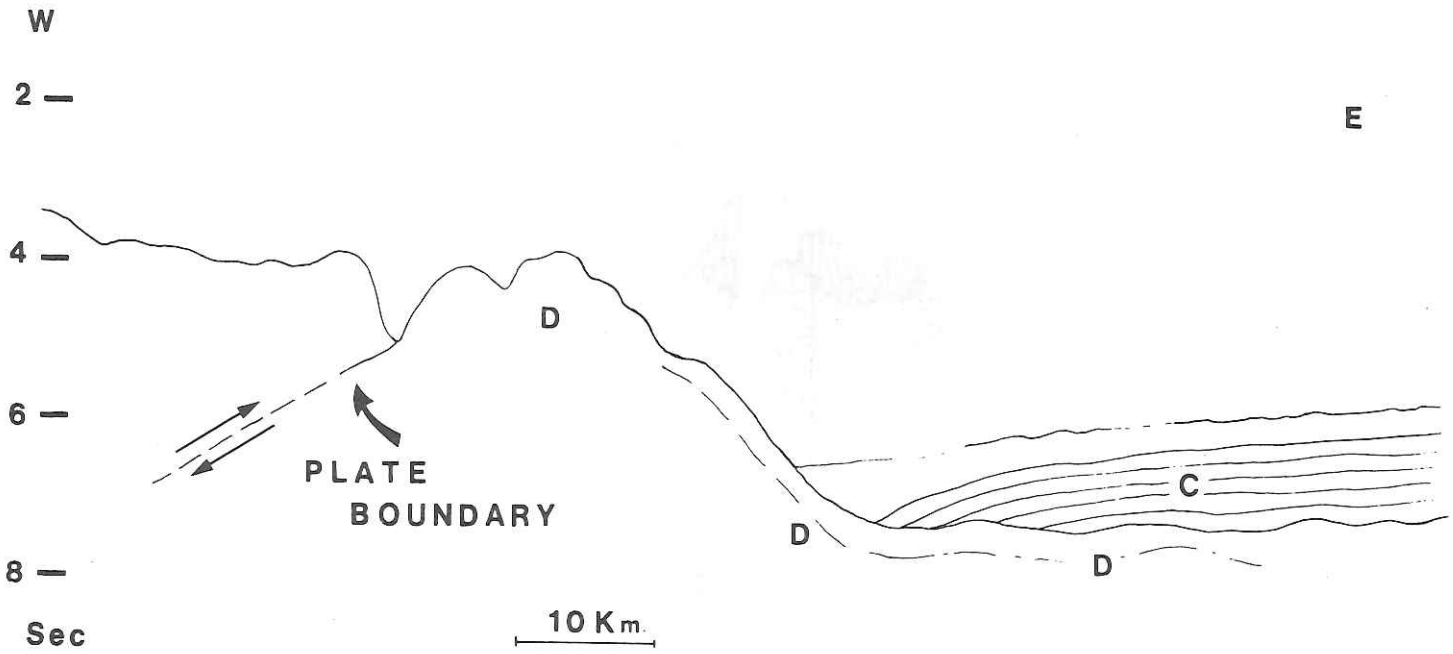

Fig. 14-16. Schematic structure along line KH-82-4-10.

APPENDIX. PRELIMINARY RESULTS OF THE R.V.TANSEI-MARU KT 82-10 (Nov.13, 1982 -Nov.20, 1982)

A-1. SCIENTISTS ABOARD THE R.V. TANSEI-MARU FOR THE CRUISE KT82-10.

KOBAYASHI,Kazuo (Chief Scientist)	Ocean Research Institute, University of Tokyo
TOMODA, Yoshibumi	Ocean Research Institute, University of Tokyo
FURUTA, Toshio	Ocean Research Institute, University of Tokyo
WATANABE, Masaharu	Ocean Research Institute, University of Tokyo
TANAKA, Takeo	Ocean Research Institute, University of Tokyo
NAITO, Yoshihiro	Department of Earth Sciences, Chiba University

A-2. OPERATION LOG OF PISTON CORE

Date 18 Nov. 1983 Ship Tansei Maru KT 82-10 Station 1
Latitude 34°44.39'N Longitude 140°32.23'E
Location north of the northeastern escarpment of Sagami Trough
Sea calm , no swell Weather clear to cloudy
Bottom Topography flat, on a bank Profiler

Length of Core Pipe 8 m Wall Thickness 7.5 mm Material Al
ID of Pipe 75 mm Core Head Wt. 350 Kg Trigger Wt. 50 Kg
Length Main Line 16 m Length Trigger Line 16 m Length Free Fall 7 m
Response at Hit clear Response at Pull-out clear
Time Lowered 12h 35m; Uncorrected Water Depth m
Time Hit 13h 00m; Uncorrected Water Depth 1983 m
Wire Angle at Hit 0°; Wire-out at Hit 1996 m

Cored Length 753 cm Trigger Cored Length 11 cm
Method of Storage cut in laboratory No. of Pipe filled 5
Length of Cores in Pipe 1. 111 cm, 2. 189 cm, 3. 185 cm, 4. 183 cm, 5. 85 cm, 6. cm.

A-3. MEGASCOPIC CORE DESCRIPTION

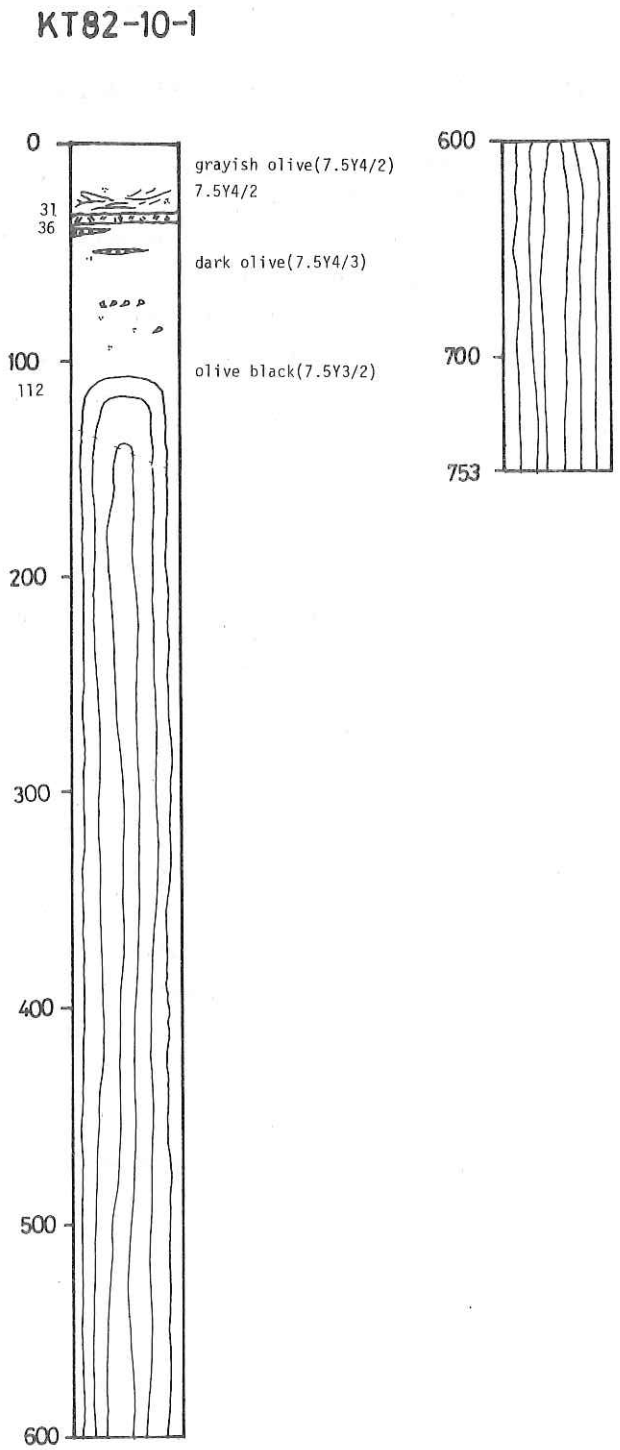

Fig. A-3-1. Megascopic description of core KT 82-10-1.

A-4. OPERATION LOG OF DREDGE

Date Nov. 19, 1982 Ship Tansei Maru KT82-10 Station No. 3
Location Sagami Trough
Weather fine Wind 7.5m/s, 240°sw Sea low swell
Bottom Topography bottom of Trough
Type of Dredge Okean Add.Wt. kg
Time lowered 07 h 57 m Uncorr. Water Depth 3400 m
Initial Time on Bottom 08 h 57m Uncorr. Water Depth 3360 m
Wire Length 3337 m Wire Angle
Ship Position Lat. 34°37.58'N Long. 140°28.96'E
Direction of Haul Ship Speed kt. (till h m)
Speed Wire-in m/sec (from h m) Winch No.
Final Time on Bottom h m Uncorr. Water Depth m
Wire Length m Wire Angle
Ship Position Lat. Long.
Time Surfaced h m

A-5. DESCRIPTION OF HARD-ROCK SAMPLES

During the cruise, some angular fragments of semi-consolidated mudstones were collected from the lower flank of the northern escarpment of the Sagami Trough. The rocks recovered were mostly bluish gray hemipelagic claystones containing a lot of calcareous nannofossils. They include yellowish brown vitric mudstones and poorly sorted siltstones rich in quartz, plagioclase and volcanic fragments.

Calcareous nannofossils are common and moderately preserved in the sediments. According to N. Ohyama, important age indicative species are as follows; *Discoaster asymmetricus* Gratner, *Reticulofenestra pseudoumbilica* Gartner, *Sphenolithus abies* Deflandre and others. These indicate the age of these sediments as middle Pliocene, upper part of CN 10 or CN 11 zone of Okada & Bukry (1981).

BATHYMETRIC MAP OF AMAMI PLATEAU AND ITS VICINITY

COMPILED BY
TAKESHI MATSUMOTO AND KAZUO KOBAYASHI
OCEAN RESEARCH INSTITUTE, UNIVERSITY OF TOKYO, 1983

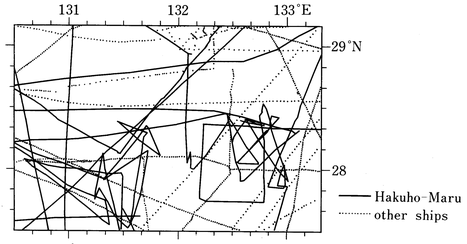

131 132 133°E

29°N 28

1/250,000 (Lat. 35°)

BATHYMETRIC MAP OF OGASAWARA FORE-ARC REGION AND ADJACENT AREA

COMPILED BY
TAKESHI MATSUMOTO AND KAZUO KOBAYASHI
OCEAN RESEARCH INSTITUTE, UNIVERSITY OF TOKYO, 1983

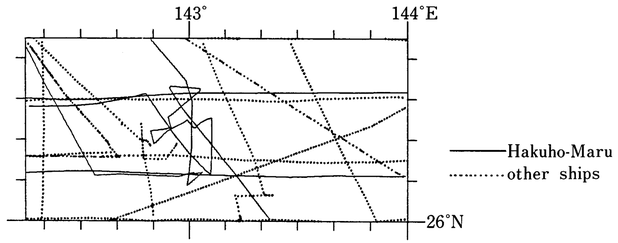

143°
144°E
26°30′
26°30′N
26°
26°
143°
144°
400
1000
2000
3000
3400
4000
5000
6000
7000
3600
2400
2600

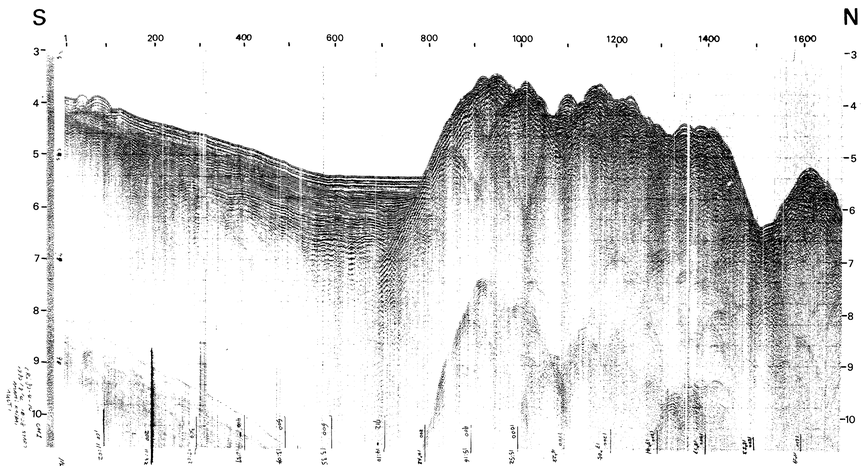

Fig. 14-4. Onboard far-trace monitor record of the line KH 82-4-14.

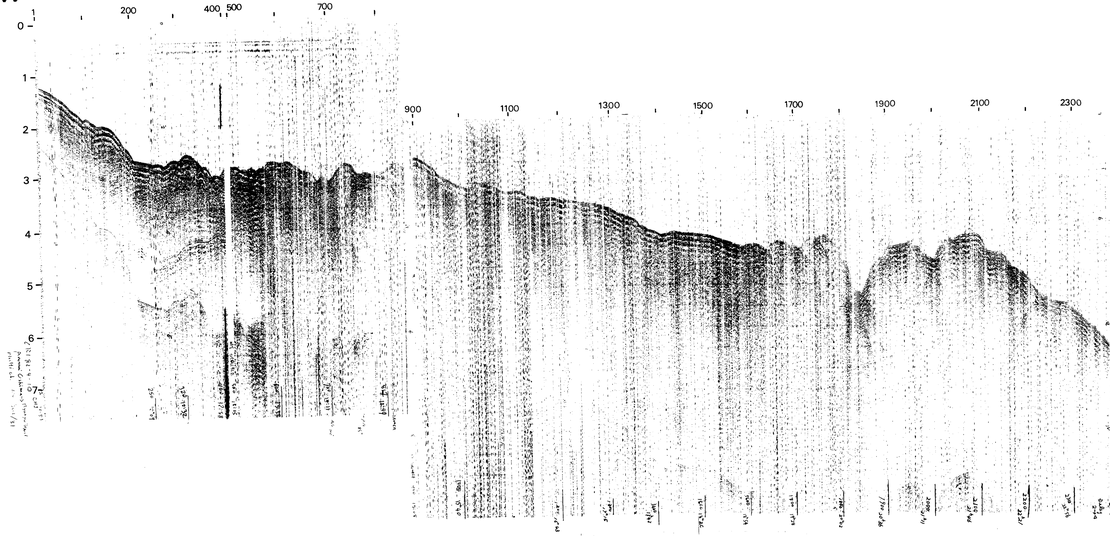

Fig. 14-12. Onboard far-trace monitor record of the line KH-82-4-10

ON BOARD FAR TRACE RECORDS OF MULTICHANNEL SEISMIC SURVEY AROUND THE AMAMI PLATEAU. KH 82-4.

Foldout attached to Preliminary Report of the Hakuhō Maru Cruise KH 82-4, Chapt. 14, H. TOKUYAMA and KONG YOUNG SAE, 1983.

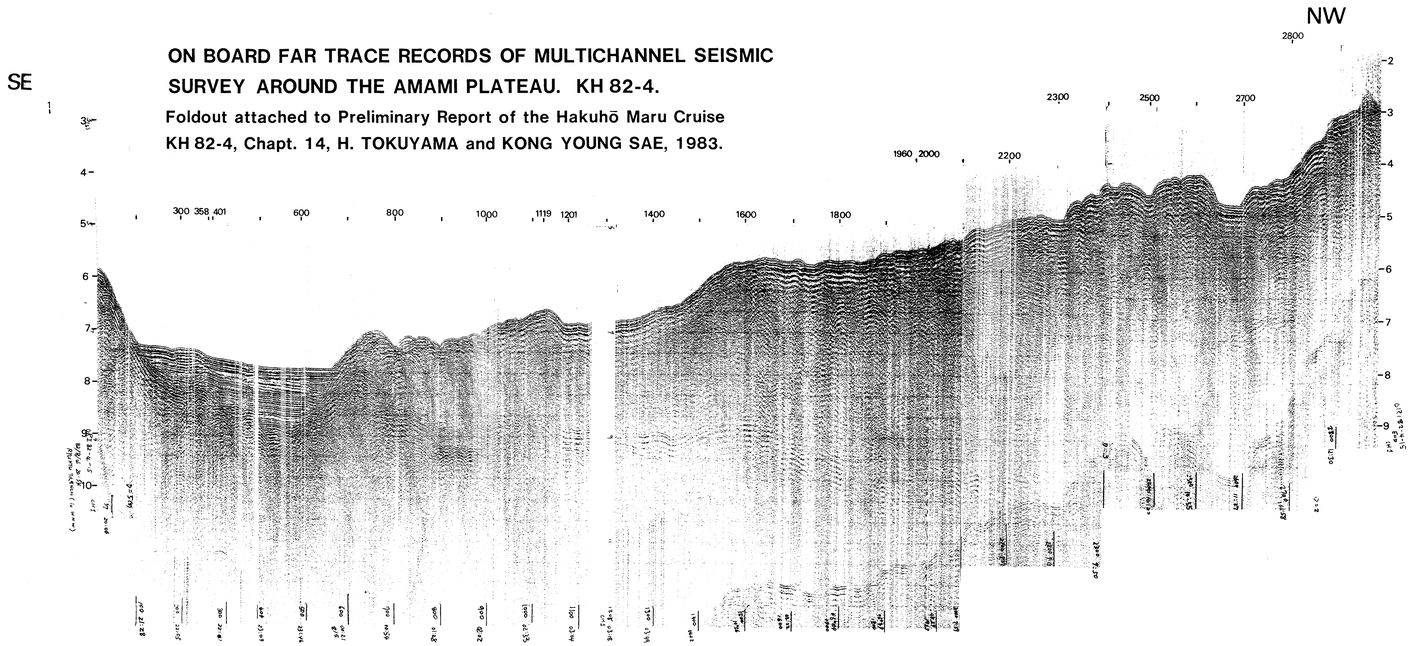

Fig. 14-8. Onboard far-trace monitor record of the line KH-82-4-15